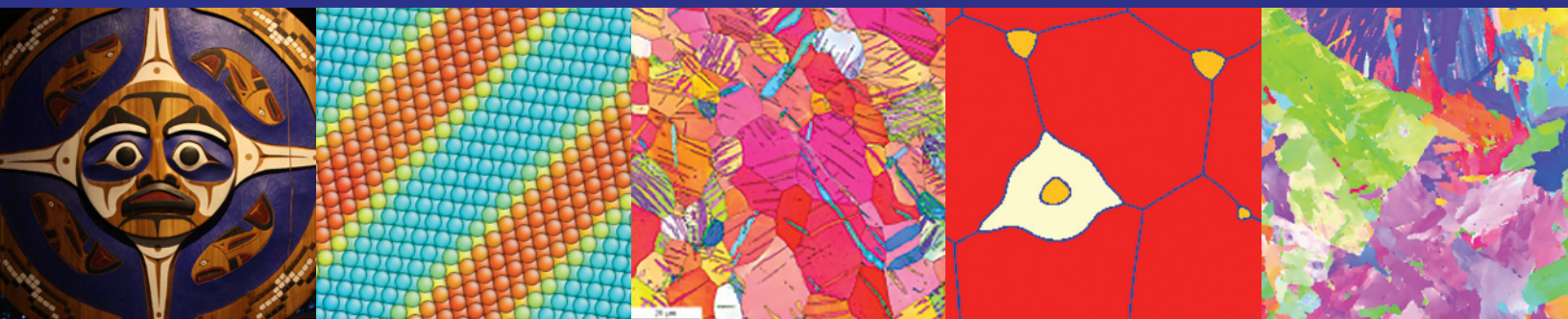




Solid-Solid Phase Transformations in Inorganic Materials

JUNE 28 – JULY 3, 2015 | WHISTLER, BC, CANADA



Thermal Mechanical Simulators

Materials researchers are frequently asked to extend the boundaries of what is possible in their industries. To help in this quest, Dynamic Systems Inc. (DSI) has developed a comprehensive line of dynamic thermal-mechanical physical simulators and testing machines.

Whether you need to characterize new materials, optimize existing processes, explore new production techniques, or simulate the conditions of new applications, you will find there is a DSI system that will help you cut costs, shorten development times, and open the door to new ideas, processes and profits.

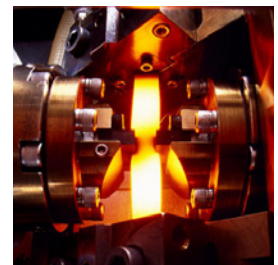
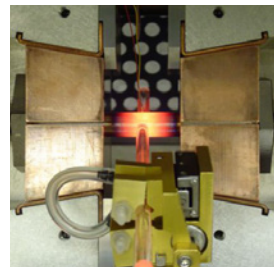
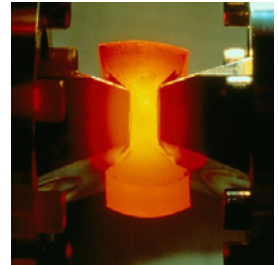


Gleeble 3800
20 Ton Maximum Force

Process Simulation Capabilities of the Gleeble include:

- Weld HAZ Cycles
- Continuous Casting
- CCT & CHT
- Friction Stir Welding
- Mushy Zone Processing
- Heat Treating
- Powder Metallurgy/Sintering
- Melting and Solidification
- Continuous Strip Annealing
- Hot Rolling
- Forging
- Quenching
- Diffusion Bonding
- Butt Welding
- Extrusion
- Embrittlement and Crack Susceptibility
- Hot / Warm Compression Testing
- Hot / Warm Tensile Testing

About DSI: Dynamic Systems Inc. (DSI) designs and manufactures the Gleeble® line of material testing and simulation systems. New materials and process improvements can be studied in a laboratory and successfully transferred to plant production lines, reducing the cost, risk, and time associated with studying new processes or materials.



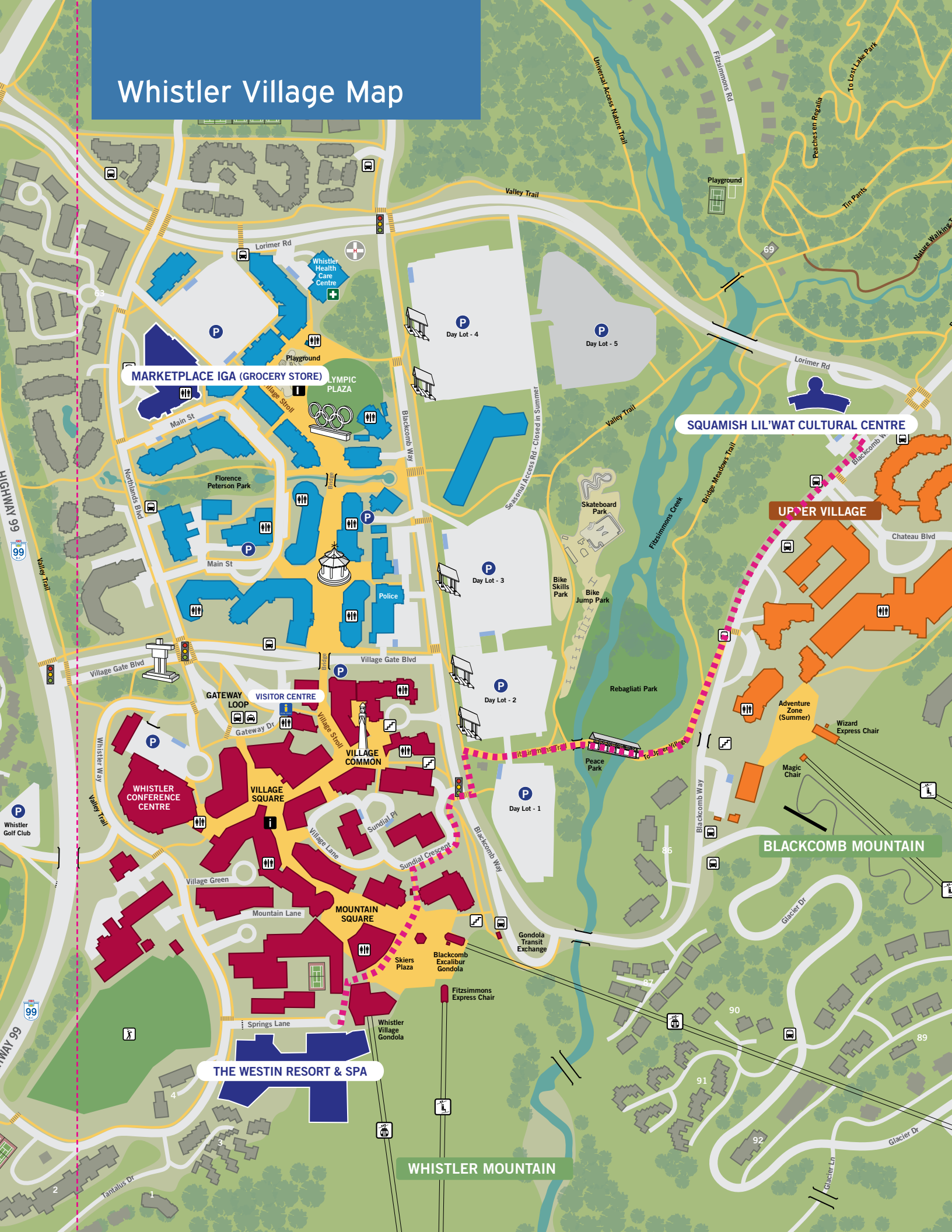
Visit us online at
www.Gleeble.com



P.O. Box 1234, 323 Route 355
Poestenkill, NY 12140 USA
(518) 283 - 5350 | Fax: (518) 283 - 3160

Specifications are subject to change.
"Gleeble" is a registered trademark of Dynamic Systems Inc.
©2015 by Dynamic Systems Inc. All rights reserved. v6.15

Whistler Village Map



MARKETPLACE IGA (GROCERY STORE)

SQUAMISH LIL'WAT CULTURAL CENTRE

UPPER VILLAGE

BLACKCOMB MOUNTAIN

THE WESTIN RESORT & SPA

WHISTLER MOUNTAIN

Table of Contents

Registration	2
Exhibition & Sponsorship	3
Venues	4
Whistler Information	5
Abstracts	6
Monday 29 June 2015	6
Tuesday 30 June 2015	14
Poster Session	19
Wednesday 1 July 2015	31
Thursday 2 July 2015	35
Friday 3 July 2015	44
Author Index	49

Also included in the Onsite Program:

- [Program at a Glance Booklet](#)
- [Map of Whistler Village](#)



International Conference Services Ltd.

Conference Secretariat

International Conference Services, Ltd.
2101 – 1177 West Hastings St.
Vancouver, BC, Canada, V6E 2K3

Tel +1 604 681 2153
Fax +1 604 681 1049

vancouver@icsevents.com
www.icsevents.com

Committees

Organizing Committee

Matthias Militzer (Chair)
*Professor, ArcelorMittal
Dofasco Chair in Advanced
Steel Processing*
The University of British Columbia
Materials Engineering Department

Gianluigi Botton
*Professor, Canada Research
Chair in Microscopy of
Nanoscale Materials*
McMaster University
Materials Science and Engineering
Department

Long-Qing Chen
*Donald W. Hamer Professor
of Materials Science and
Engineering*
Penn State University
Materials Research Institute

James M. Howe
*Thomas Goodwin Digges
Professor*
University of Virginia
Materials Science and Engineering
Department

Chadwick W. Sinclair
Professor
The University of British Columbia
Materials Engineering Department

Hatem S. Zurob
Associate Professor
McMaster University
Materials Science and Engineering
Department

Advisor to the Organizing Committee

Gary Purdy
University Professor
McMaster University
Materials Science and Engineering
Department

International Scientific Committee

Mark Asta, United States of America
Sudarsanam Babu, United States of America
Annika Borgenstam, Sweden
Francisca Caballero, Spain
Amy Clarke, United States of America
Alexis Deschamps, France
Masato Enomoto, Japan
Alphonse Finel, France
Helio Goldenstein, Brazil
Robert Hackenberg, United States of America
Ming-Xin Huang, Hong Kong
Christopher Hutchinson, Australia
Jose-Maria Rodriguez Ibabe, Spain
Pascal Jacques, Belgium
Xuejun Jin, China
Dorte Juul-Jensen, Denmark
David Laughlin, United States of America
Young-Kook Lee, Korea
Emmanuelle Marquis, United States of America
Knut Marthinsen, Norway
Goro Miyamoto, Japan
Tetsuo Mohri, Japan
Elena Pereloma, Australia
Michel Perez, France
Nik Provatas, Canada
Dierk Raabe, Germany
Eugen Rabkin, Israel
Michel Rappaz, Switzerland
Joseph Robson, United Kingdom
Colin Scott, Canada
David Seidman, United States of America
Bill Soffa, United States of America
Georges Spanos, United States of America
Ingo Steinbach, Germany
Valentin Vaks, Russia
Sybrand Van der Zwaag, Netherlands
Thomas Waitz, Austria
Jer-Ren Yang, Taiwan
Wenzheng Zhang, China

Registration

Your full congress registration includes

- Name Badge
- Onsite Program (including Abstracts)
- Proceedings USB
- Program Sessions
- Welcome Reception on Monday
- Daily Coffee Breaks; Lunch on Monday, Tuesday and Thursday
- Gala Dinner on Thursday

Registration Hours

The registration desk will be located in the Main Foyer of the Hotel

Sunday	12:00–21:00
Monday	07:00–18:00
Tuesday	08:00–18:00
Wednesday	08:00–14:00
Thursday	08:00–20:00
Friday	08:00–13:30

NETWORKING & SOCIAL EVENTS

Welcome Reception

The Welcome Reception will be held on Monday, June 29 from 18:30–20:30 at the Squamish Lil'wat Cultural Centre Whistler, B.C.

The Welcome Reception is about a 25 min. walk from the Westin. The location and route are highlighted on the enclosed map.

Poster Viewing and Extended Lunch Break

The poster session will be held Tuesday from 13:15–15:00 in the Alpine Foyer and includes lunch. Posters will be on display for the duration of the conference from Monday to Friday.

Congress Dinner

The dinner will be held on Thursday, July 2 from 20:00–22:30 in the Emerald Ballroom.

Internet Access

Complimentary internet access is available for PTM attendees in public areas of the hotel and in the guest rooms.

Technical Sessions

The plenary sessions will be held in the **Emerald Ballroom**.

The poster presentations will be held in the **Alpine Foyer** on Level 2. See the Technical Program for room locations.

All other oral presentations will be held in **Alpine ABC** and **Alpine DE, Callaghan Room** and the **Nordic Room** up on Level 2.

POLICIES

Badges

All attendees must wear registration badges at all times during the congress to ensure admission to events included in the paid fee such as technical sessions and receptions.

Photography Notice

By registering for this congress, all attendees acknowledge that they may be photographed by congress personnel while at events and that those photos may be used for promotional purposes.

Audio/Video Recording Policy

Recording of sessions (audio, video, still photography, etc.) intended for personal use, distribution, publication, or copyright without the express written consent of PTM and the individual authors is strictly prohibited.

Cell Phone Use

In consideration of attendees and presenters, we kindly request that you minimize disturbances by setting all cell phones and other devices on "silent" while in meeting rooms.

Exhibition & Sponsorship

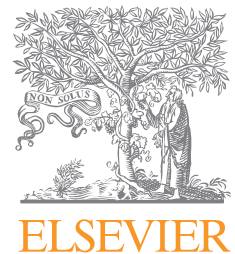
Exhibition Hours

The exhibition tables will be located in the Emerald Ballroom Foyer

Monday	10:00–16:45
Tuesday	09:45–18:30
Wednesday	11:00–13:30
Thursday	09:45–17:45
Friday	09:45–13:30

PTM would like to thank the Exhibitors and Sponsors for their gracious support of the event.

Sponsors



Co-Sponsor



a place of mind



Venues



THE WESTIN RESORT & SPA, WHISTLER

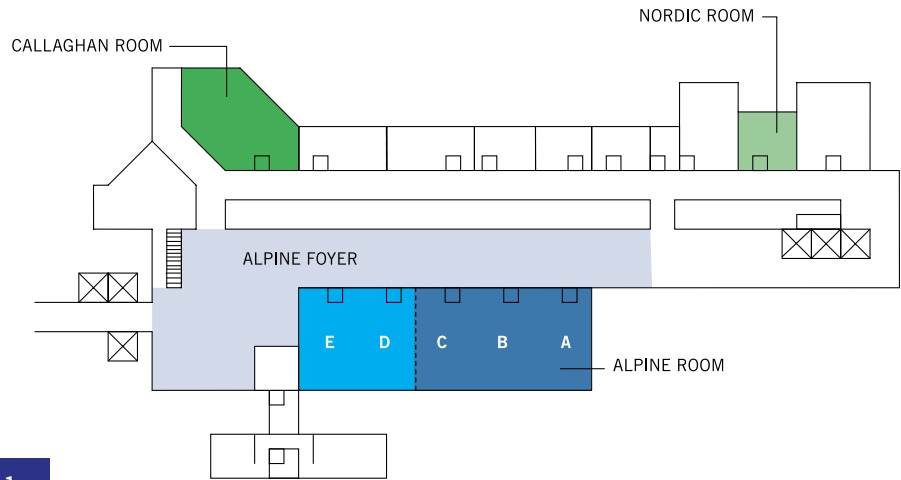
4090 Whistler Way
Whistler, BC V0N 1B4
Canada
Phone: 604 905 5000
www.westinwhistler.com



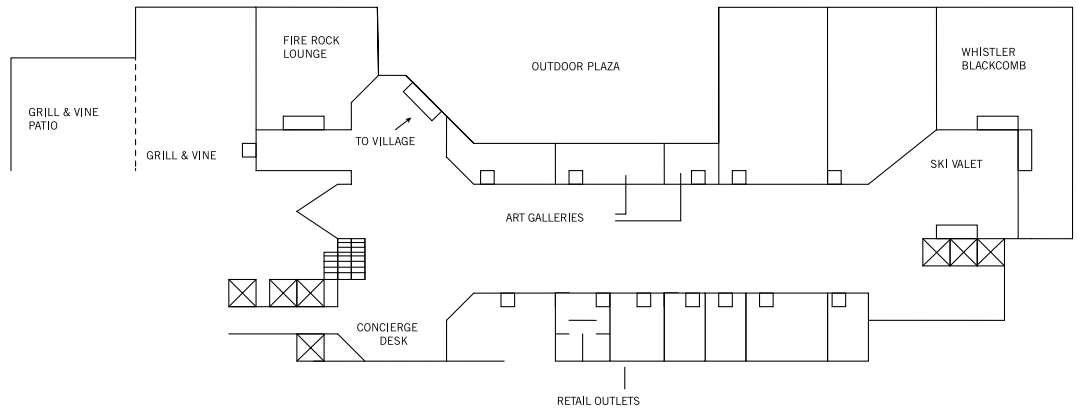
WELCOME RECEPTION LOCATION SQUAMISH LIL'WAT CULTURAL CENTRE

4584 Blackcomb Way
Whistler, BC V0N 1B4
Canada
1 866 441 SLCC (7522)
info@slcc.ca

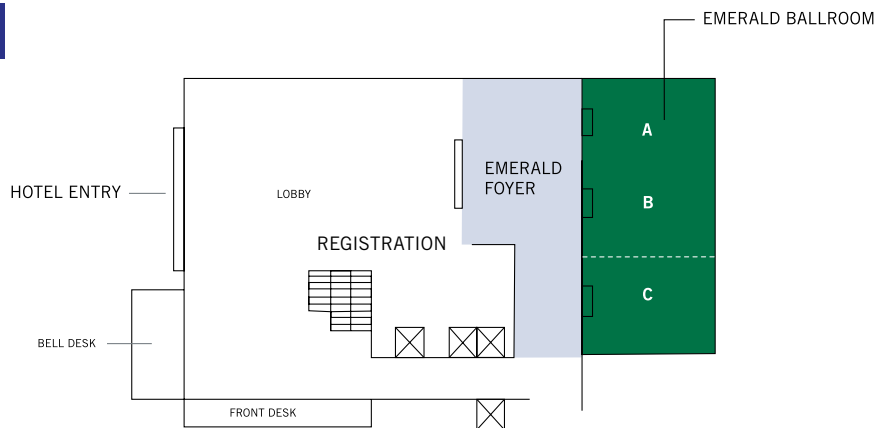
LEVEL 2



LEVEL 1



LOBBY LEVEL



Whistler Information

The Whistler Visitor Centre

www.whistler.com/whistler-visitor-centre

Phone 1.604.935.3357

Toll Free 1.877.991.9988

Email activity@tourismwhistler.com

Location 4230 Gateway Drive
(Adjacent to the Taxi/Bus loop
in the centre of Whistler Village)

Free Parking Options

Parking in Day Lots 4 and 5 is free for a maximum of 72 hours. Please see map for locations.

Emergency Services

The nationwide emergency phone number for the police, ambulance and fire is 911.

Tipping

Tipping in Canada is much the same as it is in the U.S. In most cases, a tip in the range of 15%–20% is perfectly acceptable.

Electricity

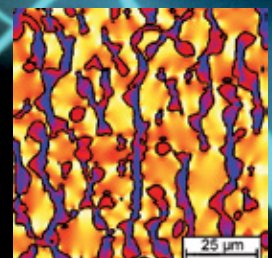
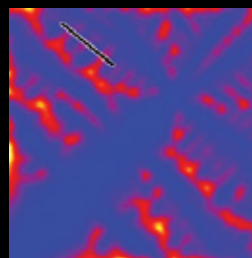
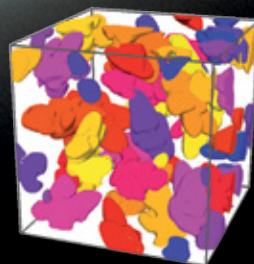
Canada's electrical supply and electrical outlets (sockets, wall plugs) are the same as those found in the United States. The electrical supply is 110 Volts and 60 Hertz (cycles per second).

microstructure evolution simulation software



Simulation of microstructure evolution in technical alloys:

- solidification
- recrystallization
- grain growth
- solid state transformations
- coupling to thermodynamic / mobility data



www.micress.de
support@micress.de
www.access.rwth-aachen.de

MONDAY | 29 JUNE 2015

Plenary 1

MONDAY AM ROOM: EMERALD BALLROOM
SESSION CHAIR: MATTHIAS MILITZER,
THE UNIVERSITY OF BRITISH COLUMBIA

08:15 Introductory Comments

08:30 Plenary

Nucleation: A Challenge in the Modelling of Phase Transformations: *John Agren*¹; ¹Royal Institute of Technology

The modelling of phase transformations, once the nucleation event has occurred, may involve tedious computations but nevertheless methods based on sharp and diffuse interfaces have been quite successful and led to a deeper insight even in complex multicomponent materials. On the other hand nucleation is much more difficult to model. The difficulties stem from deficiencies in our fundamental understanding of nature, from lack of physical knowledge as well as problems involving computational efficiency. In the talk the classical theory of nucleation as well as various modifications over the years will be reviewed. Special emphasis will be given to the thermodynamics of small clusters, kinetics of fluctuations, multicomponent effects, and the rate of nucleation and the importance of different types of defects. In particular the combination of nucleation with sharp and diffuse interface modelling of phase interfaces will be addressed.

09:30 Break

Phase Transformations in Steels: Austenite-Ferrite I

MONDAY AM ROOM: ALPINE A-B-C
SESSION CHAIR: INGO STEINBACH,
RUHR-UNIVERSITY

10:00 Invited

Interfacial Segregation for Allotriomorphic Ferrite Transformation in Fe-C-Mn Alloy: *Takafumi Amino*¹; Genichi Shigesato¹; Masafumi Azuma¹; Takayuki Nozaki¹; ¹Nippon Steel & Sumitomo Metal Corporation

In proeutectoid ferrite growth from austenite in low carbon steel, paraequilibrium (PE) mode and local-equilibrium (LE) mode have been suggested on the basis of the equilibrium theory. In addition, the transition from PE to LE modes has been confirmed during the ferrite growth. On the other hand, on the basis of the grain growth theory, it has been indicated that solute drag (SD) of substitutional alloying element affects deceleration of ferrite growth. In order to understand the effect of SD on the transition, time dependency of Mn concentration profiles at the regions across ferrite/austenite interface during isothermal transformation of Fe-0.12C-2.0Mn (mass%) was measured with sub-nm resolution analysis by means of Cs-STEM and EELS methods. The results show that Mn segregation at the ferrite/austenite interfaces occurs before Mn partitioning begins. It is suggested that the deceleration of interfacial velocity due to SD effect extend duration of the PE mode.

10:30

Carbon and Nitrogen Effects on Austenite Decomposition in a Low-alloyed Steel: *Simon D. Cateau*¹; Julien Teixeira¹; Jacky Dulcy¹; Sabine Denis¹; Moukrane Dehmas¹; Hugo P. Van Landeghem¹; Abdelkrim Redjaïmia¹; Marc Courteaux²; ¹Institut Jean Lamour; ²PSA Peugeot Citroën

The decomposition of carbon and nitrogen enriched austenites during cooling is studied in a low-alloyed steel, by dilatometry, in-situ synchrotron X-ray diffraction (HEXRD) and TEM. Samples were prepared by using a gas-carbonitriding process to obtain different controlled and homogeneous N and/or C concentrations. The newest results concern the effects of nitrogen and C+N on the isothermal transformation kinetics of the austenite. In the ferrite-pearlitic domain, an acceleration of the kinetics is observed whereas in the bainitic domain, the kinetics is slowed down. From the in situ HEXRD, it is shown that during the bainitic transformation (at 400°C) ferrite is formed first and then chromium nitrides (CrN) and cementite precipitate. From the analysis of the austenite lattice parameter evolution and peak profiles, the possible rejection of interstitial elements from the bainitic ferrite into the austenite is discussed. Formation of nanometric CrN in the bainitic ferrite is confirmed by TEM.

10:45

Alloying Effects on Microstructure of Fe-1mass%M Binary Alloys Treated by Nitriding and Quenching Process: *Hironori Kubo*¹; Goro Miyamoto²; Tadashi Furuhashi²; ¹Nisshin Steel Co.; ²Institute for Materials Research, Tohoku Univ.

In order to reduce long treatment time in nitriding and distortion in carburizing, nitriding and quenching (N-Q) process has been developed recently. In this process, surface hardening is achieved by the formation of high nitrogen austenite during nitriding at high temperature and subsequent martensite transformation by quenching. In this study, in order to clarify the influence of alloying elements, microstructure of Fe-1mass%M (M = Mn, Cr, Si) binary alloys and pure iron after N-Q process were investigated. By the addition of 1%Mn, higher hardness and deeper hardened layer (austenite before quenching) were obtained compared with those for the pure iron. The addition of Si increases the hardness with the reduction of the hardened layer thickness, while both of the hardness and thickness are decreased by the addition of Cr. Those alloying effects will be discussed in terms of precipitation of alloy nitrides, variations in nitrogen contents and austenite/ferrite phase stability.

11:00

Microstructure Characterization of a Nitrided Fe-3wt.%Cr-0.3wt.%C Model Alloy by Anomalous Small Angle X-ray Scattering: *Myriam Dumont*¹; Sébastien Jegou²; Laurent Barrallier²; ¹IM2NP-UMR 7334; ²MSMP

Nitriding is a thermo-chemical surface treatment of steels providing an improved fatigue and wear resistance. This treatment is based on nitrogen diffusion involving the precipitation of nano-scaled nitrides from the solid solution at the near surface of the nitrided piece. Nitriding involves a complex microstructural evolution both in time and depth including diffusion of nitrogen and precipitation of nitrides but also coarsening and dissolution of carbides resulting in diffusion of carbon. However the chemical composition of nano-scaled precipitates remains controversial, in particular regarding the iron content in nano-nitrides that may substitute alloying elements. In this framework, anomalous small-angle X-ray scattering was used to bring quantitative data on the distribution and composition of the nano-scaled phases in a Fe-3Cr-0.3C steel as a function of depth.

11:15 Break

Ab-Initio Simulations

MONDAY AM ROOM: ALPINE D-E
SESSION CHAIR: BRENT FULTZ,
CALIFORNIA INSTITUTE OF TECHNOLOGY

10:00 Invited

Ab Initio Description of Finite Temperature Phase Stabilities and Transformations: *Jörg Neugebauer*¹; Albert Glensk¹; Gerard Leyson¹; Fritz Körmann¹; Blazej Grabowski¹; Tilmann Hickel¹; ¹Max-Planck-Institut für Eisenforschung GmbH

The driving force behind phase transformations is the difference in the chemical potentials of the involved phases. Since for most technologically relevant structural materials the chemical potential differences are strongly temperature dependent an accurate treatment of all free energy contributions (vibrational, electronic, magnetic) is crucial. This turns out to be a major hurdle for empirical potentials as well as for ab initio computations. Over the last years we have therefore developed computationally efficient approaches that allow an accurate and fully ab initio based description of all relevant free energy contributions. The power of these approaches will be shown for examples ranging from the design of new high-strength steels, understanding failure mechanisms such as H embrittlement, or to improve ductility of light-weight alloys.

10:30

Ab Initio Description of the Ti bcc to ω Transition at Finite Temperatures: *Dominique Korbmayer*¹; Albert Glensk¹; Blazej Grabowski¹; Tilmann Hickel¹; Jörg Neugebauer¹; ¹Max-Planck-Institut für Eisenforschung

Ti-based alloys are technologically important materials. A detailed knowledge of their phase diagrams and transitions is crucial for optimizing their properties. However, the occurrence of phases that become stable only at high temperatures makes an *ab initio* computation of phase diagrams challenging. We have therefore developed and applied an ab initio methodology that allows to accurately compute free energies of unstable phases. The method employs thermodynamic integration starting from a reference of optimized embedded atom potentials that were fitted to reproduce ab initio molecular dynamics data for a narrow temperature range. We apply our technique to the bcc phase of pure Ti and compute its free energy up to the melting point. We predict a second order phase transformation at around 1000 K. A careful investigation of the trajectories allows us to identify the low temperature phase as the technologically important hexagonal ω structure.

10:45

First-principles Study of Ni Doping Effect on Mechanical Properties of Dilute Fe-Si Alloy: *Ying Chen*¹; Arkapol Saengdeejing¹; Tetsuo Mohri¹; ¹Tohoku University

A drastic change in mechanical properties at Si concentration 5-6wt.% has been intriguing since a long time ago. Our recent DFT calculations re-produced a Si concentration dependence of the elastic properties in dilute Fe-Si alloy, and found a ductile to brittle transition as Si content crosses 4.2wt.%Si. Further calculations combining CVM (Cluster Variation Method) revealed the origin of the sharp change in the mechanical properties in 4.6-5.6wt.%Si region is the interplay between magnetovolume effect and structure ordering of D03 in Fe-Si alloy. Electronic structures analysis revealed that the instability at Fermi Energy results in a degradation of ductility at 4.2wt.%Si. Simulations of Ni-doping into Fe-Si have been performed,

and we found a recovery of elastic properties at critical Si concentration, which is an encouraging experience of tailing band structures intentionally by creating specific atomic configurations which varies bonding states and generates re-distribution of electrons toward enhancing the specific physical property.

11:00 Invited

Spin Wave Method for the Total Energy of the Paramagnetic State: Practical Applications: *Vsevolod Razumovskiy*¹; *Andrei Reyes-Huamantlino*¹; *Andrei Ruban*²; ¹Materials Center Leoben; ²KTH Royal Institute of Technology

The Spin Wave method for the total energy of paramagnetic state represents an alternative to the existing methods for modeling magnetic disorder in Density Functional Theory calculations. One of the main advantages of the method is its applicability to defect calculations in pure metals and alloys. A combination of the SW-method and the supercell approach provides one with a convenient way of ab initio calculations of a number of thermodynamic and kinetic properties using methods based on Hamiltonian formalism like the PAW method as implemented in VASP. The Hamiltonian-based VASP-PAW-SW and Green's function-based EMT0-DLM methods have been used to calculate basic thermodynamic properties of paramagnetic iron and steel (including vacancy formation energy, stacking fault energy, phonon spectra etc.). The accuracy and efficiency of both methods has been assessed by comparing the obtained results to available experimental and theoretical data.

11:30 Break

Atomistic Characterization

MONDAY AM ROOM: CALLAGHAN
SESSION CHAIR: FRÉDÉRIC DANOIX,
CNRS - UNIVERSITÉ DE ROUEN

10:00 Invited

Advanced Characterisation of Precipitates in Strip Cast Steel Alloys: *Nicole Stanford*¹; *Mahendra Ramajayam*¹; *Ross Marceau*; *Thomas Dorin*; *Adam Taylor*; ¹Deakin University

During the strip casting of steels, solidification occurs in a matter of milliseconds, and complete cooling to room temperature is complete in under 1 minute. Consequently, many steel alloys are meta-stable when processed by this method. These super-saturated alloys show unusual nano-scale behaviours such as room temperature clustering, nano-precipitation, and exhibit rather complex phase transformation characteristics during austenite decomposition. This presentation will demonstrate how advanced characterisation techniques such as atom probe tomography and small-angle neutron scattering have enabled better understanding of these phenomena.

10:30 Invited

Atomic-scale Structure and Mechanisms of Phase Transformations of Precipitates in Aluminium Alloys: *Laure Bourgeois*¹; *Nikhil Medhekar*¹; *Julian Rosalie*²; *Zezhong Zhang*¹; *Philip Nakashima*¹; *Andrew Smith*¹; *Matthew Weyland*¹; *Jian-Feng Nie*¹; *Christian Dwyer*³; ¹Monash University; ²National Institute for Materials Science; ³Forschungszentrum Jülich

In precipitate-hardened alloys such as many aluminium alloys, high strength is achieved through the controlled formation of precipitate phases. These precipitates are often metastable phases which grow into high aspect ratio shapes with one or more nanoscale dimensions. Due to the experimental difficulty in characterising such embedded precipitates, much uncertainty remains regarding their bulk and interfacial structures, and consequently, the mechanisms of phase transformations for nucleation and growth. We have used aberration-corrected scanning transmission electron microscopy and first-principles calculations to characterise, at the atomic scale, the bulk and interfacial structures of several precipitate phases in aluminium, such as the classic θ' (Al₃Cu) phase. This has led to surprising findings, including that the interfaces

are not simple combinations of the structures of the bulk phases and do not correspond to the lowest energy states. The determined interfacial structures suggest mechanisms for precipitate growth and for observed behaviours of interfacial segregation.

11:00

The Role of Microscopy in Guiding Materials Simulations:

Towards Designer Structure-Property Relationships: *Simon Ringer*¹; ¹The University of Sydney

Short-range ordering, atomic clustering, segregation and site-occupancy exert a major influence on the phase transformation pathways, and transformation kinetics in many technologically important solid solutions. Therefore, the questions around how these non-periodic arrangements of solute atoms within a parent crystal lattice can be described, measured precisely and, ultimately, 'designed' to understand and create new materials property-performance space, remain of great interest. That is the focus of our recent research, and of this presentation. Firstly, I will discuss our recent theory for short-range order, which provides a framework for describing the atomistic configurations in n-component solid solutions. The characterisation of such materials for the purposes of measuring the atomic configurations will then be discussed, in detail. The challenging issues associated with scattering based approaches using X-rays, neutrons or electrons, will be mentioned and our approaches to addressing these issues using atom probe microscopy will be featured. We have recently modelled the origins of resolution in the atom probe, computed advanced spatial distribution maps, which are analogous to Patterson functions in scattering experiments, and used these new tools to devise an approach for 'lattice rectification'. In bringing us closer to atomic resolution tomography, these techniques are revealing a rich and complex hierarchical architecture of atomic structures within solid solutions, and at microstructural interfaces. This opens new opportunities for computational materials science where the input supercells can be derived directly from experiments. Intersecting atomic resolution microscopy and first principles modelling through density functional approaches has great potential impact in advancing our capacity to understand materials behaviour, conduct materials simulations and to design new materials. Examples that will be highlighted will include the design of new 3rd generation steels with remarkable combinations of high strength and ductility, and materials that exhibit magnetism and superconductivity in the same phase.

11:15

Determination of the Interfacial Atomic Structure of O Phase in Al-Cu-Mg-Ag Alloy and Its Role in O Phase Transformation: *SungJin Kang*¹; *Jian-Min Zhu*²; *Miyoung Kim*¹; ¹Seoul National University; ²University of Illinois

Interface plays a critical role in phase transformation of light alloys involving precipitation, but interfacial atomic structures of precipitates are often undetermined, even for common phases in alloys such as Al-Cu. We solved the interface structure of the O phase in Al-Cu-Mg-Ag alloy by using a combination of 3D atomic-resolution imaging obtained by aberration-corrected scanning transmission electron microscopy (ac-STEM) and spectroscopy. The structure is further refined by density functional theory (DFT) calculations. We discovered that the interface of the O phase is substantially stabilized by ordering of Ag atoms in a hexagonal arrangement within a single atomic layer and Mg atoms located in the middle of the hexagonal Ag atoms. O phase nucleates from a double layered interface, which enables Al₂Cu crystal to be form on (111)Al. This type of phase transformation seems to occur in several Al alloys providing new insight for light alloy design.

11:30 Break

Additive Manufacturing of Metals

MONDAY AM ROOM: NORDIC
SESSION CHAIR: ADAM FARROW,
LOS ALAMOS NATIONAL LABORATORY

10:00 Invited

Rationalization of Microstructural Heterogeneity in Components Produced by Additive Manufacturing and Welding: *Sudarsanam Babu*¹; ¹The University of Tennessee, Knoxville

Mechanical property of welds and additively manufactured components depend on local microstructural gradients. This paper will focus on fundamental aspects of heat and mass transfer, solidification under large (10^3 to 10^5 K/m) thermal gradients and liquid solid-interface velocities (10^{-3} to 1 m/s), as well as, solid-solid transformation during thousands of thermal gyrations. Need for measurement of these phenomena using in-situ and ex-situ characterization tools, as well as, simulation using integrated process modeling will be highlighted. Two examples will be presented. In the first example, competition between dissolution and growth of $M_{23}C_6$ during normalizing, welding and post-weld heat treatment in Cr-Mo steels was described and these changes were correlated to creep-rupture life. In the second example, the macro-scale crystallographic heterogeneity, micro-scale segregation features and nano-scale compositional distribution around age-hardening precipitates in Inconel 718 alloys built by laser additive manufacturing and electron beam powder melting process, were described using integrated process models.

10:30

Characterization of Nickel Based Superalloys Technique of Additive Manufacturing: *Yaakov Idell*¹; *Lyle Levine*¹; *Carelyn Campbell*¹; *Eric Lass*¹; *Li Ma*²; ¹National Institute of Standards and Technology

Additive manufacturing of nickel based superalloys will allow direct production of complex shaped components based on 3-D computer aided drawings. The aerospace industry is interested in exploiting this technology to reduce time and cost for production of complex parts; however, the effects resulting from repeated cycles of rapid heating, melting, cooling, and solidification on the microstructure-property relationships are not well understood. We conducted a study investigating the microstructural evolution processes that occur during direct metal laser sintering of various Ni-based superalloys. Microstructural characterization techniques including scanning and transmission electron microscopy, electron back scattering diffraction, x-ray diffraction, and synchrotron ultra small angle x-ray scattering were used to determine the residual stress distributions, porosity, phase fractions, and compositional differences as functions of varying processing conditions. These results are compared with multicomponent diffusion simulations and FEM simulations that predict the phase fraction, composition, and residual stress as functions of time and temperature

10:45

Maraging Steel Produced by Laser Additive Manufacturing: The influence of Processing Conditions on Precipitation and Austenite Reversion Behaviour: *Eric Jaegle*¹; *Zhendong Sheng*¹; *Pyuck-Pa Choi*¹; *Dierk Raabe*¹; ¹Max-Planck-Institut für Eisenforschung

Materials produced by Laser Additive Manufacturing (LAM) experience a thermal history that is markedly different from that encountered by conventionally produced materials. In particular, a high cooling rate from the melt is combined with cyclical reheating upon deposition of subsequent layers. Using SEM-EDS, EBSD and atom-probe tomography (APT), we investigated how this nonconventional thermal history influences the phase-transformation behaviour of maraging steel (Fe-18Ni-9Co-3.4Mo-1.2Ti) produced by LAM. We compared specimens prepared conventionally, by Selective Laser Melting and by Laser Metal Deposition and found differences in the microsegregation, amount of clustering and retained austenite in the as-produced state. Upon aging, three different types of precipitates, namely (Fe,Ni,Co)₃(Ti,Mo), (Fe,Ni,Co)₃(Mo,Ti), and (Fe,Ni,Co)₂Mo₆, were observed as

well as martensite-to-austenite reversion around regions of the retained austenite. The findings are discussed the light of the different processing conditions.

11:00

Texture Evolution during Laser Direct Metal Deposition of Ti-6Al-4V: *Niyanth Sridharan*¹; Anil Chaudhary²; Sudarsanam Babu¹; ¹University of Tennessee Knoxville; ²Applied Optimization

While the production of near net shapes is achievable in terms of shape, the microstructures obtained via additive manufacturing are not favorable for the full scale production of engineering materials. Titanium alloys are used in a wide variety of high performance applications and hence the processing of the titanium and the resulting microstructures has received significant attention. During additive manufacturing the processing route involves the transition from a liquid to solid state. The addition of successive layers results in a complex microstructure due to solid state transformations. Since phase transformations in titanium alloys occur with specific orientation relationships the texture in titanium alloys is expected to vary with the addition of every new layer. The aim of this work is to investigate the changes in texture and microstructure as a function of the build height and identify conditions to tailor the texture in the manufactured parts.

11:15

Prediction of Phase Transformation During Electron Beam Additive Manufacturing of Inconel 718: *Michael Kirka*¹; Allison Miller²; Grant Helmreich³; Ryan Dehoff; ¹Oak Ridge National Laboratory; ²University of Tennessee; ³University of Tennessee

Metal powder bed additive manufacturing processes such as electron beam melting (EBM) have emerged as industrial viable tools. Unlike traditional manufacturing processes that are understood and yield predictable microstructures, the EBM processes present new challenges in processing science. Through EBM, components are built layer by layer, during which temperatures are maintained at two-thirds or greater of the material's melt temperature throughout a component's build as in the case of Inconel 718, which allows for the precipitation and coarsening of phases as a function of build height. Considered in this work are the influences of EBM build parameters for Inconel 718 that ultimately control the resulting as-built component microstructure. Coupling experimental findings with computational findings obtained from JMatPro, an understanding of the phase transformations that occur during the EBM build process are derived and applied towards the development of optimal process conditions for Inconel 718 EBM components.

11:30 Break

Phase Transformations in Steels: Austenite-Ferrite II

MONDAY AM ROOM: ALPINE A-B-C
SESSION CHAIR: ANNIKA BORGSTAM, KTH

11:45 Invited

The Effect of Alloy Elements Partition on Kinetics of Deformed Austenite Decomposition in Steels: *Zhi-Gang Yang*¹; Chi Zhang¹; Yuan Xia¹; Ze nan Yang¹; ¹Tsinghua University

Due to significant difference between carbon and alloy elements diffusion coefficients, whether the partition of alloy elements during phase transformation happens or not affects the kinetics of austenite decomposition in steel remarkably. Based on the partition local equilibrium (PLE)/negligible partition local equilibrium (NPLE) theory, the formation of pro-eutectoid ferrite from deformed austenite in Fe-C-Mn alloys has been studied in this work. The nucleation rate was calculated with pillbox model on grain boundaries. Under PLE model, the promotion of ferrite nucleation by deformation relates mainly with acceleration of diffusion and increment of grain boundary, whereas under NPLE model, the increase of phase transformation

driving force dominates. The reason of grain refinement of ferrite from deformed austenite is proposed considering the kinetics of nucleation and growth at different temperatures.

12:15

Modelling the Austenite to Ferrite Phase Transformation in Low Carbon Microalloyed Steels in Terms of Grain Size Distributions: Pedro Manuel Garcia-Riesco¹; Pello Uranga¹; *Beatriz López*²; Jose Maria Rodriguez-Ibabe¹; ¹CEIT and TECNUN

In the present paper, a model to predict the ferrite grain size distribution after transformation at continuous cooling conditions in low carbon microalloyed steels is described. The use of grain size distributions instead of mean grain sizes is very interesting to predict mechanical properties, especially toughness, where the coarsest grains play an important role in fracture. The model has been applied to both, recrystallized and deformed austenite microstructures. The model uses the austenite grain size distribution present before transformation as an input and provides the final ferrite grain size distribution. In the case of deformed austenite, the effect of accumulated strain on ferrite grain size has been implemented. For the validation of the model, thermomechanical simulations were carried out by dilatometry tests. In all cases the prior austenite and the resulting ferrite microstructures were characterized. The critical parameters of the grain size distribution model could be identified.

12:30

Microstructure and Hardness Evolution During Simulated Coiling of a Direct Strip Cast Low Carbon Low Niobium Steel: *Thomas Dorin*¹; Adam Taylor¹; Nicole Stanford¹; Peter Hodgson¹; ¹Deakin University

The novel direct strip casting technology involves extremely rapid cooling. Upon cooling, the steel are maintained at a given temperature for coiling. The temperature and duration of coiling strongly affects the final microstructure and mechanical properties of these metals making it necessary to understand and control it. In this work, we study the microstructure evolution of a low-carbon, low-niobium steel for three coiling temperatures, 600°C, 700°C and 850°C. These three temperatures correspond to coiling in the ferrite, during the austenite decomposition and in the austenite. The microstructure evolution is investigated with optical microscopy, SEM and TEM. We show that the coiling temperature strongly affects the final ferrite morphology which ranges from bainite to dendritic and polygonal ferrite. We show that only coiling in the ferrite provides suitable hardening response. We finally discuss the concurrent strengthening contributions of the microstructure and of the fine Niobium-carbo-nitride precipitates that form during coiling.

12:45 Lunch

Atomistic Simulations of Interfaces

MONDAY AM ROOM: ALPINE D-E
SESSION CHAIR: NIKOLAI ZARKEVICH, AMES LABORATORY

11:45 Invited

Structural Phase Transitions in Solid-solid Interfaces and Their Effect on Kinetic Properties: *Timofey Frolov*¹; *Mark Asta*¹; ¹University of California, Berkeley

This talk will review results of recent atomistic computer simulations, investigating the nature of structural phase transitions in metallic grain boundaries, induced by changes in temperature and composition. We focus specifically on grain-boundary phase transitions that involve changes in atomic density in the interface plane, which was discovered using simulation methodologies developed to permit such variations. The nature of grain-boundary phase diagrams associated with these transitions will be discussed, along with the coupling of such structural phase transitions with solute segregation. Finally the impact of these structural phase transitions on interfacial kinetic properties such as grain-boundary diffusion and mobility will be discussed.

12:15

Free Volume of Grain Boundaries and Vacancy Absorption in the Atomic Density Function Model: *Oleksandr Kapikranyan*¹; Helena Zapolsky¹; Christophe Domain²; Renaud Pate¹; Cristelle Pareige¹; Bertrand Radiguet¹; Philippe Pareige¹; ¹GPM, Université de Rouen; ²Département MMC, E.D.F.-R&D

Grain boundaries (GB) control important physical properties in materials. For example, mechanical strength is often determined by grain boundary cohesion; electronic transport can be dominated by boundary scattering; and corrosion often proceeds rapidly along boundaries. Understanding the point-defect absorption and impurity/solute segregation at GBs is the key to the improvement of the existent alloys. The atomic density function (ADF) theory has been recently applied to model the atomic structure of grain boundaries in iron (O.Kapikranyan et al, PRB 89 (2014) 014111). In this paper we propose a new development of the ADF theory to estimate the free (excess) volume of grain boundaries. We show that using this approach the vacancy diffusion and absorption at different tilt angle GBs can be modeled. The results are discussed in respect of the GB free volume and stress field. The perspective of using our model to study the non-equilibrium segregation in steels is discussed.

12:30

An Atomistic Study on the Dynamic Clustering of Helium in Migrating Grain Boundaries of bcc-Fe: *Tegar Wicaksono*¹; Chad Sinclair¹; Matthias Militzer¹; ¹The University of British Columbia

A series of molecular dynamics (MD) simulations was performed to examine the dynamic interaction of helium clusters with grain boundaries in iron. Clustering occurs due to the low solubility of He. The cluster size distribution has been characterized as a function of temperature and He concentration and varies significantly between bulk and grain boundary regions. Clustering was also found to retard the boundary migration, its drag effect being dependent on the cluster size and mobility. When sufficient time was available for clustering, the boundary can be halted before unpinning, leaving behind immobile clusters. On the other hand, the boundary may carry along the solutes as it migrates if helium remains primarily as individual atoms, the migration rate being slower in this case as compared to He-free boundaries. These investigations provide insight that may be used to bridge classical solute drag and particle pinning models.

12:45

Predicting Structure and Energy of Dislocations and Semicohherent Heterophase Interfaces: *Aurélien Vattré*¹; Michael Demkowicz²; ¹CEA, DAM, DIF; ²MIT

Bicrystals containing semicoherent interfaces exhibit distortions produced by the superposition of coherency strains and the elastic strain fields of interface Volterra dislocations. Using an approach that combines the quantized Frank-Bilby equation with anisotropic elasticity theory, this residual elastic state is computed for semicoherent heterophase interfaces formed by face- and body-centered cubic crystals. Elastic distortions are found to be unequally partitioned between the neighboring anisotropic materials. For any given heterophase interface, these distortions determine the coherent reference state within which the Burgers vectors of the interfacial dislocations are defined. The elastic strain energies of interface dislocation arrays are computed using solutions for short-range elastic fields. The mechanical force that occurs when two adjoining regions contain different elastic properties is derived by decreasing the overall stored energy in the system, e.g., during martensitic phase transitions. Examples of applications to semicoherent heterophase interfaces are given.

13:00 Lunch

Transmission Electron Microscopy

MONDAY AM ROOM: CALLAGHAN
SESSION CHAIR: SIMON RINGER,
THE UNIVERSITY OF SYDNEY

11:45 Invited

Direct Observation of Step Nucleation and Motion in Faceted Grain Boundaries at Atomic Resolution: Ulrich Dahmen¹; Abhay Gautam²; *Colin Ophus*³; Frederic Lancon³; ¹LBNL; ²MIT; ³CEA

Using aberration-corrected transmission electron microscopy, we make direct atomic resolution observations of structural events such as step and kink motion in solid interfaces. From extended dynamic time sequences recorded at a rapid rate, atomic relaxations in the interface are measured by automated event detection followed by cumulative averaging of images between events. The approach is illustrated for HRTEM and HAADF images of structural changes that take place in a $90^\circ \langle 110 \rangle$ tilt grain boundary in Au. By splitting a series of images at sudden events such as step motion or fluctuations between structural states of the interface, image blurring due to overlapping structures can be avoided. This makes it possible to analyze the atomic structure of dynamic defects with sufficient accuracy to allow quantitative comparison with atomistic simulations. Our results highlight the importance of surfaces and other defects in the nucleation and motion of steps and kinks in flat interfaces.

12:15 Invited

Movie Mode Dynamic Transmission Electron Microscopy (DTEM): A New Tool for Observing Nanoscale Dynamics in Rapid Phase Transformations: *Thomas LaGrange*¹; ¹Integrated Dynamic Electron Solutions

Transmission electron microscopy (TEM) is an extraordinarily powerful tool for exploring the dynamics of material phase transitions. However, we are typically confined to observe phase transitions under near equilibrium conditions due to the resolution limitations of conventional analytical techniques and we often miss the rapid salient events associated the phase transitions dynamics. Now, with rapid advances in situ and time-resolved TEM (including single-shot Dynamic and femtosecond Ultrafast TEM, DTEM and UTEM), it is possible to directly observe the nucleation and growth dynamics of rapid transitions as they unfold, often under the precise physical conditions of real-world applications. This talk will present the most recent technological developments in DTEM (such as the Movie-Mode DTEM that can capture multiple images in one microsecond), along with examples drawn from materials science, chemistry, and nanoscience illustrating how this new instrumentation opens unique windows onto nanoscale phase transformations and structural dynamics associated with real applications.

12:45

TEM Studies of Structure and Magnetism in Thermally-induced Antiphase Boundary: *Yasukazu Murakami*¹; Koudai Niitsu²; Toshiaki Tanigaki³; Ryosuke Kainuma¹; Hyun Soon Park⁴; Daisuke Shindo¹; ¹Tohoku University; ²RIKEN; ³Hitachi Ltd.; ⁴Dong-A University

Antiphase boundaries (APBs) in ordered alloys/compounds induce material functionalities such as pinning of magnetic domain walls, large critical fields for magnetic saturation, magnetoresistance, etc. These functionalities are due to atomic disordering in the APB region, which deteriorates ferromagnetic spin order. Our transmission electron microscopy studies demonstrated the unusual relationship between APBs and ferromagnetism in the Fe-30at%Al alloy. The thermally-induced APBs showed a finite width (approximately 2 nm) in which significant atomic disordering was observed. Electron holography studies revealed an unexpectedly large magnetic flux density in the APB region, amplified by 60 % (at 293 K) compared with the matrix value. The observations provide renewed insights for materials engineering using thermally-induced APBs.

13:00 Lunch

Microstructure - Property Relationships

MONDAY AM ROOM: NORDIC
SESSION CHAIR: YAAKOV IDELL, NATIONAL
INSTITUTE OF STANDARDS AND TECHNOLOGY

11:45 Invited

Plasticity-enhancement in Ultra-fine Grained Steel by Deformation-induced Twinning and Transformation: *Bruno De Cooman*¹; ¹Pohang University of Science and Technology

A new class of ductile ultra-high strength materials with an ultra-fine microstructure, has been developed. The ductility enhancement is achieved by a combination of the twinning-induced plasticity (TWIP) effect and the transformation-induced plasticity (TRIP) effect, which occur in succession during straining. The application of this "TWIP+TRIP" mechanism to low alloy, ultra-fine grained, multi-phase steel, obtained by inter-critical annealing, is shown to result in an ultra-high strength and a large tensile ductility. In the present contribution, the physical metallurgy of the ductile ultra-high strength TWIP+TRIP steel will be presented. The compositional and microstructural requirements will also be discussed in detail. A model for the strain hardening in TWIP+TRIP steel, based on the dislocation density evolution during straining, will be shown to predict the mechanical properties.

12:15

Effect of Carbon Content on the Mechanical Properties in 0.1C-5Mn Martensitic Steel: *Toshihiro Hanamura*¹; Shiro Torizuka²; ¹National Institute for Materials Science

The effect of carbon on mechanical properties in a 5Mn-2Si steel has been investigated. In general tendency of strength-total elongation balance, when strength increases the total elongation of the identical steel decreases. However, in the martensite structure with different carbon content in 5Mn-2Si composition, when strength increases with increasing carbon content, the corresponding total elongation stays almost constant. The martensite structure of (0.05-0.20C)-5Mn-2Si steel has excellent total balance properties with regard to tensile strength and total elongation, in comparison to other conventional steels. In martensite, it is generally believed that when their strength is high, their ductility is rather poor. In contrast to this, the 5Mn-2Si steel exhibits excellent total balance properties. With increasing the C level farther more, however, the ductility starts to decrease. This change in mechanical properties as a function of carbon content is to be discussed with martensitic steels with the conventional composition of 1.5Mn-0.3Si.

12:30

Study of the Influence of Phase Transformations on Mechanical Properties in a Stabilized Austenitic Stainless Steel (316Nb): William Jolly¹; *Caroline Toffolon-Masclat*¹; Thomas Guilbert¹; Pierre Wident¹; Bernard Marini¹; Lucien Allais¹; François Buy²; Sylvain Ringeval²; Eric Suzon²; François Cortial³; Philippe Petit⁴; ¹CEA-Saclay; ²CEA-Valduc; ³DCNS Research; ⁴Aubert & Duval

Stabilized austenitic stainless steels (316Nb type) are usually used for components exposed to significant thermo-mechanical stresses in corrosive environments, mostly in the chemical, nuclear and oil industries. Different phases can be found in the austenitic matrix: retained δ ferrite, sigma phase, primary and secondary Nb(N,C). Depending on the cooling rate applied after high temperature heat treatment, the microstructure of these steels can evolve leading to a "sigmatization" of the δ ferrite. In the present work, the influence of phase transformations on mechanical properties has been studied by means of microstructural characterization by TEP and microhardness measurements, SEM, TEM and WDS observations, and mechanical testing. At last, the use of CALPHAD tools such as DICTRA and MatCalc, have allowed modelling the phase transformations.

12:45

Transition Carbide Formation in a 0.2C-1.54Mn-1.48Cr-1.30Si (wt. pct.) Quenched and Partitioned Steel: *Daniel Coughlin*¹; Dean Pierce²; John Speer²; Amy Clarke¹; Emmanuel De Moor²; Kester Clarke¹; ¹Los Alamos National Laboratory; ²ASP/PRC, Colorado School of Mines

Understanding the formation of transition carbides and their effect on microstructure and mechanical properties is important for the development of advanced high strength steels. Quenching and partitioning (Q&P) of steels is a process path that can be used to create microstructures with retained austenite for ductility and martensite for strength. Q&P relies on the partitioning of carbon from martensite to austenite, but the formation of η/ϵ carbides consumes carbon that could otherwise be used to stabilize austenite. Advanced microscopy techniques were used to characterize the microstructure and determine the type of transition carbides present. Additionally, differential scanning calorimetry (DSC) was used to analyze phase transitions in the heat-treated material and determine the austenite phase stability. Compositions were selected to analyze the effect of C, Mn, and Ni content on transition carbide formation and austenite phase stability.

13:00 Lunch

Pearlite

MONDAY PM ROOM: ALPINE A-B-C
SESSION CHAIR: ERNST GAMSJÄGER,
MONTANUNIVERSITÄT LEOBEN

14:00 Invited

Pearlite Revisited: *Ingo Steinbach*¹; ¹Ruhr-University

Zener's model of pearlite transformation in steels can be viewed as the prototype of many microstructure evolution models in materials science. It links principles of thermodynamics and kinetics to the scale of the microstructure. In addition it solves a very practical problem: How the hardness of steel is correlated to the conditions of processing. Although the model is well established since the 1950s, quantitative explanation of growth kinetics is still a matter of debate. The presentation will shortly review the classical model of pearlite transformation. Zener's conjecture of maximum entropy production will be annotated by modern theoretical and experimental considerations of a band of stable (sometimes oscillating) states around the state of maximum entropy production. Finally, several mechanisms are investigated quantitatively by phase-field simulations which must be active together to reproduce the observed growth kinetics of pearlite.

14:30

Divergent Pearlite in a Fe-C-Mn-Al Quaternary System: *Maria Martín-Aranda*¹; Shao-Pu Tsai²; Robert E. Hackenberg³; Jonathan Poplawsky⁴; Jer-Ren Yang²; Esteban Urones-Garrote⁵; R. Rementeria¹; Carlos Capdevila¹; ¹CENIM-CSIC; ²Department of Materials Science and Engineering, National Taiwan University; ³Materials Science and Technology Division, Los Alamos National Laboratory; ⁴Oak Ridge National Laboratory; ⁵Centro Nacional de Microscopía Electrónica (CNME), Universidad Complutense de Madrid

The roles of Mn and Al during the isothermal growth of partitioned pearlite under non-steady state conditions are analysed by comparing the phase compositions of austenite, ferrite and cementite ($\gamma+\alpha+M_3C$) within the three phase field in the Fe-C-Mn and Fe-C-Mn-Al systems. The goal is to study the kinetics and thermodynamics when divergent pearlite is obtained in both ternary and quaternary systems. Transmission electron microscopy, energy dispersive X-ray spectroscopy, and atom probe tomography (APT) measurements across the $\gamma/\gamma+\alpha$ and $\gamma/\gamma+M_3C$ interfaces were compared to theoretical values obtained by ThermoCalc software to study the LE conditions across the interfaces at different isothermal decomposition times and to establish whether the pearlite is growing under the Negligible Partitioning Local Equilibrium (NPLE) or the Partitioning Local Equilibrium (PLE) modes for both Mn and Al alloying elements. APT was conducted at the Center for Nanophase Material Science, which is a DOE Office of Science User Facility.

14:45

Elastic Strain Generated by Pearlitic Transformation: *Nobuo Nakada*¹; Norimitsu Koga²; Toshihiro Tsuchiyama¹; Setsuo Takaki¹; ¹Kyushu University; ²Yokohama National University

Pearlite is the diffusional transformation product formed via eutectoid transformation in steel and has a two-phased fine lamellar structure composed of ferrite and cementite. G.J. Shiflet et al. reported that lattice misfit between both phases is so significant that interfacial structures, i.e. microscopic steps and misfit dislocations, are introduced at the lamellar interfaces during pearlitic transformation. However, the microstructural characterization by XRD and TEM reveals that the misfit strain does not seem to be completely accommodated by the interfacial structures, and thus mostly remains as elastic strain in pearlite, leading to an obvious crystal rotation. In addition, EBSD/Wilkinson method, which is able to map the distribution of local elastic and plastic strains separately, shows that each pearlite colony has a different anisotropic elastic strain field. As a result, it is thought that the formation of pearlite colony contributes to uniform the transformation elastic strain in pearlite.

15:00

Cementation Assisted by Electric Current: *Patrice Chantrenne*¹; Damien Fabrégue²; Michel Perez²; ¹INSA Lyon

To study the influence of the current on the diffusion of interstitials, an ARMCO iron sample is placed between the two graphite punches of a Spark Plasma Sintering facility. The current between the punches is managed to regulate the temperature of the sample. Above 910°C, the ferrite transforms into austenite and carbon only diffuses into austenite. Below 910 °C, carbon diffuses in ferrite which promotes austenite. The microstructure of the sample is analyzed and micro-hardness is measured along the diffusion direction. Results are compared to carbon concentration predicted thanks to a model taking into account of the Fick's law, the solid phase change and the influence of the electric field. The latter phenomenon shifts the carbon atoms. Comparison between experiments and simulations is used to identify the carbon drift velocity. It is thus possible to get a better insight on the phenomena taking place in a SPS device.

15:15 Break

Interfaces

MONDAY PM ROOM: ALPINE D-E
SESSION CHAIR: JEFFREY HOYT,
MCMASTER UNIVERSITY

14:00 Invited

Grain Boundary Metastability and Its Implications for Grain Boundary Kinetics: *Jian Han*¹; David Srolovitz¹; Vaclav Vitek¹; ¹University of Pennsylvania

Many polycrystal properties are understood in terms of the structure and energetics of its constituent grain boundaries (GBs). These are usually described in terms of a single GB structure. In this work, we demonstrate that most grain boundaries have a very large multiplicity of structures of very similar energy and that during kinetic process GBs commonly explore many of these. We first examine the extent of this multiplicity in several materials and characterize it in terms of a GB configurational entropy. Next, we provide examples of how this multiplicity affects structural relaxation at grain boundaries and its role in determining GB efficacy as a point-defect sink. We predict the dependence of these properties on macroscopic GB structural properties and confirm the prediction via comparison with experiment and simulations.

14:30

Lattice Coupled Grain Growth with Low-angle Grain Boundaries: *Kevin McReynolds*¹; Kuo-An Wu²; Peter Voorhees¹; ¹Northwestern University; ²National Tsing Hua University

Grain growth is generally driven to minimize the interfacial energy. However, for low-angle grain boundaries the requirement that lattice planes be continuous across the boundary gives rise to a coupling between the normal motion of the grain boundary and the tangential motion of the lattice. We show through simulations using the phase-field crystal model, that for a circular grain embedded at a symmetric planar tilt grain boundary this coupling gives rise to a rigid body translation of the lattice as the grain shrinks. The process is mediated by significant climb of the dislocations in the boundary in a mechanism that involves bulk diffusion of vacancies from the trailing edge to the leading edge of the crystal. The implications of these results on the motion of partially coherent two-phase interfaces will be discussed.

14:45

Molecular Dynamics Study of the Migration Kinetics of Asymmetric Grain Boundaries: *Sherri Hadjani*¹; Blazej Grabowski¹; Christopher Race²; Jörg Neugebauer¹; ¹Max-Planck-Institut für Eisen Forschung; ²The University of Manchester

Classical molecular dynamics (MD) simulations are commonly used to explore the migration of grain boundaries. Our previous research on low sigma symmetric boundaries has shown that at conditions of low driving forces as found in actual experimental setups and when going towards system sizes exceeding those commonly employed in MD a novel mechanism becomes operational that is based on mesoscopic island nucleation. In the present study we extend our research towards grain boundaries deviating from the perfect and symmetric arrangement to investigate the kinetics of asymmetric, defective boundaries. Such grain boundaries constitute in fact the majority of experimentally observed moving boundaries. We introduce defects by deviating the boundary plane from a symmetric equilibrium boundary. The results of the simulations show how the fundamental atomistic mechanisms change as the nucleation driven motion shifts towards a step propagating one.

15:00

Multi-scale Quantum Mechanical Calculations of Solute-grain Boundary Interaction: *Liam Huber*¹; Blazej Grabowski²; Matthias Militzer¹; Jörg Neugebauer²; Jörg Rottler¹; ¹University of British Columbia; ²Max-Planck-Institut für Eisenforschung

Solutes at interfaces significantly affect phase transformation and grain growth kinetics, but density functional theory (DFT) treatment is restricted to special high-symmetry interfaces. To maintain quantum mechanical (QM) accuracy near solutes and facilitate general interfaces, we propose QM/molecular mechanical (MM) coupling. We perform this coupling by decomposing the system into a small QM region and a much larger MM region, which are elastically coupled. Since most DFT codes for metals use a plane wave basis set with periodic boundary conditions, isolation of the QM region using vacuum clusters creates deeply penetrating electronic perturbations. Thus, we introduce new "filler" atoms, replacing the vacuum surface with a less severe interface. We study the binding of solutes to a high symmetry grain boundary (GB) in Al which can be validated against periodic DFT calculations, allowing critical evaluation of errors. We then apply the method to solutes at a general GB, beyond DFT's reach.

15:15 Break

Microstructure Characterization in Steels

MONDAY PM ROOM: CALLAGHAN
SESSION CHAIR: LAURE BOURGEOIS,
MONASH UNIVERSITY

14:00 Invited

Crystallographic Analysis of Martensite and Bainite Structures by SEM / EBSD Method: *Goro Miyamoto*¹; Tadashi Furuhashi¹; ¹Tohoku University

There has been increasing attention to martensite and bainite structures in high strength steels. It is well known that martensite and bainitic ferrite (BF) hold a near K-S orientation relationship (OR) with parent austenite and 24 variants can be formed in a single austenite grain. Since inter-variant boundaries act as obstacles against deformation and fracture, understanding of crystallography of those microstructures is essential. The present authors have recently developed a novel method to quantify OR precisely even with no retained austenite. ORs of martensite and BF were found to deviate from the exact K-S/N-W ORs and the deviation increases at higher Ms and bainite transformation temperatures. Furthermore, variant analyses revealed that specific low-angle variants belonging to the same Bain group are paired in bainite structure formed at high temperature or low carbon martensite while twin-related variant pairs become more dominant in bainite at lower temperature and in higher carbon martensite.

14:30

Effect of Lamellar Orientation on the Plastic Deformation Behavior of Pearlitic Steel: *Toshihiko Teshima*¹; Makoto Kosaka¹; Nobuo Nakada²; ¹Nippon Steel & Sumitomo Metal Corporation; ²Kyushu University

Pearlitic steel has a hierarchical microstructures, consisting of pearlite colonies in which the orientation of lamellar structure is almost identical, and pearlite blocks in which the crystal orientation of ferrite is nearly the same. This complicated microstructures make it difficult to analyze the deformation process of the pearlitic steels, thus the role of each microstructure on plastic deformation has not been fully understood. In this study, we have investigated the local strain distribution along with the deformation behavior at the early stage of plastic deformation. The local strain distribution was measured by DIC (digital image correlation) method, and corresponding microstructures were analyzed with SEM-EBSD technique. It has been found that the identical local strains were confined within single colonies, and larger strains are generated at a colony, where the Schmidt factor of its ferrite is large and its lamellar orientation is close to 45 degrees to the tensile axis.

14:45

Study of Carbide Precipitation During Tempering of Martensite in Fe-Cr-C Alloys: *Ziyong Hou*¹; Peter Hedström¹; Di Wu²; Joakim Odqvist¹; ¹KTH Royal Institute of Technology; ²Northeastern University

Precipitation hardening is one of most effective strengthening mechanisms in steels, and much research has been performed in the past. However, predictive modeling of precipitation is still a challenge and in the present work, precipitation of carbides after tempering of martensitic Fe-Cr-C alloys up to 1000h has been investigated. Experimental measurements using electron microscopy and modeling using a Langer-Schwartz approach has been conducted. The importance of a proper definition of the initial microstructure for predictive modeling is discussed.

15:00

Coupled APT, EBSD, FIB and NanoSIMS Techniques for Investigation of Boron Segregation in Steel: *Claire Debreaux*¹; Frédéric Danoix¹; Didier Blavette¹; Laurence Chevalier¹; David Gibouin²; Thomas Sourmail³; Nathalie Gey⁴; Fabien Cuvilly¹; ¹GPM CNRS - UMR 6634; ²GPM CNRS - UMR 6634 and AMMIS - MERCI EA3829; ³Asco Industries CREAS; ⁴LEM3 CNRS - UMR 7239

Atom Probe Tomography is a key approach to investigate phase transformation and interfacial segregation at the nanometer scale. In this presentation, a correlative

microscopy approach is used to investigate boron segregation at prior austenite grain boundaries (PAGB) in martensitic steels. It is difficult to analyze PAGB because of the large size of grains (30-100 μ m) compared to the analyzed volume (50x50x200 nm³). Therefore, EBSD were used to locate the PAGB in the martensitic microstructure, in order to place it at the atom probe specimen apex by FIB lift-out. NanoSIMS was used to get an overall picture of the element in material. Using this combined approach, it was possible to analyze the region of interest and to get information on segregation. The influence of experimental condition, including the orientation of PAGB in specimen with respect to the analysis direction, will be investigated, and their consequences on the quantitativity of APT results discussed.

15:15 Break

Non-Ferrous Alloys

MONDAY PM ROOM: NORDIC
SESSION CHAIR: MICHAEL KIRKA,
OAK RIDGE NATIONAL LABORATORY

14:00 Invited

Looking Forward: Solid-state Phase Transformations in Flat-rolled Aluminum Products: *Babak Raeisinia*¹; Cyrille Bezencon²; Vahid Fallah³; Shahrzad Esmaili³; Simon Barker¹; ¹Novelis Global R&T Center; ²Novelis Switzerland SA; ³The University of Waterloo

Hillert's (1980) vision in comparing thermodynamics simulations to the game of chess has pretty much become a reality within the aluminum industry in that the 'game of thermodynamics' is indeed played regularly across different product lines. This has been made possible with the advent of different software packages that allow fundamental thermodynamics principles to be readily accessed and utilized in industry. Opportunities for improvement do, however, exist. In this work, we look at flat-rolled aluminum alloys and underscore areas where better understanding and prediction capability of solid-state phase transformations are necessary. In particular, we focus on precipitation in the Al-Mg-Si alloy system. First, HRTEM and 3-D phase-field-crystal (PFC) modeling studies of early-stage solute-cluster formation in this alloy system are discussed. Next, the issue of quench-rate sensitivity is examined and discrepancies between thermo-kinetic simulation predictions and experimental observations are highlighted.

14:30

Prediction of Quenching-Induced Residual Stress Distributions in 7XXX Aluminum Alloy Thick Plates using Gleeble Interrupted Quench Tests: *Nicolas Chobaut*¹; Denis Carron²; Patrick Schloth³; Sylvie Arsene⁴; Jean-Marie Drezet¹; ¹Ecole Polytechnique Fédérale de Lausanne; ²Université de Bretagne-Sud; ³Paul Scherrer Institut / Ecole Polytechnique Fédérale de Lausanne; ⁴Constellium Technology Center

In the fabrication of heat treatable aluminum parts for the aeronautic industry, quenching is a key step to obtain the required mechanical characteristics after ageing. For thick plates, thermal gradients cause non-homogeneous plastic strain resulting in residual stresses (RS) after quenching. In 7xxx alloy, precipitation phenomena may affect these RS. Quenching RS are extensively reduced by stress relief. However, RS at final temper could lead to some distortions during machining of large and complex parts. For their prediction, it is thus important to be able to model the full process and particularly the quenching. In this work a simple but realistic approach is presented to predict as-quenched RS. Instead of modelling precipitation, yield strength is characterized with a few Gleeble interrupted quench tests. The results are introduced in a finite element model and predictions are compared to residual stress measurements in plates of different thicknesses for two different 7xxx alloys.

14:45

Solid-Solid Phase Transformations During Casting of Plutonium: *Adam Farrow*¹; Jeremy Mitchell¹; Terence Mitchell¹; Deniece Korzekwa¹; Tarik Saleh¹; Cameron Knapp¹; ¹Los Alamos National Laboratory

Plutonium possesses six solid allotropes, displaying a wide range of unusual behaviors. Large volume changes, negative thermal expansion in some phases, and an assortment of low-symmetry crystal structures yield a wide variety of behaviors during cooling from high temperatures. Density changes approximately 20% from the lowest density phases to the highest, resulting in significant deformations in the part. A majority of this deformation involves orthorhombic or 2 different monoclinic crystal structures, resulting in the largest deformations in the phases least able to deform without cracking. This talk will address fundamentals related to the thermodynamics and mechanisms of transformations in this material, focusing on the relationships between homologous temperatures in allotropic materials, deformation mechanisms, phase transformation mechanisms, and microstructural changes due to annealing during casting. Control of microstructures to suppress cracking via process control will be related to these fundamentals.

15:00

Effect of Heating Rate on the Phase Transformation of Zirconium Alloys in Design Basis Accidents: *Toan Nguyen*¹; Javier Romero²; Antoine Ambard³; Michael Preuss¹; João Quinta da Fonseca¹; ¹The University of Manchester; ²Westinghouse Electric Company; ³Électricité de France R&D

The effect of heating rate on the phase transition temperature and phase fraction evolution was studied in two industrial Zr alloys: recrystallized ZIRLO[®] and cold-worked Zircaloy-4. An electro-thermal-mechanical tester was used to heat the materials at rates similar to the rates experienced during in loss-of-coolant accidents (LOCA) in nuclear fuel assemblies. The aim was to determine how these fast rates affect the kinetics of the transformation and the final texture of the different materials, which is relevant to material degradation during LOCA. By using electrical resistivity measurement and post-mortem microstructure analysis, it was found that fast heating, in the range of 10-100°Cs⁻¹, increases transition temperature and lowers β -fraction at a given temperature. After a complete $\alpha \rightarrow \beta \rightarrow \alpha$ thermal cycle, the strong starting texture of the materials is less pronounced but the alloys show different final texture components. A possible mechanism relating this change to different initial grain sizes is discussed.

15:15 Break

Bainite

MONDAY PM ROOM: ALPINE A-B-C
SESSION CHAIR: KESTER CLARKE,
LOS ALAMOS NATIONAL LABORATORY

15:30 Invited

Certain Aspects of the Bainitic Transformation in Steel: *Annika Borgenstam*¹; ¹KTH, Royal Institute of Technology

A review of certain aspects of the bainitic transformation in steel based on the diffusional theory will here be given. Underlying thermodynamics, kinetics as well as microstructure evolution will be reviewed including the effect of temperature and alloy composition. The thermodynamic barrier needed and its physical nature will be discussed together with modelling and experimental measurements of growth rates of acicular ferrite, the change in morphology with temperature and composition both with respect to ferrite and cementite, the transition between upper and lower bainite and the fact that bainite can form below Ms. The effect of the symmetry in the Fe-C phase diagram will also be considered.

16:00

Investigation of Bainite Formation in a Chemically Inhomogeneous Medium Carbon Spring Steel: *Constantinos Goulas*¹; Pina Mecozzi¹; Jilt Sietsma²; ¹Materials innovation institute (M2I)/ Delft University of Technology; ²Delft University of Technology

The effect of chemical inhomogeneity on the isothermal bainite formation is investigated in medium carbon low silicon spring steel by dilatometry and microscopy. The analysis of the microstructure at different times during transformation shows that chemical segregation of substitutional alloying elements resulting from casting strongly affects the bainite formation by retarding the transformation kinetics and limiting the maximum achievable bainite fraction. The effect of prior austenite grain size and Cr-rich carbide precipitation in the segregation bands is investigated and compared with the findings in homogenized material. A physically based model is used to simulate bainite formation and the mechanism of nucleation and growth is discussed. The calculated difference in nucleation rates between the enriched and the depleted areas is not by itself sufficient to explain the microstructures obtained and thus significant influence of growth on bainite formation is observed, which indicates that a diffusional transformation mechanism is taking place.

16:15

Role of Cementite in the Formation of Bainite in 0.3 mass% C Steels: *Jiaqing Yin*¹; Mats Hillert¹; Annika Borgenstam¹; ¹KTH Royal Institute of Technology

The role of cementite on the transformation of austenite to bainite has been studied in three 0.3 mass% C steels, with 0.5 mass% Si, 0.5 mass% Mn and both 0.5 mass% Si and 0.5 mass% Mn, respectively. Samples have been isothermally heat treated from the eutectoid temperature down to below the martensite start (Ms) temperatures and characterized using Light Optical Microscopy and Scanning Electron Microscopy. The cementite formation during the bainitic transformation has been followed and the influence of cementite on the evolution of the bainitic morphology and on the growth rate of acicular ferrite is discussed. Attention has also been paid to the role of cementite on the transition from upper to lower of bainite.

16:30

Ultrafast Granularization of Lath-like Bainite in FeNiC Alloys During Isothermal Holding: *Meriem Ben Haj Slama*¹; Sébastien Allain²; Nathalie Gey³; Lionel Germain³; Kangying Zhu⁴; ¹JJL/LEM³; ²JL; ³LEM³; ⁴ArcelorMittal Reseach Center/Maizières_lès_Metz

Evidences of a fast and unexpected lath-like bainite «granularisation» during isothermal holdings will be reported. The phenomenon is characterized by improved angular resolution EBSD and TEM, and is observed in a Fe5Ni0.13C alloy transformed at 380°C (above Ms) after an austenitic soaking. The granularisation process starts once the initial lath bainitic transformation is over (lower and upper bainites) after 1 min and is characterized by an evolution of the ferrite matrix morphology and microtexture and by a carbide ripening process. During subsequent holdings (typically 30 min), variant coalesced zones develop and rapidly grow within packets, at the expense of highly misoriented laths (60°). The resultant low misorientation angle boundaries then progressively recover and carbide films precipitate on former packet boundaries. This explains the mechanical properties decrease. The associated driving forces will be discussed. This tempering mechanism occurring with slower kinetics in more conventional FeNiMnC alloys could contribute to bainite classification.

16:45 Break

Bridging from Atomistic Simulations

MONDAY PM ROOM: ALPINE D-E
SESSION CHAIR: MARK ASTA,
UNIVERSITY OF CALIFORNIA, BERKELEY

15:30 Invited

Atomistic and Continuum Modeling of Diffusion Controlled Growth of Facetted Interfaces: Peyman Sadiq¹; Jeffrey Hoyt¹; ¹McMaster University

The kinetics of many solid-solid and solid-liquid phase transformations are governed by the diffusion controlled lateral motion of steps along a facetted interface. Despite the importance of the step flow mechanism the velocity of facetted interfaces is not completely understood. In this work we employ the boundary element method to model the composition profile and velocity of an infinite periodic array of steps along a solid-liquid interface and assume that, due to convection, a boundary layer of a specified thickness exists at the interface. In addition, a multiple scale analysis is utilized to derive an analytic expression for the growth of a stepped interface in the case of a solid-solid interface where no convection is present. Finally, the continuum results are compared to molecular dynamics simulations of facetted Si 111 growth in Al-Si liquid alloys and the transition from attachment controlled to diffusion controlled growth is discussed.

16:00

C2-NEB: The Nudged Elastic Band Method with Two Climbing Images, Validated on the Martensitic Transformation in NiTi Shape Memory Alloy: Nikolai Zarkevich¹; Duane Johnson¹; ¹Ames Laboratory

The nudged-elastic band (NEB) method is modified with concomitant two climbing images (C2-NEB) to find a transition state (TS) in complex energy landscapes, such as those with serpentine minimal energy path (MEP). If a single climbing image (C1-NEB) successfully finds the TS, C2-NEB finds it with higher stability and accuracy. However, C2-NEB is suitable for more complex cases, where C1-NEB misses the TS because the MEP and NEB directions near the saddle point are different. Generally, C2-NEB not only finds the TS but guarantees that the climbing images approach it from the opposite sides along the MEP, and it estimates accuracy from the three images: the highest-energy one and its climbing neighbors. C2-NEB is suitable for fixed-cell NEB and the generalized solid-state NEB (SS-NEB). We validate the C2-NEB method on the solid-solid phase transformations in NiTi, and find agreement with experiment.

16:15 Invited

From Nanosecond to Second: Bridging the Time Gap in the Atomistic Dynamics of Complex Materials with the Kinetic Activation-relaxation Technique: Normand Mousseau¹; Laurent Béland²; Peter Brommer³; Fadwa El-Mellouhi⁴; Jean-François Joly⁵; Gawonou N'Tsounglo¹; Oscar Restrepo⁶; Mickaël Trochet¹; ¹Université de Montréal; ²Oak Ridge National Laboratory; ³University of Warwick; ⁴Qatar Environment and Energy Research Institute; ⁵Carleton University; ⁶Texas A&M University at Qatar

Understanding atomistic diffusion and relaxation mechanisms remains one of the main challenges of materials science. How can we follow the microscopic motion of atoms on time scales relevant to describe aging, crack propagation and self-assembly? With the advent of faster computers and the development of a new class of algorithms, we are now starting to bridge this time gap in complex materials, opening the door to the numerical study of crucial, but long neglected problems. In this talk, I will present the kinetic Activation-relaxation Technique (k-ART), an off-lattice kinetic Monte Carlo algorithm with on-the-fly catalog building, a method able to follow atomistic kinetic of alloys, defective and disordered materials over more than 10 decades in time, reaching the second time scale and more. I will show recent applications to carbon diffusion in iron, relaxation of ion bombarded silicon, defect diffusion in amorphous materials and more.

16:45 Break

In-situ Techniques I

MONDAY PM ROOM: CALLAGHAN
SESSION CHAIR: NICOLE STANFORD,
DEAKIN UNIVERSITY

15:30 Invited

Stabilization of bcc Fe by Magnon-phonon Interactions: Brent Fultz²; Lisa Mauger¹; Fritz Körmann²; Blazej Grabowski²; Matthew Lucas¹; Jorge Munoz¹; Sally Tracy¹; Biswanath Dutta²; Tilmann Hickel²; Jörg Neugebauer²; ¹California Institute of Technology; ²Max-Planck-Institut für Eisenforschung

Phonon densities of states (DOS) were measured for bcc ⁵⁷Fe between 300 K and 1184 K using nuclear resonant inelastic x-ray scattering. All phonons shifted to lower frequencies with temperature, but the low transverse modes shifted especially rapidly above 700 K, showing an unusual nonharmonic behavior that followed the thermal trend of the magnetic entropy. This excess phonon shift made a contribution of 35 meV/atom to the free energy at 1100 K. A new ab-initio approach for quantitatively assessing effects of magnon-phonon interactions and lattice expansion showed that for some phonon branches, the magnon-phonon interaction is an order of magnitude larger than the phonon shift due to thermal expansion or anharmonicity. The magnon-phonon interaction makes a surprisingly important contribution to the thermodynamic stability of bcc Fe.

16:00

Differential Scanning Calorimetry as a Powerful Tool for Investigation of Solid-Solid Phase Transformations in Heating, Isothermal Annealing and Cooling: Benjamin Milkereit¹; Marco Starink²; Olaf Keßler¹; Christoph Schick¹; ¹University of Rostock; ²University of Southampton

During the recent years, we developed advanced techniques to analyze solid-solid phase transformation by Differential Scanning Calorimetry (DSC) in a very wide dynamic range. Our lab today covers the entire heating and cooling rate range of technical but also physical interest - up to eight orders of magnitude for inorganic materials (0.0001 K/s - 10,000 K/s). This talk will introduce these techniques, using reactions in aluminium alloys as examples. DSC allows to quantify characteristic temperatures and times and moreover the measured enthalpy change gives a direct link to the kinetics and thermodynamics of the phase transformations. Modelling the enthalpy change enables to determine solute content, possible supersaturation- and also precipitation-amount. Applying these methods it is possible to record time temperature transformation diagrams for various materials during heating, isothermal annealing and even during continuous cooling, making DSC to a very powerful tool for the investigation of solid-solid phase transformations.

16:15

Control of Phase Transformation During Heat Treatments Based on DSC Experiments: Philipp Schumacher¹; Stefan Pogatscher²; Olaf Keßler¹; Marco Starink³; Christoph Schick¹; Volker Mohles⁴; Benjamin Milkereit¹; ¹University of Rostock; ²ETH Zurich; ³University of Southampton; ⁴RWTH Aachen University

Phase transformation in Al-Si alloys during cooling from solution annealing was investigated with advanced DSC techniques in a wide cooling rate range (2 K/s-0.0001 K/s). Microstructural analyses show that quench-induced Si particles of different shape and size can precipitate. The dependence of formation enthalpy on cooling rate and temperature is modelled, providing a consistent physical description of precipitate volume fraction and solute Si amount during cooling. This allows control of phase transformation via precise heat treatments and thus allows generation of well-defined microstructural states. Thereby, samples having an equal amount of solute Si but different precipitation states could be tested in order to investigate the influence of different precipitate types on

the mechanical behaviour. A big advantage of this method is that the strengthening contribution of precipitates can be determined without the need to assume any - potentially inaccurate - superposition law between particle and solute strengthening.

16:30

Rotation of Single Crystal Cu Nanopillar Revealed by In Situ Electron Diffraction: Yang Hu¹; Jian-Min Zuo²; ¹University of Illinois at Urbana-Champaign

The crystal rotation and slip behavior during compression in bulk samples are well-described by Taylor rotation model and Schmid's law. However, when sample sizes are reduced to the micron or nano scale, whether the classical geometrical model could be applied is still under debate. In this study, in-situ electron diffraction experiment is performed in a transmission electron microscope to study the crystal rotation in Cu single crystal nanopillar under compression. The evolution of diffraction pattern is used to track the crystal rotation behavior and to predict the primary and critical slip systems by using Quantitative Electron Diffraction software to fit diffraction patterns. Results show that Cu single crystal rotates during compression. It first undergoes double slip on the geometrically predicted slip system, followed by single slip behavior. These detailed information are helpful to understand the deformation behavior of nanopillars under compression.

16:45 Break

TRIP Materials

MONDAY PM ROOM: NORDIC
SESSION CHAIR: SUDARSANAM BABU,
THE UNIVERSITY OF TENNESSEE, KNOXVILLE

15:30 Invited

Development of "Steels Like" Titanium Alloys Combining High Strength, High Strain Hardening and Improved Ductility: Cedrik Brosek¹; Fan Sun¹; Matthieu Marteleur²; Thierry Gloriant³; Philippe Vermaut¹; Pascal Jacques²; Frédéric Prima²; ¹Chimie ParisTech; ²Université catholique de Louvain; ³Institut des Sciences Chimiques de Rennes

Titanium alloys are attractive for industrial applications, due to their remarkable strength/density ratio and corrosion resistance. However, major drawbacks arising from low ductility (typically <20%) and a lack of strain hardening, are still limiting their potential in advanced applications when compared to steels. This work aims at designing a new family of Ti-Cr and Ti-V titanium alloys with improved mechanical properties. These alloys show an extremely high ductility (45% of plastic deformation) accompanied by both a high strength and a very high work hardening rate. Extensive microstructural characterization revealed a complex sequence of deformation mechanisms consisting in activation of intense mechanical twinning accompanied by α' stress induced precipitations. In this talk, design strategy and chronology of deformation mechanisms will be highlighted in order to understand the improvement of the work hardening. Future directions towards the development of a new family of metallic materials will be discussed.

16:00

The Interaction of Martensitic Phase Transformations in MMC Based on TRIP-steel with Zirconia Particle Reinforcement: Harry Berek¹; Christian Weigelt¹; Christos Aneziris¹; ¹TU Bergakademie Freiberg

A new class of metal-matrix composites (MMC) consists of austenitic steel showing transformation induced plasticity (TRIP) and magnesia partially stabilized zirconia (Mg-PSZ). Both components exhibit martensitic phase transformations during deformation, thus generating the potential for improved mechanical properties. The MMC can be produced in the form of cellular materials as foams and honeycombs. They enable different light weight applications. This paper deals with the interdependency of the martensitic phase transformations within steel and zirconia during deformation. Investigations based on in situ X-ray computed tomography (XCT) are described. Local phase analysis was performed by electron backscatter

diffraction (EBSD). A correlation between the degree of local deformation and the local martensitic phase transformation was found within the ceramic reinforcement. There are maxima of deformation and martensite formation within the steel at steel-ceramic-boundaries. Nevertheless the transformation of the steel starts at a higher deformation level in comparison to the ceramic.

16:15 Invited

Metastability of Austenite in High Strength Steels Associated with TRIP Effect: *Xuejun Jin*¹; ¹Shanghai Jiao Tong University

Economically manufactured Advanced High Strength Steels (AHSS) are increasingly demanding to satisfy the requirements of better structure materials for comfortable life and sustainable development. "Third Generation" of AHSS shows strength-ductility combinations significantly better than showed by the first generation AHSS (ferrite-based microstructure) but at a cost distinctively less than required for second generation AHSS (austenite-based microstructure). Considerable amount of austenite is attained through the combination of delicate composition design and sophisticated process control, which gives rise to a better mechanical performance assisted by transformation induced plasticity effect. Here, metastability of austenite is evaluated and discussed with respect to external loading or temperature change. Factors such as heterogeneous composition, grain size and surrounding constrains controlling the metastability of austenite have been studied in Quenching-Partitioning treated steels, Medium-Mn steels and Trip dual phase stainless steels. A few models are compared and applied to evaluate metastability of these newly developed AHSS.

16:45 Break

Plenary 2

MONDAY PM ROOM: EMERALD BALLROOM
SESSION CHAIR: HATEM ZUROB,
MCMASTER

17:00 Plenary

Importance of Phase Transformations in Development of Modern High Strength Steels: *Tadashi Furuhashi*¹; ¹Tohoku University

Fundamental and applied research in structural steels attracts much attentions recently. In development of modern high strength steels, importance of strength and ductility/toughness balance is increasing and more advanced and sophisticated controls of microstructure formed during phase transformations are utilized particularly. In the presentation, two major topics in high-strength low-alloy steels are discussed; 1) nano-sized precipitation of alloy carbide accompanied during ferrite transformation, i.e., interphase precipitation, which establishes high yield strength, moderate work-hardening and high local elongation in low-carbon ferritic sheet steels, and 2) substructure and transformation kinetics of bainite which should contribute to improvement of toughness of plate steels. In such design of microstructure, importance of various aspects in phase transformations, i.e., thermodynamics, kinetics and crystallography, will be emphasized.

Plenary 3

TUESDAY AM ROOM: EMERALD BALLROOM
SESSION CHAIR: GARY PURDY,
MCMMASTER UNIVERSITY

08:30 Plenary

The Dominant Role of Interface Composition on the Austenite-ferrite Transformation Behaviour at High and Low Temperatures: *Sybrand van der Zwaag*¹;
¹Technical University Delft

The kinetics of the austenite decomposition even in lean steels has been studied for many years as it is surprisingly difficult to construct a consistent model which takes into account the effects of the change in crystal structure and more importantly the effects of element partitioning at the moving austenite-ferrite and the austenite-bainite interface. Existing models make different assumptions regarding the degree of element partitioning but are equally capable of describing the experimental data for simple linear cooling. At Delft we developed the cyclic partial transformation concept to magnify the effect of the solute partitioning and to discriminate between various models. Extension of the concept to the austenite-bainite transformation confirmed the role the partitioning of the substitutional elements to the interface also for this transformation. A Gibbs-Energy-Balance model is proposed which applies to both types of transformation.

09:30 Break

Precipitation Under Non-Equilibrium Conditions

TUESDAY AM ROOM: ALPINE A-B-C
SESSION CHAIR: HÉLIO GOLDENSTEIN,
UNIVERSITY OF SAO PAULO

09:45 Invited

Possibility of Auto-tempering in Martensitic Steels Containing Carbon: *Setsuo Takaki*¹; Daichi Akama¹; Nobuo Nakada¹; Toshihiro Tsuchiyama¹; Masahiro Murakami²; Kengo Iwanaga²; ¹Kyushu University; ²NETUREN Co., Ltd.

Martensitic steels containing carbon are characterized by their high tensile strength and the solid solution strengthening by super saturated carbon has been believed to be the dominant strengthening mechanisms. However, it was pointed out recently that carbon does not exist in solid solution in martensite matrix but may precipitate as nano-sized carbide on cooling after martensitic transformation (Auto-tempering). In this study, X-ray diffraction analysis revealed that the lattice structure of as quenched martensite is not bcc but bcc independent of carbon content in the range C<0.5% at least. In addition, the theoretical analysis on the strengthening mechanism indicated the fact that the strength of as quenched martensite can be reasonably explained by the mechanism of particle dispersion strengthening based on the particle cutting model. As a result, it was confirmed that auto-tempering cannot be avoided in conventional martensitic steels under the engineering cooling condition at 100 ~ 200°C/s.

10:15

Evolution of Reverted Austenite and Martensite during Thermal Processing of Chromium Stainless Steels: *Ernst Gamsjäger*¹; Manfred Wiessner²; Marina Gruber³; Sybrand van der Zwaag⁴; ¹Montanuniversität Leoben; ²Materials Center Leoben; ³Materials Center Leoben; ⁴TU Delft

Due to their excellent mechanical properties in combination with high corrosion resistance martensitic chromium stainless steels are applied to severe conditions in cryogenic, nuclear, oil field and aerospace applications. A key for the quality of these steels is the final microstructure evolving during the heating regime. The kinetics of phase transformations is investigated by dilatometer tests and in situ-XRD measurements. During heating the transformation from the body centered phase to face centered austenite occurs in two stages accompanied by partitioning of Ni. During cooling after austenitization martensite is formed in at least two distinct stages, which has been observed at various cooling rates. The kinetics of the transformation process is simulated. It is confirmed that the distinct stages during the bcc-fcc transformation are due to regions of higher and lower mole fractions of nickel. The distinct stages during the martensitic transformation appear to be independent of the cooling rate.

10:30

On the Decomposition of Annealed Amorphous Fe-C Thin Films: *Ben Lawrence*¹; Amelie Fillon²; Chad Sinclair¹; Xavier Sauvage²; Michel Perez³; Colin Scott⁴; Thierry Epicier³; ¹University of British Columbia; ²University of Rouen; ³University of Lyon, INSA Lyon; ⁴CanmetMATERIALS

The complex sequence of metastable phases obtained via conventional thermomechanical processing makes steels extremely versatile for structural applications. Through the use of far-from-equilibrium processing strategies it is possible to access transformation pathways that pass through different metastable phases, leading to novel microstructures and properties. In this work, we have sought to study the sequence of phase transformations arising from the low temperature annealing of amorphous binary Fe-C alloys containing between 15 and 35at% C produced via magnetron sputtering. X-ray diffraction, transmission electron microscopy and atom probe tomography are used to show both the crystallographic and compositional variations that occur upon annealing. The results suggest the important role that carbon redistribution plays in determining the rate of nucleation and growth of crystalline ferrite and/or carbides in the amorphous matrix.

10:45

Tempering Behavior in a Mo-W-Ni Steel Investigated by in-situ High Temperature XRD, Dilatometry, and TEM: *Andreas Keplinger*¹; Gerald Ressel¹; Stefan Marsoner¹; Reinhold Ebner¹; ¹Materials Center Leoben Forschung GmbH

An understanding of the precipitation behavior of various phases in high alloy steels is fundamental to adjust various properties after a certain heat treatment. Therefore, the aim of the presented work was to gain a detailed understanding of how microstructures in general and in particular bainite behave during tempering. By varying cooling rates, three distinct hardening morphologies, martensitic, bainitic and mixed martensitic-bainitic were produced in steel containing molybdenum, tungsten and nickel. The tempering process was investigated by in-situ high temperature X-ray diffraction to determine differences in the tempering behavior with respect to the initial microstructure. The time dependence of crystallographic features such as the dislocation density and the tetragonal distortion were monitored and linked with the precipitation behavior and the decomposition of residual austenite. Additionally, several samples were studied by transmission electron microscopy to give a detailed insight in the microstructures before and after tempering and to depict their differences.

11:00

Precipitation in a Multicomponent System: *Thomas Philippe*¹; Didier Blavette¹; Peter Voorhees²; ¹Normandie Université; ²Northwestern University

Recent experiments in model ternary alloys have revealed that the precipitates compositions do not lie on the equilibrium tie-line, with strong deviations in the early stages of precipitation. Assuming local equilibrium at the interface, we derive the clusters properties from nucleation to the coarsening regime in a multicomponent alloy. Size and composition of a critical nucleus are derived using the capillarity theory in the framework of classical nucleation. Then, we formulate the growth law from which a general theory of coarsening is developed accounting for off-diagonal terms in the diffusion tensor. The analysis is valid for a nonideal and nondilute solution and for any multicomponent systems. The theory gives the physical reasons for the deviation in composition from the equilibrium tie-line and is compared to experiments. Since the results are analytic, clusters properties from nucleation to coarsening can be determined using CALPHAD thermodynamic databases in a straightforward fashion.

11:15 Break

Thermodynamics and Alloy Design

TUESDAY AM ROOM: ALPINE D-E
SESSION CHAIR: CHRISTOPHE SIGLI,
CONSTELLIUM CRV

09:45 Invited

Alloys by Design - A 'Materials Genome' Approach to High Strength Stainless Steels for Low and High Temperature Applications: Qi Lu¹; Wei Xu¹; Sybrand van der Zwaag¹; ¹Delft University of Technology

An artificial intelligence based design of a series of novel advanced steels is presented, following the principle of the materials genome initiative, using an integrated thermodynamics/kinetics based model in combination with a genetic algorithm optimization routine. Novel compositions and associated heat treatment parameters are identified to realize the target microstructure for applications either at the room temperature (ultra-high strength maraging stainless steel) or at high temperatures (ferritic, martensitic and austenitic creep resistant steels). Solid solution strengthening and precipitation hardening are the two strengthening mechanisms employed to improve the strength of designed steels. Either one of them or their combination is optimised in the four steel families considered. Each model is validated by analysing the strengthening contributions in existing steels and by experimental characterization of prototype alloys. Good agreement between experimental performance and model predictions is found. All newly designed alloys are predicted to outperform existing high end reference grades.

10:15

Solid Solution Formation Rules and Crystal Structure Indicators on High Entropy Alloys: *Isaac Toda-Caraballo*¹; Pedro Rivera-Díaz-del-Castillo¹; ¹University of Cambridge

High Entropy Alloys (HEAs) are multicomponent systems incorporating several elements in a nearly equiatomic configuration. The content of each solute can typically vary between 5 and 35 at%. The high entropy associated to mixing several elements can inhibit the formation of intermetallic phases in favour of FCC or BCC solid solutions. Existing rules for predicting HEAs formation are at an incipient level, generally not offering information on the crystal structure. In this work, the interatomic spacing mismatch and bulk modulus mismatch across the lattice are considered for predicting the occurrence of HEAs. The work follows similar approaches to predict the formation of intermetallic phases and bulk metallic glasses, allowing the prescription of FCC or BCC HEAs occurrence. A

statistical analysis on the reliability of the complete set of rules for predicting HEAs has been achieved by analysing approximately 400 different compositions.

10:30

Advances in the Development of OpenCalphad Software and Databases: Bo Sundman¹; *Ursula Kattner*²; Mauro Palumbo³; Suzana Fries³; Eric Lass²; ¹INSTN, CEA; ²National Institute of Standards and Technology; ³Ruhr-University Bochum

Thermodynamics is at the core of materials science. The Calphad method, a powerful tool for materials design and engineering applications, has been shown to be an excellent platform for linking experiments and theoretical, quantum mechanics based results thereby greatly contributing to the understanding of materials and their properties. Most of today's databases and software are proprietary restricting expansion and development of new models and their integration into software tools for materials simulations. This presentation describes the progress made in development of the OpenCalphad code and databases. The goal of OpenCalphad is to develop free high quality software for thermodynamic calculations and databases with parametric physical models of the pure elements as basis for multicomponent databases as well as conventional Calphad databases. OpenCalphad provides a highly structured tool that can be used, together with kinetic models, in microstructure and continuum simulations.

10:45

Stress-strain Sensitive Gibbs Energy Formulation of Alloys: *Oleg Shchyglo*¹; Mikhail Mikolaychuk¹; Ingo Steinbach¹; ¹ICAMS, Ruhr University Bochum

CALPHAD type alloy thermodynamic methods originated a burst in capability of theoretical methods for phase transformations modeling. It is nowadays a well-established approach providing the Gibbs energies for alloy thermodynamics as well as the kinetic coefficients, e.g. atomic mobilities, in terms of database entries. The influence of mechanical properties on mechanical load, however, is modeled only through the hydrostatic pressure in current CALPHAD model approaches. In order to strengthen the modeling capabilities and descriptive power of CALPHAD type methods we present a theoretical model for alloys thermodynamics which incorporates crystal lattice symmetry and full set of elastic properties. The model has the form of a generalized Gibbs energy and takes into account cross-coupling between mechanical and chemical degrees of freedom. The proposed model allows describing phase equilibria in solid multi-phase systems taking into account the effect of internal and external stresses provided e.g. by phase-field simulations including micro-elasticity.

11:00

Calculation of the Miscibility Gap and Specific Heat of bcc Fe-Cr Alloys Using Physical – Empirical Models: *Dmitry Vasilyev*¹; Aleksandr Udovskiy¹; ¹Baikov Institute of Metallurgy and Materials Science, Russian Academy of Sciences

Methodology was developed to calculate the solubility curves, the spinodal line and temperature dependencies of specific heats of alloys; including one/two-phase states in a frame of physical – empirical models, which use physical properties of alloys: Debye and Curie temperatures, the electronic specific heat coefficients, the average magnetic moments, elastic modules, Grüneisen's parameter and thermal expansion coefficients - as input parameters. The results of calculated solubility curves as well as the spinodal decomposition line and specific heats for various alloy compositions were compared with the experimental data and the calculated results obtained by other researchers.

11:15 Break

In-situ Techniques II

TUESDAY AM

ROOM: CALLAGHAN

SESSION CHAIR: GORO MIYAMOTO,
TOHOKU UNIVERSITY

09:45 Invited

Advanced Small-angle X-ray Scattering for Quantifying Complex Precipitation Kinetic Pathways: *Alexis Deschamps*¹; Frédéric de Geuser²; ¹Grenoble Institute of Technology; ²SIMAP - CNRS

Small-Angle Scattering, used with X-rays or neutrons, enables a rapid quantification of precipitate microstructures at the nanoscale. This technique is particularly well adapted to use in-situ during thermal or thermo-mechanical treatments, or for scanning samples with heterogeneous microstructures. This presentation will give an overview about the capability of such experiments to provide insight on the kinetics of precipitation in complex situations in different alloy systems: quantifying the morphology evolution of plate like precipitates and particularly the competition between lengthening and thickening (Al-Cu-Li), validating precipitation models by in-situ kinetic data in isothermal and non-isothermal situations (Al-Li-Mg and Fe-Si-Ti), understanding the coupling between plastic deformation and concurrent precipitation (Al-Zn-Mg-Cu), understanding the precipitation kinetics in severely plastically deformed materials (Al-Zn-Mg-Cu), mapping heterogeneous microstructures in welds (Al-Cu-Li)

10:15

Thermo-mechanical Simulation Coupled with Synchrotron X-ray Scattering: A Unique Tool to Explore and Develop Materials: *Antonio Ramirez*¹; Leonardo Wu¹; Guilherme Faria¹; Thais Alonso¹; Leirson Palermo¹; ¹LNNano

The development and optimization of materials and processes involves nowadays the use of countless characterization and modelling techniques. Among those, intense x-ray synchrotron beamlines present the possibility to study materials under near to application conditions in real time. When such photon sources are combined with powerful thermo-mechanical physical simulators, the possibilities to study fundamental phenomena and rapidly develop/optimize materials are enormous. This was the strategy used to design and built the x-ray scattering and thermo-mechanical simulation installation (XTMS) at LNNano/LNLS-Brazil. The possibility to simultaneously submit the sample to a well-controlled and reproducibly strain/stress and temperature conditions using a customized Gleeble® system while approaching its crystallographic characteristics by x-ray diffraction have made possible to study the fundamentals of phase transformations and to optimize processing conditions for several materials. Thus, the capabilities of such unique installation will be presented along with selected examples of fundamental studies on metallic alloys.

10:30

In Situ Measurement of Austenite Grain Size through Reverse Transformation of Low Carbon Steel: *Keiji Ueda*¹; Thomas Garcin²; Matthias Militzer²; ¹JFE Steel Corporation; ²The University of British Columbia

Microstructural refinement is a key technology of a high performance steel plate. Reverse transformation behavior is important factor to achieve final grain refinement. However an integrated common theory about austenite grain growth through reverse transformation from original martensitic and bainitic steel has still not been fully understood. Novel in-situ measurement technique for metallurgical properties by laser ultrasonic is established recently. In this study, variation of grain size for 0.17%C steel during a continuous heating was in-situ measured. It was revealed that grain coarsening was promoted when the original microstructure is coarse martensite. The reason is that reverse transformed grains with similar crystal orientation form along lath boundary and coalesce easily. Lath structure of the original coarse martensite is maintained and this acts as the habit plane for the reverse transformed nucleation under Kurdjumov-Sachs relationship.

10:45

Advanced Mathematical Treatment of Dilatometry and Calorimetry to Discriminate and Quantify Multiple Phase Transformations: *Patricio Mendez*¹; *Ata Kamyabi-Gol*¹; John Gibbs¹; ¹University of Alberta

Dilatometry and calorimetry are well-established techniques, and have been used successfully for decades; however, they are seldom used to quantify the progress of a transformation. Most often, these techniques are used to detect start and finish of transformations. When used quantitatively, current analysis of dilation data does not account for the different changes in density for the different transformed phases. Similarly, quantitative calorimetric analysis does not account for different rates of enthalpy release for different transformed phases. The technique proposed for both dilatometry and calorimetry consists on posing a differential equation based on dilation or temperature data generated under controlled experimental conditions. When integrated, this equation extracts phase fraction evolution from the experimental data. Like all differential equations, the equation posed involves coefficients and integrations constants. The work presented differs from other similar work in that the coefficients are obtained from calibration before, after, and at transition points for each transformation, with a minimum of need of previously tabulated data. The mathematical treatment will be introduced, and applications will be discussed involving solid-state precipitation in Al-Ag, precipitation during solidification in A356, martensitic transformation in creep-resistant steel, and bainitic and mael.

11:00 Break

Other Diffusional Transformations

TUESDAY AM

ROOM: NORDIC

SESSION CHAIR: MIKKO HAATAJA,
PRINCETON UNIVERSITY

09:45

Investigation of Competing Transformation Mechanisms in Titanium Copper Active Eutectoid System: *Soumya Nag*¹; *Rodrigo Contieri*²; *Arun Devaraj*³; *Eder Lopes*²; *Rubens Caram*²; *Rajarshi Banerjee*¹; ¹GE Global Research; ²University of Campinas; ³Pacific Northwest National Lab; ⁴University of North Texas

Investigation of active eutectoid systems is quite interesting both kinetically as well as crystallographically. It has been observed that these systems exhibit an extremely rapid decomposition process that cannot be suppressed even during fast quenching from the high temperature parent phase. In the present work Ti-Cu alloys of hypo-eutectoid, eutectoid and hypereutectoid compositions have been subjected to different cooling rates from single-phase beta regime and the ensuing eutectoid products have been studied. Different characterization tools like SEM, TEM and 3D Atom Probe have been employed to determine the composition and structure of various Ti-rich and Cu-rich phases. The results help in understanding the transformation pathways that generate the end products as well as deconvoluting competing influences of martensite formation versus eutectoid decomposition via pearlitic and/or bainitic mechanisms.

10:00

Morphological and Compositional Evolution of Omega Precipitates and Its Consequent Influence on Alpha Precipitation in Ti-V Alloys: *Deep Choudhuri*¹; *Talukder Alam*¹; *Rongpei Shi*²; *Yufeng Zheng*²; *Soumya Nag*³; *Yunzhi Wang*²; *Hamish Fraser*²; *Rajarshi Banerjee*¹; ¹University of North Texas; ²Ohio State University; ³GE

Embrittling omega (ω) precipitates typically exhibit cuboidal or ellipsoidal morphologies in β -stabilized Ti alloys, depending on the relative degree of the β - ω misfit. This study focuses on the coupled morphological and compositional evolution of precipitates in a model high misfit Ti-20at%V alloy via a systematic series of isothermal annealing experiments and coupling TEM and 3D-atom-probe techniques. The water-quenched specimens exhibited fine scale ellipsoidal with indiscernible V partitioning across the ω/β interface, indicating the presence of athermal.

Subsequent annealing caused progressive size increase and, crucially, morphological changes: ellipsoidal(1hr) near-cuboidal(64 hrs) cuboidal(256 hrs). Furthermore, after only 1 hr of annealing, the ω phase was substantially depleted in V, while exhibiting minimal V pile-up at the ω/β interface. Possible factors contributing to the morphological and compositional evolution of ω at lower temperatures and ω -assisted nucleation and growth of a precipitates at higher annealing temperatures will be discussed.

10:15

Interplay between Microstructure and Phase Transition Kinetics during the Conversion from sp^2 - to sp^3 -Hybridised BN under Extreme Conditions: *Christian Schimpf¹; Marcus Schwarz²; Christian Lathe²; Edwin Kroke¹; David Rafaja¹; ¹TU Bergakademie Freiberg; ²GFZ German Research Centre for Geosciences*

The kinetics of the high pressure/high temperature (HP/HT) phase transition from hexagonal to cubic boron nitride were studied by means of laboratory and in-situ X-ray diffraction under HP/HT conditions using a multi-anvil press. Hexagonal graphitic BN precursors (h-BN) were characterised with respect to their microstructure (crystallite size, microstructure defects) using the profile analysis of X-ray diffraction lines. The real structure of the samples significantly affects the phase transition kinetics and synthesis products. Kinetic parameters of the phase transition were determined in-situ at high pressure. Exemplary, quantitative results have shown that basal plane corrugations in h-BN assist the direct transition from h-BN to cubic BN without the formation of intermediate wurtzitic BN (w-BN). Contrarily, defect-poor h-BN transforms to c-BN via w-BN, thereby showing much slower nucleation and growth rate. A complementary analysis using TEM and XRD (in-situ and laboratory) was applied to reveal microscopic driving forces of the phase transition mechanisms.

10:30

Phase Transformations in Electrodeposited Cobalt-phosphorous Coatings: *Sriram Vijayan¹; Na Luo¹; Mark Aindow¹; ¹University of Connecticut*

Nanostructured Electrodeposited Co-P alloy coatings have been identified as attractive alternatives to electrolytic hard chrome coatings due to their superior corrosion and wear resistance, and the more environmentally benign electroplating bath formulations involved. Three different types of Co-P coating microstructure can be formed depending on the P content: crystalline, hybrid and amorphous. The hybrid structure forms at intermediate P contents, comprises a nanostructured mixture of crystalline and amorphous phases, and gives optimized fatigue characteristics. Here we report a study on the stability of the phases and microstructures in DC-plated Co-P coatings with 0-15 wt.% P by comparing the as-deposited coatings with those after subsequent thermal exposure. A combination of differential scanning calorimetry, x-ray diffraction and transmission electron microscopy techniques have been used to reveal the character and sequence of the phase transformations that occur upon heating as a function of P content.

10:45

Solid-state Reactive Diffusion between Sn and Iron Family Metals: *Masanori Kajihara¹; ¹Tokyo Institute of Technology*

Solid-state reactive diffusion between various metals with low-melting and high-melting temperatures is experimentally examined in our research group. For the reactive diffusion between Sn and iron family metals in the temperature range of 433-473 K, only the most Sn-rich compound is formed as a layer with visible thickness, though there exist several stable compounds in this temperature range. The layer growth is controlled by volume and boundary diffusion for the Fe-Sn and Ni-Sn compounds but by interface reaction and volume diffusion for the Co-Sn compound. Although the contribution of boundary diffusion is greater for the Fe-Sn compound than for the Ni-Sn compound, the growth rate is much smaller for the former one than for the latter one. On the other hand, the Co-Sn compound grows much faster than the Ni-Sn compound, though interface reaction is a bottleneck for the compound growth.

11:00 Break

Phase Transformations in Complex Steels

TUESDAY AM ROOM: ALPINE A-B-C
SESSION CHAIR: DANIEL COUGHLIN,
LOS ALAMOS NATIONAL LABORATORY

11:45

Quenching & Partitioning Heat Treatment on a Ductile Iron: Competition between Martensite/Austenite Carbon Partition and Bainite Reaction - Microstructure and Kinetics Measurements: *Arthur Nishikawa¹; André Melado²; Antonio Ramirez³; Hélio Goldenstein¹; ¹Department of Metallurgical and Materials Engineering of University of São Paulo; ²Department of Metallurgy of Federal Institute of Espirito Santo; ³Brazilian Nanotechnology National Laboratory*

In this work the kinetics and microstructural evolution during Quenching & Partitioning (Q&P) heat treatment applied on a ductile cast iron (DI) was studied. Heat treatments were conducted in oil and salt baths and by means of dilatometry, allowing kinetics measurements. Additionally, evolution of phase fractions and lattice parameters were also monitored by means of in situ X-ray diffraction conducted at the XTMS experimental station facilities at Brazilian Nanotechnology National Laboratory (LNNano). Real time information about kinetics of competitive reactions and changes on austenite lattice parameter was obtained based on those results providing evidences for two main mechanisms of austenite carbon-enrichment: martensite carbon partitioning and bainite reaction. Microstructural characterization was performed by Scanning Electron Microscopy and Transmission Electron Microscopy. Q&P of DI was able to produce tailored microstructures composed by tempered martensite, carbide-free bainite and carbon-enriched stabilized austenite.

12:00

Quenching & Partitioning Heat Treatment on a Ductile Iron: Competition between Martensite/Austenite Carbon Partition and Bainite Reaction - Mechanical Properties: *André Melado¹; Arthur Nishikawa²; Hélio Goldenstein²; Estéfano Vieira; ¹Department of Metallurgy of Federal Institute of Espirito Santo; ²Department of Metallurgical and Materials Engineering of University of São Paulo*

In this work, the mechanical properties and stability of austenite of a ductile cast iron after processing using the quenching and partitioning (Q&P) route was studied. Heat treatments consisted on heating the material to 880°C for 2 hours followed by quenching in oil at 140 and 170°C (temperatures between Ms and Mf). The material was directly reheated to 300 and 375°C (partition treatment) for different times between 15 to 120 minutes. Mechanical properties of the material were characterized by tensile and impact strength tests. Fracture surfaces were studied by scanning electron microscopy. The transformed austenite upon plastic deformation in the range from 0 to 20% thickness reduction of the samples was analyzed. The retained austenite and induced martensite after rupture was characterized using X-ray diffraction with Rietveld refinement. The overall results showed that the austenite stays mostly stable even after plastic deformation.

12:15

Mössbauer Spectroscopy Investigation of Transition Carbides in Quenched and Partitioned Steel: *Dean Pierce¹; Daniel Coughlin²; Don Williamson¹; Kester Clarke²; Amy Clarke²; John Speer¹; Emmanuel De Moor¹; ¹Colorado School of Mines; ²Los Alamos National Laboratory*

Quenching and partitioning (Q&P) produces steel microstructures with martensite and austenite that exhibit promising mechanical properties. Understanding reactions that compete for the available carbon, such as carbide formation, is crucial for alloy design, processing, and achieving austenite enrichment and retention during Q&P processing. Mössbauer spectroscopy and transmission electron microscopy were used to quantify and characterize carbide formation in a 0.38C-1.54Mn-1.48Si wt. pct. steel after Q&P and the results were compared with data obtained for quenched and tempered (Q&T) microstructures. The results indicate that η -carbide formed during Q&P

processing and consumed a significant percentage of the total carbon in this steel, which likely contributes to lower retained austenite fractions. Nonetheless, an even greater amount of η -carbide formed after Q&T, indicating that carbon partitioning from martensite to austenite occurs in competition with η -carbide formation (in the Q&P steel). The findings of this work will allow alloying and processing optimization of Q&P treatments.

12:30

Comparison of Continuous and Isothermal Tempering of a High Speed Steel: *Stephanie Sackl¹; Gert Kellezi²; Harald Leitner²; Helmut Clemens¹; Sophie Primig¹; ¹Montanuniversitaet Leoben; ²Böhler Edelstahl GmbH & Co KG*

High speed steels are usually used for cutting applications. The red hardness of high speed steels leads to increased tool life and enables high cutting parameters. Their outstanding mechanical properties at elevated temperatures are assigned to the precipitation of secondary hardening carbides. The continuous heat treatment becomes more and more important due to cost and time savings. Nevertheless, the precipitation behavior during tempering may alter from those of isothermal heat treatments. Therefore, this study compares the continuous tempering to the isothermal tempering of a HS 6-5-2 high speed steel. The continuous and the isothermal heat treatment are performed in a quenching dilatometer. Atom probe tomography is used to characterize the chemical composition of the secondary hardening carbides after each of the three tempering steps. Transmission electron microscopy is applied as a complementary method to investigate the evolution of the volume fraction and the growth of the MC and M₂C precipitates.

12:45

Phase Transformations in a Metastable Stainless Steel: Microstructure Evolution and Mechanical Properties: *Carola Celada Casero¹; Bo-Ming Huang²; Jesus Chao¹; Jer-Ren Yang²; David San Martín¹; ¹CENIM-CSIC; ²National Taiwan University*

Ultra-fine austenitic microstructures (~350 nm) have been obtained after applying isochronal heat treatments (0.1-100 °C/s) to cold-rolled metastable steel samples. The martensite (α')-to-austenite (γ) transformation has been investigated by using magnetization measurements and electron microscopy, and the mechanical behavior of partially and fully transformed microstructures by tensile testing. Martensitic shear reversion mechanism has not been observed. The mechanical response of mixed (α'/γ) microstructures is influenced by the mechanical stability of austenite and depends on the austenite volume fraction and the presence of Ni₃Ti precipitates, showing a wide range of strength (2.1-1.1 GPa) and elongation (3-25%) values. In fully -microstructures strength can drop to 0.35 GPa and the elongation increase to 40% depending on the grain size. Deformation proceeds initially via localized Lüders-like band formation. The TRIP effect has been observed even for the finest grain sizes (350 nm). Retained austenite after deformation amounts ~10% regardless of the grain size.

13:00

Dissolution Versus Morphological Evolution of Residual δ -Ferrite in Model Austenitic Stainless Steels: *Mahmoud Saied¹; Yves Du Terrail Couvat²; Catherine Tassin³; Jessica Delacroix¹; Muriel Véron³; Jean-Denis Mithieux¹; E. Rigal⁴; ¹APERAM; ²Univ. Grenoble Alpes; ³Univ. Grenoble Alpes; ⁴CEA Grenoble*

The dissolution kinetics of residual δ -ferrite was studied in a cast Fe-17.3%Cr-9.4%Ni austenitic stainless steel ingot by means of heat treatments at temperatures lying in the austenitic domain, between 1140 and 1300°C. Experiments show that the ferrite fraction transiently increases at early stages of the transformation, until reaching a maximum value, after which the dissolution starts, driven by Cr and Ni diffusion. The dissolution rate undergoes a slight decrease at the intermediate stage of the transformation: this slowdown is attributed to the competition between the chemical driving force and the δ/γ interfacial energy leading to a morphological change of the ferrite. To overcome the complex microstructural features (dendritic / lathy) of δ -ferrite in the cast alloy, simplified geometries have been produced using austenitic and ferritic Fe-Cr-Ni alloys, allowing a better description of the different stages of the phase transformations. Experimental results are compared to a 1D finite-difference modelling.

13:15 Lunch and Poster Session

Transformation Kinetics

TUESDAY AM ROOM: ALPINE D-E
SESSION CHAIR: URSULA KATTNER, NATIONAL
INSTITUTE OF STANDARDS AND TECHNOLOGY

11:45 Invited

Modelling Transformation Kinetics: *Bastian Rheingans*¹; Eric Mittemeijer²; ¹Institute for Materials Science, University of Stuttgart; ²Max Planck Institute for Intelligent Systems / Institute for Materials Science, University of Stuttgart

For versatile modelling of phase transformation kinetics, a kinetic model should provide a flexible framework for implementing suitable kinetic descriptions for the operating transformation mechanisms. Thus, a modular approach for modelling solid-state phase-transformation kinetics is presented, which allows combination of specific, dedicated modes of nucleation and growth to obtain an adequate description of the transformation kinetics. Examples of corresponding, successful kinetic analyses include crystallisation of amorphous materials, massive transformations, martensitic transformations and precipitation reactions [1,2]. Frequently neglected aspects of kinetic modelling will also be addressed: severely erroneous kinetic analysis as often caused by incorporation of inconsistent thermodynamics in models for nucleation and growth, and the limited ability of apparently successful kinetic models to also provide a satisfactory, complete description of the resulting microstructure, as shown for recrystallisation. [1] E. J. Mittemeijer, *Fundamentals of Materials Science*, Springer, Heidelberg, 2010. [2] B. Rheingans, E. J. Mittemeijer, *JOM* 65, (2013) 1145-1154

12:15

A Contribution to Nucleation Theory in Concentrated Alloys: *Christophe Sigli*¹; Joël Lépinoux²; ¹Constellium Technology Center; ²Univ. Grenoble Alpes

When dealing with the nucleation theory in concentrated alloys, the statistical physics of fluctuating clusters must take into account cluster competition for available space. To that effect a mean field effective pressure is introduced in the theory which affects the occupancy probability of the energy levels of each cluster. The theory will be illustrated on binary Al-Li alloys as a first case study. It will be shown that the pressure model reproduces Monte Carlo (MC) calculations in terms of equilibrium cluster distribution and phase diagram. As will be illustrated, such an approach can easily be incorporated in a cluster dynamic formalism to predict the nucleation-growth-coarsening of a new phase (here L12 Al₃Li in a fcc solid solution).

12:30

A Molecular Dynamics Simulation Study of Crystallographic Orientation Relationships during Nucleation in the Austenite-ferrite Phase Transformation: *Huajing Song*¹; Jeff Hoyt¹; ¹McMaster University

The study of the solid-state nucleation through experiment is often limited by small length and time scales and even today most of the solid-state nucleation mechanisms are estimated based on classical nucleation theory. In this study, we use the molecular dynamics (MD) method to study the nucleation of the BCC ferrite phase in pure Fe starting from a polycrystalline system of the FCC austenite phase. The simulation focuses on the heterogeneous nucleation occurring at grain boundaries. The grain boundary energy, the FCC-BCC interface energy and the crystallographic orientation relationship between the new and parent phases are monitored during the MD simulations. Consistent with previous experiments on steel, several special orientation relationships are found to dominate during the nucleation stage. The crystallographic orientation significantly affect the interface properties during the transformation process. In addition, a barrier-free heterogeneous grain nucleation phenomenon is captured and analyzed in this study.

12:45

Molecular Dynamics Simulation of the Effects of fcc/bcc Interfaces on the Nucleation and Growth of Martensite in Iron: *Xiaoqin Ou*¹; Jilt Sietsma¹; Maria Santofimia Navarro¹; ¹TU Delft

Molecular dynamics simulations have been used to study the effect of fcc/bcc interfaces in the Nishiyama-Wasserman (N-W) orientation relationship on the fcc-to-bcc transformation at 300 K in pure iron. Simulations show the growth of the original bcc phase present in the initial configuration as well as the nucleation and growth of new bcc grains inside the original fcc phase. During growth, heterogeneous and homogenous bcc nuclei both pin the propagation of the original bcc/fcc interface. In some locations, neighboring newly-nucleated bcc plates merge into a single bcc grain. The fcc phase transforms to bcc phase by a predominantly martensitic mechanism.

13:00

Diffusion and Diffusion-controlled Transformations in Bulk and Nanolayered Intermetallics: Atomistic Modelling: *Rafal Abdank-Kozubski*¹; Andrzej Biborski²; Mirosław Kozłowski¹; Piotr Sowa¹; Sylwia Brodacka¹; Christine Goyhenex³; Veronique Pierron-Bohnes³; Jolanta Janczak-Rusch⁴; Elena Levchenko⁵; Alexander Evteev⁵; Irina Belova⁵; Graeme Murch⁵; ¹Jagiellonian University in Krakow; ²Academic Centre for Materials and Nanotechnology, AGH University of Science and Technology; ³Institut de Physique et Chimie des Matériaux de Strasbourg, UMR 7504; ⁴EMPA, Swiss Federal Laboratories for Materials Science and Technology; ⁵University Centre for Mass and Thermal Transport in Engineering Materials, School of Engineering, The University of Newcastle Callaghan

Self-diffusion, decomposition, precipitation, chemical ordering and surface segregation in bulk and nanolayered intermetallics have been modeled at the atomistic scale using hybrid Monte Carlo – Molecular Statics algorithms. Three particular results are reported: (i) The experimentally observed discontinuous transformation from “in-plane” to “off-plane” L10 variant in [001]-oriented FePt nano-layers modelled with Analytic Bond-Order Potentials (ABOP); (ii) The configuration of the eutectic mixture of Ag and Cu precipitates in nano-layered Ag-40at.%Cu modelled with many-body potential derived for Ag-Cu within the Second-Moment-Approximation; (iii) Vacancy thermodynamics, self-diffusion and “order-order” kinetics modelled by means of Semirigid Canonical Monte Carlo and Kinetic Monte Carlo simulations in B2-ordering A-B system mimicking Ni-Al. Experimentally observed relationship between the activation energies for ordering and self-diffusion in NiAl is reproduced and its origin is elucidated. The study is extended upon AB nanolayers where an interplay between surface-segregation and ordering is revealed.

13:15 Lunch and Poster Session

Theory of Displacive Transformations

TUESDAY AM ROOM: CALLAGHAN
SESSION CHAIR: DANIEL SCHWARTZ,
LOS ALAMOS NATIONAL LABORATORY

11:45 Invited

Atomic-Level Study of Pure-Shuffle Mechanisms in Solid-Solid Phase Transformation: *Jian Wang*¹; ¹Los Alamos National Laboratory

Using high-resolution transmission electron microscopy (HRTEM) and atomistic simulations (density function theory and molecular dynamics), we explored zero-shear phase transformation mechanisms that occur in hexagonal close packed Ti, Zinc-blend AlN, and Wurtzite InAs. A face-centered cubic titanium (fcc-Ti) was characterized in polycrystalline titanium where the two phases have the orientation relation $\langle 0001 \rangle_{\text{fcc-Ti}} \parallel \langle 001 \rangle_{\text{hcp-Ti}}$ and $\{10\bar{1}0\}_{\text{fcc-Ti}} \parallel \{110\}_{\text{hcp-Ti}}$. We discovered that the fcc-Ti band forms via a pure-shuffle mechanism and migration of phase boundary via a shear-shuffle mechanism or a pure-shuffle mechanism. Zinc-blend AlN nanolayer was characterized in Al-AlN-TiN trilayers. Zinc-blend AlN transforms to wurtzite AlN

during mechanical loading through collective glide of three Shockley partial dislocations as one unit that has a net zero Burgers vector and corresponds to a zero-shear strain. The same transformation mechanism was also characterized in InAs nanowires. I will report on zero-shear phase transformation mechanisms and discuss potential application in designing nanostructured materials.

12:15 Invited

Martensitic Transformation Precursors: Phonon Theory and Critical Experiments: *Yu Wang*¹; Yongmei Jin¹; ¹Michigan Tech

Anomalous precursor effects are observed in cubic austenite phases prior to martensitic transformations, which are difficult to explain from conventional phase transition theories. Based on incomplete phonon softening that generally occurs above martensite start temperature, a Grüneisen-type phonon theory of martensitic precursors is developed. The theory considers phonon free energy contribution and addresses the effects of deformation-dependent incompletely-softened low-energy phonons on the structural, thermal, acoustic and elastic behaviors of pre-martensitic cubic crystals on the same physical footing of thermal expansion. It shows that martensitic precursor effects are natural consequences of anharmonic lattice dynamics in cubic crystals that undergo incomplete phonon softening. In-situ 3D phonon diffuse scattering and Bragg reflection experiments using high-energy synchrotron X-ray single-crystal diffraction are performed to test the theory. Exotic domain behaviors are observed in pre-martensitic austenite phases, which are fundamentally distinct from usual ferroelastic domain switching behaviors and are explained from phonon point of view.

12:45 Invited

Continuous Martensitic Transformation and Invar and Elinvar Anomalies: Dong Wang¹; Liangxiang Zhang¹; Xiaobing Ren²; *Yunzhi Wang*³; ¹Xi'an Jiao Tong University; ²National Institute for Materials Science; ³Ohio State University

Martensitic transformation (MT) is a typical first-order diffusionless solid state phase transformation accompanied by a discontinuous structural change at the transition temperature. Long-range elastic interactions dominate the microstructural evolution, with strong autocatalysis leading to an avalanche of self-accommodated strain domains (martensitic variants) via nucleation and growth. Such transition characteristics are too sharp and nonlinear for certain applications. By creating martensitic embryos with a broad distribution of degrees of maturity and hence of different MT start temperatures, suppressing the autocatalysis, and regulating the spatial extent of domain growth via random fields from point and extended defects, we show that this sharp MT can be rendered continuous. Accompanying such a continuous MT, there could be many special properties, including superelasticity of nearly zero hysteresis, nearly zero thermal expansion (Invar anomaly), and low and temperature-independent elastic modulus (Elinvar anomaly) over a broad temperature range. The simulation predictions agree well with experimental observations.

13:15 Lunch and Poster Session

Ferrous Austenite

TUESDAY AM

ROOM: NORDIC

SESSION CHAIR: MASATO ENOMOTO,
IBARAKI UNIVERSITY

11:45 Invited

Some Metallurgical Issues Concerning Austenite Conditioning in Microalloyed Steels Processed by Near-net-shape Casting and Direct Rolling Technologies: *Jose Rodriguez-Ibanez¹; Beatriz López¹;*

¹CEIT

As steel grades with higher strength/toughness requirements combined with smaller total reductions are requested, austenite conditioning during hot working of as-cast microstructures becomes a key step that needs to be properly analyzed. If this conditioning prior to transformation is not well achieved, in the final microstructure coarse high angle boundary crystallographic units can be present which impair toughness. The complexity of this austenite conditioning has increased due to the displacement from single to multiple microalloying additions (usually Nb combined with other elements such as Ti, Mo or V) and to the development of new hot rolling configurations and rolling strategies with smaller reductions. It is worth emphasizing that these microalloying combinations can affect the softening-strain induced precipitation interactions associated with Nb microalloying. This manuscript analyzes some of the microstructural features that should be taken into account during austenite conditioning, with special emphasis in Ti-Nb and Nb-Mo microalloyed grades.

12:15

Austenitization Kinetics of Medium Mn Steels during Intercritical Annealing: *Haiwen Luo¹;* ¹University of Science & Technology Beijing

Medium Mn steels which usually contain 5-10 wt.% Mn are the promising candidate for the 3rd generation automotive steels as they exhibit an excellent combination of strength and elongation. The key production process of these steels is intercritical annealing, during which part of ferrite shall transform to austenite. Austenitization kinetics determine the amount and stability of austenite formed intercritically and then retained after cooling, which accounts for the improved tensile properties via TRIP effect. The austenitization kinetics and partition of the solutes between ferrite and austenite during intercritical annealing were not only measured experimentally but also simulated numerically. We found a discrepancy between the measured and simulated results on the partition of Mn, and then discussed the possible reasons.

12:30

Austenite Decomposition and Properties of Mo-Nb Containing Press Hardening Steels: *Fateh Fazeli¹;* Colin Scott¹; ¹CanmetMATERIALS

Press hardening steels with strength exceeding than 1.5 GPa enable significant down gauging of the structural parts of lightweight vehicles without compromise of crash performance. Austenite decomposition of blank sheets during forming operation controls microstructure and crashworthiness of fabricated parts; particularly the fraction and microstructural features of martensite which depend on alloy composition and forming parameters. Modified 22MnB5 steels with Mo-Nb addition were developed for improved press hardenability and enhanced crash performance. Dilatometric study and microstructural analysis were carried out to assess the role of processing parameters, i.e. forming temperature, applied strain and thermal path. Dynamic recovery of austenite during forming and its subsequent softening upon die cooling were analyzed to understand the interaction between austenite deformation and decomposition. Further, hat-section parts were fabricated to provide specimens for tensile and three-point bend tests. The transformation behaviour of the developed alloys and the interplay among microstructure-processing-properties are discussed in details.

12:45

Microstructures and Mechanical Properties of High Strength Medium Manganese Steel: *XiaoLong Yang¹;* Yunbo Xu²; Ying Zou¹; Xiaodong Tan¹; Zhiping Hu¹; Yongmei Yu¹; Di Wu¹; ¹Northeastern University

With the development of microalloyed steels, the excellent combination of high strength and high ductility becomes a target in modern industry. Due to the low price of manganese and excellent mechanical properties, the medium manganese steels are attracted much more attention recently. Based on TMCP and UFC technology, the microstructures and mechanical properties of medium manganese steel were studied in this paper. The hot-rolled medium manganese steel was treated by reheating quenching process. The mechanical properties of medium manganese steel were measured by tensile and impact test, and microstructures were observed by optical microscopy (OM), scanning electron microscopy (SEM) and transmission electron microscopy (TEM). The excellent mechanical properties were obtained in this study, and relationship between microstructures and mechanical properties was further investigated in order to acquire a good combination of high strength, high ductility and excellent impact toughness.

13:00

In Situ Study of Austenite Reversion Kinetics during Intercritical Tempering of a 12Cr-6Ni-2Mo Supermartensitic Stainless Steel: *Julian Escobar¹;* Guilherme Faria²; Leonardo Wu²; Paulo Roberto Mei¹; Antonio Jose Ramirez²; ¹State University of Campinas; ²Brazilian Nanotechnology National Laboratory

With the development of microalloyed steels, the excellent combination of high strength and high ductility becomes a target in modern industry. Due to the low price of manganese and excellent mechanical properties, the medium manganese steels are attracted much more attention recently. Based on TMCP and UFC technology, the microstructures and mechanical properties of medium manganese steel were studied in this paper. The hot-rolled medium manganese steel was treated by reheating quenching process. The mechanical properties of medium manganese steel were measured by tensile and impact test, and microstructures were observed by optical microscopy (OM), scanning electron microscopy (SEM) and transmission electron microscopy (TEM). The excellent mechanical properties were obtained in this study, and relationship between microstructures and mechanical properties was further investigated in order to acquire a good combination of high strength, high ductility and excellent impact toughness.

13:15 Lunch and Poster Session

Poster Session

Poster Session

TUESDAY 13:15-15:00

ROOM: FOYER

SESSION CHAIRS: CHAD SINCLAIR,
UNIVERSITY OF BRITISH COLUMBIA;
HATEM ZUROB, MCMASTER

Diffusional Transformations

P-A1: Effect of Heating Rate on the Microstructure Formation during Inter-critical Annealing of Cold-rolled Low-carbon Steels.: Anish Karmakar¹; Madhumanti Mandal¹; Abhisek Mandal¹; Subrata Mukherjee²; Debalay Chakrabarti¹; ¹Indian Institute of Technology, Kharagpur; ²Research and Development, Tata Steel

Two different heating rates (~ 1K/s and ~300K/s) were used for inter-critical annealing of cold-rolled low-carbon steels having ferrite-pearlite or ferrite-martensite starting structures (with blocky / fibrous martensitic morphologies). The cold-rolled samples were annealed at different temperatures (773-1173K) and water-quenched. Alternate layers of fine ferrite and martensite in ferrite-fibrous martensite starting structure showed the finest ferrite grain sizes (3-6 μm) and uniform distribution of martensitic islands after annealing, offering the best tensile properties among all the investigated samples irrespective of the heating rate. The microstructures obtained after rapid annealing have been explained in view of the strain partitioning in cold-rolled structure as determined by EBSD analysis. Detailed study has been carried out on the recrystallization kinetics, transformation kinetics and recrystallization-transformation interaction as the function of heating rate. Austenite islands were formed around carbide particles and at the ferrite grain boundaries depending on the heating rate.

P-A2: Effect of Ni-based Amorphous Foil on Transient Liquid Phase Bonding of CLAM/CLAM Steels: Xiaosheng Zhou¹; Chenxi Liu¹; Yongchang Liu¹; Liming Yu¹; Huijun Li¹; ¹Tianjin University

Transient liquid phase bonding is employed to join China low activation martensitic (CLAM) steels, with Ni-based amorphous foil as interlayer. The effect of the Ni-based amorphous foil on the microstructure and mechanical performance of the joint is investigated. During bonding, as the temperature reaches the start temperature of austenite transformation, boron, a melting point depressant in amorphous foil, can diffuse along austenite boundaries, resulting in compounds containing boron in the fine-grain zones adjacent to the interlayer. Owing to the melting of interlayer and the dissolution of substrate material, the final width of the interlayer is increased. At the interlayer close to the joint interface, small voids can be observed, associated with the difference between Fe and Ni diffusion rates. It should also be noted that the bonded CLAM/CLAM steels always fracture at the interlayer.

P-A3: Effect of Interphase Precipitation in Ferrite on Strain Hardening Behavior DP Steels under Deformation: Shao-Pu Tsa¹; Chih-Hung Jen¹; Yuan-Tsuong Wang²; Ching-Yuan Huang²; Jer-Ren Yang¹; ¹NTU; ²CSC

Dual-phase steels are widely used in automobile industry due to good formability and excellent mechanical properties since 1970's. In order to further improve ferrite hardness, interphase precipitation (IP) is introduced into ferrite to effectively strengthen the soft phase. Different strain hardening behavior is observed in conventional and IP strengthened dual-phase steels, which is believed to be associated with the different ferrite characteristic. In order to elucidate the effect, strain hardening rate is divided into three stages, where tensile tests are applied to both specimens. To make a linkage between substructure and mechanical properties, TEM techniques are used to observe dislocation microstructure. It is found out that higher strain hardening rate in IP dual-phase steels

in the first stage is attributed to enhanced dislocation multiplication and impingement caused by precipitates. Equal strain hardening rate in the second stage is due to the balanced effect of dynamic recovery and dislocation entangle.

P-A4: Effect of Cooling Rate after Solution Treatment on Phase Separation in Fe-Cr Alloys: Xin Xu¹; Peter Hedström¹; Joakim Odqvist¹; ¹KTH Royal Institute of Technology

It is known that the solution treatment of bcc Fe-Cr alloys will affect subsequent low temperature aging and phase separation kinetics. There are several factors contributing and their individual effect is not clear. Hence, in the present work we have tried to isolate and study the effect of the cooling rate after solution treatment on the phase separation kinetics in Fe-Cr alloys. The alloys were cooled at different rates after solution treatments and subsequently aged. The microstructure was characterized and mechanical properties were measured. The effect of cooling rates on the kinetics of the phase separation during subsequent aging, and the resulting microstructure and mechanical properties is discussed.

P-A5: Isothermal Decomposition of Austenite below Ms and during Tempering on a C-Si Steel: José da Cruz Junior¹; Dagoberto Santos¹; Arthur Nishikawa²; Hélio Goldenstein²; ¹Metallurgical, Materials and Mining Engineering Department of Universidade Federal de Minas Gerais; ²Department of Metallurgical and Materials Engineering of University of São Paulo

Experimental investigations were performed on the formation of the microstructure in SAE 9254 steel during isothermal heat treatments below the martensite start (Ms) temperature, in the range of 200-270°C. After the isothermal heat-treatment, the same steel was subjected to tempering at various temperatures (350-450°C). Isothermal and non-isothermal dilatometry experiments were performed to characterize the kinetics of phase transformations during the initial austenite decomposition and during the subsequent tempering heat treatment.

P-A6: The Structure Property Relationships Governing Solute-Boundary Binding Energies in Austenite: Michael Hoerner¹; Mark Eberhart¹; John Speer¹; E. Damm²; ¹Colorado School of Mines; ²TimkenSteel Corporation

Austenite grain size and austenite boundary motions play an important role in ferrous phase transformations and property control. Solute atoms are known to interact with austenite grain boundaries, but the nature of these interactions is not well understood. To understand these interactions, *ab-initio* density functional theory calculations have been performed on a number of grain boundaries with varying degrees of symmetry in the FCC Fe system. The binding energy of solutes to the boundary has been determined. In low symmetry environments traditional parameters that drive site segregation, such as site volume, have been difficult to calculate. Analysis of the changes in the local charge density that are caused by the introduction of solute atoms has been performed in the present work. This analysis was found to provide a meaningful way to understand the origin of solute-boundary binding energy in low symmetry boundaries.

P-A7: Phase Field Modeling of the Austenite-ferrite Transformation in Fe-C-Mn Alloys: Hao Chen¹; Benqiang Zhu¹; Matthias Militzer¹; ¹University of British Columbia

Three different approaches for considering the effect of Mn on the austenite-ferrite interface migration have been coupled with a phase field model (PFM). In the first approach (PFM-I), only long range C diffusion is considered while Mn is assumed to be immobile. Both C and Mn diffusions are considered in the second approach (PFM-II). In the third approach (PFM-III), C diffusion is considered in combination with the Gibbs energy dissipation due to Mn diffusion inside the interface. PFM-I, PFM-II and PFM-III are all applied to simulating the isothermal transformation and the cyclic transformation in Fe-C-Mn alloys. PFM-II can predict the stagnant stage and growth retardation phenomenon experimentally observed during

cycling transformation whereas PFM-III can only replicate the stagnant stage but no growth retardation and PFM-I predicts neither the stagnant stage nor growth retardation. This study suggests a significant role of Mn redistribution near the interface on reducing transformation rates.

P-A8: Austenite Stability in Low Density Steels: Ian Zuazo¹; Aurelien Bauche¹; Patrick Barges¹; Xavier Garat¹; ¹ArcelorMittal

High aluminium steels of the FeMnAlC system are an alternative to current automotive steels due to a higher strength coupled to a density reduction from 8-10% and higher. In the two-phase austenite-ferrite (Duplex) family, the stability of austenite plays an important role on mechanical behaviour. In this alloys TRIP behaviour is observed to depend strongly on annealing parameters (temperature and time) that modify austenite: grain size, partitioning, internal structure, etc. In addition sub-zero cooling down to liquid nitrogen leads to mixed structures where the apparition of martensite, enhanced by the presence of aluminium in an otherwise highly alloyed and stable austenite, also depends on annealing parameters. These aspects will be discussed in relation with the resultant mechanical properties from room temperature to sub-zero testing.

P-A9: Precipitation in Strip Cast Austenite: Adam Taylor¹; Peter Hodgson¹; Nicole Stanford¹; ¹Deakin University

The precipitation behaviour of a strip cast model austenitic alloy (Fe-29Ni-0.17Nb-0.14Mn-xC wt.%) was investigated. This particular alloy was chosen as it retains its austenitic structure on cooling to room temperature and thus allows the precipitation behaviour in austenite during the strip casting process to be studied directly. The fast cooling times associated with strip casting process results in a different microstructure when compared to the conventionally cast material. These rapid cooling rates can also result in chemical segregation and the formation of solute clusters and nano-precipitates. The unique precipitation behaviour of this alloy/process combination is studied utilising a combination of atom probe tomography (APT), transmission electron microscopy (TEM) and scanning electron microscopy (SEM) with energy dispersive spectroscopy (EDS).

P-A10: A Model for the Growth Rate of Bainitic Ferrite: Lindsay Leach¹; Annika Borgenstam¹; John Ågren¹; Lars Höglund¹; ¹KTH Royal Institute of Technology

The appeal of bainitic steels lies in their immense potential for improved mechanical properties as is evident in the good combination of strength and toughness they exhibit, a development which can be facilitated by computational tools. The aim of this work is to develop a predictive model for the formation of bainite. At this point, it is solely the ferritic component of bainite that is considered. A model for the lengthening rate of bainitic ferrite has been developed. The critical conditions of formation and thermodynamic driving forces are used to delineate thermodynamic barriers. The growth kinetics has been conducted within a diffusional framework and a maximum lengthening rate concept has been applied. It is demonstrated that under these conditions, the growth rates of bainitic ferrite can be predicted to a sufficient extent thus laying the foundation for further development of a quantitative model to predict the degree of transformation.

P-A11: Nano-sized Precipitates in an Fe-13Cr Alloy Formed Under Oxidizing Water Vapor: Leonardo Agudo¹; Maria Mosquero¹; Gert Nolze¹; Fernando Rizzo²; ¹BAM; ²PUC Rio de Janeiro

Oxidation of a Fe-13Cr alloy under water vapor at 600C produced a zone of nano-sized precipitation underneath the outside scale formed by iron oxides and Fe-Cr spinel. The precipitated particles present an orientation relationship to the ferritic matrix. The precipitates have a lath morphology with main axes parallel to <100> ferritic directions. The majority of the spinel layer also shows a fixed orientation relationship to the ferritic matrix. EDS and EBSD were used to characterize the oxide layer. The precipitates were investigated by TEM of specimens extracted by FIB to target an area previously characterized

by EBSD, consisting of the base material, the precipitation zone and the spinel layer. Energy filtered selected area diffraction (SAD) and dark field in the conventional (C) TEM mode, as well high angle annular dark field (HAADF) imaging and EDS in the scanning (S)TEM mode were also employed in the characterization of the specimens.

P-A12: Experimental and Numerical Analysis on Transformation from Martensite to Austenite during the Intercritical Annealing of 13Cr-5Ni Steel: *Lu Liu¹; Zhi-Gang Yang²; Chi Zhang²; Yuan Xia²; Pengcheng Song²*; ¹State Nuclear Power Research Institute; ²Tsinghua University

Microstructure evolution from martensite to austenite and partitioning behavior of alloying elements during the intercritical annealing from 550°C to 700°C with different durations at a heating rate of 10°C/min in a 13Cr-5Ni steel were examined experimentally and analyzed numerically by Thermo-Calc and DICTRA. In a lower intercritical annealing temperature, filmlike austenite preferentially formed at martensite lath boundaries, while higher temperatures produced granular austenite inside the laths in addition to filmlike austenite. The volume fraction of austenite at room temperature after intercritical annealing firstly increased with the annealing temperature, exhibiting a maximum at 625°C and then decreased at higher temperatures. Annealing for longer durations resulted in a larger volume fraction of austenite and thicker austenite laths with an enrichment of Ni. The thickening of the austenite lath was simulated under local equilibrium. Formation of austenite was controlled by diffusion of Ni in martensite.

P-A13: Hierarchical Control of Eco-friendly Fe-Si Based Alloys for Thermoelectric Applications: *Wade Jensen¹; Naiming Liu¹; Eva Rosker¹; William Soffa¹; Jerry Florio²*; ¹University of Virginia

Hierarchical optimization of the structure and properties of semiconducting β -FeSi₂ could result in a competitive thermoelectric material. Eutectoid decomposition α -FeSi₂ \Rightarrow β -FeSi₂ + Si can result in Si nanorods embedded in β -FeSi₂. The increased heterointerface density strongly reduces thermal conductivity. To further increase phonon scattering while simultaneously engineering band alignments between the phases, additional alloying with 4 at% Ge has been attempted by arc melting. This produces coarse eutectic lamellar structures of Si_{1-x}Ge_x and α -FeSi₂ upon solidification, with a non-equilibrium FeSi B20 phase present. However, melt-spinning the alloy markedly decreases the lamellar length scales to the nanoscale regime, and eliminates FeSi. Ternary equilibrium has not been reported in this region of the Fe-Si-Ge phase diagram, and we are beginning to map out the liquidus surface. This poster will discuss how the microstructure results from the combined eutectic/eutectoid decomposition process, and how this affects thermoelectric properties.

P-A14: Investigation of Microstructural Mechanisms Occurring in Lean Duplex Stainless Steel During Ageing: *Jean-Yves Maetz²; S. Cazottes²; C. Verdu²; X. Kléber²*; ¹University of British Columbia; ²Université de Lyon, INSA Lyon

Lean duplex stainless steels have low Ni and Mo contents and an austenite-ferrite phase ratio of approximately one. The microstructure evolution of a 2101 lean duplex stainless steel during isothermal ageing was investigated in the embrittlement temperature range, at 690 °C, from a few minute to several months using a multi-technique and multi-scale approach. To highlight the main microstructural changes the ageing kinetics was followed using thermoelectric power (TEP) measurements and in this way specific ageing stages were selected to be qualitatively and quantitatively characterized using scanning electron microscopy (SEM), electron back-scattered diffraction (EBSD), transmission electron microscopy (TEM) and focused ion beam nano-tomography (FIB-nt). Particular attention was paid to the phase stability during long-term ageing, especially to the δ -ferrite transformation into γ 2 secondary austenite and σ -phase and the subsequent transformation of γ -austenite into α' -martensite during cooling.

P-A15: The Frenkel Effect during Diffusion Process: *Bartek Wierzbą¹; Patrycja Wierzbą¹; Wojciech Skibinski²*; ¹Rzeszow University of Technology; ²AGH, University of Science and Technology

In this paper numerical description of the reactive diffusion process including Frenkel effect is shown. The

vacancy generation and voids evolution is discussed in terms of numerical simulations. The proposed approach based on the generalized Darken approach where the volume velocity is essential in defining the local material velocity at non-equilibrium. The voids formation in β NiAl-Cu system is experimentally discussed and modeled.

P-A16: Competition between Kirkendall, Frenkel and Backstress Effects during Diffusion Process: *Wojciech Skibinski¹; Bartek Wierzbą²; Stanislaw Wedrychowicz²*; ¹AGH University of Science and Technology; ²Rzeszow University of Technology

In this work the relation between Kirkendall and backstress effects induced in the diffusion process is discussed. Both effects are caused by the difference in intrinsic diffusion coefficients in the system. The Kirkendall plane shift is simulated and experimentally verified. Several simulations methods are discussed – trajectory, velocity curve and entropy density. This approach is based on the bi-velocity (Darken) method which combines the Darken and Brenner concepts proposing that the volume velocity is essential in defining the local material velocity at non-equilibrium.

P-A17: Mechanisms of Void Shrinkage in Aluminium: *Zezhong Zhang¹; Tianyu Liu¹; Andrew Smith²; Nikhil Medhekar¹; Philip Nakashima¹; Laure Bourgeois³*; ¹Department of Materials Engineering, Monash University; ²School of Physics, Monash University; ³Monash Centre for Electron Microscopy, Monash University

voids in aluminium can significantly affect materials performance and key question is their evolution. We performed in-situ annealing in a high-resolution transmission electron microscope and found that void shrinkage is a two-stage process. The void first shrinks anisotropically from a non-equilibrium to an equilibrium shape and then shrinks progressively keeping its equilibrium shape until its collapse. This phenomenon can be explained through a surface energy analysis: the void shrinks so to maximise the total surface energy reduction per vacancy emitted. We explain the measured void shrinkage rates using bulk diffusion kinetics modified to take into account electron beam irradiation. This provides an explanation for the common presence of a specific, non-equilibrium void shape before shrinkage starts.

P-A18: In Situ Investigations of Partitioning Mechanisms in Q&P Steels by Synchrotron Diffraction Experiments: *Sébastien Allain¹; Guillaume Geandier¹; Jean-Christophe Hell²; Michel Soler²; Frédéric Danoix³; Mohamed Gouné⁴*; ¹Institut Jean Lamour; ²ArcelorMittal Maizières Research SA; ³GPM; ⁴ICMCB

Quenching & Partitioning is a new annealing route proposed to produce the third generation of Advanced High Strength Steels. It relies on the generation of a mixed martensite and austenite microstructure by an interrupted quench (Quenching) followed by a carbon redistribution from supersaturated martensite to austenite (Partitioning) at higher temperature. We will report the results of such an annealing treatment on high C TRIP steels studied by the mean of X-Ray diffraction experiments using a synchrotron source. The high energy monochromatic beam enables high acquisition rates adapted to the study of the 'real time' Q&P processes on bulk samples. A single in situ experiment permits thus to follow all the different metallurgical processes operating during the different steps of Q&P (phase transformation, interface mobility, partitioning, carbide precipitation). A special attention will be paid to the sensitivity of these processes to the manufacturing parameters.

P-A19: Growth of Compounds during Reactive Diffusion between Sn-base Alloys and Conductor Metals at Solid-state Temperatures: *Misako Nakayama¹; Masanori Kajihara¹; Makoto Inomoto²*; ¹Tokyo Institute of Technology

Tin-base solders are widely used in the electronics industry. If a multilayer Au/Ni/Cu conductor is interconnected with the Sn-base solder, the Au layer quickly dissolves into the molten solder during soldering, and then the Ni layer is directly contacted with the solder. Owing to reactive diffusion at the interconnection between the Ni layer and the solder, Ni-Sn compounds are formed during soldering, and then gradually grow during energization heating at solid-state temperatures. After prolonged heating, however, the Ni layer will be completely depleted by the compound growth. Due to the depletion of the Ni layer, the Cu-base conductor is directly contacted with the solder. In

such a case, the reactive diffusion between the conductor and the solder occurs at the interconnection. In the present study, the kinetics of the solid-state reactive diffusion between binary Sn-base alloys and conductor metals was experimentally observed at temperatures of 433-473 K.

P-A20: Investigation of Intermediate Phase Layers Growth in the Interdiffusion of Cu-Cd Metal System: *Jaanis Priimets¹; Ülo Ugaste¹; Jana Paju¹; Mart Viljus²; Veronika Shirokova¹; Tõnu Laas¹*; ¹Tallinn University, Institute of Mathematics and Natural Sciences; ²Tallinn University of Technology, Faculty of Chemical and Materials Technology, Centre for Materials Research

A number of investigations have shown that in certain cases the phases apparent in equilibrium phase diagrams will not emerge in the diffusion zones of real samples. This occurs most frequently in zones with narrow field of homogeneity. As the mechanism behind such phenomena is not yet fully understood, further experimental and theoretical investigations are necessary. The interdiffusion process in multiphase Cu-Cd binary metal system has been studied. The experiments have been carried out at temperatures below the eutectic (300 °C), with variation of the annealing time from 2 to 288 h. The structure of the diffusion zone and distribution of concentration have been studied by metallographical analysis, optical microscopy, scanning electron microscopy and electron probe microanalysis. In the diffusion process two intermediate phases were observed: ϵ -phase and CuCd₂. The growth rate and temperature dependence of the phase growth was investigated.

P-A21: Aging of Al Based Composites with Spherical Al₃Ti Particles: *Takaaki Hirako¹; Yoshimi Watanabe¹; Hisashi Sato¹*; ¹Nagoya Institute of Technology

In this study, aging behavior of Al based composites containing spherical Al₃Ti particles is studied. Spherical Al₃Ti intermetallic compound particles were prepared by gas atomization method. The sieved particles in the range of 75-150 μ m and 150-212 μ m were sintered with pure aluminum particles by spark plasma sintering (SPS), where volume fraction of Al₃Ti particles within the composites was fixed to be 10 Vol.%. When the composites are aged at elevated temperature, the spherical Al₃Ti particles are divided into smaller parts. This is because the spherical Al₃Ti particles prepared by gas atomization method are poly crystal.

P-A22: Precipitation Hardening in Ti-Mo-N Coating Deposited by Reactive Sputtering: *Yuji Sutou¹; Shoko Komiyama¹; Katsunari Oikawa¹; Daisuke Ando¹; Junichi Koike¹*; ¹Tohoku University

In order to enhance the functionality of TiN hard coating, simultaneous improvements are strongly required in terms of hardness, oxidation resistance, wear resistance etc. Ti-Mo-N coating with δ -phase (NaCl) is known to show lower friction coefficient and wear rates than TiN coating due to the self-formation of lubricious Mo oxide debris. However, the increase of hardness by Mo addition is only 10% or so. In this study, the effects of heat treatment on the hardness of Ti-Mo-N coatings were investigated. We found that in Ti₃₄Mo₂₈N₃₈ film the hardness increased by heat treatment due to the precipitation of bcc phase in δ matrix and a maximum hardness of around 35 GPa was obtained by heat treatment at 1000°C. Moreover, Ti₁₄Mo₃₅N₄₁ film was found to show an increase of hardness (26 GPa \rightarrow 34 GPa) by heat treatment at 700°C, which is caused by phase separation into δ -TiN (NaCl structure) and γ -Mo₂N (NaCl structure).

P-A23: Determination of HCP/BCC Boundaries and the Mechanical Properties of Dual-phase Alloy in Binary Mg-Sc System: *Yukiko Ogawa¹; Daisuke Ando²; Yuji Sutou²; Junichi Koike²*; ¹Tohoku University; ²Department of Materials Science, Graduate School of Engineering, Tohoku University

Mg alloy has been expected for next generation structural material for long time because of its high specific strength. However, conventional Mg alloys have poor formability due to hcp structure. Mg-Li alloy with HCP/BCC dual-phase is known to show good ductility, but the alloy exhibits low tensile strength and poor corrosion resistance. In this study, we propose binary Mg-Sc system as high strength HCP/BCC dual-phase Mg alloy. From Mg/Sc diffusion couple methods, HCP/BCC boundaries were found to exist in much higher Mg content region than those in reported Mg-Sc phase diagram. Moreover, it was found that Mg-Sc alloy

with a BCC/HCP dual-phase shows several times higher tensile strength than Mg-Li alloys. In the presentation, we will discuss on the relationship between mechanical properties and microstructure (two-phase structure, texture, age hardening etc) in Mg-Sc alloys.

P-A24: Role of Zn Addition on the Precipitation Sequence and Creep Properties of Mg-RE Alloys: Deep Choudhuri¹; David Jaeger¹; Srinivasan Srivilliputhur¹; Mark Gibson¹; *Rajarshi Banerjee*¹; ¹University of North Texas

Controlling the sequence of precipitation in Mg-rare earth (RE) alloys is crucial towards improving their high temperature creep properties. Using TEM and 3D-atom-probe, we have examined the role of Zn addition on second phase precipitation and creep properties of a Mg-Nd-based alloy. While Mg-Nd-based alloys exhibited the precipitation sequence: SSSS→GP zones→β¹→β²→β³, addition of only a minor quantity of Zn (0.3 at%) resulted in an entirely different sequence: SSSS→GP zones→β¹→β². The Mg-Nd-Zn based alloy contained a substantially higher number density of fine scale precipitates compared to the non-Zn alloy; along with Zn segregation at defect structures. The stability of these different precipitate phases, i.e. β¹, β², and β³ was investigated using first-principles DFT-based computations. Possible factors contributing to the altered precipitation sequence and improved creep resistance, due to Zn addition, will be discussed.

P-A25: Two-step Age-hardening Behavior of Cu-Be and Cu-Ti Alloys Processed by High-pressure Torsion: *Chihiro Watanabe*¹; Ryoichi Monzen¹; Seiichiro Ito²; Koichi Tsuchiya²; ¹Kanazawa University; ²National Institute for Materials Science

Age-hardening behavior of Cu-1.8wt%Be-0.2wt%Co and Cu-3wt%Ti alloys severely deformed by high-pressure torsion (HPT) at room temperature has been investigated on two-step aging condition; natural aging and then subsequent artificial aging. Application of HPT processing under an applied pressure of 5 GPa for 10 revolutions at 1 rpm to the alloys produced ultra-fine grained structures. The hardness of the Cu-Be and Cu-Ti alloys increased with equivalent strain and then saturated to constant values of 400 and 330 Hv, respectively. Natural aging at 293 K up to 2.6 × 10⁶ s did not essentially change the hardness of both alloys. Attained peak hardness of the Cu-Be alloy on subsequent aging at 593 K decreased with natural aging time. On the other hand, no influence of the natural aging on the age-hardening behavior of the Cu-Ti alloy during aging at 623 K was observed.

P-A26: Phase-field Simulation of Magnetic Field-induced Preferential Variant Selection in Al-L10 Disorder-order Transformation: *Hiroshi Akamine*¹; Sahar Farjami¹; Hidetsugu Sakaguchi¹; Minoru Nishida¹; ¹Kyushu University

Near-equiatomic Co-Pt and Fe-Pd alloys undergo cubic-tetragonal disorder-order transformation and form three tetragonal orientation variants. It has been reported that magnetic field-induced preferential nucleation of a certain variant in initial stage of ordering gives a rise to preferential growth of the same variant in the later magnetic field-free stage [1]. In this study, effect of preferential nucleation on microstructure evolution in the later stage was studied by phase-field method. The simulation results indicate that the elastic strain energy is the most important factor affecting preferential growth in the later stage. The increase in volume fraction of preferred variant strongly depends on nucleation ratio between the variants. Consequently, when the nucleation ratio of the certain variant is larger in the initial stage, preferential growth completes at less time steps in the magnetic field-free stage. [1] S. Farjami, M. Yasui, T. Fukuda and T. Kakeshita, *Scr. Mater.*, 58 (2008) 811.

P-A27: Influence of Applied Tensile Stress on Formation and Growth of Ellipsoidal ω Precipitates in a Ti-20wt%Mo Alloy: *Ryoichi Monzen*¹; Ryutarō Kawai¹; Chihiro Watanabe¹; ¹Kanazawa University

The effects of tensile stress on the nucleation and growth of ellipsoidal ω phase precipitates have been investigated for a Ti-20wt%Mo alloy aged at 300°C. Application of a tensile stress promotes not only the nucleation but also the growth of ω precipitates. Estimates of the average misfit strains along the loading and the transverse directions from measurements of the length change and the lattice parameter reveal preferential formation of specific ω

variants among crystallographically-equivalent four ones. The average size of the precipitates in the alloy aged under no stress follows initially a parabolic growth law, whereas when aged under a stress from 400 to 500 MPa the precipitate size increases linearly with aging time. This indicates that the growth of ω precipitates is governed by diffusion of Mo from the ω/β interface to the β matrix at the initial stage of aging, but is interface-controlled under tensile stress.

P-A28: The Effect of Pre-deformation on Precipitation in Al-Mg Alloys Containing Small Cu Additions: *Sebastian Medrano*¹; Chad Sinclair¹; Frédéric de Geuser²; Alexis Deschamps²; DaeHoon Kang³; Babak Raeesinia³; ¹Department of Materials Engineering, The University of British Columbia; ²SIMAP, INP Grenoble – CNRS – UJF; ³Novelis Global Research and Technology Center

By manipulating the interaction between precipitation and dislocations one can tailor the evolution of the mechanical response of materials during thermomechanical processing. While precipitation can be used to directly harden, it can also be used to help stabilize the strength of wrought alloys. Wrought aluminum alloys containing scandium have been shown to be particularly good at maintaining their strength even on relatively high temperature exposure, this due to the effectiveness of Al₃Sc precipitates at slowing recovery and recrystallization. In this work we have looked at lower cost alloys, using pre-deformed Al-Mg alloys containing < 1wt% Cu to see whether similar stability can be achieved. Measurements of hardness, electrical resistivity and small angle x-ray scattering have been used to evaluate the evolution of microstructure during long-term thermal exposure. The evolution of the precipitation state in pre-deformed material has been compared to that in undeformed material otherwise treated in the same way.

P-A29: Effect of Cu and Cr Additions on the Ostwald Ripening in Fe-Ni-Al Alloys: Nicolas Cayetano-Castro¹; *Victor Lopez-Hirata*²; Hector Dorantes-Rosales²; Maribel Saucedo-Muñoz²; Jorge Gonzalez-Velazquez²; ¹Instituto Politecnico Nacional (CNMN); ²Instituto Politecnico Nacional (ESIQIE)

The results of present work showed that the growth kinetics of coarsening process followed the behavior predicted by the modified Lifshitz-Slyozov-Wagner theories for diffusion-controlled coarsening during the aging of Fe-10at.%Ni-15at.%Al, Fe-10at.%Ni-15at.%Al-1at.%Cu and Fe-10at.%Ni-15at.%Al-1at.%Cr alloys at 750, 850 and 950 °C for different times. The coarsening kinetics was observed to occur more slowly in both of the aged quaternary alloys. The copper remains in the beta precipitates since the solubility of Cu is low solubility in the bcc Fe matrix and it has a good solubility in Ni and more than 4 at. % in Al, while the chromium was found to be in the ferrite matrix since it has a higher solubility in the ferrite matrix. This element partitioning is the responsible for the increase in coarsening resistance. Additionally, the highest aging peak hardness was observed to occur in the Cu-containing alloy and the lowest value corresponded to the Fe-Ni-Al alloy.

P-A30: Formation of GP Zones and β Precipitate at the Early Stage of Ageing in a Mg-Gd Binary Alloy: *Zhenyan Zhang*¹; Liming Peng¹; Yijin Tang¹; Wenjiang Ding¹; ¹Shanghai Jiao Tong University

The precipitates in a Mg-Gd binary alloy aged at 225°C were studied by high-angle annular detector dark-field scanning transmission electron microscopy (HAADF-STEM). A unit structure containing only three Gd atoms was proposed for the zigzag chain and hexagonal ring shaped GP zones forming at the early stage of ageing. This unit structure was suggested to begin from one Gd atom in the Mg-Gd solid solution, and self-assemble via the vacancy diffusion and the binding between vacancies and Gd atoms. The atomic-scaled formation models of GP zones and β precipitate were established on the basis of this unit structure.

P-A31: A Study of the Effect of Strain on Spinodal Decomposition in Fe-Cr: *Frédéric Danoix*¹; Helena Zapolsky²; Peter Hedström³; Joakim Odqvist³; ¹CNRS; ²University of Rouen; ³KTH - Royal Institute of Technology

When bcc Fe-Cr alloys are used in service at elevated temperatures embrittlement due to spinodal decomposition may occur. It is then important to consider whether the alloy is exposed to deformation since it is known to affect the kinetics of decomposition. The detailed understanding

of the effect of deformation on decomposition is however lacking and in the present work we have used a combination of atom probe tomography and phase-field modeling to elucidate these details. The effect of strain on the decomposition mechanism and the kinetics is discussed.

Displacive Transformations

P-B1: An In-situ Method to Identify Lattice Correspondences for High Temperature Ceramic Phase Transformations: Ryan Haggerty¹; Zachary Jones¹; Pankaj Sarin¹; *Waltraud Kriven*¹; ¹University of Illinois at Urbana-Champaign

Using in-situ synchrotron powder diffraction technique, planar thermal expansions are measured and plotted in 3-D using a computer algorithm (CTEAS) which depicts the quadric surface for all of the observed {hkl} d-spacings. In the case of non-orthogonal crystals such as monoclinic, the principal strains are not oriented along unit cell axes. By following the principal thermal expansion strains from one phase to another through a phase transition, a 3-D lattice correspondence can be postulated. It is assumed that the principal thermal expansion strains correlate with atomic motifs within a unit cell and that the dominating coordination polyhedra in the parent structure continue their role into the product structures. Thus a 3-D lattice correspondence can be identified and the basis for a transformation mechanism is laid. This approach is illustrated by in situ high temperature studies of the monoclinic to tetragonal transformation in hafnia (HfO₂) at 1750 °C on heating.

P-B2: Kinetics of the fcc-hcp Phase Transformation in the Cu-Ge System Studied by X-ray Diffraction: *Efthymios Polatidis*¹; Nikolay Zotov²; Eric Mittemeijer³; ¹Max Planck Institute for Intelligent Systems; ²Max Planck Institute for Intelligent Systems; ³Max Planck Institute for Intelligent Systems (formerly Max Planck Institute for Metals Research) and University of Stuttgart, Institute for Materials Science

The thermally-induced precipitation of the hcp-phase from fcc supersaturated Cu-Ge solid solutions (in the range of 8.8-11.1 at.% Ge) was claimed in the past to be an isothermal martensite transformation exhibiting C-type transformation curves in TTT diagrams [1, 2]. However, the kinetics of the hcp-phase formation upon isothermal ageing were not determined until now and therefore the above statement has not been validated until now. Against this background, in the present study in-situ X-ray diffraction studies on Cu-Ge powders (with 10.8 at.% Ge) were performed at different temperatures in the range of 200-400 °C to quantitatively study the fcc-hcp transformation kinetics and thereby to reveal the underlying transformation mechanism. [1] P.J. Moroz, R. Taggart, D.H. Polonis, J. Mater. Sci., 22 (1987) 839-852. [2] P.S. Kotval, R.W.K. Honeycombe, *Acta Metallurgica*, 16 (1968) 597-607.

P-B3: Effect of Cr and Ni on the Martensitic Transformation in Ternary Fe-Cr-Ni Alloys: *Ye Tian*¹; Annika Borgenstam¹; Peter Hedström¹; ¹KTH Royal Institute of Technology

The athermal and deformation-induced martensitic transformation in high-purity Fe-Cr-Ni alloys has been investigated. The aim is to study the effect of Cr and Ni on the microstructure of martensite as well as on the martensitic transformation behavior. The microstructural investigations are conducted using light optical microscopy, electron channeling contrast imaging and electron backscatter diffraction in the scanning electron microscope. Furthermore, the transformation regime of athermal and deformation-induced martensite is discussed based on the change of Cr or Ni content and it is related to the austenite stacking fault energy (SFE) via X-ray diffraction measurements. The relation between SFE, thermodynamic driving force and microstructure is discussed.

P-B4: Comparative Grain-scale Characterization of Mechanical Twinning in Austenitic Steel and Beta-Ti: Matthieu Marteleur¹; Perrine Tanguy¹; Frédéric Prima²; Pascal Jacques¹; ¹UCL; ²Chimie-ParisTech

Since its discovery by Sir Hadfield in the late 1800s and the first experimental evidences by TEM characterization in the 1960s, the TWIP (Twinning Induced Plasticity) effect in Fe-Mn-C steels has drawn more and more attention due to the outstanding mechanical properties exhibited by these steels. TWIP effect has also been observed in β titanium alloys from the 1970s, and those alloys also show improvement of the work hardening with the activation of mechanical twinning. This work investigated at the grain-scale, the activation of the TWIP effect in both steels and Ti alloys. Specific patterning depending on grain size is observed in both systems with some proportionality in the characteristic lengths of the mechanical twins. It is proposed that this patterning influences in a large way the mechanical response of these materials.

P-B5: Formation of Widmanstätten Ferrite in a C-Mn Steel at Temperatures High in the Austenite Phase Field: Clodualdo Aranas¹; Rupanjit Grewal¹; John J. Jonas¹; ¹McGill University

Compression tests were carried out on a 0.06%C-0.3%Mn-0.01%Si and a 0.09%C-1.0%Mn-0.41%Si-0.04%Al-0.040%Nb steel over the temperature range 1000°C to 1300°C. Strains of 0.7 were applied at a strain rate of 1s⁻¹. The double differentiation method was employed to determine the critical strains for the initiation of dynamic transformation (0.12) and dynamic recrystallization (0.20). The occurrence of dynamic transformation was detected at temperatures up to 1300°C. Optical and EBSD images indicated that Widmanstätten ferrite plates were being formed in the austenite phase field and that the plates coalesced into polygonal grains during straining. These results are interpreted in terms of the flow softening model of the transformation by calculating the driving forces promoting the transformation and the energy obstacles that oppose it. Comparison between the behaviors of the plain C and Nb steels shows that the addition of Nb delays both the forward and reverse transformation.

P-B6: Phase Transformation of Nanostructured Bainite after High-strain Rate Deformation: Yu-Ting Tsaï¹; Hung-Wei Yen¹; Jer-Ren Yang¹; Woei-Shyan Lee²; ¹National Taiwan University; ²National Cheng Kung University

In this research, a split Hopkinson pressure bar is used to study the microstructure evolution of nanostructured bainite at high strain rate, and the results indicate very high strength (>2GPa) and high fracture strain (>0.3). Scanning electron microscopy results show that large blocky austenite allows bainite sheaves to rotate, therefore accommodating more strain. Transmission electron microscopy results show that after deformation, retained austenite thin films are heavily twinned in one major variant, with tiny second or third variants nanotwins and some evidence of strain-induced martensite formation inside internal twins. On the contrary, blocky retained austenite component exhibits complex phase transformation behavior, and multiple twinning band and irregular-shaped martensite was found. Significant dislocation structure change inside nanostructured bainitic ferrite is found by scanning transmission electron microscopy. Finally, the work-hardening rate is explained by the sequential phase transformation behavior.

P-B7: Detection of the Martensitic $\gamma \rightarrow \alpha'$ a Phase Transformation on a Metastable Austenitic Steel, Using Spontaneous Magnetic Emission (SME): Edgar Apaza Huallpa¹; Julio Antonio Capó Sánchez²; Hélio Goldenstein¹; ¹Universidade de São Paulo; ²Universidad de Oriente

In this study samples from a metastable austenitic steel AISI 301 are mechanically tested in tension at room temperature in the presence of a magnetic emissions detection system. This steel is known for presenting strain-induced martensitic transformations ($\gamma \rightarrow \epsilon$ and $\gamma \rightarrow \alpha'$). It was possible to follow the transformation to α' martensite induced by deformation thanks to the detection of magnetic pulses, similar to Magnetic Barkhausen Noise (MBN), but more intense, synchronized with the advance of plastic deformation. The results indicate that the α' phase begins after the elastic part of the tensile test. The issue of magnetic pulses during the martensitic transformation, a phenomenon called SME (Spontaneous

Magnetic Emission), had previously been described during cooling at cryogenic temperatures of metastable austenite. The results were discussed in light of results for Magnetic Barkhausen Noise (MBN), X-ray diffraction and microstructures obtained before and after the tests.

P-B8: Deformation Induced Martensitic Transformation in 304 Austenitic Stainless Steel: Djamel Kaoum¹; Francois-Liguori Paul¹; Junliang Liu¹; ¹The University of South Carolina

Deformation-induced phase transformation in 304 austenitic stainless steel has been studied in tension at room temperature and cryogenic temperatures (-50 °C and -100 °C) in-situ in a Transmission Electron Microscope. The experiments were done on two types of 304 stainless steel: (i) a cold-rolled sheet and (ii) stress-relieved 304 bar. In the cold-rolled material, phase transformations could be observed during the cooling to cryogenic temperatures without external stress applied. The nucleation and growth of the martensitic phase developing under strain were monitored in-situ and captured on video. The processes involved in the phase transformation were studied. The presentation will report the observations done and analysis especially at room temperature.

P-B9: Influence of Quenching and Partitioning Conditions on the Microstructures and Mechanical Properties of a 0.2C Steel: Pierre Huyghe¹; Cédric Georges²; Stéphane Godet¹; ¹Université Libre de Bruxelles; ²CRM Group

The Quenching and Partitioning process consists of an interrupted quench between Ms and Mf from intercritical annealing or full austenitization, followed by a partitioning step in order to stabilize the austenite through carbon enrichment. In order to maximize the carbon transfer, the use of specific alloying elements and the design of appropriate Q&P parameters are required to eliminate competing mechanisms such as carbide formation and austenite decomposition. In the present work, Q&P heat treatments were carried out in a quench dilatometer on 0.2- and 0.4wt.%C-2.3wt.%Mn-1.5wt.%Si-0.2wt.%Cr steels. The kinetics of the phase transformations, especially martensite transformation, carbon partitioning and austenite decomposition were evaluated. The microstructure evolution was characterized using SEM, EBSD and XRD. The tensile properties of selected samples were measured. The mechanical properties are shown to be highly dependent on phase volume fractions and the stability of retained austenite. This is critically discussed and compared to ferrite/bainite/austenite (TRIP) microstructures.

P-B10: Variant Selection of Bainite Nucleated at Austenite Grain Boundaries: Takeshi Kaneshita¹; Goro Miyamoto¹; Tadashi Furuhashi¹; ¹Tohoku University

Bainitic ferrite (BF) has a near K-S orientation relationship with the prior austenite, leading to the formation of 24 equivalent variants. High angle inter-variant boundaries impede slip deformation and crack propagation. Therefore, variant pairing of neighboring BFs is a key to determine the mechanical properties. Moreover, specific variant BFs tend to be preferentially formed at austenite grain boundary, which is called variant selection. However, details of variant selection in practical low alloy steel have not been investigated. Therefore, the present study aims to clarify the effects of transformation temperature and carbon content on variant selection of BF isothermally formed in Fe-2Mn-C alloy. It was found that most of BF variants nearly holds the K-S orientation relationship with respect to both of adjacent the austenite grains, while this tendency is weakened at high carbon content and lower transformation temperature because of enhanced self-accommodation.

P-B11: Surface Effects on Martensitic Phase Transformation, a Simultaneous In Situ XRD and Dilatometry Study: Guilherme Faria¹; Julian Escobar¹; Antonio Ramirez²; ¹Brazilian Nanotechnology National Laboratory

Martensitic transformation temperatures are largely dictated by this transformation nucleation driving force. In FCC to BCC/BCT martensitic transformations, one of the most influential terms in this driving force is the strain energy, given the difference in atomic densities between the initial and final phases. At the surface of metallic samples, there is a direction in which the newly formed nuclei can expand freely, implying that at this region the strain energy term will be smaller than at the

core, and that the transformation will happen at different temperatures. In this work, this difference is assessed through simultaneous in situ X-ray diffraction and laser dilatometry. Transformation temperatures determined by both techniques for the sample surface and core showed differences up to 140°C. Anisotropic elasticity calculations allow the qualitative determination of the evolution of the surface martensite stress state during the test.

P-B12: On the Martensitic Transformation of AISI D2 Tool Steel through Cryogenic Cooling: Hadi Ghasemi Nanesa¹; Mohammad Jahazi²; Tom Levasseur³; ¹Ecole de Technologie Supérieure; ²Ecole de technologie supérieure; ³DK SPEC Company

In this research, high resolution BÄHR dilatometer DIL805 (A/D) was utilized to study martensitic transformation in AISI D2 tool steel at two cooling rates of 10 K.s⁻¹ and 50 K.s⁻¹ (above critical cooling rate to obtain full martensitic microstructure). Austenitizing was carried out at 1300K for 20 min then continuous cooling until 173 K was applied. The dilatometry diagrams revealed two distinct behaviors: 1) regular behavior where a single change in the slope of the curve is observed and associated with martensitic transformation; 2) an atypical behavior where another inflection point is appeared in the curve. For the regular behavior section of the curve an original equation is proposed which accurately describes the martensitic transformation and could be used for predicting such transformations in similar steels. An analysis is proposed to account for the atypical behavior which is based on the occurrence of dynamic straining of austenite during austenitization.

P-B13: Understanding the Role of Prior Austenite Grain Size in Isothermal Bainite Formation Kinetics: Ashwath M. Rav¹; Jilt Sietsma¹; Maria J. Santofimia¹; ¹Delft University of Technology

Prior austenite grain size (PAGS) is one of the key factors which influences bainite formation kinetics in steels. Previous studies indicate that austenite grain refinement increases the nucleation rate which generally results in acceleration of bainite kinetics. These studies provide, mainly, an outlook on the effects of PAGS on overall transformation kinetics. In this work, the kinetics of the bainite formation during isothermal treatments in low silicon steels is investigated. Information regarding the fraction of bainite which evolves solely due to grain boundary nucleation as well as the fraction of bainite which nucleates solely by autocatalysis is independently retrieved from dilatometry experiments. Using this approach, an attempt to provide a deeper insight into the role of PAGS on the transformation kinetics as well as on autocatalytic nucleation is carried out.

P-B14: Elastocaloric Effect in the Fe-31.2Pd (at.%) Single Crystal: Fei Xiao¹; Xuejun Jin¹; Takashi Fukuda²; Tomoyuki Kakeshita²; ¹Shanghai Jiao Tong University; ²Osaka University

In typical shape memory alloys exhibiting an obvious first-order martensitic transformation, significant elastocaloric effects appear only in the parent phases. However, we report here that a significant elastocaloric effect appears both in the parent and martensite phases in an Fe-31.2Pd (at.%) alloy, which exhibits a weak first-order martensitic transformation. When a compressive stress of 200 MPa applied in the [001] direction was removed, the specimen exhibits an adiabatic temperature decrease of more than 1.5 K in a wide temperature range of between 175 K and 335 K. The refrigeration capacity is calculated in this temperature range to be 5 MJ/m³.

P-B15: Functional Properties of Iron Based Shape Memory Alloys Containing Finely Dispersed Precipitates: Philipp Krooß¹; Peter Kadletz²; Malte Vollmer¹; Johannes Guenther¹; Christoph Somsen³; Yuri Chumlyakov⁴; Hans Maier⁵; Thomas Niendorf¹; ¹Tu Freiberg; ²Ludwig-Maximilians-Universität; ³Ruhr-Universität Bochum; ⁴Tomsk State University; ⁵Leibniz Universität Hannover

Shape memory alloys (SMAs) are promising candidates for actuation and damping applications in numerous industries. This is mainly due to their higher work output compared to other functional materials. Established SMAs such as NiTi often suffer from high processing costs which limits their usage only to expensive niche applications. In this regard, iron based SMAs (Fe-SMAs) are able to

overcome these issues since established processing routes from steel industries are well suited for fabrication of Fe-SMAs. Recent promising Fe-SMAs, such as FeNiCoAlX and FeMnAlNi show up to 13% reversible strain which makes them very attractive for actuation and damping devices. However, cyclic instability is the key issue preventing Fe-SMAs from widespread applications. Thus, this study investigates the cyclic stability in Fe-SMAs in order to identify microstructural features accountable for functional degradation. In-situ testing, electron microscopy and neutron diffraction was used to correlate between the phase transformation and microstructural features.

P-B16: In Situ SEM Observations of Nucleation and Growth of Thermoelastic Martensitic Transformation in Shape Memory Alloys: Yohei Soejima¹; Takayuki Miyoshi¹; Tomonari Inamura²; Minoru Nishida¹; ¹Kyushu University; ²Tokyo Institute of Technology

The nucleation, growth, forward and reverse transformation processes of thermoelastic martensite in polycrystalline Ti-Ni, Cu-Al-Mn and Ni-Mn-Ga shape memory alloys have been investigated by in-situ SEM cooling and heating observations. The clear information was obtained by electron channeling contrast images with back scattered electrons. For instance, the characteristic strain contrast associated with martensite formation was clearly visualized in the residual parent phase. Homogeneous nucleation was observed in Ti-Ni alloys. The homogeneous nucleation in Ti-Ni alloy was confirmed by FIB/SEM serial sectioning. On the other hand, heterogeneous nucleation from grain boundaries was observed in Cu-Al-Mn and Ni-Mn-Ga alloys. There was no microstructure memory effect of martensitic phase in the three alloys upon thermal cycles. The interaction between habit plane variants clusters of B19' martensite in Ti-Ni alloys is also presented. The evidence of thin foil effect in in-situ TEM observations will be provided.

P-B17: High Temperature TiPd Shape Memory Alloys Subjected to Severe Plastic Deformation: Thomas Waiatz¹; Mitsuhiro Matsuda²; Michael Kerber¹; Ajit Panigrahi¹; ¹University of Vienna; ²Kumamoto University

TiPd high temperature shape memory alloys show a transformation between the B2 austenite and the B19 martensite. Ti-50at.%Pd was subjected to high pressure torsion (HPT) to study its impact on the martensitic phase transformation. HPT samples were analysed by X-ray diffraction using Rietveld refinement methods. Considering possible lattice structures of TiPd (B2, B19, B19' and L10) the positions of most of the peaks agree with B19 while intensities indicate (partial) disordering or a strong texture. Additional peaks agree with a L10 lattice structure. Heating in a differential scanning calorimeter yields an exothermic signal at a temperature of about 425°C that might arise by ordering. Upon heating also recovery and grain growth occur prior to the onset of the B19 to B2 reverse transformation. Therefore the martensitic transformation occurs at almost the same temperature as in the initial undeformed alloy. Financial support by the Austrian COMET program is gratefully acknowledged.

P-B18: Two-Way Shape Memory Ni-Ti Alloys with Small Transformation Hysteresis Prepared by Rapid Solidification and Constrained Aging: Xiao Ma¹; Yuanyuan Li¹; Shanshan Cao¹; Xiping Zhang¹; ¹South China University of Technology

A simple yet effective method for fabricating Ni-Ti alloys with two-way shape memory behavior and a small transformation hysteresis is reported. Ni-Ti button ingot was prepared by vacuum arc melting, and the molten master alloy was sucked into a water-cooled copper mould under vacuum condition to obtain rapidly solidified stripe. The stripes were then subjected to thermal aging under constraint condition in specially designed moulds of different shapes bringing about series of initial bending strains. Results showed that both the aging temperature and dwelling time have significant influence on phase transformation behavior and two-way shape memory effect of Ni-Ti alloy. Deformation features of the Ni-Ti alloy stripes during cooling and heating were characterized, which are well responding to the forward and reverse R-phase transformations respectively. The small transformation hysteresis characteristic of the stripe making it a promising candidate for fabricating artificial anal sphincter.

P-B19: Effect of Ausforming Strain on Martensite Start Temperature: Binbin He¹; Wei Xu²; Mingxin Huang¹; ¹The University of Hong Kong; ²ArcelorMittal Global R&D Gent

Ausforming is generally believed to decrease the martensite start (Ms) temperature. However, the present experiment found that Ms temperature firstly increased at small strain and then decreased at large strain. This interesting finding may be explained by the competing role of dislocation played in martensitic transformation. The austenite grain boundary is the potent nucleation site of martensite. The plastic deformation of polycrystalline material results in the distribution of geometrically necessary dislocation (GND) at the austenite grain boundaries. The large deformation can result in the formation of subgrain boundaries in austenite grain interior. The pile-up of GND at the austenite grain boundary may increase the potency of martensite embryo by facilitating its plastic initiation, resulting in an increase of Ms temperature after small deformation. The formation of subgrains in austenite grain interior inhibits the propagation of the martensite glissile interface, leading to a decrease of Ms temperature after large deformation.

Advances in Experimental Techniques

P-C1: Microstructural Evolution of Severely Plastically Deformed Austenitic Stainless Steel Using Precession Electron Diffraction: Yaakov Idell¹; Jorg Wiezorek²; ¹National Institute of Standards and Technology; ²University of Pittsburgh

The properties of austenitic stainless steel can be vastly improved through thermo-mechanical processing using severe plastic deformation (SPD) techniques. Quantifying the microstructure-property relationships for the ultrafine- and nano-scale grain refined and often two-phase microstructures with conventional experimental tools is challenging. An orientation imaging microscopy (OIM) technique using automated acquisition and indexing of precession electron diffraction patterns in the transmission electron microscope (TEM) enables determination of structural metrics, such as grain size and morphology, phase fraction, texture, and grain boundary character, with local specificity from statistically significant and representative data sets with the required nanometer spatial resolution. We conducted a cross sectional study of the depth-dependent microstructure in austenitic stainless steel following SPD by linear plane-strain machining and its evolution during annealing at temperature up to 650°C. Complemented by X-ray diffraction, conventional TEM, hardness indentation and magnetometry, microstructure-property relationships have been determined. We acknowledge support from the Nuclear Regulatory Commission, NRC-38-009-935.

P-C2: Atomic Structure and Bonding of the Interfaces between Gold Nanoparticles and Epitaxially-Regrowth Oxide Substrates: Wei Zhou¹; Paolo Longo²; Guo-zhen Zhu¹; ¹Shanghai Jiao Tong University; ²Gatan

Equipped with aberration correctors and an electron energy-loss spectrometer, transmission electron microscopy allows the study of chemical composition and bonding information at atomic resolution, and thus becomes the ideal tool to investigate the interfacial complexions, which usually includes a few monolayers with intricate atomic structures. By applying the above advanced techniques, we investigated a few unique metal/oxide interfacial complexions formed between gold nanoparticles and oxide substrates, such as TiO₂ and MgAl₂O₄. The clarification of these atomic structures provides deep insights in the understanding of the abnormal epitaxial growth of a previous stable substrate (e.g. TiO₂ and MgAl₂O₄) under gold nanoparticles. In addition, this can also shed the light on the understanding of the strong metal-support interaction mechanism for heterogeneous catalysts such as Au/TiO₂ and Au/MgAl₂O₄.

P-C3: Misfit Induced Changes of Lattice Parameters in Two-Phase Systems: Coherent/Incoherent Precipitates in a Matrix: Maryam Akhlaghi¹; Tobias Steiner²; Sai Ramudu Meka³; Andreas Leineweber³; Eric Mittemeijer⁴; ¹Max Planck Institute for Intelligent Systems; ²Max Planck Institute for Intelligent Systems and Robert Bosch GmbH Heat Treatment Processes and Heat

Treatment Technology (CR/APM⁴); ³Max Planck Institute for Intelligent Systems; ⁴Max Planck Institute for Intelligent Systems and Institute for Materials Science, University of Stuttgart

Elastic accommodation of precipitation induced or thermally induced misfit leads to lattice-parameter changes in crystalline polyphase systems. Formulae for calculation of such misfit induced lattice-parameter changes are presented for the aggregate (matrix + second phase particles) and for the individual phases, recognizing the occurrence of either coherent diffraction or incoherent diffraction by matrix and second phase particles. Experimental data and theoretical predictions agree well for various cases available in the literature.

P-C4: In Situ Characterization of Precipitate Formation and Dissolution in an Al-Zn-Mg-Cu Alloy by Electrical Resistivity Measurement: Fulin Jiang¹; Hatem S. Zurob²; Gary R. Purdy²; Hui Zhang³; ¹Hunan University/McMaster University; ²McMaster University; ³Hunan University

In situ electrical resistivity measurements were employed to follow precipitation and dissolution processes in an Al-Zn-Mg-Cu alloy under non-isothermal conditions (continuous heating and cooling processes). The initial state of the material (i.e. volume fraction of pre-existing precipitates) was varied in order to highlight the competition between the various precipitation reactions. The precipitate formation and dissolution kinetics could be reliably inferred from the evolution of resistivity. The data indicates that the kinetics of η and T precipitation (and dissolution) is much faster than those of the S phase. The resistivity results were further validated using Differential Scanning Calorimetry and hardness testing.

P-C5: Transmission Electron Microscopy Study of Microstructure Evolution in Cryotreated AISI D2 Tool Steel: Hadi Ghasemi Nanesa¹; Mohammad Jahazi¹; Tom Lévasseur²; ¹Ecole de technologie supérieure; ²DK SPEC Company

After austenitization at 1300 K, samples of AISI D2 tool steel were cooled down to 173K. The evolution of the microstructure was studied by transmission electron microscope (TEM). Field-emission gun scanning electron microscope (FEG-SEM) was also used to investigate other microstructural features. Thanks to the precision and accuracy of the sample preparation and 3D imaging capability, it was possible to distinguish the complex microstructure of the investigated alloy, which was comprised of carbides, allothromorphic ferrite, Widmanstätten ferrite, acicular ferrite, and mostly bainite instead of traditionally expected martensite. The obtained results are compared with the fully martensitic microstructure obtained when a cooling rate of 50 K.s⁻¹ is used.

P-C6: Ni₃Ti₃ Investigation in an ARSMA Using ASTAR Orientation Imaging Microscopy and Phase Mapping: Xiyang Yao¹; Yuanyuan Li²; Shanshan Cao²; Xiao Ma²; Xiping Zhang²; Dominique Schryvers¹; ¹University of Antwerp; ²South China University of Technology

Applications of Ni-Ti-based shape memory alloys strongly depend on the existence and arrangement of nano- or micron-sized Ni₃Ti₃ precipitates, produced by an appropriate ageing. Obtaining quantitative and statistically relevant data on these precipitates remains a problem due to their small size and the four orientation variants in which they can appear. In the present work we have applied the new technique of automated crystal orientation and phase mapping, now available in a TEM and able to reach nanoscale resolution, to samples prepared for all-round shape memory applications (ARSMA). In these samples the configuration of Ni₃Ti₃ samples varies inside the material and quantified data on grain sizes and orientation, precipitate volume fractions, local strain fields, etc. is indispensable for further development of the material. This approach will be combined with in-situ TEM tensile testing to observe the stress-induced martensitic transformation and its variant selection due to the different precipitate configurations.

P-C7: Texture Analysis in Vacuum Arc Remelted Ingots of Ti-6Al-4V Using EBSD: *Joo-Hee Kang*¹; Seong Moon Seo¹; Chang-Seok Oh¹; Jong-Taek Yeom¹; ¹Korea Institute of Materials Science

Titanium alloys are used in a wide variety of high performance applications. The evolution of microstructure and texture during phase transformation and plastic deformation plays a significant role in determining the final microstructure and properties. In particular, the relationship between the texture of the beta phase and that of alpha phase is of great interest because many thermomechanical processing steps are conducted in the beta phase region. Therefore, the understanding of the inhomogeneous microstructure in a cast ingot is important for controlling of the microstructure in final products. In the present study, the textures of the alpha and beta phases of a large scale Ti-6Al-4V ingot were investigated using electron backscatter diffraction. The preferred growth orientation of beta phase was <100> in columnar grains. Whereas, the equiaxed grains at the center and chill region had random beta orientations. The burgers relation was validated from direct measured alpha and beta orientations.

P-C8: X-ray Absorption Fine Structure Investigation of Long Period Stacking Ordered Structure Formation in Mg-Zn-Gd Alloys: *Satoru Yoshioka*¹; Tomokazu Yamamoto¹; Kazuhiro Yasuda¹; Syo Matsumura¹; ¹Kyushu University

Magnesium based alloys in Mg-Zn-Gd with long period stacking ordered (LPSO) structure have superior mechanical properties. The specific structure is formed by the aging procedure at high temperature (623 K). Additionally, this system has many crystal structures and morphologies depending on aging temperatures and holding times. In this study, our final goal is to determine the local structure behaviors around Zn and Gd on precipitation process of LPSO phase from Mg₃Zn₁Gd₃ cast alloy. We adopt x-ray absorption fine structure (XAFS) method. The peak top position of white line Gd L3-edge X-ray absorption near edge structure for annealed sample is located at higher energy than that of as-cast sample by 0.5 eV. The shape of Zn K-edge spectrum is also changed by aging. These XANES spectrum differences between as-cast and annealed samples suggest for the local structure changes of each Gd and Zn from the as-casted sample.

P-C9: In Situ Evaluation of the hcp to bcc Transformation in Commercially Pure Titanium Using Laser Ultrasonics: *Alyssa Shinbini*¹; Thomas Garcin¹; Chad Sinclair¹; ¹University of British Columbia

The mechanical properties of titanium alloys are strongly related to microstructure developed during thermomechanical processing. An ability to follow such phase transformations in-situ would provide key information for tailoring microstructure and properties. In this work, the Laser Ultrasonics for Metallurgy (LUMet) sensor has been used to examine, in real time, the hcp to bcc phase transformation in titanium. While this technique has been shown to reliably measure transformations in steels, it has not been previously used for titanium. Here, LUMet measurements of the hcp/bcc transformation kinetics have been evaluated from ultrasound velocity measurements and compared with ex-situ metallography in order to establish the validity of the LUMet technique.

P-C10: In Situ Grain Size Measurement in a Cobalt Super Alloy Using Laser-ultrasonics: *Mahsa Keyvani*¹; Thomas Garcin¹; Damien Fabrègue²; Matthias Miltzer³; Kenta Yamanaka³; Akihiko Chiba³; ¹The University of British Columbia; ²INSA de Lyon ; ³Tohoku University

Laser ultrasonics for metallurgy (LUMet) is dedicated to in-situ monitoring of microstructure evolution during thermo-mechanical treatments. In this technique, broadband ultrasound pulses are generated and detected with lasers. For anisotropic materials, ultrasonic attenuation is caused by scattering at grain boundaries and can be related to grain size. The objective of this work is to further explore the LUMet potential for in-situ grain size measurements. The response of ultrasonic attenuation to grain growth is evaluated during isothermal annealing at various temperatures in cobalt super alloy. Correlations have been found between the average grain size and the frequency dependence of attenuation. The applicability of these relationships to quantify the changes in grain size distribution during abnormal grain growth is examined. The results of this investigation establish LUMet as a powerful tool to study evolution of microstructure in cobalt super

alloys during their processing at high temperatures to get the best mechanical strength.

P-C11: Combined Analytical Electron Microscopy and Atom Probe Tomography Characterization of Internal Interfaces in Steels: *Frédéric Danoix*¹; Xavier Sauvage¹; Mohamed Gouné²; Claire Debreux¹; Thomas Sourmail³; ¹CNRS - Université de Rouen; ²ICMCB Bordeaux - UPR CNRS 9048; ³Asco Industries -CREAS

The chemistry of internal interfaces plays a key role in modern physical metallurgy, in particular for the development of the new generations of steels. Despite the tremendous instrumental developments over the last decade, the atomic scale characterization of these interfaces in steels is still a very challenging problem. Electron microscopy and atom probe tomography are two techniques with spatial and analytical resolutions making them suitable for such analyses. In this poster, we will show the first results related to quantitative chemical analysis of interfaces obtained combining analytical electron microscopy (EDX and EELS in STEM mode) and atom probe tomography. The potential for quantitative determination of C and B in steels, and the consequences of the interface orientation in both TEM and APT specimens will be discussed.

Advances in Modelling and Simulation

P-D1: A Thermodynamic Description of Ferrous Martensite with Carbon Trapped at Dislocations: *Jiayi Yan*¹; Annika Borgenstam¹; John Ågren¹; ¹KTH Royal Institute of Technology

Ferrous martensite has been treated in computational thermodynamics simply as carbon-supersaturated ferrite for a long time, neglecting the high density of dislocations as carbon traps. As a result, in the simulations of quench-and-partition treatment, the austenitic fraction tends to be over-predicted. A thermodynamic modification of ferrite is made to account for the carbon trapped by dislocations, using the classic works on the Cottrell atmosphere and the early stage of martensitic tempering, as well as recently published atom-probe studies. The consideration of carbon trapping contributes to a general picture including the effects of the martensitic tetragonality and Zener ordering, for the purpose of a full thermodynamic description of martensite and a better prediction of the partitioning process.

P-D2: Modelling the Kinetics of Secondary Carbides Precipitation in an Industrial HP Steel: *Karolina Maminska*¹; *Anna Fraczkiewicz*²; *Jader Furtado*²; ¹MINES St-Etienne; ²Air Liquide

The main asset of austenitic stainless steels of HP type (FeCrNi-C, containing Nb, Ti and Si) is their long-time ability to support high (1000 °C) temperatures. Their mechanical resistance is mainly due to the presence of fine-scale carbide precipitation, especially NbC and M₂₃C₆. The kinetics of carbides co-precipitation has been studied experimentally (SEM, TEM) and modelled by ThermoCalc / PRISMA software at different temperatures (600 – 950°C). Experimental analysis was used to identify physical parameters necessary for modelling; especially, the interface energy values for both NbC and M₂₃C₆ carbides, hardly available from literature, could be deduced from our TEM quantitative analyses. We have shown that at 700°C, values of gamma NbC = 0.26 mJ/m² and gamma M₂₃C₆ = 0.22 mJ/m² lead to a satisfactory description of co-precipitation kinetics in terms of particle mean size. Yet, the gamma values are strongly depending on temperature, as well as the M₂₃C₆ equilibrium composition is.

P-D3: On the Tuning of Austenite Stability in a Medium Mn TRIP Steel: *Fei Huyan*¹; Jiayi Yan¹; John Ågren¹; Annika Borgenstam¹; ¹KTH Royal Institute of Technology

The influence of intercritical annealing on the austenite stability of a medium Mn steel was studied with experiments and simulations in the present work. During the intercritical annealing between 500 and 650°C, austenite nucleates and grows in between the martensite laths. Martensite relaxes into ferrite due to carbon depletion, and austenite is stabilized by enrichment of carbon. The fine mixture of austenite and ferrite with an in-lathellar distance of a few

hundred nanometers is obtained after quenching to room temperature. The Ms of the retained austenite is lower than room temperature and the TRIP effect is thus exhibited. By tuning the annealing temperature and time, the Ms of the austenite was adjusted approximately to room temperature, aiming to obtain best mechanical properties from the TRIP effect. The microstructure was simulated using Thermo-Calc and DICTRA, and Ms was predicted by a thermodynamic model. Both results showed good agreement with experiments.

P-D4: Simulation of Austenite-to-ferrite Transformation in Fe-C-Mn Alloy Using Non-equilibrium Multi-phase-field Model Coupled with CALPHAD Database: *Masahito Segawa*¹; Akinori Yamanaka¹; Sukeharu Nomoto²; ¹Tokyo University of Agriculture and Technology; ²ITOCHU Techno-Solutions Corporation (CTC)

Multi-phase-field (MPF) model has attracted much attention as one of the most powerful tool to simulate microstructure evolution during austenite-to-ferrite (γ - α) transformation in steel. Many studies have already reported the MPF model to simulate the γ - α transformation in Fe-C-Mn alloy [e.g. M. Miltzer et al. Acta Mater., 54 (2006), 3961-3972]. However, most of previous studies assumed para-equilibrium condition: only carbon atom can be redistributed during the transformation. In this study, we have developed a MPF model coupled with CALPHAD database (i.e. ThermoCalc software) to simulate the γ - α transformation in Fe-C-Mn alloy without the assumption of the para-equilibrium condition on the basis of the non-equilibrium MPF model proposed by Steinbach et al. [I. Steinbach et al., Acta Mater., 60 (2012), 2689-2701]. We have also developed the MPF model using the assumption of quasi-equilibrium. Using two MPF models, we discussed the effect of diffusion of Mn atom on the γ - α transformation behavior.

P-D5: Electronic Structure and Tetragonal Distortion in Disordered Fe-Pt and Fe-Pd Magnetic Shape Memory Alloy: *Sukeyoshi Yamamoto*¹; Tomohito Yokomine¹; *Kazunori Sato*²; Masako Ogura¹; Takashi Fukuda¹; Tomoyuki Terai¹; Tomoyuki Kakeshita¹; Hisazumi Akai²; ¹Osaka University; ²ISSP, The University of Tokyo

To discuss the electronic origin of the martensitic transformation in Fe-Pd and Fe-Pt alloys, we perform first-principle calculations by using the Korringa-Kohn-Rostoker (KKR) coherent potential approximation method. For describing delicate dependence of the total energy on the deformation, full-potential (FP) KKR method has been employed [1]. According to our total energy calculations of disordered Fe₃Pt, it is shown that the system has complex energy landscape with the tetragonal distortion, i.e., the FP-KKR predicts not only FCC (c/a=1) structure but also meta-stable BCC (c/a=1/√2) and FCT (c/a=0.93) structures. We show how the ground state changes by varying composition and degree of order. In addition to the comparison with the experiments, we also discuss the relation between tetragonal distortion and the electronic structure [2]. References: [1] M. Ogura and H. Akai, J. Phys.: Cond. Matter 17 (2005) 5741. [2] T. Yamamoto et al., Mat. Trans., 51 (2010) 896.

P-D6: Modeling of Nucleation in Materials at Large Driving Forces: *Alexander Umantsev*¹; ¹Fayetteville State University

In many material systems the process of nucleation proceeds far away from equilibrium that is, at large driving forces. In these conditions the standard approach of the stationary nucleation rate is not applicable. Examples are crystallization of organic fluids, colloids, low dimensional systems, etc. In this presentation I discuss a new approach based on the concept of lifetime of a metastable state. We use the Ginzburg-Landau-Langevin method where the internal thermal noise is modeled as an additional stochastic force of specified intensity. To calibrate the method we calculate the equilibrium properties of the metastable state using the perturbation theory and Feynman diagrams and compare the results with the simulations. We use the method to calculate the lifetime of a metastable state as a function of the supersaturation, noise intensity, and system-size. We obtained the 3D critical nuclei with large degree of ramification and non-traditional lifetime/volumed relationship.

P-D7: Statics and Dynamics of Point Defects in TiC: *Hossein Ehteshami¹; Weiwei Sun¹; Pavel Korzhavnyi¹; ¹KTH Royal Institute of Technology*

Titanium carbide incorporates many carbon vacancies whose effects on the properties are well-known. Little is known about other possible defects in TiC. We perform a systematic study of point defects in titanium carbide. The electronic spectra and atomic structures for the metal and non-metal vacancies, interstitials, and antisite defects are calculated using density functional theory and projector augmented wave method as implemented in VASP package. In many cases the symmetric point defect configurations are found to be unstable against a symmetry-breaking distortion via the Jahn-Teller mechanism. An enhanced stability of titanium dumbbells is obtained for sub-stoichiometric TiC where the dumbbells form clusters with the carbon vacancies. Possible migration pathways for point defects and their clusters in TiC are explored. The obtained electronic and phonon spectra of point defects, as well as their formation and migration energies, can be useful in spectroscopic characterization and atomistic modeling studies of TiC.

P-D8: Tracking Fe Solid Solution Level through the Whole Processing Route of Commercial Purity Aluminum Alloys: *Qiang Du¹; Yanjun Li²; Knut Martinussen²; ¹SINTEF; ²NTNU*

It has been found in the commercial purity aluminum alloys, the solid solution level of Fe has a profound effect on softening kinetics. In this paper, a through process modeling approach will be employed to predict the Fe solid solution level during casting, homogenization heat treatment, hot rolling and annealing. The models' predictions will be compared with the reported experimental results. It is expected this exercise could identify the missing links for the existing through process chain model framework to make reliable through process predictions on microchemistry evolution.

P-D9: Cation Ordering in Cuprite, CuOH: *Yunguo Li¹; Cláudio Lousada²; Inna Soroka²; Pavel Korzhavnyi²; ¹Royal Institute of Technology (KTH); ²Royal Institute of Technology (KTH)*

Cuprite is a solid form of cuprous hydroxide, whose structure was established in computational studies of Cu-O-H compounds and rationalized as a hybrid between the structures of cuprite Cu₂O and ice-VIII H₂O [1]. In contrast to Cu₂O, but similar to ice, the cuprite CuOH possesses configurational degrees of freedom associated with distributing the cations near the anions. In previous studies it was assumed (but not proved) that all the possible structures of CuOH would be degenerate in energy. We have found the ground state structure of CuOH by enumerating and searching through 82944 configurations. The cation ordering pattern in cuprite is similar to that in ice-VIII (ordered form of ice-VII). Simulated diffraction pattern for the obtained ground-state structure is similar to the one recorded from the yellow precipitate of cuprous hydroxide synthesized in this work. The electronic and phonon spectra of the obtained cation-ordered structure of CuOH are also reported.

P-D10: Phase Field Crystal Simulation of Dislocation Annihilation Mechanism of Grain Boundary under Strain at High Temperature: *Gao Yingjun¹; ¹Guangxi University*

In this work, the annihilation process of subgrain boundary (SGB) and splitting of low-angle grain boundaries (GBs) during plastic deformation near but below the melting point were simulated using the phase field crystals (PFC) model, respectively. The results show that SGBs with opposite sign move close to each other at certain distance to form a dipole of dislocation pair in relative stability. Owing to the shear stress, the dislocation pair in the SGBs changes its direction two times. In this process, the interaction of dislocation of different types occur, and also the generation of new dislocations and annihilation of dislocation by gliding, which will result in the change of Burgers vector of dislocation and the exchange of types of dislocation.

P-D11: An Analysis of the Thermal Properties of Metals: New Application of the Cluster Variation Method: *Yasunori Yamada¹; Tetsuo Mohri¹; ¹Tohoku University*

Cluster Variation Method (CVM) is an efficient statistical tool to describe phase equilibria of a given system. The original formula was proposed by late Prof. Kikuchi, and he calculated phase transformation behavior of Ising model. We propose a new extension of the CVM formalism to calculate the free energy of phonon. The advantage of the present scheme is the fact that we do not have to calculate many samplings of the dispersion relation as conventional phonon calculations, and then we diagonalize only a small number of matrixes which are defined by interatomic force constants for each cluster. Thereby, we analyzed the thermal properties of metals.

P-D12: Simulation of Impurity Atom Segregation Formation in the Vicinity of Dislocations and Crack Tips: *Andrei Nazarov¹; Alexander Mikheev²; ¹National Research Nuclear University (MEPhI); ²Moscow State University of Design and Technology*

We use new equations for the interstitial impurity diffusion fluxes under strain to study impurity atom redistribution in the vicinity of crack tips or dislocations taking into account the strain generated by mentioned defects. Two levels of simulation are applied. First one is evaluation of coefficients that determine the influence of strain tensor components on interstitial diffusion fluxes in FCC and BCC structures for different kinds of atom jumps. For this purpose we have developed a model into the framework of molecular static method taking into account an atom environment as near the interstitial site as for the saddle-point configuration. The second level is modeling of interstitial segregation formation based on nonlinear diffusion equations taking strains generated by defects. The results show, that the distribution of the interstitials near the crack tip has a quite complicated character and the hydrogen distribution has qualitatively different character as compared with carbon distribution.

P-D13: Evaluation of Parameters Influencing Recrystallization: A Simulation Study: *Panthea Seppehrband¹; Shahrzad Esmaili²; ¹Santa Clara University; ²University of Waterloo*

Mechanical properties of polycrystalline materials are highly dictated by size and distribution of their grains. Thermomechanical processing consisting of a cold-deformation process followed by an annealing treatment is a common technique to manipulate grain structure characteristics. Proper control of grain structure evolution requires deep understanding of the phenomena occurring during annealing, and more specifically during recrystallization. Isolating the individual phenomenon and analyzing its effect through experimental analysis is a very hard task to achieve, if not impossible. In this research, a microstructural simulation technique is used to study the impact of various parameters affecting progress of recrystallization, and the resultant grain structure. The parameters studied include concurrent recovery, stored-energy distribution, large intermetallic particles, and precipitates size and distribution. Simulation carried out using a Monte Carlo approach. The simulation results show that among the parameters studied, the nature of stored-energy distribution has the most dominant effect on the grain structure evolution.

P-D14: An Atomistic and Mesoscopic Investigation of Nb Precipitation in NbZr Alloys: *Maeve Cottura¹; Emmanuel Clouet¹; ¹CEA*

Niobium-containing zirconium alloys are currently used in nuclear power plants. Our goal is to understand Nb precipitation under irradiation and its consequences on the alloy behavior. Under irradiation, coherent niobium precipitates (b.c.c. structure) presenting a platelet shape lying in the basal planes appear in the Zr matrix (h.c.p.). In the present work, a multi-scale approach combining atomistic and mesoscopic simulations has been followed to understand the factors leading to this morphology. An ab-initio study has been carried out on coherent interfacial energies for NbZr systems. The different interface orientations evidenced by high resolution electron microscopy has been investigated to analyze the anisotropy of the interface energy. At a different scale, the phase field approach has been employed to understand the role of inhomogeneous and anisotropic elasticity during the formation of the precipitates using the interface energies obtained from the ab-initio calculations.

P-D15: On the Differences between Continuum and Discrete Approaches for Solute Drag Calculation during Interface Migration: *Damon Panahi¹; Hatem Zurob¹; Gary Purdy¹; ¹McMaster University*

Having an accurate description for calculation of free energy dissipation associated with diffusion of alloying elements within the interface is of significant importance in understanding kinetics of phase transformation in different alloying systems. Usually, this energy dissipation is evaluated through continuum models in which a sharp transition in interface properties within the interface is assumed. However, considering short range of atomic bounds in metallic systems, recently there has been a growing interest among researchers to adopt discrete-jump approaches for describing atomic diffusion across the interface in these systems. In this regard, it is important to have a systematic study to compare results of these two approaches. As a result, the present study deals with outcomes of these two treatments under different interface conditions. Possible differences and their subsequent effects on the kinetics of the interface migration during austenite to ferrite transformation in steels will be highlighted.

P-D16: A Novel Criterion for Determining the Optimum Value of Twist in the Topological Model of Martensitic Phase Transformations: *Xiao Ma¹; Zhaozhao Wei¹; Xiping Zhang¹; ¹South China University of Technology*

Recently, a topological model of transformations has been presented wherein the habit plane is a semi-coherent structure, and the transformation mechanism is shown explicitly to be diffusionless. In previous works of applying the topological model to martensitic phase transformations, the value of twist angle was determined based on the consideration of habit plane matching, where the physical realization of the so predicted interfacial defect networks may require reorientations of defect line directions by short-range diffusion, though no long-range diffusion is needed. In the present work, a novel criterion for determining the optimum value of twist is proposed so that the predicted interface defects are not only able to fulfill the function of fully accommodating the coherency strains arising on the terrace plane, but also capable of reaching the required position at the habit plane without long- or short-range diffusion.

Emerging Areas

P-E1: Formation of Nanocrystalline (Fe,Ni,Co) Phases on the Ti Sheet under Severe Plastic Deformation Induced by Ball Collisions: *Sergey Romankov¹; Yun Chang Park²; Jeong Mo Yoon¹; Dong Jun Shin¹; ¹Chonbuk National University; ²National Nanofab Center*

Surface severe plastic deformation induced by repeated ball collisions has recently received much consideration because of its simplicity and efficiency. One of the main problems associated with ball treatment is impurities introduced into the material from the grinding media used in the milling process. However, contamination can be favorable and provide a new approach for the fabrication of nanocrystalline composite materials. In the present work, a source of Ni and Fe contaminations was deliberately introduced into the ball treatment process. We demonstrated that Ni and Fe contaminations could be used for producing nanocrystalline magnetic (Fe,Ni) layer on the metal sheets. During processing, Ni and Fe fragments were transferred and alloyed to the surface of a Ti sheet by ball collisions. The combined effects of the deformation-induced plastic flow and mechanical intermixing resulted in the formation of the (Fe,Ni) phase. The average size of the (Fe,Ni) grains was 8 nm.

P-E2: In Situ High Temperature Synchrotron Studies of Ceramics: *Waltraud Kriven¹; Pankaj Sarin¹; Ryan Haggerty¹; Zlatomir Apostolov¹; Robert Hughes¹; Zachary Jones¹; Joachim Angelkort¹; Steven Letourneau¹; Patrick Driemeyer¹; Kevin Seymour¹; ¹University of Illinois at Urbana-Champaign*

Phase transformations in oxide ceramics can occur at exceedingly high temperatures up to 2,000°C and beyond. Here we discuss an in situ powder diffractometry technique using synchrotron radiation. The experimental

apparatus is a four-halogen lamp furnace heating to 2,000°C in air. The data is analyzed by the Rietveld profile fitting method, from which are extracted lattice parameters and (hkl) d-spacings as a function of temperature. In situ high temperature studies have been made of the displacive, monoclinic to tetragonal transformations in hafnia (HfO₂) at 1750°C and zirconia (ZrO₂) at 1170°C, respectively, on heating. The pure ferroelastic transformations in the rare earth niobates (YNbO₄, DyNbO₄, LaNbO₄) transform at ~860°C as well as the tantalates and niobates. Several reconstructive transformations have been observed in the rare earth tungstates (3Ln₂O₃•WO₃) to 1350°C and rare earth titanates Ln₂O₃•TiO₂ (to 1680°C), as well as in di-zirconium phosphate.

Industrial Applications

P-F1: Investigation of Nano-scale Precipitation Phenomena in Al-Fe and Al-Cu-(Fe) Alloys Processed Via Direct Strip Casting: *Thomas Dorin*¹; *Rajeev Gupta*²; *Ross Marceau*¹; *Nicole Stanford*¹; *Peter Hodgson*¹; ¹Deakin University; ²University of Akron

The recycling of Al-Cu-(Fe) alloys is often limited due to an increase in impurity content such as Fe during re-processing. Direct strip casting (DSC) is an emerging technology that shows tremendous potential to improve the recycling of these alloys. We demonstrate that the extremely rapid solidification (>1000°C/s) during DSC permits the retention of Fe in solid solution above equilibrium concentration. We first reveal that dissolved Fe results in significant precipitation strengthening in a binary Al-Fe alloy when submitted to subsequent thermo-mechanical treatment. We then examine the co-precipitation phenomenon of Cu and Fe in an Al-Cu-Fe system. The precipitation kinetics are investigated with in-situ Small Angle X-Ray Scattering and Transmission Electron Microscopy. The corrosion behaviour is explored with metastable pitting tests on ex-situ samples. We demonstrate that DSC results in a significant improvement of the corrosion properties of these alloys thus enhancing their recyclability.

P-F2: Synergic Effects of Aging and Severe Plastic Deformation on Strength of a Cu-Ti Alloy: *Shota Ichiji*¹; *Tomotaka Miyazawa*¹; *Toshiyuki Fujii*²; *Hiroyasu Horie*²; *Kazuki Kammuri*²; *Toshiyuki Ono*²; ¹Tokyo Institute of Technology; ²JX Nippon Mining and Metals

Structural and mechanical properties of a Cu-3.15 mass% Ti alloy processed by a combination of heat treatment and severe plastic deformation were investigated. Cylindrical shaped specimens were solution-treated and quenched into water. The solution-treated specimens were aged at 723 K for 10 h and were then severely deformed by equal channel angular pressing (ECAP) for 4 Passes. The ECAPed specimens were again aged at 623 K, 673K, and 723 K for up to 8 h. A modulated structure along the <100> directions was found to be developed by aging. Grain refinement and twin formation occurred simultaneously during ECAP. The maximum hardness of 385 Hv was obtained from the ECAPed specimen after the secondary aging at 673 K for 30 min. It was found that the aging prior to ECAP gives a dominant contribution to the strength of the alloy.

P-F3: The Effect of Niobium on Austenite Decomposition for High Strength Linepipe Steels: *Isaac Robinson*¹; *Thomas Garcin*¹; *Warren Poole*¹; *Matthias Militzer*¹; ¹University of British Columbia

Niobium is a common micro-alloying addition in the production of HSLA steels for the formation of carbonitrides that restrict recrystallization and grain growth during hot rolling and welding passes. However, Nb dissolved upon heating has been found to increase the hardenability of the steel via solute drag during austenite decomposition. These coupled effects produce a range of strength and toughness through the heat-affected zones of Nb-bearing steels. It is of interest to quantify the decomposition products to gain insight into the optimal composition of steels which are welded. In this study, three experimental steels of high Nb content and differing C content were austenitized then cooled using relevant conditions obtained from experimentally measured temperature-time histories from weld trials. The thermal histories were then selected to vary

prior austenite grain size, precipitation/solution condition of Nb, and cooling rate during austenite decomposition.

P-F4: Toughening of High Strength Low Alloy Steel by Ausforming and the Plant Trial of Yield Strength 900 MPa Grade Steel Plate: *Zhaodong Li*¹; *Xinjun Sun*¹; *Zhi-Gang Yang*²; *Qilong Yong*¹; ¹Central Iron and Steel Research Institute; ²Tsinghua University

Instead of off-line quenching and tempering (QT), on-line controlled rolling was employed to improve the toughness of low alloy steel with yield strength (YS) exceeding 900 MPa. Low carbon content ensured a high level of upper shelf energy, while ultrafine martensite block transformed from pancaked austenite decreased ductile-to-brittle transition temperature and compensated the strength loss due to carbon reduction. Two mechanisms for the refinement of martensite block were proposed: One was the austenite grain refinement in the direction of thickness, and the other was the self-accommodation of martensite variants due to austenite grain hardening. In the plant trial of the YS900 MPa grade low alloy steel plate, more than 200 J of Charpy V-notch impact absorbed energy at 233 K was obtained by the on-line toughening process, which was much higher than that by the traditionally QT treatment.

P-F5: Deformation Substructure of Austenite Evaluated by Crystallographic Reconstruction and Its Influence on Microstructure Inheritance in Low Carbon Steels: *Elodie Boucard*¹; *Nathalie Gey*¹; *Lionel Germain*^{1,3}; *Meriem Ben-Haj-Slama*^{1,3}; *Sebastian Cobo*²; *David Barbier*²; ¹Laboratoire d'Etude des Microstructures et de Mécanique des Matériaux, CNRS, Université de Lorraine; *Ile du Saulcy, Metz, F-57045 CEDEX 1, France;* ²ArcelorMittal Maizières Research SA, 57283 Maizières-lès-Metz Cedex, France; ³Laboratory of Excellence for Design of Alloy Metals for Low-mass Structures ('DAMAS' Labex), Université de Lorraine, France

Hot deformation of austenite in low carbon steels is known to influence the microstructure of the transformation product [1]. However, contradictory conclusions rise up from the literature; Growth of martensite and bainite packets has been reported as well as refinement of the transformation product or formation of a granular structure. Actually the major problem relies on the lack of knowledge concerning the substructure of deformed austenite as the phase transformation prevent its direct observation. In this contribution, we apply our crystallographic reconstruction tool MERENGUE 2 [2] to evaluate the hot deformed substructure of a 0.06%C-2.4%Mn grade steel. The result shows interesting insight to analysis the complexity of the quenched microstructure. [1] N. Yu Zolotarevskii et al, Metal Science and heat treatment, vol.55, N°9-10, 2014 [2] Germain L., Gey N., Mercier R., Blaineau P., Humbert M., Acta Materialia (2012) 60, pp 4551-4562

Mechanisms of Precipitations

TUESDAY PM ROOM: ALPINE A-B-C
SESSION CHAIR: ALEXIS DESCHAMPS,
GRENOBLE INSTITUTE OF TECHNOLOGY

15:00 Invited

A Correlative Five-dimensional Study of a First-order Phase Transformation in Ni-Al Alloys at the Subnano-to-nanoscale Levels: *David Seidman*¹; ¹Northwestern University

The temporal evolution of ordered gamma-prime (L12)-precipitates in a disordered gamma (f.c.c.) matrix is studied for Ni-12.5 Al and Ni-13.5 at.% alloys aged between 773 and 873 K for times ranging from 0.08 to 4096 h. They are studied at the subnano-to-nanoscale levels utilizing three-dimensional atom-probe tomography (3-D APT), vacancy-mediated lattice kinetic Monte Carlo (LKMC) simulations, transmission electron microscopy, and microhardness measurements. The LKMC simulations include vacancy-solute binding energies through 4th nearest-neighbor distances and it is demonstrated that the gamma-gamma-prime interfacial width depends on the range of the vacancy-solute binding energies. The rate constants for the temporal evolution of the mean-radius of the gamma-prime precipitates and the aluminum supersaturations are utilized to calculate the interfacial free energy of the gamma-gamma-prime interface and the diffusivity of Al as a function of temperature and Al concentration. The results of this study taken in concert demonstrate that this transformation is diffusion controlled.

15:30

Coupled Carbon Diffusion and Precipitation in a Dissimilar Steel Weld: *Fanny Mas*¹; *Catherine Tassin*¹; *François Roch*²; *Patrick Todeschini*³; *Yves Bréchet*¹; ¹Univ. Grenoble Alpes; ²AREVA NP; ³EDF R&D

Several phase transformations occur during post-weld heat-treatment in the vicinity of the fusion line between a low-alloy steel and an austenitic stainless steel, driven by large gradients of carbon chemical potential across adjacent regions (bainite / martensite / austenite). Bainite decarburization with cementite dissolution leads to ferritic grain growth in the low-alloy side and provides carbon which diffuses towards martensite and austenite where Cr-rich carbides precipitate. Crystal structures, volume fractions and size distributions of carbides were quantified as a function of the distance from the fusion line by ACOM-TEM and 3D reconstruction after FIB serial cuts, as well as carbon content in the martensitic matrix by APT. Results are interpreted on the basis of local compositions measured for carbon, chromium and nickel by WDS and SIMS. They allow to identify the key points for phase transformation modeling in this complex three-phase configuration.

15:45

Orientation Relationships in Iron Carbonitride Compound Layers and their Relation with Diffusional Transformations: *Andreas Leineweber*¹; *Stefan Kante*²; *Norbert Schäfer*²; *Holger Goehring*³; *Eric Mittemeijer*³; ¹TU Bergakademie Freiberg; ²University of Stuttgart; ³Max Planck Institute for Intelligent Systems (formerly Metals Research)

Nitrocarburising of workpieces from iron and iron-base alloys, including steel, usually leads to formation of compound layers, which, together with the diffusion zone underneath, can lead to favourable property changes. The compound layer typically consists of one or several iron carbonitride phases (epsilon, gamma) but occasionally also of cementite. We have characterized the microstructure development of such compound layers generated by gaseous nitrocarburising, sometimes followed by some additional heat treatment, in view of the constitution of the Fe-N-C phase diagram (e.g. Metall. Mater. Trans. A 43 A (2012) 2401). Here we present additional results from microstructural characterization of such compound layers by electron-backscatter diffraction. Characteristic orientation relationships between cementite and epsilon as well as between epsilon and gamma were observed. These orientation relationships will be discussed in view of the crystal structures but also in view of diffusional phase-transformation processes occurring in such layers.

16:00

Precipitate Growth Kinetics in Systems with Interfacial Energy and Mobility Anisotropy: A Phase-field Study: *Arijit Roy*¹; *M P Gururajan*¹; ¹Indian Institute of Technology - Bombay

A combination of Allen-Cahn and Cahn-Hilliard equations have been used to model precipitate growth kinetics recently in systems with isotropic mobility. We have extended such models to study the precipitate growth kinetics (of an isolated beta-phase particle growing from a supersaturated alpha-phase matrix) in 1-D, 2-D and 3-D systems with anisotropy in both interfacial energies and atomic mobility. In this presentation, we show the formulation and results for cubic and hexagonal anisotropies in interfacial energy and atomic mobility. Our numerical implementation is based on Fourier spectral technique. We show that the morphologies which result from interfacial anisotropy are quite different from those which result from atomic mobility anisotropy. Further, the late stage microstructures are also very different in these two cases.

16:15 Break

Phase Field Modelling I

TUESDAY PM ROOM: ALPINE D-E
SESSION CHAIR: KEN ELDER,
OAKLAND UNIVERSITY

15:00 Invited

Scale Bridging by Phase-field Models: A Thermodynamically Consistent Pearlite Model Above the Lamellar Scale: *Markus Apel*¹; *Bernd Böttger*¹; ¹Access e. V.

The fine lamellar microstructure of pearlite requires a high spatial resolution which inherently limits the feasible domain size for fully resolved phase-field simulations. Different attempts to overcome this limitation have been reported, e.g. to model pearlite as an own "phase" which requires to construct a phase diagram description. We will present an alternative, thermodynamically consistent approach which naturally fits into the phase-field concept and allows direct coupling to thermodynamic databases. Using a "diffuse phase" approximation, phase-fields for ferrite and cementite are allowed to intermix on a length scale of a pearlite grain. The "diffuse pearlite" recovers the local equilibrium phase fraction of ferrite and cementite without resolving the lamellar structure. An additional parameter allows to take into account the curvature undercooling, i.e. the lamellar spacing. We will discuss the model assumptions and also give simulation examples for industrial applications, e.g. phase transformation in the heat affected zone in welding.

15:30

Phase Field Modeling of Spinodal Decomposition Fe-Cr Based Alloys: *Thomas Barka*¹; *John Ågren*²; *Joakim Odqvist*²; *Lars Höglund*²; ¹KTH Royal Institute of Technology; ²KTH Royal Institute of Technology

In ferritic steels, especially with high Cr content, 475°-embrittlement can occur during service at elevated temperatures. This deterioration in mechanical properties is, at least in part, due to phase separation in the ferrite. Therefore, better understanding and predictability of this phenomenon is desired. In this work, modeling of the decomposition behavior for Fe-Cr based alloys has been performed using the Cahn-Hilliard equation. Special attention is given to multicomponent effects and the non-linearity of various coefficients, which many times is regarded as constant in the literature. The impact of non-linear coefficients will be discussed and compared to the simpler models normally used.

15:45

Optimisation Strategies for Phase Field Model of Concurrent Nucleation and Growth: *Ramanarayan Hariharaputran*¹; *Pavlo Rutkevych*¹; *David T Wu*¹; ¹Institute of High Performance Computing, Agency for Science, Technology and Research, Singapore

Microstructural evolution during phase transformation is significantly dependent on the characteristics of nucleation and growth phenomena which is exploited by different manufacturing processes to tune effective properties through varied microstructural outcomes. In this talk, we present a phase field model using Fourier spectral method with optimized approach for concurrent nucleation and growth to study microstructure evolution. The model handles both interface limited and diffusion limited growth and accommodates homogeneous and heterogeneous nucleation process. The nucleation and growth characteristics are dictated by the processing condition variations such as thermal history and external stresses which in turn determines the driving force for the transformation. We discuss the optimization strategies which were undertaken to address the modeling of the problem and present some results in the form of time dependent nucleation and growth rates and the characteristic microstructural outcomes such as grain size distribution as function of the processing conditions.

16:00

Application of the Extended GEB Model to Predict the Shape and Fraction Evolution of Ferrite as a Function of the Transformation Temperature for a Lean Steel Containing 1.9 w.t. % Mn: *Ze nan Yang*¹; *Wei Xu*¹; *Zhi-Gang Yang*; *Sybrand van der Zwaag*¹; ¹Faculty of Aerospace Engineering, TU Delft

In this work, the austenite-ferrite transformation in Fe-0.23C-1.86Mn alloy is studied by a 2-D model based on Gibbs-Energy-Balance considerations at the moving interface. Plate-lengthening, plate-thickening and isotropic growth are calculated. Growth with a plate-like morphology leads to the fastest reduction in Gibbs energy when the transformation takes place at 500°C and 600°C. On the contrary, isotropic (i.e. spherical) growth is preferential at 650°C. The concept, stasis for thickening of single plate, is put forward. The conditions for the single bainitic shear stasis correspond nicely to the conditions for macroscopic stasis.

16:15 Break

Crystallography

TUESDAY PM ROOM: CALLAGHAN
SESSION CHAIR: JIAN WANG,
LOS ALAMOS NATIONAL LABORATORY

15:00 Invited

FCC-BCC Martensitic Transformations: Let's Roll the Iron Atoms: *Cyril Cayron*¹; ¹EPFL

It is assumed that face centered cubic (fcc) to body centered cubic (bcc) martensitic transformations result from combinations of shears: the Bain distortion (1924) has been complemented by (shape and lattice) shear components in the phenomenological theory; and the physical models of Kurdjumov and Sachs (1930), Nishiyama (1934), or Bogers and Burgers (1964) are based on discontinuous sequences of shears and shuffles. We recently proposed a new model in which the distortion occurs directly without any ad-hoc assumption. The iron atoms move continuously as rolling balls from fcc to bcc positions in Pitsch, Nishiyama or Kurdjumov-Sachs orientations. The analytical matrices of distortion depend on only one parameter, and they are naturally decomposed into a product of Bain and a rigid body rotation. Surprisingly, they are not of shear type. This approach permits to qualitatively discuss some microstructural characteristics of martensite such as the habit planes, internal misorientations, variant grouping etc.

15:30

Crystallographic Analysis of Intervariant Boundary Planes in a Lath Martensite: *Hossein Beladi*¹; *Gregory Rohrer*²; *Anthony Rollet*²; *Vahid Tari*³; *Peter Hodgson*¹; ¹Deakin University; ²Carnegie Mellon University; ³Mississippi State University

In the current study, the crystallographic of intervariant boundary planes distribution in the lath martensite has been measured as a function of lattice misorientation

and boundary plane orientation using five macroscopic parameters approach. The distribution revealed a relatively high anisotropy with a tendency for the lath interfaces to terminate on (110) planes. This results from the crystallographic constraints associated with the shear transformation rather than a low energy interface configuration. The lath martensite habit plane was determined to be mostly (110) or near (110). The relative populations of boundaries with [111] and [110] misorientations were greater than other high index misorientations, mostly characterised as (110) symmetric tilt and (110) twist boundary types, respectively.

15:45

In Situ Observation and Crystallographic Analysis of Martensitic Transformation in Low-carbon and Low-alloy Steel: *Shoichi Nambu¹; Mayumi Ojima¹; Junya Inoue¹; Toshihiko Koseki¹*; ¹The University of Tokyo

The development of a martensitic structure in a low-carbon and low-alloy steel was investigated using in-situ observation and crystallographic analysis, including the nature of variant selection. A low-carbon and low-alloy steel (Fe-0.18C-1.5Cr-3Ni) was prepared. After polishing the observation surface, the sample was heated up to 1623 K and then immediately gas quenched. During cooling, the changes in surface morphology were detected by confocal laser scanning microscopy. The samples subjected to in-situ observation were also analyzed by EBSD. The results demonstrated that the initial stage of transformation involves the partitioning of the austenite grain into packets, after which the rate of transformation is gradual. The variant selection during transformation is not random, but is affected by the relationship between the shape deformation direction and the free surface.

16:00

Effect of Ms Gradient on Variant Selection of Lath Martensite in Ni Steel: *Yuzo Kawamoto¹*; Junya Inoue¹; ¹The University of Tokyo

The effect of the gradient of the driving force for martensitic transformation on the variant selection in lath martensite was quantitatively investigated by means of electron backscatter diffraction (EBSD) analysis in conjunction with in-situ confocal laser-microscope observation. A diffusion couple composed of 22%Ni and 30%Ni ultra-low carbon steels was heat-treated at 1473K for several different holding times to achieve various one-dimensional Ms temperature gradients ranging from 0.2K/ μm to 4K/ μm . From the in-situ observation during continuous cooling, one-dimensional stepwise growth of martensite blocks from 22%Ni to 30%Ni steel was clarified. Judging from the morphology of the martensite blocks at the growth tip, some specific variants appear to be selected. The EBSD analysis confirmed that the variants whose longitudinal direction has lower angle with Ms temperature gradient direction were predominantly selected at the growth tip. The mechanism controlling the variant selection in the Ms temperature gradient will be further discussed.

16:15 Break

Ferrous Martensites

TUESDAY PM

ROOM: NORDIC

SESSION CHAIR: EUGEN RABKIN,
TECHNION

15:00 Invited

A New Look at Martensite Tempering in 4340 Steel: *Amy Clarke¹; Michael Miller²; Robert Field³; Daniel Coughlin¹; Paul Gibbs¹; Dean Pierce³; Bjorn Clausen¹; Donald Brown¹; Kester Clarke¹; David Alexander¹; John Speer³; Emmanuel DeMoor³; George Krauss³*; ¹Los Alamos National Laboratory; ²Oak Ridge National Laboratory; ³Colorado School of Mines

Quenching and tempering of medium carbon, low-alloy steel martensite produces a wide range of useful mechanical property combinations. Although martensite in steels has been extensively studied over the last century, opportunity still exists to further understand the subtle

microstructural changes (e.g., carbon redistribution, transition carbide and/or cementite formation, and austenite decomposition) that occur during tempering with advanced characterization techniques. Here we characterize the location and distribution of carbon and other alloying elements in 4340 steel with atom probe tomography after quenching and tempering from 100 to 575°C. Transmission electron microscopy and complementary techniques reveal the nano-scale structural changes that occur and clarify the progression of microstructural evolution. These observations provide a comprehensive perspective on martensite tempering in 4340 steel and insight into the location of alloying elements with respect to carbides. Such new perspectives will contribute to the design of next generation steel alloying and processing concepts.

15:30

Evolution of Microstructure during Tempering and Its Influence on the Mechanical Behavior of 2.25Cr-1Mo Bainitic Steel: *Sylvain Dépinoy¹; Caroline Toffolon-Masclat¹; Anne-Françoise Gourgues-Lorenzon²; Ernst Kozeschnik³; Bernard Marini¹; François Roch⁴*; ¹CEA; ²Mines ParisTech - PSL Research University; ³Vienna University of Technology; ⁴AREVA

This work focuses on the effects of heat treatments on the microstructure and consequently on the mechanical properties of a forged 2.25Cr-1Mo bainitic steel, and in particular on tempering conditions between 650°C and 725°C for times up to 24 hours. Carbide precipitation sequences have been investigated by means of quantitative TEM and SEM characterizations of carbon extractive replicas. Electro-etching extraction procedure is used to produce complementary analyses on phases characteristics. Within the range considered in this study, the nature of carbides does not depend on tempering conditions, even if equilibrium is far from being reached as shown by thermodynamics computations and experimental characterizations. On the other hand, the morphology, chemical composition and number fraction of the various types of carbides evolve with time and temperature. The influence of microstructural parameters on tensile and impact properties have been investigated for selected tempering conditions in order to define an optimum microstructure.

15:45

A New Martensitic Creep Resistant Steel Strengthened by MX Carbonitrides with an Extremely Low Coarsening Rate: *Qi Lu¹; Wei Xu¹; Weijie Ma²; Wei Yan²; Ke Yang²; Yoshiaki Toda³; Sybrand van der Zwaag¹*; ¹Delft University of Technology; ²Institute of Metal Research, Chinese Academy of Sciences; ³National Institute for Materials Science

An integrated computational alloy design approach based on thermodynamics and thermokinetics, a precipitation coarsening model and a genetic algorithm optimization routine is presented. This approach is applied to the design of a novel martensitic creep resistant steel strengthened by tailored MX carbonitrides which exhibit an extremely low coarsening rate. The model takes into account the gradients in the thermodynamic potentials at the precipitate-matrix interface and the diffusion coefficients of alloying elements involved. The experimental alloy quenched to a martensitic state and a high end commercial reference martensitic steel P92 are subjected to a fixed ageing temperature of 650°C for different times up to 1000 h. The microstructure evolution and resulting hardness during the ageing are studied. Experimental results show that the newly designed steel displays a much slower decrease in hardness with time compared to that of P92, owing to the extremely low coarsening rate of the MX precipitate.

16:00

Nano-precipitation Hardening of Ultra-low Carbon Martensite: Towards the Development of Lean Maraging Metallurgy: *Wenwen Sun¹; Ross Marceau²; Christopher Hutchinson¹; David Barbier³*; ¹Monash University; ²Deakin University; ³ArcelorMittal

The current challenges in the automotive steel industry consists in developing solutions with ultra high resistance, in particular, yield strength (YS>1400MPa), while maintaining sufficient ductility and in-use properties such as weldability. Such developments are potentially good candidates for lightweight solutions leading to CO₂ savings. In this context, the current work investigates

the potential development of lean 'Maraging type' steels. Using a Genetic Algorithm coupled to a computational thermodynamic database a range of alloy chemistries have been designed that exploit nanoscale precipitation of the G Phase, an intermetallic silicide, leading to yield strengths approaching 2GPa. The precipitation of the G phase has been characterized as a function of aging time and temperature using a combination of small-angle x-ray scattering and 3D atom probe tomography. The number densities of G phase precipitates formed approach the highest densities of solid state precipitates observed in any alloy system.

16:15 Break

Precipitation: Early Stages

TUESDAY PM

ROOM: ALPINE A-B-C

SESSION CHAIR: DAVID SEIDMAN,
NORTHWESTERN UNIVERSITY

16:45 Invited

Nucleation in Metals, the Basis for the Microstructure: *Jiit Sietsma¹*; ¹Delft University of Technology

In spite of its importance, nucleation remains one of the least understood aspects of phase transformations. This is especially true for solid-state transformations in crystalline metals, in which nucleation involves structural defects and local strain at the atomic scale. The Classical Nucleation Theory indicates certain trends and explains the thermally activated character of nucleation, but is by no means a predictive model. This directly implies a limited predictive value of models of microstructure formation. A basic problem in studying nucleation is the experimental difficulty to be at the right place at the right time, with the right resolution, but a concerted effort to consider combinations of experimental and modelling results can advance the insight. In the present study, experimental results on nucleation by means of EBSD and synchrotron-based diffraction will be considered together with microstructural and atomistic simulations.

17:15

The Scientific and Industrial Relevance of the Delta-Ferrite to Austenite Phase Transformation in Iron-Carbon Alloys of Near-Peritectic Composition: *Rian Dippenaar¹; Stefan Griesser¹*; ¹University of Wollongong

We have earlier quantified the dependency of early nucleation events on the presence of diffusion fields in the direct vicinity of a newly forming cluster. We have shown that the Gibbs free energy barrier to the nucleation of an intermediate phase is highly influenced by atomic mobility and hence, cannot be neglected in nucleation theory. In the present investigation, we have applied these principles to a study of the industrially important and scientifically interesting δ -ferrite to austenite phase transition in the Fe-C system, which occurs at temperatures in excess of 1670K. By using high-temperature laser-scanning confocal microscopy, we have observed in-situ, in real time and at temperature that this reaction can occur by the progression of a planar growth front, by a cellular/dendritic morphology or by a massive-type of transformation. We will present our experimental results and propose an explanation for the occurrence of the massive-type of phase transformation.

17:30

Atom Probe Tomography (APT) Characterization of the Sequence of Phase Nucleation in a 17-4PH Steel: *Guma Yel¹; Maria Auger¹; George Smith¹; Paul Bagot¹; Michael Moody¹*; ¹University of Oxford

A major concern for 17-4PH steels operating at elevated temperatures is embrittlement due to Fe-rich (α) and Cr-enriched (α') phase separation, along with precipitation of other detrimental phases. In this study atom probe tomography (APT) has characterized the sequence of microstructural changes at the atomic scale in 17-4PH for two different heat treatments (480°C and 590°C). In the earliest stages of heat treatment at both temperatures, small Nb precipitates and NbN/CrN segregation along dislocations and lath boundaries was observed, providing heterogeneous nucleation sites for Cu-rich precipitates

(CRPs). Later at the lower temperature (480°C), Cr-rich α -phase also nucleates. Later still, the Ni, Mn, Si rich G-phase was observed to nucleate at the surface of CRPs. The evolution in scale and composition of Cr-rich α -phase and G-phase, neither of which were observed at the higher temperature (590°C), has been quantified and the sequence of nucleation will be discussed.

17:45

Early Stages of Cu Precipitation in 15-5 PH Maraging Steel Revisited: Experiments and Modelling: *Sophie Primig*¹; Georg Stechauner²; Ernst Kozeschnik³; ¹Montanuniversität Leoben; ²TU Vienna; ³Christian Doppler Laboratory ESOP TU Vienna

Even though Cu precipitation during isothermal aging of Cu alloyed maraging steels has been studied thoroughly, no detailed investigations of the early stages of Cu clustering have been carried out so far. During continuous aging with a heating rate around 15 K/min of 15-5 PH maraging steel in a differential scanning calorimeter, two exothermal reactions are observed, one around 300°C and the other one around 500°C. These signals are attributed to the nucleation and growth of Fe-rich Cu clusters in the lower temperature range, followed by Cu-enrichment of these clusters and seamless transformation into bcc-Cu precipitates at higher temperatures. This investigation focuses on the characterization and modelling of the mechanisms governing these reactions. We first present a comprehensive experimental analysis based on dilatometry, differential scanning calorimetry, hardness testing, and atom probe tomography. The interpretation of the reactions is supported by thermo-kinetic simulations which substantially aid in understanding the underlying mechanisms.

18:00

Nano-size Metallic Oxide Particle Nucleation in High-Purity Fe-10%Cr Alloy by Ion Implantation: Ce Zheng; *Aurèle Gentils*¹; Joël Ribis²; Vladimir Borodin³; ¹CNSM Univ Paris-Sud & CNRS; ²CEA, DEN, DMN, SRMA; ³NRK Kurchatov Institute

Ion implantation can work as an alternative way to synthesize nano oxide particles and study their transformation behaviors under well-controlled conditions. We report the results of metallic oxide particles formation by ion implantation and subsequent thermal annealing in Fe-10wt.%Cr alloy, which is used as model materials to study particles transformation behaviors (nucleation, coarsening...) during the industrial production route (powder co-grinding and high-pressure thermo-mechanical treatment) of the Oxide Dispersion Strengthened (ODS) steels, which are promising candidates for structural components of future nuclear plants. Compositional and structural details of particles were analyzed by a range of TEM techniques (conventional TEM, high resolution TEM, energy-filtered TEM...) combined with atom probe tomography (APT) before/after thermal annealing. These experimental results are correlated with modeling data in order to clarify the mechanisms governing the formation of oxide particles. Our study can be fed back into the optimization of the production processing of ODS steels.

18:15 Break

Phase Field Modelling II

TUESDAY PM ROOM: ALPINE D-E
SESSION CHAIR: ALPHONSE FINEL,
ONERA

16:45 Invited

Estimation of Materials Parameters by Data Assimilation with Phase-field Method: *Toshiyuki Koyama*¹; Yuhki Tsukada¹; Yuichiro Kawai¹; ¹Nagoya Institute of Technology

Recently, direct simulation of microstructure changes during phase transformation has been attained by phase-field method, and calculation of materials properties dependent on their internal microstructure have also been advanced by image-based calculation method.

However, there often exist materials parameters that values are unknown in the calculation. On the other hand, a large amount of precise microstructure data has been available through advanced several experimental methods. Furthermore, both mathematical base and computational environment on data assimilation have also been established. (Data assimilation is the process by which observations are incorporated into a computer model of a real system.) Therefore, unknown materials parameter values will be estimated efficiently through the data-assimilation where experimental microstructure data and phase-field simulation are combined. In this study, we explain the general concept of this approach and estimate the gradient energy coefficient in a phase-field simulation by using the particle-filter technique in data assimilation method.

17:15

A Phase-field Simulation Study on the Correlation between Dislocation and Habit Plane Formation during Martensitic Transformation: *Yuhki Tsukada*¹; Toshiyuki Koyama¹; Yoshinori Murata²; ¹Nagoya Institute of Technology; ²Nagoya University

During fcc-bcc martensitic transformation in low-carbon steels, dislocations occur in both austenite and martensite phases. In this study, the martensitic transformation and the evolution of dislocation density field are simulated simultaneously by the phase-field method. Dislocations in both austenite and martensite phases are taken into account, and the eigenstrain field of dislocations in the austenite phase is assumed to be inherited by the martensite phase near the interphase boundary region. Simulation results are summarized as follows: (1) the martensitic transformation progresses with the formation of the stress-accommodating cluster composed of the three tetragonal domains of the martensite phase; (2) dislocation density in the martensite phase is higher than that in the surrounding austenite phase; (3) habit plane is formed near the (575) plane of the austenite phase. It has been found that the (575) habit plane formation is attributable to the dislocations introduced during the martensitic transformation.

17:30

Origin of Monoclinic Distortion in Nanodomained Ferroelectrics: Liwei Geng¹; *Yongmei Jin*¹; Yu Wang¹; ¹Michigan Technological University

Monoclinic phases and nanoscale domains are commonly observed in ferroelectric solid solutions near morphotropic phase boundaries. In this work we employ complementary computational tools, namely, first principles density functional theory and phase field model, to investigate the interrelations between these two phenomena. We show that monoclinic distortion is a natural and essential consequence of nanodomains in ferroelectrics. Combining density functional theory calculations and phase field simulations, it is shown that the monoclinic distortion has an electrostatic origin due to the internal electric field, which is generated by the electric double layer of bound charges associated with polarization gradient across domain walls; and the monoclinic distortion increases with decreasing domain size. Thus, monoclinic phases are nonequilibrium "nanophases" in nanodomained ferroelectrics. Based on this finding, a morphotropic phase boundary-based phase diagram is constructed, where nanophases of monoclinic distortions are sandwiched between conventional rhombohedral and tetragonal phases, in agreement with experimental observations.

17:45

Analysis of Phase Decomposition in Al-Zn and Al-Zn-Cu Alloys by Phase Field Method: *Victor Lopez-Hirata*¹; Erika Avila-Davila²; Maribel Saucedo-Muñoz¹; Jose Villegas-Cardenas³; Arturo Ortiz-Mariscal¹; ¹Instituto Politecnico Nacional (ESIQIE); ²Instituto Tecnológico de Pachuca; ³Universidad Politécnica

The application of phase field method, based on the Cahn-Hilliard equation, was investigated to simulate the early stages of phase decomposition during the isothermal aging of Al-Zn and Al-Zn-Cu alloys. The simulation results indicated that the start of phase decomposition, increase in modulation amplitude, took place during the aging of binary alloys at temperatures of 100-300 °C for times of 10-600 s, while the start of phase decomposition occurred during the aging of ternary alloys at temperatures of 400-550 °C for times equal to or longer than 3600 s. This analysis also showed that the morphology of the decomposed phases

is irregular and interconnected in both of the aged alloys. Likewise, the equilibrium composition of the decomposed phases for both alloys was in good agreement with the predicted values in the equilibrium phase diagrams.

18:00 Break

Ferroelectric & Magnetocaloric Materials

TUESDAY PM ROOM: CALLAGHAN
SESSION CHAIR: JEREMY MITCHELL,
LOS ALAMOS NATIONAL LABORATORY

16:45 Invited

Formation of Monoclinic Nanodomains at the Morphotropic Phase Boundary of Ferroelectric Systems: *Xiaoqin Ke*¹; Dong Wang¹; Yunzhi Wang²; Xiaobing Ren¹; Xi'an Jiaotong University; ²The Ohio State University

The monoclinic (M) phase reported recently in ferroelectric solid solutions having compositions at the morphotropic phase boundary (MPB) between the tetragonal and rhombohedral phases could be responsible for the extraordinary piezoelectric properties of these materials, but its very existence is under serious debate. In this work we show by computer simulation that using a sixth order Landau free energy polynomial with small polarization anisotropy at the MPB and taking into account the electrostatic and elastic interactions, a hierarchical structure consisting of M phase nanodomains is formed within a composition or temperature range enclosing the MPB. It is found that the M phase, even though unstable according to the Landau free energy, is stabilized by the long-range elastic and electrostatic interactions. A new phase diagram containing the M phase is established based on the simulation results.

17:15

Defect Strength and Strain Glass State in Ferroelastic Systems: *Dong Wang*¹; Duchao LV²; Yipeng Gao²; Yu Wang¹; Xiaobing Ren¹; Yunzhi Wang²; ¹Xi'an Jiaotong University; ²The Ohio State University

It has been shown both experimentally and by computer simulations that stress-carrying defects can change a normal sharp first-order martensitic transformation (MT) to a continuous strain glass transition in ferroelastic systems and offer unique properties. However, strain glass state has been found only in limited ferroelastic systems with relatively small transformation strains by means of impurity doping. We show in this paper that there exists a critical value of defect strength relative to the strength of MTs for creating a strain glass state. Using Ti48.5Ni51.5 as an example, we show that the equivalent Von Mises strain caused by anti-site defect with randomly distribution is 7/8.9 times of that created by the stress free transformation strain of Martensitic phase in order to produce an R/B19 strain glass state. This finding may shed light on developing new strain glasses of much larger transformation strains for broader applications through defect engineering.

17:30

The Influence of Different Cooling Rates on the Magnetostructural Properties of Ni-Mn-Sn Compounds for Magnetic Refrigeration at Room Temperature: *Anne-Sophie Kalbfleisch*¹; Gufei Zhang²; Johan Vanacken²; Pascal Jacques¹; ¹Université catholique de Louvain (UCL); ²Katholieke Universiteit Leuven (KUL)

Magnetocaloric materials have recently attracted significant interest due to their possible applications for high-efficiency and environmentally friendly heat pumps and refrigerators. The magnetocaloric effect (MCE) occurs due to the reversible temperature change of a magnetic material upon the application or removal of a magnetic field. The present study deals with Ni-Mn based Heusler alloys that present large MCE through a first-order magnetostructural transition. The influence of the processing path on the martensitic transition temperatures was scrutinized both by calorimetric and magnetization measurements. It was shown that, as the cooling rate

increases, the phase transformation temperatures tend to decrease. This study aims at considering the influence of the degree of order or the level of residual stresses on the shift of transformation temperatures. This understanding could help to improve the overall efficiency of refrigeration devices, in particular by allowing an optimal grading of the magnetocaloric material.

17:45 Invited

Improved Magnetocaloric Performance of Polycrystalline Ni₂MnGa Alloys Subjected to Isobaric Thermal Cycling by Introduction of Preferred Orientation: Michael McLeod¹; Bhaskar Majumdar¹; Sven Vogel²; Donald Brown; H. Matthias Reiche; ¹New Mexico Institute of Mining and Technology; ²Los Alamos National Laboratory

Magnetocaloric materials take advantage of large changes in magnetic entropy that accompany ferromagnetic to paramagnetic transitions, to bring about refrigeration in the solid state. Both experimental work and theory suggest that the magnetocaloric effect is greatest if a structural transformation (e.g., martensite to austenite) occurs simultaneously with the magnetic transition. It has been observed that there is as much as 80% increase in magnetocaloric performance when samples are subjected to thermal cycling between the austenite and martensite phase under constant compressive stress. The rationale is that the favorable twin variants would permit easier alignment of magnetic domains, and thereby produce greater magnetization in the ferromagnetic martensite state. To answer the influence of the texture on the improved properties after isobaric cycling, we utilized neutron texture analysis of specimen after treatment as well as during in situ texture measurements at temperatures between room temperature and 100°C to simulate the thermal cycling.

18:15 Break

Microstructure Development in Steels I

TUESDAY PM

ROOM: NORDIC

SESSION CHAIR: PETER HODGSON,
DEAKIN UNIVERSITY

16:45 Invited

Mechanism of Ultra-fine Microstructure Formation during ART-annealing of a Medium-Mn Steel: Artem Arlazarov¹; Mohamed Gouné²; Alain Hazotte³; Olivier Bouaziz³; Frédéric Kegel⁴; ¹ArcelorMittal/Université de Lorraine-LEM³; ²Institut de Chimie de la Matière Condensée de Bordeaux (ICMCB), CNRS UPR 9048; ³LEM3, Université de Lorraine, CNRS UMR 7239; ⁴ArcelorMittal Research and Development

The medium Mn steels are a topic of interest from both practical and scientific point of view. Many studies were focused on the microstructure characterization, but only some of them addressed the mechanisms of austenite formation and stabilization. Hence, there are still remaining questions regarding the link between the optimum retained austenite fraction and stability and the austenite formation including both the morphological and kinetics aspects. In this work, different ART annealing treatments were performed on a cold rolled 0.1C – 4.7Mn (wt.%) steel. SEM and TEM observations as well as XRD and magnetic measurements were done to characterize the resulting microstructures. Microstructure evolution was analyzed as a function of soaking time: precipitation and dissolution of cementite; austenite nucleation, growth and stabilization. The experimental observations were compared with the predictions from thermodynamic calculations. Based on the obtained results, a mechanism of austenite formation and stabilization during ART annealing is proposed.

17:15

Retained Austenite Fractions in Medium Mn Steels with Varying Mn, C, Al, Si and Cr after Intercritical Annealing: Emmanuel De Moor¹; Singong Kang²; John Speer²; ¹ASPPRC Colorado School of Mines; ²Colorado School of Mines

Medium manganese steels are being vigorously issued for automotive applications requiring high strength and formability. Retained austenite fractions predicted to be stable at room temperature after intercritical annealing were calculated for such steels with varying Mn, C, Al, Si and Cr additions, as the basis for designing a series of experimental steels containing less than 5% Mn. The phase fraction and chemical composition of each phase at the intercritical temperature were obtained under the assumption of ortho-equilibrium solute distribution using Thermo-Calc[®] with two databases. The fraction of martensite transformed during quenching was calculated based on the austenite chemical composition. The effects of alloying additions on the retained austenite fraction with varying annealing temperature are reported and discussed in terms of four critical phase transformation temperatures. Selected behaviors of experimental steels designed based on this approach are compared with the model results.

17:30

Effect of Mn and C Segregation on the Microstructure Development of Q&P Steel: Farideh Hajy Akbary¹; Kees Kwakernaak¹; Jilt Sietsma¹; Maria Santofimia²; ¹Delft University of Technology

Optimum mechanical properties in Quenching and Partitioning (Q&P) steels are reached by adequate austenite stabilization and a limited fraction of fresh martensite. Theoretical understanding of the Q&P process has allowed the design of alloys and thermomechanical parameters to reach the desired microstructures in steels with homogenous chemical compositions. However, homogeneous chemical compositions are rarely the case in industrial steels. This research is focused on the microstructural development during the Q&P process of a 0.3C-1.6Si-3.5Mn (wt. %) steel with an inhomogeneous chemical composition by applying in-situ EPMA, SEM and EBSD techniques. It was found that during the initial quenching of the Q&P process, the Mn/C-poor regions transform to martensite and thin films of austenite are stabilized via C partitioning process. However, relatively large blocks of austenite, which form in Mn/C-rich regions, have low chance to become stable and might transform to fresh martensite during final quenching, which is detrimental for ductility.

17:45

Ultrafast Heating of Advanced High Strength Steels: Roumen Petrov¹; Athina Puype¹; Dorien De Knijf¹; Leo Kestens¹; ¹Ghent University

Microstructure, texture and the tensile properties of a 70% cold rolled advanced high strength steel with microstructure of ferrite and pearlite were studied after reheating with different heating rates and subsequent quenching. Sub-size tensile samples were reheated with rates of 10, 150, 500 and 1000°C/s to temperatures below Ac₁, between Ac₁ and Ac₃ and above Ac₃ and subsequently quenched without isothermal soaking and with isothermal soaking of 30 s and 60s. By following the microstructure and texture changes it was found that after reheating with 500°C and 1000°C the recrystallization was suppressed and the alpha-gamma phase transformation starts in non-recrystallized or partially recrystallized matrix. Significant grain refinement and increase of both tensile strength and elongation was observed in the samples after ultrafast heating and subsequent quenching without isothermal soaking. The isothermal soaking erased the grain refining effect of the ultrafast heating even if it was as short as 30s.

18:00

Bainite Formation Kinetics and Properties of an Ausformed 0.7wt% Carbon Plate: James Saragosa¹; Fateh Fazeli¹; Jason Lo¹; Gianluigi Botton²; ¹Canmet Materials; ²McMaster University

Carbide-free bainite formed below 275°C consisting of nanoscale bainitic ferrite and retained austenite demonstrates strength beyond 2GPa; so-called super bainite. A modified super bainite alloy with 0.7wt% carbon and cobalt addition was designed to achieve faster bainite formation and improved toughness. Dilatometric

study was carried out to measure transformation start time, rate and final fraction of bainite and to optimize processing conditions. Different thermo-mechanical cycles varying ausforming parameters, transformation temperature and time were carried out using pilot-scale facilities to produce prototype plates. Microstructure and properties, namely tensile and Charpy impact toughness of the plates, for various processing conditions were assessed. Electron backscattered diffraction microscopy was used to characterize the effects of ausforming on bainite morphology and variant selection. Guidelines for alloy design and processing of super strong bainitic plates with adequate toughness are discussed based on thermodynamic and kinetic concepts.

18:15 Break

Plenary 4

TUESDAY PM

ROOM: EMERALD BALLROOM

SESSION CHAIR: LONG QING CHEN,
PENN STATE UNIVERSITY

18:30 Plenary

Cluster Variation Method as a Theoretical Tool for the Study of Phase Transformation: Tetsuo Mohri¹; Tohoku University

Cluster Variation Method (CVM) has been applied to various phase transformation studies. The free energy within CVM is approximated by a finite set of cluster probabilities, and the larger the basic cluster is, which is the largest cluster considered in the entropy, more accurate result one can obtain. The computational burden associated with the introduction of larger basic clusters has been relieved along with the development of high performance computers. Major application of the CVM is the first-principles phase equilibria calculations including the stability analysis in k-space leading to the concept of spinodal ordering. The extension of the CVM to time domain has been attempted in two directions. One is the atomistic kinetics study based on Path Probability Method, and the other is CVM-PFM study which leads to multiscale calculations. Recent development of Continuous Displacement CVM opens up a possibility of unified study of replacive and displacive transformations.

Plenary 5

WEDNESDAY AM ROOM: EMERALD BALLROOM
SESSION CHAIR: JAMES HOWE,
UNIVERSITY OF VIRGINIA

08:30 Plenary

Diffusional Phase Transformations: Some Examples of Kinetic Coupling and Applications in Industrial Situations: *Yves Bréchet*¹; ¹Grenoble-INP

Diffusional phase transformations have been extensively studied and modelled in relatively simple situations where they occur as a unique phenomenon, in isothermal treatments in a macroscopically homogeneous composition field. This sound corpus of knowledge can be used in more realistic situations where several transformations compete, and where long range diffusion occurs. Example of such situations will be taken to illustrate the potential of physically based modelling to treat quasi industrial situations. The coupling of allotropic phase transformations and precipitation, the precipitation kinetics in a long range chemical flux, the coupling between grain growth and precipitation and the occurrence of abnormal grain growth, the coupling between precipitation recovery and recrystallization kinetics will be applied to the understanding of microstructure generation in microalloyed steels, to defect generation in forgings and extrusions, and to annealing kinetics in dissimilar welds.

09:30 Break

Aaronson Awards Session

WEDNESDAY AM ROOM: EMERALD BALLROOM
SESSION CHAIRS: JAMES HOWE,
UNIVERSITY OF VIRGINIA;
LONG QING CHEN, PENN STATE UNIVERSITY

09:45

On the Nature of the Bainitic and Ferritic Transformation Stasis in Steels: *Hao Chen*¹; Sybrand van der Zwaag²; ¹University of British Columbia; ²Delft University of Technology

The transformation stasis phenomenon during the isothermal formation of ferrite and bainitic ferrite in a series of Fe-C-X (X = Mn, Mo, Ni, Si) alloys has been analyzed. A so-called Gibbs energy balance approach based on solute drag theory, in which the dissipation of Gibbs energy due to diffusion inside the interface and interface friction is assumed to be equal to the available chemical driving force, is applied to theoretically predicting the transformation stasis phenomenon. Theoretical predictions are compared with experimental observations. The good agreement between experiments and predictions over several alloy systems demonstrates that the transformation stasis during the isothermal formation of ferrite and bainitic ferrite is caused by diffusion of alloying elements into the migrating interfaces, and the occurrence of transformation stasis depends on the kind of X and its concentration.

10:00

Phase Transformations in Au-Fe Particles and Thin Films: Size Effects at the Micro- and Nano-scales: *Dor Amram*¹; Oleg Kovalenko¹; Leonid Klinger¹; Eugen Rabkin¹; ¹Technion - Israel Institute of Technology

Thin Fe-Au bilayers (3-30 nm in total thickness) were deposited on sapphire substrates. Annealing in a temperature range of 600-1100°C under a reducing atmosphere (ArH₂) resulted in solid-state dewetting and the subsequent formation of micro- and nano-particles. Electron microscopy, atomic-force microscopy and in-situ X-ray diffraction were employed to systematically

study two phase transformations in the Fe-Au system: (1) precipitation of α -Fe from supersaturated Au particles; (2) (bcc) \leftrightarrow (fcc) transformation in Fe and Fe-Au thin films and particles. In both cases behaviors different than bulk were observed already for sub-micron (100nm – 1 μ m) particles. These were explained by the low defect concentration in the particles, slow diffusivity on facets and Au segregation. Diffusion and nucleation models were developed to describe these results. The main conclusion is that, contrary to the current paradigm, phase transformation proceed differently even in sub-micron particles, not only in nanoparticles. Some implications for designing particle morphologies are discussed.

10:15

Finding Critical Nucleus for Heterogeneous Nucleation at Grain Boundaries During Solid-State Phase Transformations: *Rongpei Shi*¹; Yunzhi Wang¹; ¹The Ohio State University

Despite its technological significance, heterogeneous nucleation of precipitates at grain boundaries remains poorly understood. This deficiency stems mainly from the complexity in accounting simultaneously for the orientation relationship between the nucleus and the parent grains if any, low energy facets of the nucleus and their interactions with the grain boundary plane and the force balance at the triple junctions. In this study we employ the nudged elastic band method to explore the total free energy landscape of a multi-component system formulated by the multi-phase field theory and to determine the properties of a critical nucleus (including size, shape and activation energy) as a function of grain boundary energy, interfacial energy, relative orientation between the low-energy facets of the nucleus and the grain boundary. The findings allow us to resolve some of the critical issues related to variant selection of a low-symmetry precipitate phase by grain boundaries in different alloy systems.

10:30

Application of 3D Atom Probe Tomography to the Segregation of Solutes at Austenite/Ferrite Interfaces: *Hugo Van Landeghem*¹; Brian Langelier¹; Damon Panahi¹; Gary Purdy¹; Hatem Zurob¹; ¹McMaster University

A recent model accounting for solute-drag proved able to reliably predict the transformation rate of austenite into ferrite in several ternary systems (Fe-Cr-C, Fe-Mn-C, Fe-Mn-N, Fe-Ni-C, Fe-Mo-C) at various temperatures. However, the model requires an accurate thermodynamic description of the interface in order to calculate the energy dissipated by its interaction with substitutional solutes. This interaction is directly related to the segregation of solute at the austenite/ferrite interface. We show that the segregation of substitutional alloying elements can be reliably measured by 3D atom probe analysis of interfaces obtained through decarburization experiments. These experiments yield highly planar layers of ferrite with practically constant thickness, attesting to the control they allow over the velocity of the moving interface. We also establish that the use of these segregation measurements in conjunction with a solute-drag-based model leads to a more robust estimation of the binding energies of substitutional elements to the mobile interface.

10:45

Integrated Experimental and Computational Studies of Non-conventional Transformation Pathways in Titanium Alloys: *Yufeng Zheng*¹; Robert Williams¹; Dong Wang¹; Rongpei Shi¹; Soumya Nag²; Yunzhi Wang¹; Rajarshi Banerjee¹; Hamish Fraser¹; ¹The Ohio State University; ²Xi'an Jiaotong University; ³GE Global Research Center; ⁴University of North Texas

The precipitation of hcp alpha phase in bcc beta phase matrix is critical for titanium alloys due to its significant influence on mechanical properties. The nucleation of alpha phase can be affected strongly by the structural and compositional instabilities within the beta matrix and so may follow non-conventional transformation pathways. In this research, the pathways for super-refined intragranular precipitation of the alpha phase in Ti-5Al-5Mo-5V-3Cr was studied using aberration-corrected electron microscopy and 3D atom probe tomography. Experimental results indicate clearly that the omega phase can influence this

super-refined precipitation. Phase field modeling based on structural and compositional information obtained from experiment shows that the presence of the omega phase can modify the stress and compositional field in the beta matrix and therefore provide an extra driving force, and nucleation site, for alpha precipitation. A detailed understanding of non-transformation pathway controlling super-refined alpha microstructure in Ti-5553 will be described.

11:00 Break

Austenitization

WEDNESDAY AM ROOM: ALPINE A-B-C
SESSION CHAIRS: JER-REN YANG,
NATIONAL TAIWAN UNIVERSITY;
SETSUO TAKAKI, KYUSHU UNIVERSITY

11:30 Invited

Effect of Heating Rate and Microstructural Scale on Austenitization: *Kester Clarke*¹; Amy Clarke¹; Robert Hackenberg; Chastity Vigil¹; Chester Van Tyne²; ¹Los Alamos National Laboratory; ²Colorado School of Mines

The effect of heating rate and prior microstructure on austenitization kinetics has been evaluated for induction hardenable steels with ferrite-pearlite or spheroidized initial microstructures. Initial microstructural conditions were used to vary microstructural scale. Dilatometry at various heating rates was used to assess austenitization heat-treatments. As-quenched hardnesses were determined as a function of heating rate and maximum temperature for each microstructural condition. The initial microstructural scale and alloy composition are shown to cause significant variation in the as-quenched microstructure and material properties, particularly for the highest heating rates. Diffusion simulations support the observed microstructural and material property differences observed between the various initial microstructures and the plain carbon and alloy steel compositions.

12:00

Study of Austenitization Kinetics by In Situ Synchrotron X ray Diffraction for Different Initial Microstructures: *Benoit Denand*¹; Vladimir Esin²; Quentin Le Bihan¹; Moukrane Dehmas¹; Julien Teixeira¹; Guillaume Geandier¹; Sabine Denis¹; Thomas Sourmail³; Elisabeth Aebly-Gautier¹; ¹Institut Jean Lamour - UMR 7198 CNRS - Université de Lorraine; ²MINES ParisTech; ³Ascometal - CREAS

The formation of austenite during slow and fast heating (0.25–100°C/s) was investigated for three initial microstructures (ferrite-pearlite, bainite or tempered martensite) of low-alloy steel. New observations from high-energy X-ray diffraction (HEXRD) concern in-situ tracking of the amount of all phases: not only ferrite and austenite, but also cementite. Moreover, results reveal two kinetics regimes of austenite formation, corresponding to simultaneous transformation of ferrite and cementite, followed by progressive disappearance of remaining ferrite for each initial microstructure. While this is well known for ferrite-pearlite, it is not yet documented for bainite and tempered martensite. In addition, lattice parameters evolutions were characterized. These measurements reveal a non-linear evolution with temperature for the retained austenite in the initial bainite microstructure. Also, the time required to homogenize the austenite is examined. Microstructure evolution calculations based on a diffusion-controlled mechanism helped rationalize the differences observed between the three initial microstructures.

12:15

Influence of Heat Treatment on the Stability of Austenite in a High Co-Ni Secondary Hardening Steel: Marina Gruber¹; Gerald Ressel¹; Manfred Wiessner¹; Sarah Ploberger²; Stefan Marsoner¹; Reinhold Ebner¹; ¹Materials Center Leoben Forschung GmbH; ²Böhler Edelstahl GmbH & Co KG

In high Co-Ni steels thin layers of austenite have beneficial effect on toughness properties. As the positive impact on toughness is rather related to reverted austenite than to retained austenite layers, this work presents an experimental study corroborated with thermodynamic simulations to characterize the differences between retained and reverted austenite and their evolution during tempering. To this end chemical composition and the phase arrangement of retained and reverted austenite and martensite were characterized by atom probe tomography and transmission electron microscopy at different stages of tempering. Additionally, correlation of these experimental findings with thermodynamic simulations allowed a more detailed understanding of austenite evolution. The investigations revealed that the composition of retained austenite remained unchanged during tempering because of diffusional inability of austenite on the one hand and that the reverted austenite was mainly formed as a result of nickel diffusion in martensite towards the retained austenite layers.

12:30

The Growth of Austenite from Martensite during Continuous Heating in a Fe-0.1C-2Mn Steel: Koutarou Hayashi¹; Toshinobu Nishibata¹; Masato Enomoto²; ¹Nippon Steel & Sumitomo Metal Corporation; ²Ibaraki University

The growth of austenite from martensite during continuous heating was studied at a heating rate of 28 °C/s in an Fe-0.1C-2Mn alloy. Under the assumption that austenite precipitated at martensite lath boundaries with a 200 nm thickness, the planar growth of austenite/martensite interface was simulated by DICTRA. The volume fraction of austenite determined by dilatometry was much smaller than that simulated under paraequilibrium, and was even that under local equilibrium except near the time of completion. This is probably because nucleation was not taken into account in the simulation. The Ac3 temperature at which austenitization was completed was well above the Ae3 of the alloy and even that of a Fe-2Mn alloy, presumably due to the depletion of Mn as well as carbon during the growth of austenite from the martensite matrix.

12:45

Growth of Austenite-Ferrite Boundaries at a Late Stage of Austenitization in an Fe-0.1C-3Mn-1.5Si Alloy: Ran Wei¹; Masato Enomoto²; ¹International Research Institute for Steel Technology, Wuhan University of Science and Technology; ²Emeritus Professor of Ibaraki University

The growth of austenite at a late stage of austenitization was studied with focus on the possible shrinkage of austenite which was discussed in a previous paper [R. Wei et al, Acta Mater., 61(2013), 697]. The overall volume fraction of austenite which nucleated at martensite lath boundary did decrease by holding at longer times than previously. The result of STEM-EDX analysis in an Fe-0.2C-5Mn alloy that a high Mn concentration region formed near the boundary in austenite lends support to this observation. The shrinkage of austenite seems to occur from the formation of a non-partitioned austenite at early stages and the subsequent diffusion of Mn from the high concentration region near the boundary to the inside Mn-lean region after the growth of austenite essentially stopped. The conditions in which the boundary moves back at a later stage will be discussed.

13:00

Mechanism of Austenite Formation in an Intermediate 3.5Mn Steel with Mn-enriched Cementite: Qingquan La¹; Mohamed Gouné²; Astrid Perlade³; Thomas Pardoën¹; Olivier Bouaziz²; Yves Bréchet⁶; ¹The University of British Columbia; ²CMCB-CNRS; ³ArceleMittal Global R&D; ⁴Université catholique de Louvain; ⁵Université de Lorraine; ⁶Université de Grenoble

The re-austenitization from spheroidized microstructure during intercritical annealing was studied in a Fe-0.1C-3.5Mn alloy, in which the cementite is enriched with Mn. The austenite grains dominantly nucleate at the intergranular

cementite but not at the intragranular cementite. The austenite growth is accelerated by increasing annealing temperature. The simulation by DICTRA, assuming local equilibrium condition, reproduces the austenite growth kinetics at various temperatures. The predicted C and Mn activity profiles show that, when the cementite Mn content is high, the austenite growth is essentially composed of two stages: a partitioning growth controlled by Mn diffusion in ferrite, and a stage controlled by Mn diffusion in austenite for final equilibration. The partitioning growth results in homogeneous carbon distribution within austenite, which is supported by NanoSIMS carbon mapping. A parametric study predicts that if the cementite Mn content is sufficiently decreased, the initial negligible-partitioning growth controlled by carbon diffusion in austenite becomes significant.

13:15

Phase Field Modeling of Cyclic Phase Transformations in Low-carbon Steels: Benqiang Zhu¹; Hao Chen²; Matthias Militzer¹; ¹University of British Columbia; ²Tsinghua University

A phase field model has been developed to describe microstructure evolution during cyclic phase transformations for two low-carbon steels (Fe-0.1wt%C, Fe-0.1wt%C-0.5wt%Mn). The austenite-ferrite transformations are assumed to occur under negligible-partition conditions for Mn and only long-range diffusion of carbon is considered. A Gibbs-energy dissipation model has been integrated with the phase field model to describe the stagnant stages during cyclic phase transformations in the ternary alloy. Experimental results, e.g. length of stagnant stages and the cyclic phase transformation kinetics, have been successfully duplicated with 2D phase field simulations.

Phase Transformations in Ceramics and Minerals

WEDNESDAY AM ROOM: ALPINE D-E
SESSION CHAIRS: JILT SIETSMAN,
DELFT UNIVERSITY OF TECHNOLOGY;
ERIC LASS, NATIONAL INSTITUTE OF STANDARDS
AND TECHNOLOGY

11:30 Invited

Phase Transformations in Fergusonite Type Rare Earth Tantalates: Robert Hughes¹; Zlatomir Apostolov¹; Pankaj Sarin¹; Waltraud Kriven¹; ¹University of Illinois at Urbana-Champaign

Rare-earth tantalates have received a lot of attention due to their potential use in environmental and energy related applications. They have high chemical and electrochemical stability and can demonstrate ion conductivity, luminescence and photoelectronic activity. They have potential applications as phosphors, as catalysts and in fuel cells. The orthotantalates have several different structures, dependent on temperature and synthesis route. The normal room temperature phase is that of fergusonite, (Y, RE)NbO₄, monoclinic I2/a. When made by lower temperature solution based routes, the M' P2/a structure is formed. At high temperatures (>1300 °C) both structures transform to a scheelite phase, tetragonal I4_a. We present a study of the phase transformations of fergusonite RE₂TaO₄ (RE = Nd, Sm, Gd, Dy, Ho, Er) through in-situ synchrotron X-ray diffraction carried out at NSLS and APS up to 1700°C and DSC experiments up to 1550 °C, and discuss the order and mechanisms of the transformation.

12:00

A Microstructure Study on the Decomposition of Ti-Zr-C: Taoran Ma¹; Peter Hedström¹; Andreas Blomqvist²; Ida Borgh³; Joakim Odqvist¹; ¹KTH- Royal Institute of Technology, Sweden; ²Sandvik Coromant R&D; ³Sandvik Mining AB, R&D Rock Tools

The mixed carbide (Ti,Zr)C is a promising candidate as the main hard phase in cermets and as an additional hard phase along WC in cemented carbide. Furthermore, it can be deposited as a coating to improve the performance of cutting tool inserts. In the present work, a near-single

phase (Ti,Zr)C has been synthesized and subsequently aged at different temperatures up to 500 h. X-ray diffraction, scanning electron microscopy and electron backscatter diffraction was performed to characterize the microstructure after aging. Based on the results, the mechanism of the phase separation is discussed.

12:15

The Characterization of the Orthorhombic to Hexagonal Phase Transformation in Dy₂TiO₅: Kevin Seymour¹; Daniel Ribero¹; Waltraud Kriven¹; ¹University of Illinois at Urbana-Champaign

The relationship between the orthorhombic and hexagonal phases in the Ln₂TiO₅ (where Ln = Gd, Dy, and Y) system is not well understood, and conventional laboratory equipment is not sufficient to fully characterize the transformation. In this study, *in situ* high temperature synchrotron X-ray diffraction in conjunction with differential scanning calorimetry was employed to shed light on the kinetics and mechanisms behind this transformation. The thermal expansion behavior in both the parent and product phases was also examined to bring additional clarity and understanding of the mechanism at the transition temperature. The transformation was found to be reconstructive and first ordered in nature, and fit well with the Avrami nucleation and growth kinetic model.

12:30 Invited

Element Partitioning at Reaction Interfaces in a Reactive Diffusion Setting: Spinel Layer Growth in the MgO-Al₂O₃ System, Experiment and Thermodynamic Model: Rainer Abart¹; Jiri Svoboda²; Petr Jerábek³; Erwin Povoden-Karadenitz⁴; Gerlinde Habler¹; ¹University of Vienna; ²Institute of Physics of Materials, Academy of Sciences of the Czech Republic; ³Charles University Prague; ⁴Technical University Vienna

Corona structures formed by reactive diffusion are common phenomena in rocks. From their phase content, composition patterns, and microstructure the formation conditions can be reconstructed, if the underlying processes are calibrated. We report on experimental layer growth of magnesio aluminate spinel (MgAl₂O₄) at periclase (MgO) corundum (Al₂O₃) interfaces aiming at identifying and quantifying these processes. Periclase and corundum were contacted and annealed at 1623K and ambient pressure for 5 to 160 hours. Along the contact a spinel layer formed showing parabolic growth. The spinel exhibits monotonic decrease in Al content from the spinel-corundum interface to the spinel-periclase interface, where local spinel-periclase equilibrium is closely attained. In contrast, at the spinel-corundum interface the Al content increases with run duration approaching but never attaining local equilibrium. Based on the experimental data a thermodynamic model accounting for dissipation due to long-range diffusion, interface migration, and generation/annihilation of vacancies at reaction interfaces is calibrated.

13:00 Invited

Evolving Microstructures, Deformation, and Fracture in Solid Oxide Fuel Cell Anode Materials: Mikko Haataja¹; ¹Princeton University

Energy conversion processes in solid oxide fuel cell (SOFC) materials are strongly affected by a nonlinear coupling between mass/charge transport, heat transport, and morphology at nanometer and micrometer length scales in a multi-phase/multi-component system. Furthermore, under continuous operation, these complex morphologies and local compositions evolve over time in response to a multitude of physical, chemical, and mechanical cues at elevated temperatures. In the first part of my talk, I will present our recent work on quantifying coarsening kinetics of metallic particles within SOFC cermet anode materials based on large-scale diffuse-interface model simulations. In the second part of my talk, I will focus on the development of elastic stresses and resulting mechanical failure in SOFC anode materials driven by re-oxidation of the metallic particles by employing a diffuse-interface fracture mechanics model within a finite deformation framework.

Displacive Transformations in Non-Ferrous Alloys

WEDNESDAY AM ROOM: CALLAGHAN
SESSION CHAIRS: YU WANG, MICHIGAN TECH;
YUNZHI WANG, OHIO STATE UNIVERSITY

11:30 Invited

Stress-induced Transformations During the Compression of a Ti 1033 Alloy: Mansur Ahmed¹; Azdiar Gazder¹; Ahmed Saleh; David Wexler¹; Elena Pereloma¹; ¹University of Wollongong

Realisation of transformation-induced plasticity and/or twinning-induced plasticity is a promising pathway to combat the low ductility of Ti alloys. Near- β Ti-10V-3Al-3Fe (wt.%) alloy containing after thermo-mechanical processing different fractions of α phase was compressed to 40% reduction. Detailed microstructure evaluation was carried out using high resolution scanning transmission electron microscopy and electron back scattering diffraction. For the first time, deformation-induced $\beta \rightarrow \alpha'$ and $\beta \rightarrow \omega$ transformation products together with $\{332\}\langle 113 \rangle \beta$ and $\{112\}\langle 111 \rangle \beta$ twinning systems were simultaneously detected in a meta-stable β alloy with α phase. The effects of the strain rate and β phase stability on the preferential activation of these reactions were analysed. It was found that stress-induced phase transformations became restricted with increase in β phase stability and strain rate. On the other hand, compared to $\{112\}\langle 111 \rangle \beta$, $\{332\}\langle 113 \rangle \beta$ twinning was more dominant in the least stable β condition and twinning fraction was enhanced with increase in strain rate.

12:00

In Situ Investigation of Plasticity Mechanisms in β -Metastable Titanium Alloys Presenting Synergetic TRIP and TWIP Effects: Matthieu Marteleur¹; Pascal Jacques¹; Frédéric Prima²; Hosni Idrissi¹; Steven Van Petegem³; ¹Université Catholique de Louvain; ²Chimie-ParisTech; ³Paul Scherrer Institute

β -Ti alloys with plasticity driven by dislocation glide suffer from a lack of work hardening, which is most of the time a major drawback. Recently, several β -metastable Ti grades have been designed to exhibit simultaneous TRIP and TWIP effects in order to improve mechanical properties of as-quenched β phase. Indeed, work hardening rates never reached before by Ti alloys seem to result from the activation of α' stress-induced martensitic (SIM) phase as well as from mechanical twinning with ω phase precipitation. In this work, we investigate the mechanisms of β twinning and $\beta \rightarrow \alpha'$ SIM transformation during tensile loading with *in-situ* synchrotron XRD, EBSD and TEM microscopy in as-quenched Ti-12 wt.% Mo alloy, as well as their own role in the global improvement of the mechanical properties.

12:15

Stability of the Two-phase Microstructure of Shocked Zircirconium: Donald Brown¹; Jonathan Almer; Ellen Cerreta¹; Bjorn Clausen¹; ¹Los Alamos National Lab

The microstructure of two-phase (α/ω) shocked zirconium was studied in-situ during heating with high energy X-ray diffraction techniques. The volume fraction of the metastable ω -phase was monitored as the reverse phase transformation occurred: the start and finish temperatures being 470K and 550K, respectively, during heating at 3K/min. Phase strains were monitored and separated in terms of thermal expansion and mechanical strains due to local phase constraints. Stresses in the α zirconium were estimated to be a superposition of a hydrostatic component (of order -50MPa) and uniaxial component (of order -600MPa) along the c-axis. A high dislocation density was observed in both the α and ω phases in the as-shocked state. The dislocation density of the ω phase decreased preceding the reverse transformation suggesting that it is the presence of the high concentration of defects in the ω phase which retarded the reverse transformation to the stable α phase.

12:30

Aging and the δ -to- α' Transformation in Pu-Ga Alloys: Jeremy Mitchell¹; Franz Freibert¹; Terence Mitchell¹; Daniel Schwartz¹; ¹Los Alamos National Laboratory

Face-centered cubic δ -phase plutonium that has been stabilized to room temperature with small amounts of Ga (<3 at. %) will transform to monoclinic α' at \sim -100°C. This martensitic transformation results in a very large volume contraction, has a large temperature hysteresis, and saturates at \sim 30% α' phase fraction. Defects associated with processing can inhibit or even prohibit transformation onset, and annealing above 150°C can reset the microstructure such that normal transformation is possible. In this presentation, we will describe ongoing work on how aging and radiation damage influence the δ -to- α' transformation as studied using dilatometry. In particular, we will focus on sequential annealing studies and what they reveal about transformation behavior.

12:45

Heating-cooling Asymmetry in the δ - γ Transformation in Plutonium: Clausius-Clapeyron Considerations: Daniel Schwartz¹; Jeremy Mitchell¹; ¹Los Alamos National Laboratory

On heating, the regions of plutonium allotropic stability and phase transformation onset temperatures are well-defined. Cooling behavior is quite different, and the δ - γ cooling transformation displays a burst character, with an anomalously large region of metastable coexistence of the δ -Pu and γ -Pu phases. The structure of this phase transformation will be described in detail. Pu phase transformations were examined quantitatively in terms of the Clausius-Clapeyron relation to get information about the pressure-temperature behavior of Pu near its critical points. Compared to the other solid-state transformations in the Pu system, δ - γ has an unusually large P-T slope, suggesting that a pressure-arrest mechanism may be operating to produce the burst phenomenon. The mechanism will be described in detail. C-C arguments do not explain why bursting only occurs upon cooling, but recent work examining the detailed atomic movements required to transform from δ to γ structure provide insight into the asymmetry.

13:00

On the Mechanism of Nucleation and Growth of Omega Phase in Beta Titanium Alloys: Robert Williams¹; Yufeng Zheng¹; Talukder Alam²; Deep Choudhuri²; Rajarshi Banerjee²; Dipankar Banerjee³; Hamish Fraser¹; ¹The Ohio State University; ²University of North Texas; ³Indian Institute of Science

The omega phase forms in many beta titanium alloys following fast quenching. It is generally accepted that the mechanism is displacive, involving the collapse of {111} planes in the beta phase. In contrast, the results of the present research are consistent with a mechanism of atom shuffle and diffusion. Thus, full and partial collapse of {111} planes were characterized in the as-quenched state for various Ti-Mo binary systems using aberration-corrected electron microscopy. Solute diffusion between omega phase and parent beta phase was studied in multi-component systems using 3D atom probe and x-ray energy dispersive spectroscopy. The results, obtained from direct observation of the nucleation and growth of omega, support a mechanism of formation involving the shuffle of every two of three neighboring {222} atom planes along $\langle 111 \rangle$ direction. The composition of omega phase is achieved by the solute diffusion across omega/beta interface. The transformation is characterized a mixed mode.

13:15

Cahn-Rosenberg Distortion and the Orthorhombicity of Titanium Martensites: Jiayi Yan¹; Gregory Olson²; ¹KTH Royal Institute of Technology; ²Northwestern University

The orthorhombicity of martensitic structure in Ti alloys can be explained by an anisotropy of pair correlations due to short-range ordering (SRO), as proposed by Cahn and Rosenberg. We use first-principle supercell calculations and configurational entropy to obtain equilibrium short-range ordering degrees at temperature in eight binary Ti systems. The composition dependence of martensitic orthorhombicity shows a system-dependent sensitivity to the SRO anisotropy. Such SRO sensitivities falls into strong and weak groups, which correlate with the atomic radii of the alloying elements.

Microstructure Development in Steels II

WEDNESDAY AM ROOM: NORDIC
SESSION CHAIRS: ERIC JAEGLER,
MAX-PLANCK-INSTITUT FÜR EISENFORSCHUNG;
AMY CLARKE, LOS ALAMOS NATIONAL
LABORATORY

11:30 Invited

The Control of Transformation in Steels Through Conventional and Novel Processes to Produce New Products: Peter Hodgson¹; Ilana Timokhina; Hossein Beladi; Nicole Stanford; ¹Deakin University

Steel products rely on the control of the phase evolution to develop microstructures suitable for a wide range of applications. The nature and scale of the transformation phases and the evolution of precipitates and solutes are all important in determining the strength, ductility and toughness as well as other properties. This paper will review recent work related to the control of the microstructure under conventional deformation and cooling conditions as well as the more radical conditions experienced under new processes such strip casting. In the latter case the cooling rates during the initial phase transitions are extremely rapid and lead to unique microstructures both in terms of the nature of the phases but also the precipitates and solutes. These can have a dramatic effect on downstream processing as they interact with the deformation and recrystallization reactions. For conventional processing there are two major aims. The first is to reduce the scale of the microstructure to obtain ultrafine or nanoscale transformation products, while the second is to also control the evolution and size and stability of the precipitates.

12:00

Advanced Experimental Approach Using EBSD to Quantify the Influence of Nb on Phase Transformations in X80 Linepipe Steel: Jennifer Reicher¹; Matthias Militzer¹; Warren Poole¹; ¹The University of British Columbia

The graded microstructure in the heat affected zone (HAZ) of state-of-the-art girth welded pipelines consists primarily of complex bainitic transformation products. The details of these HAZ microstructures depend on the welding technique and the associated thermal profiles that also affect the amount of Nb in solution as a function of the distance from the fusion line. An X80 linepipe steel has been investigated and tools were established to characterize and quantify complex bainitic transformation products occurring in the HAZ. Electron BackScatter Diffraction (EBSD) was used to distinguish bainitic transformation products based on their orientation relationship with the parent austenite. Thermal profiles were designed to study different amounts of Nb in solid solution prior to continuous cooling phase transformation. Nb in solid solution shifts the transformation start to lower temperatures resulting in finer microstructural sub-structures. Using EBSD the increase of high angle boundary density can be related to the transformation temperature.

12:15

Microstructure Evolution During Thermomechanical Processing of a High Strength Sheet Steel: Doug Boyd¹; Hayley Scott¹; Luana Siqueira¹; Gagan Sidhu¹; Fateh Fazeli²; Xiang Wang³; Keith Pilkey³; ¹Queen's University; ²CanmetMATERIALS; ³McMaster University

The formability of high strength sheet steel is sensitive to microstructure on several length scales. The goal of this research is to delineate the microstructural evolution during thermomechanical processing (TMP) of a commercial hot-rolled stretch-flangeable steel (low-C, microalloyed, 780 MPa UTS). Final microstructures produced by different cooling schedules were characterized by OM, SEM, and TEM, and austenite transformation kinetics were studied by deformation dilatometry. The microstructures are a complex mixture of polygonal ferrite (PF), granular bainite (GB), lath bainite (B), martensite/austenite (M/A), and 'coarse' (\sim 100 nm) and 'fine' (\sim 10 nm) (Ti,Nb)(C,N) precipitates. A pancaked (unrecrystallized) austenite condition promotes the formation of PF to higher cooling rates and the formation of GB to higher temperatures. The cooling temperature controls the relative amounts of B and M/A, as well as the type and distribution of precipitates.

Based on these insights, TMP schedules can be designed to produce desired final microstructures and properties.

12:30

Formation Mechanism of Acicular Ferrite during the Heat Treatment of High Strength Low Alloy Steel: *Yongchang Liu*¹; *Lei Shi*¹; *Yan Chen*¹; *Chenxi Liu*¹; *Liming Yu*¹; ¹Tianjin University

Although Acicular ferrite (AF) has been widely considered one of the most attractive candidate microstructures for HSLA steels, the formation mechanism has not been clarified up to now. In this approach, the formation mechanism of acicular ferrite was firstly discussed according to the effect of dissolution and precipitation of Nb on the subsequent phase transformations of undercooled austenite. Then the effects of different intercritical quenching and intercritical normalizing treatments of the HSLA steels were explored. It is recognized that the morphology of AF exhibits a lath-type when an intercritical normalizing treatment is adopted, instead of the formation of polygonal and acicular ferrites after a traditional normalizing treatment. Further intercritical tempering treatment would bring a fibrous and tempered AF structure. The formation mechanism of the lath-type, fibrous acicular ferrites and their morphological evolution are addressed in view of diffusion- or interface-controlled growth mechanism.

12:45

Control of Nano-scale Mx Dispersion in Grade 91 Steel through Thermo-mechanical Treatment: *Benjamin Shassere*¹; *Yukinori Yamamoto*²; *Sudarsanam Babu*¹; ¹University of Tennessee; ²Oak Ridge National Laboratory

Detailed microstructure characterization of Grade 91 (modified 9Cr-1Mo, ASTM A387) steel was performed after a thermo-mechanical treatment (TMT). This process includes rolling at temperatures above or below the α - γ phase field with varying plastic strains, followed by an isothermal aging in the α - γ phase field, which aims at enhancing very fine MX (M: Nb and V, X: C and N) dispersion in the base metal. Such pre-existing MX precipitates are expected to be stable during welding and improve the creep resistance of the fine grained heat affected zone in contrast to standard "normalization and tempering" heat-treatment. Dense MX precipitates were dispersed readily after TMT, resulting in improving cross-weld creep properties in comparison to standard heat-treated samples. The paper will discuss the competition between MX and $M_{23}C_6$ precipitation, as well as, their correlation to high-temperature strengthening mechanisms. Research sponsored by US-DOE, Office of Fossil Energy, the Crosscutting Research Program.

13:00

The Contribution of TEM-EELS to Understanding the Behaviour of Carbon in the Fe-C System: *B. Shalchi-Amirkhiz*¹; *Fateh Fazeli*¹; *Chad Sinclair*; *Colin Scott*¹; ¹CanmetMATERIALS

Carbon is the most important addition element in determining the physical properties of structural ferrous alloys. Despite this, there remains much to be discovered about the basic behaviour of interstitial carbon atoms and the stable and metastable iron-carbides that form. Driven by recent improvements analytical techniques, important advances have been made in the past decade. This is particularly true for the study of carbon in non-equilibrium environments like quenched martensite, supersaturated ferrite and during cementite decomposition. Here, we provide an overview of an important analysis technique used for carbon quantification, Electron Energy Loss Spectroscopy (EELS) in the TEM. In particular, it will be shown that the near edge fine structure observed in EELS spectra can be interpreted to provide not only quantitative (i.e. atomic concentration) but also chemical (coordination number, bonding) information in the Fe-C system. Applications including martensite, Fe_3C_{1-x} thin films and third generation automotive steels will be discussed.

13:15

Impulse Internal Friction Analysis of High-damping Fe-Mn Alloys: *Sunmi Shin*¹; *Won Seok Choi*²; *Jongbae Jeon*³; *Bruno De Cooman*²; ¹Pohang University of Science and Technology; ²Pohang University of Science and Technology; ³Korea Institute of Industrial Technology

Fe-Mn alloys are being considered for the production of automotive panels. Their high-damping properties are

expected to reduce substantially noise levels and prevent fatigue failures. Their use requires the precise matching of the material's maximum damping relaxation peak with the in-service vibration frequency and temperature. The damping spectrum of high damping Fe-Mn is characterized by diffusion-controlled phase transformations, martensitic transformations and magnetic transformations. The damping properties of Fe-Mn high-damping alloys and the effect of critical alloying additions, such as carbon, were characterized by means of the impulse internal friction technique and dilatometry. The results showed that the movement of magnetic domains contributed significantly to the damping. The thermo-elastic martensitic transformation was found to coincide with the anti-ferromagnetic phase transformation. The influence of the strain amplitude on the damping of Fe-Mn alloys was studied, and effects related to interface break-away were clearly observed.

Plenary 6

THURSDAY AM ROOM: EMERALD BALLROOM
SESSION CHAIR: CHAD SINCLAIR,
UNIVERSITY OF BRITISH COLUMBIA

08:30 Plenary

Importance of Atomic Scale Modeling in Describing and Predicting Properties of Solids and Interfaces:
*George Sawatzky*¹; ¹University of British Columbia

My field of solid state physics and strongly correlated electron systems seems far removed from the real world dealt with in most of the presentations at this meeting, so one might wonder if what I have to say is of any use to this broad audience. However perhaps now that multi-scale modelling has become very fashionable also in the descriptions of construction materials maybe we can in fact learn from each other. In my world the biggest problem is to deal with strong electron correlation effects which we believe are at the source of the wide diversity of physical properties of materials involving 3d transition metal atoms and rare earth elements resulting in things like strongly localized magnetic moments, quantum spin fluctuations, high temperature superconductors, and a multitude of phase transitions involving the lattice, spin, and even the atomic quadrupole moments. Obviously atomic physics in such systems plays an equally important role to that of the translational symmetry and band structure effects. In this field the last decade has also brought in new ideas and concepts which are especially relevant for the properties of interfaces between systems such as for example a thin layer of LaAlO₃ grown on top of SrTiO₃ both perovskite structures and electrical large band gap insulators but resulting in an interface that is metallic and even superconducting. This has opened a huge new field of research in which interface engineering is slowly emerging as a way to generate new properties and also new potential devices. I will try to describe some of these developments and describe some of the challenges in trying to explain observed properties in which indeed also defects both extended and point defects play a very important role.

09:30 Break

Carbide Precipitation in Steels

THURSDAY AM ROOM: ALPINE A-B-C
SESSION CHAIR: WENZHENG ZHANG,
TSINGHUA UNIVERSITY

09:45 Invited

Transmission Electron Microscopy Investigation of the Transition from Interphase-precipitated Carbides to Fibrous Carbides in Fe-V-C Steels: *Jer-Ren Yang*¹;
¹National Taiwan University

For vanadium steels, the previous research work indicated that interphase-precipitated carbides were changed into fibrous carbides in localized regions of the ferrite matrix, and suggested that the most coherent regions of the ferrite/austenite interface are the most sluggish and thus have the best possibility of developing fibrous precipitate. However, the exact circumstances bringing about the formation of fibrous carbides in the face of competing interphase-precipitated carbides have not yet been clarified. In this work, through the isothermal treatments, the attempt to produce the fibrous carbides adjacent to the interphase-precipitated carbides has been achieved in vanadium-containing medium-carbon steels. Thereby, transmission electron microscopy can provide direct orientation information about the transition. The transmission electron microscopy reveals that in the same ferrite matrix, the interphase-precipitated carbides can be intimately connected with the fibrous carbides. From the analysis of

orientation relationships, the correlation between these two precipitation modes has been proposed.

10:15

Effect of Vanadium, Titanium and Tungsten on Secondary Precipitation of Metallic Carbides in High Temperature Austenitic Modified HP Alloys: *Robin Guiz*¹; *Anna Fraczkiewicz*¹; ¹Ecole Nationale Supérieure des Mines de Saint-Etienne

Centrifugally cast HP alloys (Fe-Ni-Cr-C with Nb, Ti and Si additions) were designed to endure high temperature conditions. In these materials, simultaneous precipitation of two phases in the austenitic matrix is to be considered during service: NbC and M(Cr)₂₃C₆. The precipitation of these fine secondary carbides, resulting from the dissolution of primary as-cast carbides, improves the mechanical properties of the alloy. Though, after long-time service at high temperature, these particles will be subject to coarsening, leading slowly to the weakening of the material and its severe damaging. This work aims at studying the evolution of the secondary precipitation state on chemically modified alloys, cast in the laboratory. Their compositions were chosen on the basis of results obtained with Thermo-Calc and TC-PRISMA softwares, as well as on literature results. Thus, the effects of new alloy elements on the precipitation have been investigated (SEM imaging, TEM, EBSD) after aging at high temperature.

10:30

Dominating Factor on the Dispersion of VC Interphase Precipitation in V-added Steels: *Yongjie Zhang*¹; *Goro Miyamoto*¹; *Kunio Shinbo*¹; *Tadashi Furuhashi*²; ¹Tohoku Univ.

Nano-sized interphase precipitates formed at migrating ferrite (α)/austenite (γ) interface during a transformation attracts increasing attention due to its excellent precipitation strengthening. However, the effects of various factors, e.g. transformation temperature, alloying content, on its dispersion have not been clarified yet quantitatively. Therefore, the present study aimed to clarify the dominating factor(s) on VC interphase precipitation through the quantification on the number density of precipitate by using three-dimensional atom probe (3DAP). A series of V-added steels with different V and C contents were transformed at various temperatures between 873K and 993K. It is found that, compared with the migrating rate of α/γ interface, the number density of VC shows better correlation with the driving force for its precipitation.

10:45

Precipitation and Growth of Intragranular Proeutectoid Cementite in an Ultrahigh Carbon Steel: *Matthew Hecht*¹; *Bryan Webler*²; *Yousuf Picard*²;
¹Carnegie Mellon University; ²CMU

A heat treatment for commercial 2C-4Cr ultrahigh carbon steel (UHCS) was found to result in extensive precipitation of discrete equiaxed cementite particles within the microstructure, with morphology similar to the idiomorphic cementite of the Dubé/Aaronson classification. The resultant carbide distribution indicates partitioning of carbon away from the cementite network which lines grain boundaries in UHCS. As others have shown, network breakup increases the toughness in UHCS by removing brittle pathways for crack propagation. Nucleation of cementite, studied by in-situ confocal scanning laser microscopy (CSLM), was observed around 950°C during rapid heating. Effects of varying chromium content and hold temperature were also studied to better understand the kinetics and driving force for nucleation and growth. A quantitative network analysis method for SEM and optical images was developed to help predict the network reduction needed for a given toughness level.

11:00

Precipitation Processes in High Manganese Steels: *Ian Zuazo*¹; *Patrick Barges*¹; ¹ArcelorMittal

Further improvement of strength in high manganese steels or TWIP steels for automotive applications can be achieved via precipitation of vanadium or niobium carbonitrides. In order to improve the understanding of the precipitation processes in this class of steels several

compositions were casted with varying additions of C, V, Nb and N. Intragranular carbonitrides with different morphologies and arrangements have been detected at and above 800°C in homogenized and non-homogenized samples. At the lowest temperature discontinuous precipitation is observed after long treatments times. The nature of precipitates agrees well with calculations from a new thermodynamic database developed for high manganese steels. The precipitate compositions measured via EELS and the precipitate volume fractions obtained by a chemical dissolution method have been compared with equilibrium predictions. Transitions at temperatures below 600°C are also discussed.

11:15 Break

Phase Field Modelling III

THURSDAY AM ROOM: ALPINE D-E
SESSION CHAIR: MARKUS APEL,
ACCESS E. V.

09:45 Invited

Dynamics of Phase Transformation in LiFePO₄ Particles in Battery Electrode: *Hui-Chia Yu*¹; *Bernardo Orvananos*¹; *Oncu Akyildiz*¹; *Katsuyo Thornton*¹;
¹University of Michigan

Lithium iron phosphate (LFP) has been a successful material for Li-ion battery cathodes due to its enhanced safety and rate capability. For cathodes consisting of LFP nanoparticles, the current-voltage response in macroscopic electrochemical measurements exhibits a feature indicative of solid-solid phase transformation during the charge-discharge processes. However, the Li concentration evolution within individual nanoparticles remains to be elucidated. Thus, understanding the phase evolution in LFP nanoparticles is of great importance. Using phase field modeling, we investigated the effects of a variety of material parameters and their anisotropies on the phase morphological evolution in cathode nanoparticles, including Li diffusivities, interfacial energies, surface insertion rate, electronic conductivity, and misfit strain. The effect of conductive surface coatings on the nanoparticles was also examined. Finally, we will introduce a thermodynamic model with the simulations, which provides an explanation of recent experimental observations of highly inhomogeneous Li concentration distribution in LFP particles.

10:15

Phase Field Modeling of Sigma Phase Formation in Duplex Stainless Steel: *Amer Malik*¹; *Lars Höglund*¹; *John Ågren*¹; *Joakim Odqvist*¹; ¹KTH Royal Institute of Technology

Duplex stainless steels have an excellent combination of strength, toughness and corrosion resistance. However, due to their high alloy content they are prone to precipitate various undesirable phases such as sigma phase and chi phase. Even relatively small fractions of the sigma phase could drastically lower the impact toughness and resistance to pitting corrosion. In order to study the formation of sigma phase in duplex stainless steel a phase field model has been developed. The model uses thermodynamic and kinetic quantities from CALPHAD databases. Multicomponent and multiphase simulations starting from different morphologies of the austenite-ferrite matrix as well as during continuous cooling have been performed.

10:30

3D Modeling of Ferrite Transformation in Deformed-austenite Using Multi-phase-field Method and Crystal Plasticity Fast Fourier Transformation Method: Akinori Yamanaka¹; ¹Tokyo University of Agriculture and Technology

Recently, the multi-phase-field (MPF) model has been frequently used for investigating the effects of chemical composition, temperature and deformation condition of austenite phase on microstructure evolution during the austenite-to-ferrite (γ - α) transformation. In the previous study [A. Yamanaka, T. Takaki, Y. Tomita, ISIJ Int., 52 (2012) 659-668], we developed a simulation model to describe the γ - α transformation in deformed austenite phase using the crystal plasticity finite element method (CPFEM) and the MPF method. Using the developed model, we investigated the effect of plastic deformation in austenite phase on the transformation behavior in 2D space. In this study, we propose a computationally efficient methodology to simulate the γ - α transformation in deformed austenite phase using crystal plasticity model based on the fast Fourier transformation (CPFFT) and the MPF model. On the basis of the results, the effects of plastic deformation in austenite phase on the nucleation and growth of ferrite grain are discussed.

10:45

Kinetics of Orientational Phase Ordering near Line Defects in Crystals: Christina Bjerkén¹; Ali Massih¹; ¹Malmö University

General properties of directed ordering of second-phase near line defects in elastic crystals undergoing phase transition are studied using the two-component time-dependent Ginzburg-Landau equation, which describes two different low symmetry phases. The corresponding potential accounts for a first-order transition and it comprises the elastic properties, the singularity that characterizes the defect and a biquadratic anisotropy term. The phase diagram of the system is delineated and the effect of line defects on phase domains is demarked. After quenching the system below its transition point, the temporal evolutions of the order parameter components in the vicinity of the defect are evaluated, and the effect of the anisotropy on the temporal evolution is analyzed. The development of topological defects, i.e. vortices, is explored and their interaction with the structural defect is examined. Finally, applications of the model to the case of phase transitions in improper ferroelectrics in light of experimental data are discussed.

11:00

Domain Pattern Evolution in Hexagonal Systems: Fei Xue¹; Xueyun Wang²; Yanzhou Ji¹; Sang-Wook Cheong²; Long Qing Chen¹; ¹Penn State University; ²Rutgers University

The solid phase transitions in hexagonal systems lead to fascinating domain patterns. Here we employ phase-field method to investigate the domain patterns in hexagonal systems using YMnO_3 and Sb_2O_3 as examples. The improper ferroelectric YMnO_3 exhibits antiphase domain structures made up of six types of domains. The domains connect at vortices and antivortices, so called "topological defects". The vortex, antivortex, and domain walls connecting them form domain wall networks, which can be categorized into two types based on the configurations of the six types of antiphase domains. The transition between the two types is demonstrated by phase-field simulations. On the other hand, the ferroelastic Sb_2O_3 shows straight domain walls between three domain ferroelastic variants. The three domain variants lead to the formation of three-pointed stars at different spatial hierarchies. From symmetry and phase-field simulations, we demonstrate that there are four types of domain stars and six types of star parings.

11:15 Break

Shape Memory Alloys

THURSDAY AM ROOM: CALLAGHAN
SESSION CHAIR: GREGORY ROHRER,
CARNEGIE MELLON UNIVERSITY

09:45 Invited

TEM/SEM Studies on Nucleation and Growth of Precipitates in Various Martensitic Systems: Dominique Schryvers¹; ¹University of Antwerp

The use of shape memory materials as reversible switches, superelastic wires, actuators, etc. is based on the underlying displacive martensitic transformation occurring between a high temperature high symmetry austenite phase and a low temperature low symmetry martensite phase. In many of these alloy systems, however, the actual transformation process or even the possibility for practical applications depends strongly on the existence of precipitates formed during the material preparation, training or ensuing product application. The fundamental conditions for nucleation and growth of precipitates, which usually also include atom diffusion, thus need to be well understood to allow further improvement of these systems. In the present contribution an overview will be given of early day and more recent results of the characterisation of precipitation in Ni-Al, Ni-Ti, ... by various TEM techniques aiming for quantification of structural and chemical parameters such as interface structures, strain fields, concentration gradients, etc.

10:15

In Situ X-ray Diffraction Studies of the Austenite-martensite Transformation upon Load Cycling of Superelastic NiTi Shape Memory Alloys: Ethymios Polatidis¹; Nikolay Zotov¹; Eric Mittemeijer²; ¹Max Planck Institute for Intelligent Systems (formerly Max Planck Institute for Metals Research); ²Max Planck Institute for Intelligent Systems (formerly Max Planck Institute for Metals Research) and University of Stuttgart, Institute for Materials Science

Components made of NiTi shape memory alloys exhibiting superelasticity may undergo numerous stress-induced austenite-martensite transformation cycles during their service life. Consequently, it is important to understand the effect of cyclic loading on the transformation behavior of superelastic NiTi alloys and to be able to predict the change of their superelastic behavior. The effect of previous cyclic tensile loading (100 cycles) on the transformation behavior of superelastic NiTi (50.3 at.% Ni) was investigated by in-situ synchrotron and laboratory-based X-ray diffraction techniques during displacement-controlled tensile loading/unloading at ambient temperature. It was found that with load cycling the character of the reversible austenite-martensite transformation changes from localized (via the propagation of transformation fronts) to uniform. Changes in the strain-stress curves (strain hardening, decrease of the dissipated energy) with cycling are discussed and correlated to the changes in the transformation behavior and the evolution of the martensite fraction as deduced from the diffraction analysis.

10:30

Magneto-thermo-mechanical Coupling Effects on the Dynamic Performance of NiMnGa Magnetic Shape Memory Alloy: Yongjun He¹; Oana Zenaida Pascan¹; Ziad Moumni¹; ¹ENSTA-ParisTech

Ferromagnetic Shape Memory Alloy (FSMA) is a smart material coupling magnetic, thermal and mechanical fields that leads to many potential applications (actuators, energy harvesting, refrigeration, etc.). FSMA is a candidate for high-frequency actuators as it provides large recoverable deformation with fast-changing magnetic fields. The existing prototypes of high-frequency FSMA actuators can work only at short periods due to temperature rise caused by eddy current and twin-boundary friction. In the experiments on the martensite reorientation in NiMnGa under magnetic fields of various frequencies, we quantified these two modes of energy dissipation. It was found that the energy dissipation of the high-frequency twin boundary motion was much less than that in quasi-static loadings; but the twin-boundary friction was still the main heat source for the temperature rise. Accompanying the temperature variations, the FSMA dynamic performance shifts during the cyclic loadings. Understanding such thermo-magneto-

mechanical coupling is important in academic study and engineering applications.

10:45

Constitutional Study and Thermodynamic Evaluation of the Ni-Ti-Hf Shape Memory Alloy System: Chang-Seok Oh¹; Hak Sung Lee¹; Jong-Taek Yeom¹; Jaekwon Hong¹; ¹Korea Institute of Materials Science

The Ni-Ti-Hf ternary shape memory alloy system was systematically investigated through constitutional study and thermodynamic assessment combined with the first-principles calculation. A series of alloys with compositions of Ni-rich and Ti-rich shape memory alloys were fabricated and their microstructures were analyzed by means of SEM/EDS and XRD. The Gibbs energies of individual phases in the Ni-Ti-Hf system were described by the compound energy model and optimized based on the available experimental data, in which DFT energy calculations for metastable end-members from sub-lattice descriptions were performed. The calculated phase equilibria with obtained thermodynamic parameters for selected alloys are presented and compared with the experimental data.

11:00

The Zigzag Pattern Revisited in Fe-31Ni-0.155C: Loïc Malet¹; Stéphane Godet¹; ¹Université Libre de Bruxelles

The most striking feature of lenticular martensite is its burst kinetics and the zigzag pattern associated with it. In the present work, the crystallography of burst configurations in a coarse-grained Fe-31Ni-0.155C alloy is revisited, based on a thorough analysis at different scales using optical micrography, EBSD and TEM. The crystallographical path deduced from those configurations can be rationalized by considering mechanical couplings between variants. More precisely, the formation of the first, biggest, variant is shown to trigger both self-accommodating and autocatalytic couplings. Self-accommodating couplings occur between variants of the same plate group and manifest themselves as zigzag patterns responsible for the portioning of the initial austenitic grain. Subsequent transformation in the austenite pockets left untransformed is triggered by autocatalytic coupling between variants pertaining to perpendicular plate groups. The transformation is therefore proposed to occur sequentially over several length scales and is believed to be driven by the undercooling below M_s .

11:15 Break

From Lab to Application

THURSDAY AM ROOM: NORDIC
SESSION CHAIR: JOSE RODRIGUEZ-IBABE,
CEIT

09:45 Invited

Flying Martensite: Transformations in Materials Design: Greg Olson¹; ¹Northwestern University

Martensitic steels represent the first examples of successful integrated computational materials design and AIM qualification, meeting the technology acceleration goals of the national Materials Genome Initiative (MGI). Parametric design of alloy composition and process specifications employs mechanistic transformation theory in predictive control of martensitic M_s temperatures, precipitation rate constants, and critical particle size. Detailed process optimization employs efficient transformation simulators such as the CryoMART code for cryogenic treatment and the PrecipiCalc code for final heat treatment. For Ni-based superalloys, coupling of PrecipiCalc to heat transfer simulations accelerates process optimization of complex components such as aeroturbine discs. Under the DARPA Open Manufacturing program, accelerated optimization of additive manufacturing addresses both precipitation hardening and recrystallization. New microstructural simulation tools play a vital role in the NIST-funded Chicago-regional CHiMaD Center for Hierarchical Materials Design in support of the MGI.

10:15

Microstructure Evolution and Precipitation of a Low Carbon Low Alloyed Steel by the Two-step Intercritical Treatment: Chengjia Shang¹; Zhenjia Xie¹; Zhiqun Wang¹; Wenhao Zhou¹; S.V. Subramanian¹; ¹University of Science and Technology Beijing

Stable retained austenite (9 vol.%) and multi-scale precipitates were obtained in a 0.08C-0.5Si-2.0Mn-0.5Ni-0.9Cu-0.14(Nb+V+Mo) (wt%) steel by the two-step intercritical treatment. The first step of intercritical annealing creates a mixed microstructure of preliminary alloy-enriched martensite and lean alloyed intercritical ferrite. The second step of intercritical tempering is helpful for producing film-like stable reverted austenite along the reverted structure. The two-step austenite reverted transformation associated with intercritical partition of C, Mn and Ni is believed to be the underlying basis for stabilization of retained austenite during the two-step intercritical heat treatment. Fine niobium-containing precipitates of size ~2-10 nm and copper precipitates of size ~10-30 nm were obtained in the ferrite and retained austenite. The combination of multiphase microstructure, the transformation-induced-plasticity effect of retained austenite and strengthening effect of nanometer-sized precipitates contributes to yield strength greater than 840 MPa, uniform elongation greater than 10% and excellent low temperature impact toughness.

10:30

Direct Pearlite Spheroidization : Industrial Dream and Laboratory Reality: Matteo Caruso¹; Benjamin Pohu¹; Stéphane Godef¹; ¹CRM Group; ²Université Libre de Bruxelles

It is well-known that cold rolling of eutectoid steels requires a prior annealing step that ensures the spheroidisation of the cementite lamellae. In this work, two potential direct spheroidisation methods are analysed: the divorced mechanism during cooling and the strain-induced spheroidisation during hot rolling. Both processes are studied at the laboratory scale and the critical microstructural and thermomechanical parameters are identified. The possible scale-up to the industrial scale is evaluated with tests at the pilot scale that are critically discussed.

10:45

Development of Thermodynamic and Kinetic Model for Ferrite and Pearlite Transformation in Case Hardening Steels: Hideaki Ikehata¹; Hirofumi Ito¹; Kouji Tanaka¹; ¹Toyota Central R&D Labs Inc

In order to study ferrite and pearlite transformation in case hardening steels, we investigated effects of the alloy element during the isothermal phase transformation using Fe-0.2C-X (X=Si, Mn, Cr) (in mass %) and Fe-0.2C-1Cr-0.8Mn-0.2Si-0-0.2Mo model steels. The progress of the phase transformation was estimated by the change of the specimen's dilatation, and the quantification of the microstructures obtained by an optical microscope. The experimental results showed the importance of the negligible-partitioning local equilibrium condition caused by Mn and the solute drag effects by Mo, resulting in strong inhibition of ferrite transformation. Results also suggested partition of Cr during pearlite transformation. By implementation of these phenomena, we developed a thermodynamic and kinetic model for predicting microstructures (ferrite and pearlite) during isothermal and continuous cooling conditions, and confirmed that the model was able to reproduce the experimental results well.

11:00

Significant Age Hardening Response of BCC/HCP Dual Phase Mg-Sc Alloys: Daisuke Ando¹; Yukiko Ogawa¹; Tetsu Suzuki¹; Yuji Soutou¹; Junichi Koike¹; ¹Tohoku University

Mg alloys have poor ductility due to their HCP structure. Meanwhile, Mg-Li alloys with above 15at.%Li have BCC/HCP dual-phase and show good ductility. However, Mg-Li alloys have low tensile strength. Thus, we will propose Mg-Sc alloys with BCC/HCP dual-phase. According to phase diagrams, a beta-Sc BCC phase exists in high Mg content and a BCC/HCP dual-phase can be obtained. It is possible to control the microstructure through thermo-mechanical or ageing treatment after beta solution treatment. If such a microstructural control is possible in Mg-Sc alloy, the mechanical properties can be drastically enhanced. In this study, the age-hardening behavior in solution-treated beta

Mg-15at.%Sc alloy was investigated and we found that a very high hardness of over 200 Hv was obtained by ageing treatment at 473 K. Such a significant age hardening response was caused by the formation of a very fine alpha phase in the beta matrix phase.

11:15 Break**Precipitation in Non-Ferrous Alloys: Aluminum Alloys**

THURSDAY AM ROOM: ALPINE A-B-C
SESSION CHAIR: JOSEPH ROBSON,
UNIVERSITY OF MANCHESTER

11:45 Invited

Coupled Precipitation, Yield Strength and Hardening Modelling for Non-isothermal Treatments of a 6061 Aluminium Alloy: Michel Perez²; Didier Bardel¹; Daniel Nelias²; Sylvain Dancette¹; ¹Université de Lyon - INSA de Lyon - MATEIS - UMR CNRS 5510; ²Université de Lyon - LaMCoS - INSA

In age-hardening alloys, high-temperature processes, such as welding, can strongly modify the precipitation state, and thus degrade the associated mechanical properties. The aim of this talk is to present a coupled approach able to describe precipitation, associated yield stresses and kinematic/isotropic hardening for non-isothermal treatments of a 6061 aluminium alloy. The precipitation state (in terms of volume fraction and precipitate size distribution) is modelled thanks to a recent implementation of the classical nucleation and growth theories for needle-shaped precipitates. The precipitation model is validated through small-angle neutron scattering and transmission electron microscopy experiments. The precipitation size distribution is then used as an entry parameter of a micromechanical model for the yield strength and kinematic/isotropic hardening of the alloy. Predicted stress/strain curves are compared to tensile cyclic tests performed with various heating conditions, representative of the heat-affected zone of a welded joint.

12:15

Kinetics of Solute Clustering in Multi-constituent Aluminum Alloys: Rosen Ivanov¹; Frédéric de Geuser¹; Alexis Deschamps¹; ¹Univ. Grenoble Alpes, CNRS, SIMAP

Aluminum alloys exhibit age hardening at room temperature linked to the formation of small solute clusters from a supersaturated solid solution. The kinetics and extent of clustering of the solute elements in multi-constituent alloys depends both on the interaction between the solute species and between the solutes and the quenched-in vacancies. Using Small-Angle X-ray Scattering, Differential Scanning Calorimetry and hardness we investigate several Al-Cu based model alloys with combined additions of Mg and Li. Al-3.0Cu, Al-3.5Cu-0.9Li, Al-2.5Cu-1.5Mg and Al-3.5Cu-0.9Li-0.3Mg (all wt%) are employed to demonstrate changes to cluster size, volume fraction and related hardness occurring during natural ageing. The stability of the clusters formed at room temperature is evaluated by monitoring their evolution during reversion experiments. The results show that the additions of Mg and Li to Al-Cu have a drastically different effect on the formation rate of the clusters and their stability.

12:30

Combinatorial Approach to Investigate the Influence of Minor Alloying Elements in AlCuLi Alloys: Eva Gumbmann¹; Frédéric de Geuser²; Christophe Sigli³; Williams Lefebvre⁴; Alexis Deschamps²; ¹Grenoble INP; ²Univ. Grenoble Alpes, SIMAP, F-38000 Grenoble, France; ³CNRS, SIMAP, F-38000 Grenoble, France; ⁴Constellium Technology Center; ⁵Groupe de Physique des Matériaux, UMR CNRS 6634, University of Rouen,

Al-Cu-Li alloys are hardened by the T1 - phase that precipitate on {111}Al planes as thin platelets. Several studies show that an effective nucleation of T1 is possible only in the presence of dislocations and minor alloying additions, particularly Ag and Mg. However, there is so far no study that determines the minimum amount

of these elements necessary to achieve the described effects. We apply a combinatorial approach based on monitoring the precipitation kinetics on materials based on Al-3%Cu-1%Li, where a gradient in Ag and Mg minor alloying elements has been achieved, using time- and space-resolved Small-Angle X-ray Scattering performed in-situ during precipitation heat treatments. The obtained microstructural data (size and fraction of precipitates as a function of solute content and heat treatment time) allow, in conjunction with hardness measurements, to determine the critical minor solute contents and better understand their role in promoting nucleation and avoiding precipitate coarsening.

12:45

Quantitative In Situ X-ray Powder Diffraction Studies of Phase Transformations in Al Alloys: Mark Styles¹; Mark Gibson¹; Christopher Hutchinson²; ¹CSIRO; ²Monash University

In situ synchrotron X-ray powder diffraction is a powerful tool for studying phase transformations in engineering alloys, which, when combined with Rietveld-based data analysis methods, allows the phase composition of an alloy to be quantified as a function of variables such as time or temperature. This approach has recently been used to gain new insights into phase transitions within two Al alloy systems. In situ isothermal aging experiments have confirmed that the decomposition sequence in Al-Cu-Mg alloys involves a metastable variant of the S (Al₂CuMg) phase, and enabled the kinetics of the transformation between metastable and equilibrium S phases to be investigated. In addition, continuous heating experiments have been used to investigate crystallisation pathways in Al-Ni-Y metallic glasses, and have revealed that the mechanism switches from a two stage process involving α-Al, to a three stage process involving Al₃Ni₂ and a transient excess of Al₃Ni, with increasing Ni concentration.

13:00

On the Effect of Iron and the Precipitation Behaviour of Iron during Annealing of a Cold Deformed Commercial Purity Aluminium Alloy: Sindre Bunkholt¹; Erik Nes²; Knut Marthinsen²; ¹Hydro Aluminium Rolled Products AS; ²Norwegian University of Science and Technology

Iron is always present in any aluminium alloy and usually as an impurity element. In commercial purity alloys the concentration of iron is typically so large that iron has a strong influence on the material properties due to its low diffusivity and low solubility in aluminium. In the present work the effect of iron in solid solution and the precipitation behaviour of iron during annealing of a cold-deformed commercial purity aluminium alloy have been investigated. Iron in solution is found to have a strong retarding effect on the softening kinetics. The resulting recrystallization texture has a distinct Cube component and some weak deformation texture components. By additional cold rolling and inter-annealing, the solute content is reduced significantly by precipitation of mainly Al₃Fe and some alpha-AlFeSi phases. Doing so speeds up the softening kinetics by a factor of ~1000 and causes a considerable strengthening of the Cube in the recrystallized texture.

13:15 Lunch

Simulation of Ordering and Pattern Formation

THURSDAY AM ROOM: ALPINE D-E
SESSION CHAIR: CHRIS WOLVERTON,
NORTHWESTERN UNIVERSITY

11:45 Invited

Self-Organization Reactions Under Irradiation: Toward the Design of Radiation-Resistant Materials: *Pascal Bellon*¹; Robert Averback¹; ¹University of Illinois

Irradiation can drive materials into non-equilibrium states, induce phase transformations, and nanoscale structuration through self-organization. These nanostructures could impart radiation resistance by providing a large density of interfacial sites for point defect elimination, while at the same time improving mechanical properties. We will present two approaches that have been identified for alloys comprised of immiscible elements. In a first approach, for instance observed in Cu-Nb-W, nanoprecipitation of a highly immiscible solute (W in Cu) takes place during displacement cascade, providing a fractal-like template for the precipitation of a second and less immiscible solute (Nb). Atomistic kinetic Monte Carlo (KMC) simulations reveal that, under these conditions, nanoprecipitates can be completely resistant to thermal coarsening. In a second approach, the competition of ballistic mixing with thermal diffusion can lead to self-organized nanoprecipitates, which are thus coarsening resistant by design. KMC reveal that effective point-defect sinks can extend this nanopatterning to elevated temperatures.

12:15

Thermo-kinetic Modeling of Mg-Si Couples Formation as a Precursor to Precipitation in Al-Mg-Si Alloys: *Yao Shan*¹; Jiri Svoboda²; Franz Fischer³; Ernst Kozeschnik⁴; ¹Materials Center Leoben Forschung GmbH; ²Institute of Physics of Materials, Academy of Sciences of the Czech Republic; ³Institute of Mechanics, Montanuniversität Leoben; ⁴Institute of Materials Science and Technology, Vienna University of Technology

As the first step a thermodynamic model describing the Gibbs energy of the system accounting for Mg-Si co-cluster formation in an Al-Mg-Si matrix is developed. The equilibrium concentration of co-clusters is obtained by minimizing the Gibbs energy of the system for a given temperature, chemical composition and the trapping energy, describing the decrease of energy due to Mg-Si cluster formation relatively to isolated Mg and Si atoms. In the second step, the evolution equations describing the kinetics of dimer formation are derived by means of the Onsager (Ziegler) thermodynamic extremal principle. The studies based on this model, can significantly contribute to a better understanding of the early stages in nucleation of complex precipitates. The predictions of our model are compared to similar approaches in open literature, such as the models of Howard and Lidiard, and of Starink et al., which use different approaches to the treatment of the configurational entropy.

12:30

Grain and Interphase Boundary Anisotropy and Growth Pattern Formation: Theory, Experiments and Numerics: *Silvere Akamatsu*¹; Sabine Bottin-Rousseau¹; Gabriel Faivre¹; Supryio Ghosh²; Mathis Plapp²; ¹CNRS - UPMC; ²Ecole Polytechnique

The anisotropy of the free energy of solid-solid boundaries in alloys often plays a determining role in the formation of growth microstructures during phase transformation. In a recent work, we showed that a rotating directional-solidification method, during which the crystal orientation can be varied continuously, can give experimental access to the interfacial anisotropy of grain or interphase boundaries left behind the solidification front in a polycrystal or eutectic solid. We will present an approximate theory that formalizes this statement (it refers to the local-equilibrium condition at solid-solid-liquid trijunctions), and experimental observations that supports it. We also performed (2d) numerical simulations of tilted lamellar eutectic growth patterns with two different methods – phase field and dynamic boundary integral – by implementing various (model) anisotropy functions without and with Herring-unstable orientations. They confirm the general validity

of the theoretical analysis, and give an estimate of the accuracy of the above mentioned experimental method.

12:45 Invited

Ordering of Two Dimensional Strained Films: *Ken Elder*¹; ¹Oakland University

In this talk I would like to discuss the ordering of ultrathin films grown on various substrates. The lattice mismatch between the film and substrate leads to strain induced patterning and phase transitions. The talk will focus on using amplitude representations of the phase field crystal model to study large scale ordering of triangular films on triangular substrates (relevant for systems such as Cu/Ru(0001) and Ag/Cu(111)) and honeycomb films on triangular substrates (relevant for graphene on various metallic substrates). This approach bridges the gap between atomistic details such as dislocations and large scale ordering on micron length scales.

13:15 Lunch

Characterization of Displacive Transformations in Ferrous Alloys

THURSDAY AM ROOM: CALLAGHAN
SESSION CHAIR: DONALD BROWN,
LOS ALAMOS NATIONAL LAB

11:45 Invited

Atom Probe Tomography Investigation of Carbon Segregation and Redistribution from Supersaturated Virgin Fe-C Martensites: *Frédéric Danoix*¹; Sebastien Allain²; Mohamed Gouné³; Helena Zapolsky¹; ¹CNRS - Université de Rouen; ²IJL Nancy; ³CMCB Bordeaux – UPR CNRS 9048

Due to its renewed importance in modern steels, numerous works have been carried out for years to explain the strength of as-quenched martensitic steels. The relation between microstructure and tensile properties is still a matter of debate, partly because fine scale microstructural defects acting as obstacles for dislocation motion are not known in details. The difficulty lies in the autotempering, which strongly depends on the cooling rate. In order to avoid it, we study 'virgin martensites', where carbon diffusion is almost completely suppressed before ageing. Even in such unaged martensites, different types of C 'heterogeneities' are observed, from segregations to structural defects, to homogeneous Fe-C phase separation by a spinodal mechanism. C (re)distribution in virgin martensite is investigated mostly by atom probe tomography, and the observed microstructures are compared with the tensile behavior in order to better understand the influence of fine scale microstructural parameters on their mechanical properties.

12:15

Quantitative Metallography for Industrial Use on Martensitic Steels: *Albin Stormvinter*¹; Annika Borgenstam²; Goro Miyamoto³; Tadashi Furuhashi³; Hans Kristoffersen¹; ¹Swerea IVF AB; ²KTH Royal Inst. of Technology; ³Institute for Material Research, Tohoku University

The performance of powertrain components and rock tools relies on the inherent strength and hardness of ferrous martensite. Currently the industry uses experimental measurements of surface hardness and case depth to qualify their hardening processes. Often there are additional requirements on microstructure constituents, although there are no quantitative methods available to characterize ferrous martensite. Here such methodology is discussed in relation to SEM-EBSD measurements on the full practical range of Fe-C alloys. The orientation relationships between austenite and martensite along with the variant pairing tendency of martensite are determined from the EBSD data. These results are related to the well-known morphological transition from lath to plate martensite in Fe-C alloys. Quantitative metallography using SEM-EBSD has the potential to complement hardness- and residual-stress measurements when qualifying new steel grades and hardening processes in the industry. It may also

prove important when researching the coupling between material properties and fatigue performance.

12:30

Phase Transformation of Cu Precipitates in an Fe-3Si-2Cu Alloy: *Yoon-Uk Heo*¹; Dong Hwi Kim¹; Sung-Joon Kim¹; ¹Pohang University of Science and Technology

Phase transition of Cu precipitates during aging of an Fe-3Si-2Cu alloy was studied by transmission electron microscopy. The precipitation of 3–5 nm sized BCC Cu in ferrite matrix was confirmed by HAADF-STEM imaging. The BCC Cu precipitates transformed to 9R Cu as they grow. Many of 9R Cu precipitates were twinned, however untwinned 9R Cu particles were also observed. The 9R Cu transformed to twinned FCC Cu by the glide of $\pm a/3$ [100]9R Shockley-type partial dislocations. Finally, twins in FCC Cu precipitates were disappeared to form stable FCC Cu particles. The transformation sequence of Cu precipitates in α -matrix is concluded as follow; BCC Cu 9R Cu Twinned FCC Cu FCC Cu. Formation of 3R structure previously reported could not be confirmed in this study. The importance of electron beam orientation-dependant moiré fringes in the correct identification of Cu structure will be discussed in detail.

12:45

The Growth of Bainitic Ferrite at the Early Stages of Transformation in a High Silicon Steel: *Ilana Timokhina*¹; Dierk Raabe²; Klaus Liss³; Hossein Beladi¹; Peter Hodgson¹; Khushboo Rakha¹; Xiang-Yuan Xiong⁴; ¹Deakin University; ²Max-Planck-Institut für Eisenforschung; ³Australian Nuclear Science and Technology Organisation; ⁴Monash University

In-situ neutron diffraction, transmission electron and atom probe microscopy have been used to study the initial stages of the bainite transformation in a high Si steel, when only a single bainitic ferrite layer formed. It appeared that the carbon redistribution between the bainitic ferrite and retained austenite at the early stages of the bainite transformation occurs in the following sequence: (i) formation of retained austenite with higher and lower carbon contents at the beginning of the transformation, (ii) segregation of carbon to the dislocations near the austenite/ferrite interface, and (iii) homogenous redistribution of carbon within the retained austenite with the progress of transformation and the formation of bainitic ferrite colonies. It was found that bainitic ferrite can nucleate at internal defects as well as at the prior austenite grain boundary.

13:00

Large Lattice Strain in Fe₃Pt Exhibiting a Second-order-like Martensitic Transformation: *Takashi Yamaguchi*¹; Takashi Fukuda¹; Tomoyuki Kakeshita¹; ¹Osaka University

An Fe₃Pt has an ordered L12-type structure, and the alloy with its degree of order of 0.75 exhibits a second-order-like martensitic transformation from an L12-type cubic structure to an L60-type tetragonal structure in the cooling process at a temperature near 90 K. We have investigated lattice strain of the Fe₃Pt under compressive stress applied in the [001] direction by neutron diffraction at BL-19 (TAKUMI) in J-PARC. We found that a large lattice strain of approximately 6% appears under a stress of -280 MPa near the transformation temperature. The lattice strain drastically decreases with increasing test temperature. These results are the consequence of significant softening of elastic constant C₁₁.

13:15 Lunch

Order-Disorder Transformations

THURSDAY AM ROOM: NORDIC
SESSION CHAIR: STEPHANE GORSSE,
ICMCB-CNRS

11:45 Invited

On the Characterisation of the Order - Disorder Transitions of Fe₂VAl-based Ternary Thermoelectric Heusler Compounds: *Pascal Jacques*¹; Philippe Bellanger¹; Geoffrey Roy¹; Aude Simar¹; Camille van der Rest¹; ¹UCL

Compounds based on Fe₂VAl are good candidates for large-scale devices devoted to the harvesting of low grade heat from industrial processes through the thermoelectric effect. However, their thermoelectric properties are badly influenced by disorder, especially at higher temperatures. The present study investigates order-disorder transformations in Fe₂VAl ternary Heusler compounds. An inherent problem of these compounds is the close atomic numbers of Fe and V making their atomic scattering factor almost similar for X-rays scattering. Hence, the D03 and L21 structures, corresponding to Fe-V antisite defects, are hardly distinguishable by XRD. Anomalous scattering and neutron diffraction were combined with differential scanning calorimetry to highlight the order-disorder transformations in Fe₂VAl-based compounds. Based on these characterisations, specific heat-treatments were defined to promote the formation of the L21 ordered phase.

12:15

A simple Model for the Disorder/Order Transformation Preceding Fe₃C Precipitation in Martensite: *Walter Mayer*¹; Yao Shan²; Ernst Kozeschnik¹; ¹Institute of Materials Science and Technology, Vienna University of Technology; ²Materials Center Leoben Forschung GmbH, Leoben

We present a new theoretical approach to simulate the sequence from metastable disordered C-rich cluster formation and defect segregation to stable cementite (Fe₃C) precipitation in low and medium carbon martensitic steel. The freshly quenched virgin bct martensite is treated as a highly supersaturated solid solution of C in a heavily defect-loaded Fe matrix where, on tempering, a strong driving force for precipitation of carbides exists that are, however, experimentally not observed. In our model, in the 0th stage of tempering, C atoms either segregate to lattice defects (dislocations, grain and phase boundaries) or form Fe-rich C-clusters. These metastable configurations delay, or even suppress, the precipitation of Fe₃C at low temperature. Using the thermo-kinetic software MatCalc we simulate tempering, taking into account the full sequence of C trapping to dislocations, the formation of C clusters and, finally, transformation to stable Fe₃C carbide precipitates with an (ordered) orthorhombic crystal structure.

12:30

On the Interactions between Recrystallisation and Ordering Phenomena in Fe₂VAl-based Heusler Compounds: *Camille van der Rest*¹; Philippe Bellanger¹; Geoffrey Roy¹; Aude Simar¹; Pascal Jacques¹; ¹Université Catholique de Louvain

Compounds based on Fe₂VAl are considered as promising materials to harvest low grade heat from industrial processes through the thermoelectric effect. On the one hand, conditions leading to hot ductility of this intermetallic compound were analysed through hot uniaxial compressive strength tests. Recovery and recrystallisation phenomena were characterised during and after hot-rolling, particularly with the aim of grain refinement. On the other hand, ordering (B2, D03 or L21) is of prime importance in Fe₂VAl-based compounds as their thermoelectric properties are greatly enhanced in the ordered state. The influence of the temperature as well as of the presence of defects was assessed. The interactions between recovery/recrystallisation and ordering in specific temperatures ranges were characterised owing to X-ray diffraction and transmission electron microscopy.

12:45

Simulations of TDGL Equations for B2 Type Ordering with Two Step Phase Separation in Fe-Ni-Al Alloys: *Ryuichiro Oguma*¹; Syo Matsumura²; Minoru Doi³; Satoshi Hata²; Keisuke Ogata²; ¹Fukuoka University; ²Kyushu University; ³Aichi Institute of Technology

Present authors developed a time-dependent Ginzburg-Landau (TDGL) formulation for ordering processes of B2 and D03 in binary alloys. Coauthors have investigated domain structures in two-step phase separation of Fe-based Fe-Ni-Al alloys. Micro-structures in the superalloys consist of B2 ordered domains and A2 disordered matrices in the first stage of phase separation. The second stage during a subsequent aging leads to formation of B2 domains and A2 phase regions in the former A2 matrices and B2 domains, respectively. The evolution of 3D domain structures has been analyzed by electron tomography imaging and energy-dispersive X-ray spectroscopy. In this work the authors have applied the TDGL formulation to this alloy system, and performed 3D numerical simulations assuming the thermal processing. The results of the simulations well reproduced the characteristics of the microstructures obtained from the observations.

13:00 Lunch

Coupled Precipitation

THURSDAY PM ROOM: ALPINE A-B-C
SESSION CHAIR: JIAN-FENG NIE,
MONASH UNIVERSITY

14:15 Invited

Lamellar and Nonlamellar Decomposition in U-Nb: Energy Sinks and Approach to Equilibrium: *Robert Hackenberg*¹; Clarissa Yablinsky¹; Anna Llobet¹; Heather Volz²; Pallas Papin¹; Tim Tucker¹; Kester Clarke¹; Megan Emigh²; ¹Los Alamos National Laboratory; ²University of Illinois (Urbana-Champaign)

Kinetics prediction is complicated by the wide variety of thermodynamically permissible reaction paths, and the envelope of permissible paths expands with increasing supersaturation. Tracking the magnitudes of free energy changes along actual reaction paths provides important clues to understand the selection of length scales, growth rates, and phase compositions. This energy-tracking approach is applied to the diffusional monotectoid decomposition of binary Uranium-Niobium alloys. Niobium partitioning occurs over 3 stages: general precipitation (GP), discontinuous precipitation (DP), and discontinuous coarsening (DC). Each stage irreversibly consumes a portion of the available chemical driving force while also storing some energy in reversible energy sinks such as interfaces and strain. The driving forces of the DP and DC reactions are augmented by the release of energies stored in the predecessor reaction products. Diverging lamellae and non-steady state growth of DP and DC provide added complexity that will be quantified and discussed.

14:45

Competitive Continuous and Discontinuous Precipitation in Magnesium-Aluminium-Zinc Alloys and their Effect on Twinning: *Joseph Robson*¹; ¹University of Manchester

The magnesium-aluminium-zinc system forms the basis of the most widely used commercial magnesium alloys, such as AZ91. These alloys are age hardenable and form precipitates during heat treatment by continuous precipitation (CP), discontinuous precipitation (DP), or a mixture of modes. The type of precipitation that occurs has important consequences for the mechanical properties of the alloy, with DP generally considered to be undesirable. In this work, a classical kinetic model has been developed to predict the competition between CP and DP and used to understand the interaction between these modes. It is demonstrated that the removal of solute into continuous precipitates can have a strong effect in suppressing DP. Finally, the interaction of precipitates of both types with twinning, which is an important deformation mode in

magnesium, is considered. It is shown that shear resistant precipitates, whether DP or CP, can produce strong obstacles to twin growth.

15:00

Aspects of Discontinuous Precipitation (DP) Reactions in Ag-7.5Cu: *Shirley Northover*¹; Peter Northover²; Alison Wilson³; ¹The Open University; ²Oxford University; ³University of Cambridge

Since the crystallographic orientation of a cellular colony derives from the grain it grows away from, experimental interest in discontinuous precipitation has centred on how nucleation and growth rates are affected by the misorientation of the initiating grain boundary. Little attention has been paid to the nature of the interface at the reaction front. Ageing experiments on Ag-7.5Cu at 250C showed there to be two DP colony populations with distinctly different growth behaviours. EBSD studies have shown that as the colonies grow there is a build-up of misorientation behind the reaction front and eventually the fast growing colonies are surrounded by interfaces close to particular low Σ coincident site lattice (CSL) misorientations with respect to the grain into which they are growing. On the other hand, slow growing colonies are characterised by misorientations close to a different set of low Σ CSLs. The growth mechanisms behind this behaviour will be discussed.

15:15

Time and Composition Resolved Precipitation Characterization and Modelling in (Cu) - (Cu-2%Co) Diffusion Couples: *Frédéric de Geuser*¹; Mark Styles²; Christopher Hutchinson³; Alexis Deschamps⁴; ¹SIMAP - CNRS - Univ. Grenoble Alpes; ²CSIRO; ³Monash University; ⁴SIMAP - Univ. Grenoble Alpes

Precipitation models such as the so called 'class-model' are capable of reproducing complex situations such as anisothermal heat treatments and providing the evolution of the size and volume fraction of precipitates. They are now routinely used in particular in the field of precipitation strengthening. To feed the model with realistic thermokinetic properties of the alloy, a direct comparison with experimental data is needed. While this can be performed relatively easily on a single composition of an alloy, testing different compositions in multiple conditions can become very tedious. We have used time- and space-resolved in situ small angle X-ray scattering (SAXS) on diffusion couples prepared from pure Cu and Cu-2at%Co to study the kinetics of precipitation for all the intermediate supersaturations. The data obtained at different temperatures (450°C, 500°C and 550°C) provides an extensive set of information that can then be directly compared to class-model simulations.

15:30

Numerical Simulation of Precipitation in Multicomponent Alloys: *Manon Bonvallet*¹; Thomas Philippe¹; Xavier Sauvage¹; Didier Blavette¹; ¹GPM - Université et Insa de Rouen - UMR CNRS 6634 - France

A model dealing with nucleation, growth and coarsening simultaneously and accounting for particle size distribution has been developed for the simulation of precipitation of an ordered phase in multicomponent alloys. Zeldovich theory of nucleation has been implemented in this model that is based on a Kampmann-Wagner approach [1]. In multicomponent alloys, growth and coarsening of precipitates result from a competition between thermodynamics and diffusion flux-couplings [2] that has been taken into account. Compared to Rougier et al. approach [3], our model does not require CALPHAD thermodynamics database for the determination of the interfacial compositions as they are implicitly included in growth and coarsening laws. Predictions are confronted to APT experiments in NiCrAl and CoAlW superalloys. [1] R. Kampmann, R. Wagner, Sonnenberg, Pergamon; 1984. [2] T. Philippe et P.W. Voorhees, Acta Mater. 61 (2013) 4237. [3] L. Rougier et al., Acta Mater. 61 (2013) 6396.

15:45 Break

Modelling of Precipitation

THURSDAY PM ROOM: ALPINE D-E
SESSION CHAIR: JESPER FRIIS,
SINTEF

14:15 Invited

The Use of Density Functional Theory to Explore Precipitation-hardened Alloy Systems: *Chris Wolverton*¹; ¹Northwestern University

To fully optimize the large strengthening response of alloying additions to many metals, one would like to understand the energetic stability and morphology precipitate phases as well as be able to provide predictions of new precipitation-hardened alloy systems. These types of materials discovery and alloy design processes may be greatly aided by the use of computational methods, particularly those atomistic methods based on Density Functional Theory (DFT). In this talk, we present an overview of recent applications of DFT for a variety of alloy systems and precipitates. Examples will be shown for known and predicted precipitate phases in a variety of systems (e.g., Mg-, Al-, and Co-based).

14:45

A Hierarchical Computational Thermodynamic and Kinetic Approach to Discontinuous Precipitation in the U-Nb System: *Thien Duong*¹; Robert Hackenberg²; Alexander Landa³; Sean Gibbons¹; Saurabh Bajaj⁴; Andrei Ruban⁵; Levente Vitos⁵; Patrice Turchi³; Raymundo Arroyave¹; ¹Texas A&M University; ²Los Alamos National Laboratory; ³Lawrence Livermore National Laboratory; ⁴California Institute of Technology; ⁵Royal Institute of Technology

Uranium-niobium alloys decompose via discontinuous precipitation (DP) over a broad span of aging conditions, adversely affecting properties. The growth kinetics, lamellar spacings, and Nb partitioning magnitudes have been measured, but the thermodynamic and kinetic factors underlying these specific transformation characteristics and reaction paths, vis-a-vis the monotectoid reaction, are not fully resolved. In this work, a hierarchical computational thermodynamic and kinetic approach was carried out to investigate DP. The hierarchical approach started with density functional investigations of ground-state formation energies of bcc-uranium-niobium. The estimated energetic data was then utilized as an imposed first-principles constraint to improve the consistency of CALPHAD thermodynamic and, subsequently, kinetic assessments of uranium-niobium. Phase-field simulations were then carried out to study DP's microstructure evolution using the assessed CALPHAD thermodynamic and kinetic representations. Good agreements with experiments on different physical/length scales were achieved, which validates the present theoretical contributions to a better understanding of DP in uranium-niobium alloys.

15:00

Simulation of Simultaneously Occurring Coupled Inward Diffusion and Internal Precipitation: *Minsu Jung*¹; Sai Ramudu Meka¹; Bastian Rheingans²; Eric Jan Mittermeijer¹; ¹Max Planck Institute for Intelligent Systems (formerly Max Planck Institute for Metals Research); ²Institute for Materials Science, University of Stuttgart

Precipitation from homogeneously supersaturated solid solutions is more or less well understood. However, the precipitation occurring upon inward diffusion of one of the solutes, leading to depth-dependent degree of solute supersaturation, has not been modeled accurately. This is attributed to the difficulty in coupling the simultaneously occurring processes of internal precipitation and inward diffusion. To this end a model was developed which describes coupling of the inward diffusion of an element I into a substrate and the simultaneous precipitation, i.e. nucleation, growth, and coarsening, of a compound M_nI_m , with M as alloying element initially dissolved in the substrate. The model was applied to the gaseous nitriding of iron-based alloys, incorporating the role of excess nitrogen and the ammonia-dissociation kinetics at the surface of substrate. The simulation results, e.g. the variation with depth of the precipitate-size distribution, show good agreement with experimental results.

15:15 Invited

Modeling the Interaction of Precipitation and Recrystallization during Hot Deformation of Microalloyed Steel: Heinrich Buken¹; Pavel Sherstnev²; Ernst Kozeschnik¹; ¹Vienna University of Technology; ²Leichtmetallkompetenzzentrum Ranshofen

Recrystallization is a phenomenon where the polycrystalline microstructure of metallic materials is entirely rebuilt after plastic deformation and subsequent thermal treatment. Nowadays, the kinetics of recrystallization can be well described computationally in many alloy systems. In contrast, physical models describing the influence of recrystallization on precipitation and, in particular, on coarsening of precipitates located at the recrystallization front and subsequent release of the pinned recrystallization front, are lacking. In the present work, we introduce a new modelling approach that describes this phenomenon of recrystallization stop by precipitation and continuation of recrystallization due to precipitate coarsening in the framework of thermo-kinetic simulation. The computational treatment is verified against experimental data from literature, where good agreement is achieved.

15:45 Break

Martensitic & Bainitic Transformations in Steels I

THURSDAY PM ROOM: CALLAGHAN
SESSION CHAIR: CYRIL CAYRON,
EPFL IMX LMTM

14:15 Invited

Effect of Free Surface on Martensitic Transformation in Individual Retained Austenite Grains: *Mingxin Huang*¹; ¹The University of Hong Kong

The stability of retained austenite depends on the chemical composition, morphology, grain size and hardness of the surrounding matrix. Different to these aspects, the present work explores the effect of free surface on the stability of retained austenite. The first part is to employ FIB milling to create free surface around individual retained austenite grains. It was found that martensitic transformation took place automatically in the retained austenite grain when a free surface was introduced, without applying external stress. This is due to the fact that the martensite nucleation energy barrier can be lowered as the strain energy induced by martensitic transformation is largely lowered when the matrix constraints were removed. The second part investigates martensitic transformation in micron-sized pillars which were fabricated by FIB from individual retained austenite grains. It was found that that α' -martensite formed in micron-sized pillars was nearly dislocation free due to the free surface effect.

14:45

3-dimensional Microstructural Observation of Butterfly-type Martensite in Fe-Ni-Cr-C Alloy by Serial Sectioning Method: *Hisashi Sato*¹; Kousuke Fujimoto¹; Tomoyuki Tanaka¹; Yoshimi Watanabe¹; ¹Nagoya Institute of Technology

Butterfly-type martensite is formed at formation temperature between lath-type and lenticular-type martensites. Although the butterfly-type martensite has more complicate shape comparing with other types, 3-dimensional shape and its crystal orientation distribution are not clear. In this study, microstructure of butterfly-type martensite in Fe-18mass%Ni-0.7mass%Cr-0.5mass%C alloy is 3-dimensionally investigated by serial sectioning method and electron backscatter diffraction (EBSD). The butterfly-type martensite in the Fe-Ni-Cr-C alloy consists of two martensite needles and has butterfly-like shape. Moreover, angle between these needles of the butterfly-type martensite is about 140°. Habit plane of the butterfly-type is mainly close to {225} of austenite matrix. Furthermore, large orientation gradients are formed in martensite and austenite phases around tip of the martensite needle. Based on the crystal orientation distribution and the 3-dimensional image of the butterfly-type martensite, growth process of the butterfly-type martensite is discussed.

15:00

Excellent Mechanical Properties of Fine 0.1C-2Si-5Mn Fresh Martensite: *Shiro Torizuka*¹; Toshihiro Hanamura²; ¹University of Hyogo; ²National Institute for Materials Science

0.1%C-5% Mn steels have a high tensile strength of more than 1400MPa and a high total elongation of 17% and are considered to be very attractive in industrial application. However, the phase transformation behavior in middle Mn steels, e.g. 5.0%Mn steel, has not fully been investigated. In this study, the effect of Mn content in the range of 1.5 - 6.0% in 0.1%C-2.0%Si steels on their transformation behavior has been examined from the points of CCT and TTT. The effect of Mn and prior austenite grain size on tensile properties and work hardening behavior are investigated.

15:15

Effect of Pre-existing Martensite on the Isothermal Transformation Kinetics below the Ms Temperature in a Low-C High-Si Steel: *Alfonso Navarro-Lopez*¹; Jilt Sietsma²; Maria J. Santofimia¹; ¹Delft University of Technology

Thermomechanical processing of Advanced Multiphase High Strength Steels often includes isothermal treatments around the martensite start temperature (Ms). Investigations show that the presence of martensite prior to these isothermal treatments accelerates the kinetics of the subsequent transformation. This kinetic effect may be attributed to the creation of potential nucleation sites in martensite/austenite interfaces. The aim of this study is to determine whether the presence of a small volume fraction of martensite affects the nucleation kinetics of the subsequent transformation as well as to qualitatively and quantitatively determine this contribution. For this purpose, dilatometry experiments were performed at different temperatures above and below Ms in a low-carbon high-silicon steel. The combination of experimental and theoretical analysis of the nucleation processes led to the identification of the isothermal product as bainite and the proposition of a possible mechanism by which pre-existing martensite affects subsequent transformations below the Ms temperature.

15:30

Grain Refinement by Cyclic Displacive Forward/Reverse Transformations: *Tadachika Chiba*¹; Goro Miyamoto¹; Tadashi Furuhashi¹; ¹Tohoku University

Cyclic transformation has been applied to refine microstructure of low-alloyed steels, where diffusional austenite reversion takes place during heating, followed by martensite transformation during cooling. It was reported that finer austenite grain after a few cycles leads to the refinement of final microstructure. On the other hand, we focus on cyclic transformation of displacive reverse and forward transformations by lowering transformation temperature, e.g. high Ni alloys. It is expected that a high density of dislocations is introduced in each transformation and large strain is accumulated without applying explicit deformation and thus, final martensite structure can be refined effectively. Therefore, in this study, we investigated microstructure change in Fe-18Ni and Fe-18Ni-0.1C(mass%) alloys with cyclic transformations. It was found that austenite grain size does not change by cyclic transformations due to austenite memory phenomena while martensite structure got finer, in particular the small amount of carbon markedly enhances refinement of martensite.

15:45 Break

Microstructure & Alloy Design

THURSDAY PM

ROOM: NORDIC

SESSION CHAIR: PHILIP NAKASHIMA,
MONASH UNIVERSITY

14:15 Invited

The Distribution of Grain Boundary and Interface Plane Orientations in Transformed Microstructures:

Hossein Beladi¹; Gregory Rohrer²; ¹Deakin University; ²Carnegie Mellon University

The properties of interfaces depend not only on the lattice misorientation, but also on the interface plane orientation. Extensive studies of grain boundaries led to the conclusion that in systems evolving by grain growth, the relative areas of different grain boundary planes are inversely correlated to their relative energies. In other words, the low energy grain boundary planes make up a larger part of the population than the higher energy grain boundary planes. The hypothesis of this work is that the interface plane orientation distribution in transformed microstructures depends more on the mechanism of formation than on the relative energy. After a discussion of methods for measuring interface plane orientations, results will be presented for lath martensite in a low carbon steel and for martensite in a Ti-6Al-4V alloy processed in two different ways to promote a displacive transformation in one case and a diffusional transformation in the other.

14:45

Development of High Strength High Entropy Alloys (HEA) Based on CoCrFeMnNi System: Anna Fraczkiewicz¹; Michal Mroz²; Matthieu Lencic¹; ¹MINES St-Etienne

HEA (high entropy alloys) are a new challenge in the field of modern metallurgy. Since the concept was first proposed by Cantor and Yeh (2004), numerous different structures and chemical systems have been investigated. Among them, the FeCrNiMnCo system offers interesting set of properties. In this work, different alloys from FeCrNiMnCo system have been studied. Starting from a classic equiatomic composition, modifications of chemical composition have been proposed on the basis of ThermoCalc calculations. The so-chosen alloys have been cast and forged or rolled. Beneficial effects of chemical composition modification are shown: for an optimal proportion of the five elements, at room temperature, yield strength above 800 MPa with a fracture elongation of 35 % could be obtained in alloys that still conserve a ductile austenitic structure even at LN2 temperature. The microstructure and deformation mechanisms leading to so exceptional mechanical behavior will be discussed.

15:00

Alloy Design and Processing Routes for Novel High Modulus Steels: Hauke Springer¹; Rosaura Aparicio-Fernandez¹; Jazmin Duarte¹; Han Zhang¹; Christian Baron¹; Aleksander Kostka¹; Dierk Raabe¹; ¹Max-Planck-Institut für Eisenforschung GmbH

Metal-matrix-composites show great potential for future lightweight structural materials due to the possibility of significantly improving the stiffness/density-ratio compared to established metallic materials. Fe-based composites, termed high modulus steels (HMS), are of special interest due to the high Young's modulus and the multitude of phase transformations. However, a major challenge for the development of HMS remains the embrittling effect induced by the required large particle fractions and the need for suitable liquid metallurgy synthesis routes to ensure cost effective production. In this work, microstructures of Fe-TiB₂ metal-matrix-composites formed in-situ from Fe-Ti-B based melts were investigated with atomic resolution characterisation techniques. Special emphasis is laid on the influence of the solidification rate and alloying additions on particle size, morphology and distribution as well as their relation to mechanical properties. Innovative routes for the refinement—down to nano-metric ranges—and dispersion-control of TiB₂ particles for optimised matrix-co-deformation are discussed.

15:15

Further Developments in Rapidly Solidified Al-Mn-Ce Alloys: Francisco Coury¹; Claudemiro Bolfinari¹; Walter Botta¹; Claudio Kiminami¹; Michael Kaufman²; ¹Universidade Federal de São Carlos; ²Colorado School of Mines

Rapidly solidified Al-Mn-Ce alloys were previously reported to form fine quasicrystals dispersed in an Al matrix and were of interest as high specific strength Al alloys. In this work, Al-Mn alloys containing varying amounts of Ce were chill cast in a copper mold and then subjected to different heat treatments. The phases formed in the as-cast samples and after different heat treatments were identified using x-ray diffraction, scanning and transmission electron microscopy. The results are in contrast to the literature report in that no quasicrystals were observed in the ternary alloys when the Mn was lower than 10% with more than 2% of Ce. However, in an Al-6Mn-2Ce (at%) alloy, a finely-distributed metastable ternary phase (Al₂₀Mn₂Ce - Fd3m) was observed that, upon heat treating, appears to be relatively resistant to coarsening or decomposition due to a protective Al₆Mn layer that forms at the ternary phase/-Al interface.

15:30

Precipitation in Ultrafine Grained Aluminium Alloys Processed by Severe Plastic Deformation: Xavier Sauvage¹; Yana Nasedkina¹; Elena Bobruk²; Maxim Murashkin²; Nariman Enikeev²; Ruslan Valiev²; ¹University of Rouen, CNRS; ²IPAM-USATU

In this presentation, it is proposed to review the influence of large levels of deformation on precipitation mechanisms and kinetics in aluminium alloys. The motivation of this research is the application of severe plastic deformation processes to combine ultrafine grained structure and nanoscaled precipitates to achieve high strength alloys. Different alloys (AlMg, AlZn, AlCu, AlMgSi) were processed in the solubilized state by torsion under high pressure at various strain level and different temperatures. Analytical microscopy data (TEM and APT) revealed some deformation induced solute drag, segregation and precipitation. The high density of crystalline defects significantly enhances the atomic mobility and provides favourable nucleation sites. Such segregations and dynamic precipitation have an influence on grain refinement mechanisms but also on the age hardening behaviour. It will be shown that deformation induced vacancies and solute drag by moving boundaries are the main mechanisms controlling microstructure evolutions and thus final properties.

15:45 Break

Precipitation: Crystallography, Morphology and Kinetics

THURSDAY PM

ROOM: ALPINE A-B-C

SESSION CHAIR: ELENA PERELOMA,
UNIVERSITY OF WOLLONGONG

16:00 Invited

New Progress on Precipitation Crystallography Based on GMS Distribution and Evolution Simulation: Wenzheng Zhang¹; Fu-Zhi Dai¹; ¹Tsinghua University

Transformation crystallography, as a fundamental aspect for understanding of phase transformations, has been investigated with two approaches. One is based on the patterns of good matching site (GMS) for a general system. A preferred orientation relationship (OR) must ensure the GMS clusters to form. The structure within a GMS cluster indicates a matching lattice correspondence. The shape and distribution of the clusters suggest the geometry for preferred interfaces. The other approach is based on atomic simulations. Evolution of crystallographic features at early stage of precipitation in a Cu-Cr alloy was simulated, showing interesting results. The OR is close to the N-W OR for a small coherent precipitate, and it jumps towards the K-S OR discontinuously upon generating a dislocation loop during the precipitate growth. The habit plane orientation is evolved toward the one corresponding to a local minimum of interfacial energy. The simulation results agree with the available experimental results.

16:30

Atomic Resolution Investigation of Nitride Transformation and Amorphous Interfaces in Steel: Hilmar Danielsen¹; ¹Technical University of Denmark

9%Cr high temperature martensitic steels used for power plant applications rely upon MN type precipitates for long term creep strength, where M may be V, Nb or Ta. Increasing Cr content to 12% for better oxidation resistance provokes the precipitation of a new precipitate type, CrMN, which replaces the MN and causes a drop in creep strength. Investigation of the CrMN nucleation using HRTEM shows it is a transformation rather than a nucleation in the matrix. Cr was observed to diffuse from the matrix into the MN precipitates transforming them both by chemical composition and crystallography into CrMN. Investigations of the interface between Nb/Ta nitrides and the ferrite showed the presence of an amorphous shell a few nm thick enveloping the precipitates, separating the two crystalline phases. The shell had the chemical composition of the nitride and was observed to crystallise under the electron beam when removing the matrix.

16:45

On the Shape Strain of Plate-shaped Transformation Products: Jian-Feng Nie¹; ¹Monash University

Crystallographic features associated with invariant plane/line strain transformations have received considerable interest in the last 60 years, and some elegant models have been developed that can quantitatively describe the orientation relationships, interface orientations and interface structures. What remains to be firmly established is whether a shape change occurs in the formation of precipitate plates and, if so, whether the shape change can be also quantitatively described. This presentation will report a simple model that can predict the shape strain associated with invariant plane strain transformations. The validity of the model will be examined by selected examples. It will be demonstrated that many of those diffusional phase transformation products, that are traditionally classified as non-displacive, exhibit in fact a remarkable shape change and that the shape change can even be a simple shear.

17:00

PTCLab: A Free and Open Source Program for Calculating Phase Transformation Crystallography: Xinfu Gu¹; Tadashi Furuhara¹; ¹Institute for Materials Research, Tohoku University, Japan

PTCLab (Phase Transformation Crystallography Lab) is a free and open source program to calculate the phase transformation crystallography. This program covers the crystallographic theories of martensitic and diffusional transformation and allows users to represent the results in stereo graphic projection. The crystallographic models treated in PTCLab include classical phenomenological theory of martensite crystallography (PTMC), double shear version of PTMC, invariant line model, O-line model, and recently developed 3-D NCS method and Edge-to-Edge matching model etc. In addition, a number of basic crystallographic calculations for single or multiple crystal structures could be done with PTCLab. High quality composite stereographic projection figures or transmission electron diffraction patterns can be also obtained by present application. PTCLab is written in python, runnable on cross platform and is distributed at <https://sourceforge.net/projects/tclab/>.

17:15

Hydrides Formation and Dissolution Processes in Zirconium Alloys: Crystallographic Orientation Relationships and Stability after Temperature Cycling: Egle Conforto¹; Xavier Feaugas¹; ¹University of La Rochelle

The precipitation of several hydride phases in zirconium alloys has been studied by TEM, SEM-EBSD, and XRD in zirconium alloys as a function of different contents of hydrogen. The orientation relationships (ORs) observed between the hydride phase and the substrate were similar to those previously observed in Titanium hydrides grown on Titanium. Dislocation emission from the hydride precipitates has been directly related to the relaxation of the misfit stresses appearing during the transformation. The stability of the hydride phases after several dissolution-precipitation cycles have been studied by DSC, TDS and XRD for different total hydrogen content. In each case studied, the energy of precipitation is lower than that of dissolution. The dissolution and precipitation temperatures evolve as a function of the cycle number. This point is actually questioned in term of hydride phases stability, misfit dislocations, hydrogen redistribution.

17:30 Break

Simulation of Transformation Plasticity

THURSDAY PM ROOM: ALPINE D-E
SESSION CHAIR: PASCAL BELLON,
UNIVERSITY OF ILLINOIS

16:00 Invited

Phase Field Modeling and Plastic Activity: *Alphonse Finel*¹; Pierre-Antoine Geslin²; Pierre-Louis Valdenaire¹; Yann Le Bouar¹; Benoît Appolaire¹; ¹ONERA-CNRS; ²Northeastern University

Because of the various length and time scales involved in dislocation dynamics, the modeling and coupling of plastic activity to microstructure evolution is not straightforward. We address two aspects of this problem. First, we present a multiscale modeling of climb, which is important at high temperature. We propose a new analytical expression of the climb rate of a periodically jogged dislocation. We then show how to upscale this closed-form expression to the phase field scale through an asymptotic analysis of a recently proposed phase-field model of climb. Second, we address a key issue in the theory of crystal plasticity, namely the transition between the discrete, where individual dislocations are resolved, and the continuum, where dislocations are represented through densities. We in particular focus on the underlying coarse-graining procedure and discuss its implication on the resulting correlation-induced local stresses and transport equations that control the plastic flow at the continuum level.

16:30

General Approach to Diffusion under a Strain in Metals and Alloys: *Andrei Nazarov*¹; Alexander Mikheev²; ¹National Research Nuclear University (MEPhI); ²Moscow State University of Design and Technology

Our approach takes into consideration, that the strains can alter the surrounding atom configuration near the jumping one and consequently the local magnitude of the activation barrier and a rate of atom jump. The rates of atom jumps in different directions define the flux density of the defects. Now we take into account, that strain values are different in the saddle point and in the rest atom position. As a result in the development of our approach the general equations for the vacancy fluxes and impurity fluxes are obtained for fcc and bcc metals. These equations give the possibility for using at low temperatures and differ sufficient from equations that was obtained earlier. In our presentation we are going to discuss the main features of the theory of diffusion under strain, the ways of its development and its applications that are realized by computer simulation.

16:45

Elasto-plastic Phase-field Model Based on Mechanical Jump Conditions: *Daniel Schneider*¹; Oleg Tschukin²; Abhick Choudhury³; Michael Selzer¹; Britta Nestler¹; ¹Karlsruhe Institute of Technology; ²Karlsruhe University of Applied Science; ³Indian Institute of Science

Computational models based on the phase-field method typically operate on a mesoscopic length scale resolving structural changes of the material and provide valuable information about microstructure and mechanical property relations. An accurate calculation of the stresses and mechanical energy at the transition region is therefore indispensable. We derive a quantitative phase-field elasticity model based on force balance and Hadamard jump condition at the interface. Comparing the simulated stress profiles in a plate with a round inclusion under hydrostatic tension with the theoretical predicted stress fields and stress field calculated with Voigt/Taylor and Reuss/Sachs, we show the quantitative characteristics of the model. In order to validate the elastic contribution to the driving force of the phase transition, we demonstrate the absence of interfacial excess energy, in one dimensional equilibrium condition of serial and parallel material chain as well as in two dimensional system through the Gibbs-Thomson condition.

17:00

Influence of Plastic Relaxation on the Formation of Widmanstätten Structures: *Maeva Cottura*¹; Benoît Appolaire¹; Alphonse Finel¹; Yann Le Bouar¹; ¹LEM - Onera/CNRS

Many metallic alloys such as steels, brass or Ti-based alloys exhibit colonies of acicular precipitates called Widmanstätten microstructures. These structures share generic features: they consist of parallel lamellae that display the same crystalline orientation and, in isothermal conditions, they follow a highly anisotropic stationary growth process. Recently, we brought new insights on the still debated mechanism selecting the velocity and tip shape by highlighting the prominent role of the elastic driving forces. In this contribution, we proceed further by analyzing in what respect plastic activity changes or not our previous conclusions using a Phase Field approach recently coupled to a viscoplasticity model.

17:15 Break

Martensitic & Bainitic Transformations in Steels II

THURSDAY PM ROOM: CALLAGHAN
SESSION CHAIR: DOUG BOYD,
QUEEN'S UNIVERSITY

16:00

Influence of Heating/Cooling Conditions on the Martensitic Transformation in a Stainless Steel AISI 420: *Microstructure and Properties:* Carola Celada Casero¹; Jesus Chao¹; *David San Martín*¹; ¹CENIM-CSIC

After cold forming and, to obtain the optimum strength, grade AISI 420 is given a high temperature heat treatment to transform the initial microstructure (ferrite+carbides) to a mixture of martensite and some residual austenite. Some undissolved carbides might be present depending on the austenitization conditions. This research focusses on the influence of the austenitization temperature (950-1200 °C) and cooling rate (0.1-100 °C/s) on the martensitic transformation. This transformation has been characterized by using high resolution dilatometry. The final microstructure has been characterized by scanning and transmission electron microscopy and by magnetic measurements. It has been observed that the higher the temperature and the faster cooling rate, the lower the martensite start temperature (Ms) temperature is. However, for a given austenitization condition, cooling above 20 °C/s seems to inhibit carbide precipitation and the Ms temperature remains roughly constant. The strength of the steel has been evaluated using tensile testing experiments.

16:15

Martensite Formed around B2 Precipitates in Fe-Ni-Al Alloys: *Tomokazu Moritani*¹; Hideki Fujiyama¹; Yuta Horibe¹; Hisashi Sato¹; Takao Kozakai¹; ¹Nagoya Institute of Technology

It is well-known that some Fe-24-40at.%Ni-10-12at.%Al alloys have γ -austenite + B2 two phase microstructure at 1123K. When the alloys are quenched into liquid nitrogen temperature, not only thin plate martensite but also disordered bcc phase are formed in γ -austenite, and the bcc phase appear between B2 particle and thin plate martensite. As results of AED lineal analyses and EDS local chemical analyses in TEM, Ni depletion layer was found around B2 particle, and this layer corresponds to disordered bcc region. Strain field of the region around the bcc phase was detected by means of EBSD-Wilkinson method and thereby the amount of distortion around the bcc field is found to be larger than that around B2 precipitate without bcc region. It is concluded from the above results that the bcc phase is like lath martensite, which introduces slip for its self-accommodation.

16:30

Partitioning and Supersaturation of Carbon in Low-temperature Bainite: *Mathew Peef*¹; Chris Hulme-Smith¹; Howard Stone¹; ¹University of Cambridge

In low-temperature bainite, transformation leads to carbon-supersaturated bainitic ferrite. The large supersaturation results in a greater fraction of ferrite forming than is otherwise expected. Carbon inhomogeneity in ferrite has been found to be associated with carbon clustering at dislocations. A finite difference model is used for the partitioning of carbon from the ferrite plates, in the temperature range 200-350 °C. Given the diffusivities, it should be expected for carbon to be uniformly distributed in both phases as the isothermal holding times are more than sufficient for partitioning to complete. The carbon content of ferrite only slowly decreases during tempering despite being conspicuously above the equilibrium solubility limit for body-centred cubic iron. In other work it has been proposed that this can be explained by tetragonality of the ferrite, *in-situ* synchrotron experiments are analysed to investigate this possibility.

16:45

Improving the Thermal Stability of Bulk Nanocrystalline Steel: *Chris Hulme-Smith*¹; ¹University of Cambridge

Bulk nanocrystalline bainite is a novel class of steel that exhibits high strength and toughness due to a fine grain size. The microstructure consists of ferrite grains \approx 100nm wide embedded in a matrix of austenite films \approx 50 nm wide and austenite blocks \approx 1 μ m wide. No fast cooling is necessary, so the microstructure can be formed in samples which are large in three dimensions. This is especially relevant for industrial applications. Current bulk nanocrystalline bainites are not stable when heated. Retained austenite decomposes into a brittle combination of cementite and martensite. This is not suitable for use in aerospace or automotive applications. The current work uses thermodynamic modelling to develop a new alloy that forms nanocrystalline bainite with improved thermal stability. Toughness, strength and fatigue performance are presented, along with time-resolved synchrotron X-ray and neutron diffraction data to assess thermal stability.

17:00

Microstructural Evolution during Ultrafast Heat Treatment of Medium Carbon Steels: *Spyros Papaefthymiou*¹; *Constantinos Goulas*²; *Jilt Sietsma*³; *Felipe Castro*⁴; *Roumen Petrov*⁴; ¹National Technical University of Athens; ²Materials innovation institute (M²i) / Delft University of Technology; ³Delft University of Technology; ⁴Gent University

The initial microstructure, its local composition and phase morphology determines the final microstructure in ultra fast heat treatment processes (UFHT). In the present study, we designed and performed via dilatometry UFHT processes involving heating rates $>250^\circ\text{C/s}$, peak austenitization and helium quenching. This UFHT leads to a carbon gradient within the austenite, as confirmed by thermodynamic and diffusion calculations. With microscopic techniques we shed light on the microstructure evolution of steels with different compositions and initial microstructures. The most commonly achieved microstructure from UFHT in medium-carbon-steels is a mixture of fine bainite and martensite, which results from the low- and high- carbon areas respectively. Undissolved cementite, carbides and other microstructural features could be identified in similar condition to the original, even after UFHT.

17:15

Effect of Hetero-phase Boundaries on Displacive Transformation in Steel: *Kojiro Motoyama*¹; Shoichi Nambu¹; Junya Inoue¹; Toshihiko Koseki¹; ¹The University of Tokyo

To achieve higher-strength steels containing of martensite or bainite, it is important to control the size, morphology and the amount of those displacive transformation products. In this study, the effects of hetero-phase boundaries, such as austenite-ferrite boundary and austenite-inclusion boundary, on the bainite and martensite formation in steel were investigated to explore the possibility of controlling the displacive transformation. An ultra-low-carbon steel and a high-alloyed steel were joined above the Ac3 temperature of the alloyed steel and below the Ac1 of the ultra-low-

carbon steel to produce the austenite-ferrite boundary, and quenched to cause displacive transformation in the alloyed steel. It was found that martensite formed at the interface had close-packed plane or close-packed direction nearly parallel to the austenite-ferrite interface. Also, different non-metallic compound particles were embedded in steels and displacive transformation starting from the compounds was investigated with an emphasis on the crystallography and morphology of the transformation products.

17:30 Break

Nanostructures

THURSDAY PM ROOM: NORDIC
SESSION CHAIR: XAVIER SAUVAGE,
UNIVERSITY OF ROUEN, CNRS

16:00 Invited

Phase Transformations and Plasticity in Metal Nanoparticles Obtained by Solid State Dewetting of Thin Films: *Eugen Rabkin*¹; Dor Amram¹; Oleg Kovalenko¹; ¹Technion

We produced arrays of Fe and Fe-Au alloy nanoparticles on sapphire substrate employing the solid state thin film dewetting technique. The Fe particles exhibited an extraordinary high strength approaching the theoretical shear strength of Fe. The in-situ X ray diffraction studies demonstrated that these particles can be overheated by 200°C above the alpha-gamma transformation temperature. The transformation did occur in the particles of Fe-Au alloys, and in some of the thin Fe films during in-situ dewetting. The morphology of the two-phase Fe-Au nanoparticles was determined by the surface segregation of Au on Fe. We discuss the extraordinary strength and phase stability of the nanoparticles in terms of unifying concept of their structural perfection.

16:30

Field Theory of Amorphous Nanophases: *Alexander Umantsev*¹; ¹Fayetteville State University

A number of very different recent experiments with nanoparticles produced very similar results: in NPs of sizes above critical the sequence of transformations is similar to that of the bulk while in NPs of sizes below the critical novel, amorphous phases appear and remain stable in significant domains of variation of the control parameters. A natural question arises: What is the origin of this phase? In a series of recent publications the author has developed a field theory of the nanophase stability, which claims that the phase that appears in NPs of sizes below the critical is a transition state between the stable bulk phases in the space of the order parameter that distinguishes between the symmetries of the bulk phases. The theory claims that the two-phase state is energetically impossible due to high 'energy cost' of the phase separating interface and is replaced by the homogeneous transition state.

16:45

Separation Transitions in Alloy Nanoparticles and Finite-size Scaling: Modeling the Dependence of Critical Temperatures on Size and Shape: *Micha Polak*¹; Leonid Rubanovich¹; ¹Ben-Gurion University of the Negev

Temperature-dependent chemical-order in platinum-iridium truncated-octahedron and rectangular-prismatic nanoparticles as model systems was studied using the free-energy concentration expansion method [1,2]. In order to cope with large nanoparticles, the number of concentration variables was reduced via grouping atomic sites in layers. Phase-separated nanostructures stable at low temperatures were found to transform into disordered structures at size-dependent critical temperatures, exhibiting a remarkable finite-size scaling behavior with respect to the total number of atoms. More universal fit with distinct critical exponents was found by introducing extra scaling with respect to the shape-dependent number of surface atoms. Possible surface segregation effects are currently explored. It is the first study demonstrating that alloy nanoparticles can exhibit second-order-type

transitions and critical behavior in accordance with finite-size scaling theory. [1] M. Polak and L. Rubanovich, Phys. Chem. Chem. Phys., 16 1569 (2014). [2] M. Polak and L. Rubanovich, Surface Science Reports, 38, 127 (2000).

17:00

Can Bonding Electron Distribution be Measured in a Nano-structured Material?: *Philip Nakashima*¹; Tianyu Liu¹; Laure Bourgeois¹; Joanne Etheridge¹; ¹Monash University

When rapidly quenched to room temperature from just below its melting point, aluminium can form octahedral voids of a few tens of nanometres in size, truncated with {001} facets. This geometry sets up an interesting optical scenario for convergent-beam electron diffraction (CBED) in transmission through parallel facets. The resulting CBED patterns are extremely sensitive to the three thicknesses describing the two slabs of perfectly coherent crystal and the free space that they sandwich. Furthermore, we show that by considering such a system as a layered material within the volume of the electron probe, and by implementing the multislice formalism for calculating electron diffraction patterns, we can resolve features in the bonding electron distribution surrounding the nanovoid. In this manner, we attempt to make the first bonding measurements in an inhomogeneous nano-structured material.

17:15

Effect of Interfacial Monolayers on Gold-assisted Growth of Crystalline Stable Substrates: *Wei Zhou*¹; Xin Li¹; *Guo-zhen Zhu*¹; ¹Shanghai Jiao Tong University

We discovered the growth of crystalline oxide nanostructure from a previous stable substrate, facilitated by the presence of an Au over layer and the application of heat. The self-assemble nano-structures consist of crystalline oxide bases, epitaxially aligned gold nanoparticles, and in-between, unique thin interfacial layers with completely different crystal structures. This phenomenon has not been previously reported in any other similar metal-oxide system. By clarifying the atomic structure of these thin interfacial layers by aberration-corrected transmission electron microscopy, we believe that these interfacial monolayers, as examples of the interfacial complexion, induce the atomic transport from substrates to gold-substrate nano-structures. The unique interfacial structures can provide deep insights in the strong metal-support interaction mechanism for heterogeneous catalysts such as Au/TiO₂ and Au/MgAl₂O₄.

17:30 Break

Plenary 7: Hillert-Cahn Lecture

THURSDAY PM ROOM: EMERALD BALLROOM
SESSION CHAIR: GARY PURDY,
MCMASTER UNIVERSITY

17:45 Plenary

Coarsening of Two-phase Mixtures: From Particles to Bicontinuous Phases: *J. Thompson*¹; E.B. Gulsoy¹; C.-L. Park²; *Katsuyo Thornton*²; *Peter Voorhees*¹; ¹Northwestern University; ²University of Michigan

Two-phase mixtures can evolve with time by the diffusion of mass from regions of high to low interfacial curvature, a process known as coarsening. Through the experiments on the International Space Station, we have employed a model two-phase mixture that both satisfies all the assumptions made by theory and in which all the materials parameters needed to compare theory and experiment are known. We find that the observed exponents and amplitudes of the temporal power laws for the average particle size and number of particles per volume, as well as the particle size distributions match those predicted by theory. We thus conclude that interfacial energy driven ripening is well described by existing theory. Extensions of this theory to systems in which the coarsening domains have spatially varying curvature, such as those found following spinodal decomposition or ordering, will be also discussed.

Plenary 8

FRIDAY AM ROOM: EMERALD BALLROOM
SESSION CHAIR: MATTHIAS MILITZER,
THE UNIVERSITY OF BRITISH COLUMBIA

08:30 Plenary

Building Microstructures from the Atoms Up: Microstructural Science Supporting ICMSE: *Elizabeth Holm*¹; ¹Carnegie Mellon University

Using microstructure as a design variable is one of the goals of integrated computational materials engineering (ICME). However, significant scientific and engineering challenges must be overcome to achieve a predictive microstructural design capability. In this talk, we will survey these issues, including calculating the atomic-scale properties of microstructural features, developing physically-based mesoscale models for microstructural evolution, connecting microstructural data to materials performance, and creating and utilizing microstructural databases and archives. The focus will be on strategies for stabilizing bulk nanocrystalline structures against low temperature coarsening, but the approaches apply more generally to understanding and predicting microstructural evolution in polycrystalline materials of all types.

09:30 Break

Phase Transformations in Titanium

FRIDAY AM ROOM: ALPINE A-B-C
SESSION CHAIR: PASCAL JACQUES,
UCL

09:45 Invited

Large Scale Phase Field Simulations of Microstructure Evolution during Thermal Cycling of Ti-6Al-4V: *Bala Radhakrishnan*¹; Sarma Gorti¹; Sudarsanam Babu¹; ¹Oak Ridge National Laboratory

During laser additive manufacturing of Ti-6Al-4V, layer bands are formed in approximately three layers below the heat source as it experiences multiple heating and cooling that straddles the alpha to beta transformation temperature. Within the layer band the microstructure is essentially a colony structure while outside the bands a basketweave structure is obtained. The transition in the microstructure leads to significant anisotropy in the fatigue properties between the build and normal directions. We present large-scale phase field simulations incorporating realistic thermal boundary conditions, and energy contributions from thermodynamics, interface and elastic strain to capture the thermal boundary conditions under which above microstructural transition occurs. Research sponsored by the Laboratory Directed Research and Development program and Center for Computational Sciences at Oak Ridge National Laboratory, managed by UT-Battelle, LLC, under contract DE-AC05-00OR22725 for the U.S. Department of Energy.

10:15

Phase and Microstructure Evolution during Ti-6Al-4V/TiB Composite Processing: *Moukrane Dehmas*¹; Ludovic Ropars¹; Sophie Gourdet²; Elisabeth Aey-Gautier¹; Jérôme Delfosse²; David Trickeys³; ¹Institut Jean Lamour; ²Airbus Group SAS, Airbus Group Innovations; ³Materion AMC

Phase transformations occurring during the production of Ti-6Al-4V/TiB composites by powder metallurgy, from Ti-6Al-4V powders and TiB₂ reinforcement have been investigated using in situ high energy X-ray diffraction, SEM, TEM/EELS/EDS and EBSD. Two main transformations

kinetics were characterized during heating and further cooling: the transformation from TiB₂ to TiB and the $\alpha+\beta \rightarrow \beta \rightarrow \alpha+\beta$ transformations in the matrix. HEXRD and SEM/TEM observations evidenced at first the formation of a metastable phase TiB-Bf, which appears as small needles around TiB₂ particles and dispersed also in the matrix. TiB-Bf transforms into the stable TiB-B27 at temperatures higher than 1100°C. The conversion mechanisms are discussed, based on crystallographic and chemical aspects. The matrix presents an increase of the MMC transus temperature, due to an increase in O and N during the fabrication process, as supported by thermodynamic calculations. The final morphology is discussed in regard of the MMC transus temperature and the nucleation sites.

10:30

Phase Transformations Kinetics of Ti-6Al-4V during Very Fast Heating Using In Situ High-energy X-ray Diffraction (HE-XRD): *Andi Idnil Ismail*¹; Moukrane Dehmas¹; Elisabeth Aey-Gautier¹; Benoît Appolaire²; ¹JL, CNRS-Université de Lorraine; ²LEM, CNRS-ONERA

In-situ experiments were performed to characterize the transformation kinetics during very fast heating using the synchrotron radiation facilities (HE-XRD) as well as electrical resistivity measurements. The phase amounts and the mean lattice parameter variations were characterized during continuous heating up to the single β -phase domain with heating rates ranging from 0.25 °C/s to 200 °C/s. For both techniques, results clearly evidence a shift of the β -phase transformation kinetics toward higher temperatures as the heating rate increases. A poor effect of the initial size of the α grains is characterized. In addition, at temperatures lower than 600°C, the average lattice parameter of the β -phase shows a deviation from linearity, which amplitude depends on the heating condition. The transformation kinetics variations are discussed in regard of calculated dissolution rates. In addition, the β -phase lattice parameter variations are analyzed in regard of internal stress relaxation or changes of chemical composition.

10:45

Influence of Phase Transformation Kinetics on Variant Selection and Microtexture Development Associated with Alpha Precipitation at Beta Grain Boundaries in a Beta Metastable Titanium Alloy: *Matthieu Salib*¹; Lionel Germain²; *Julien Teixeira*³; Nathalie Gey²; Elisabeth Aey-Gautier¹; ¹Institut Jean Lamour - CNRS - Université de Lorraine; ²LEM3 - CNRS - Université de Lorraine

The influence of phase transformation kinetics on variant selection and microtexture development associated with heterogeneous precipitation of alpha at beta/beta grain boundaries is studied in the Ti17 beta-metastable alloy, by using the EBSD technique. Precipitation of alpha at beta/beta GBs was accelerated by reducing the isothermal transformation temperature. Faster kinetics induced formation of more variants inside each prior beta grain, which weakened the final alpha microtexture. Deforming previously the parent beta phase accelerated further the precipitation by introducing new nucleation sites. This increased drastically the number of variants and weakened further the microtexture. Variant selection (VS) at beta/beta GBs occurred frequently and influenced the final alpha microtexture. Different VS criteria have been examined, by developing an automated analysis of statistical EBSD data. In addition, some GB planes were determined by 3D characterization. New results regarding VS are compared to those documented in the literature.

11:00

Thermal Stability of HPT-induced Omega Phase in Biocompatible Ti-16.1Nb Alloys: *Ajit Panigrahi*¹; Matthias Bönisch²; *Thomas Waitz*²; Mariana Calin²; Werner Skrotzki³; Jürgen Eckert²; Michael Zehetbauer¹; ¹University of Vienna; ²IFW Dresden; ³Dresden University of Technology

TiNb alloys are potential materials for orthopaedic implants due to their excellent biocompatibility and low Young's modulus of the cubic β and orthorhombic α' lattice structure. In the present work, phase transformations of Ti-16.1 wt.% Nb induced by severe plastic deformation and subsequent annealing were systematically studied. Upon

high pressure torsion, the parent α' martensite transforms into a bulk nanocrystalline α -phase. The formation of the α -phase is triggered both by pressure and strain. In-situ heating experiments using synchrotron radiation show that the α -phase starts to decompose into the hexagonal α and the cubic β equilibrium phases at a temperature of about 320°C. The phase transformation is complete at a temperature of 460°C. The pathway via an intermediate nanocrystalline ω -phase provides a new processing route for the production of a bulk material with an ultrafine and equiaxed α/β phase structure. Funding by EC (ITN BioTiNet – 264635) is gratefully acknowledged.

11:15 Break

Modelling and Experiment

FRIDAY AM ROOM: ALPINE D-E
SESSION CHAIR: GREG OLSON,
NORTHWESTERN UNIVERSITY

09:45 Invited

Detailed Structure Analysis of Precipitates Combining TEM and DFT: *Jesper Friis*¹; Sigurd Wenner²; Calin Marioara¹; Randi Holmestad²; ¹SINTEF; ²Norwegian University of Science and Technology (NTNU)

The age-hardenable Al-Mg-Zn-Cu alloys are important as structural materials for automotive and aerospace applications. In this work, we have studied the structure of some of the precipitates, of which the plate-like β' phase is the most important for hardening when the amount of Cu is low. Structure models including the precipitate-matrix interface, are derived from high angle annular dark field scanning transmission electron microscopy and validated with calculations based on density functional theory (DFT). Cu additions to the alloys do not affect the β' structure. Instead, some Cu substitutes Zn sites. The level of substitution has been estimated using energy-dispersive X-ray spectroscopy. For the β' precipitate, this agrees well with DFT, which predicts a minimum in the formation enthalpy when about 25% of the Zn is substituted with Cu. DFT calculations also show that the dense Zn-columns are energetically favoured to substitute, followed by the Zn atoms at the interface.

10:15

Microstructure Evolution During the Homogenization Heat Treatment of Aluminum Alloys: Modeling and Experimental Results: *Qiang Du*¹; Chenglu Liu²; Hamid Azizi Alizamini²; Warren Poole²; ¹SINTEF; ²University of British Columbia

A model has been developed recently to track the microstructure evolution during homogenization heat treatment of aluminum alloys. It features full coupling with CALPHAD software (i.e. chemistry dependent) and explicit treatment of diffusion at the scales of the dendrite arm spacing and inter-dispersoid spacing. With very few tuning parameters the model is able to predict the precipitation kinetics of intra-granular dispersoids, the transformation between inter-granular constituent particles and the evolution of Dispersoid Free Zones (DFZ). In this contribution, the homogenization model is introduced and its predictive power is demonstrated by successfully reproducing experimentally measured microstructure features for various industrial alloys. As such, the model represents a valuable tool for optimizing the design of industrial aluminum alloy homogenization heat treatment parameters and compositions.

10:30

Open Problems in Grain Boundary Segregation and Embrittlement: Case Study for Nickel and bcc Iron: *Pavel Lejček*¹; *Mojmir Sobš*²; ¹Institute of Physics, AS CR; ²CEITEC MU

One of the dangerous failures of materials is intergranular brittle fracture. This phenomenon is closely related to the chemistry of surfaces and grain boundaries. Numerous data on grain boundary and surface segregation obtained both experimentally and by computer simulations have been published in literature. These data have been frequently used to quantify the embrittling potency of individual solutes. In this contribution, we summarize the available values of the energy of segregation and on the strengthening/embrittling energy for wide spectrum of solutes in nickel and bcc iron, discuss their reliability from the viewpoint of limitations of individual approaches used to determine the segregation and strengthening/embrittling energies and show the limitations of experimental and theoretical approaches providing the values of the segregation energy. Reliable data are indispensable for further modeling and prediction.

10:45 Invited

Pressure Induced Alpha to Epsilon Transformation in Iron at 15 GPa: Modeling and Experiment: *Christophe Denoual*¹; *Aurélien Vaitré*¹; ¹CEA

The modeling of pressure induced martensitic transformation of iron is challenging for numerous reasons. The pressure to transition (~15 GPa) imposes to consider non-constant elasticity tensor to reproduce the equation of state (EoS). Cycling forward transformation (from BCC to HCP) and reversion (HCP to BCC) may split the original alpha BCC crystal into an increasing number of alpha variants. The resulting distortion includes rotations, which entails the use of large strain formalism. The variant multiplication imposes to consider a potential with numerous energy well, e.g. 19 metastable states are necessary to model forward and the first reverse transformation. We present a modeling of martensitic transformation able to describe variant multiplication, non-linear elasticity (and therefore EoS), and plasticity in a consistent thermodynamic framework. Application to the BCC to HCP transition in iron at 15 GPa will be presented and compared to recent experiments.

11:15 Break

Deformation Induced Transformations in Steels

FRIDAY AM ROOM: CALLAGHAN
SESSION CHAIR: BRUNO DE COOMAN, POHANG UNIVERSITY OF SCIENCE AND TECHNOLOGY

09:45 Invited

Dynamic Transformation of Austenite at Temperatures above the Ae3: *John Jonas*¹; *Clodualdo Aranas*¹; *Chiradeep Ghosh*²; ¹McGill University; ²Tata Steel

Experiments are described, carried out on eight steels of increasing carbon contents, in which specimens are deformed in the austenite phase field. Widmanstätten ferrite is observed to form displacively as self-accommodating plates about 200 nm in width. During deformation, the ferrite plates coalesce into polygonal grains several microns in diameter. On holding after deformation, the ferrite slowly retransforms into austenite by means of diffusional processes. It is shown that the driving force for the forward transformation is the softening associated with the replacement of work-hardened austenite by softer, strain-free ferrite. Critical strains of about 0.10-0.14 are observed, which increase with temperature interval above the Ae3. The driving force developed is used to overcome: i) the free energy difference between the phases, as well as ii) the work of dilatation and of iii) shear accommodation. The role of the applied stress in promoting variant selection is under current investigation.

10:15

Strengthening and Ductilization in Lean Duplex Stainless Steels by TRIP and TWIP: *Jeom Cho*¹; *Kyung-Tae Park*²; *Heung Nam Han*³; ¹POSCO; ²Hanbat National University; ³Seoul National University

TRIP has long been utilized to develop advanced high strength steels with extended ductility. Strain induced martensite transformation occurs at in-grain nucleation sites such as intersections of ϵ -martensite bands and mechanical twins depending on the stacking fault energy of austenite. Mechanical twins themselves also greatly enhance strength and ductility by dynamic Hall-Petch effect, so called TWIP. It is plausible that, by controlling SFE, higher strength and ductility can be achieved by consecutive operation of TWIP followed by TRIP. This concept was applied to development of advanced lean duplex stainless steels(LDSS). A series of investigations revealed that TRIP LDSSs exhibited the excellent strength - ductility combinations over 1000 MPa and 50 % and mechanical properties of TWIP/TRIP LDSSs were comparable to or even better than those of TRIP LDSSs. In this study, effects of alloying elements on TRIP and TWIP behaviors in LDSSs are described in association with microstructural evolution.

10:30

Deformation Induced Transformation Behaviour of Retained Austenite in Model TRIP Steel Microstructures: *Alison Mark*¹; *Doug Boyd*¹; *M.A. Gharghour*²; ¹Mechanical and Materials Engineering, Queen's University; ²Canadian Neutron Beam Centre

Transformation induced plasticity (TRIP) steels have potential applications in lightweight automotive structures and elsewhere. In this study the microstructural factors that influence the transformation of retained austenite (RA) to martensite (M) were isolated by creating four model microstructures using a standard Si - TRIP steel composition. Detailed characterization, reported previously, revealed that the model microstructures represented a wide range of size, shape and surrounding phases for the RA. In-situ tensile tests during neutron diffraction measurements of phase fraction and lattice strain provided a measure of RA transformation as a function of strain, as well as the strain/stress partitioning between RA and the surrounding phases. The optimum RA transformation behavior was exhibited by the lamellar model microstructure, in which the RA particles are surrounded by elongated ferrite sub-grains and bainite particles.

10:45

Difference in Martensitic Transformation Behavior between Carbon- and Nitrogen-added Metastable Austenitic Stainless Steels: *Takuro Masumura*¹; *Nobuo Nakada*²; *Toshihiro Tsuchiyama*¹; *Setsoo Takaki*¹; *Tamotsu Koyano*²; *Kazuhiko Adachi*³; ¹Kyushu University; ²University of Tsukuba; ³Nippon Steel & Sumitomo Metal Co.

In order to evaluate the effects of carbon and nitrogen additions on the stability of austenite, athermal and deformation-induced α' -martensitic transformation behaviors were investigated in type 304 metastable austenitic stainless steels containing 0.1 mass% carbon or nitrogen. Since carbon-added steel has a lower stacking-fault energy (SFE) than nitrogen-added steel, deformation-twin and ϵ' -martensite were preferentially formed in carbon-added steel, whereas a dislocation cell structure developed in nitrogen-added steel. Crystallographic analysis using electron backscatter diffraction method revealed that the difference in the deformation microstructure has a significant influence on the growth behavior of deformation-induced α' -martensite. The interface of the deformation-twin and ϵ' -martensite completely suppress the growth of α' -martensite, whereas dislocation cell boundaries have little influence on that. As a result, the mechanical stability of carbon-added steel is slightly higher than that of nitrogen-added steel, although the thermal stabilization effect of carbon is much lower than that of nitrogen.

11:00

Phase Transformation and Deformation Mechanisms Induced by Nanoindentation in Metastable Austenitic Stainless Steels: *Ina Sapezanskaia*¹; *Joan Josep Roa*¹; *Antonio Manuel Mateo*¹; *Abdelkrim Redjaimia*²; ¹Universitat Politècnica de Catalunya; ²Université de Lorraine, Institut Jean Lamour, CNRS

Deformation and phase transformation mechanisms in metastable austenitic steels are crucial for the functional performance of those materials. Understanding the austenite to martensite transformation at both microscopic and nanoscopic scales is of utmost importance for the automotive industry, in order to properly tailor the manufacturing. The presented work contributes to this understanding by means of nanoindentation, which has been applied as a micro/nano-probe to induce deformation at subgrain level by monotonic and cyclic tests. Analysis of the nanoindentation curves including the reloading behaviour allowed conclusions about material properties as a function of cycle number and local crystalline orientation. Remarkably, stepwise hardness drops occurred with increasing indentation cycles, resulting in an enlarged hysteresis. The involved deformation mechanisms were studied by electron microscopy (TEM) and diffraction. It was found that with increasing cycle numbers the phase transformation induced by nanoindentation propagates until the grain boundary, and can extend to neighbour grains.

11:15 Break

Novel Processing & Novel Materials I

FRIDAY AM ROOM: NORDIC
SESSION CHAIR: CHRISTOPHER HUTCHINSON, MONASH UNIVERSITY

09:45 Invited

Thermoelectric Silicides: Microstructures, Properties and Metallurgical Recipes: *Stephane Gorsse*¹; *Solange Vivès*¹; *Philippe Bellanger*¹; ¹ICMCM-CNRS

Thermoelectric materials allow to directly convert a temperature gradient into electricity and, thus, can harvest and turn waste heat into a power source. Good thermoelectric materials should be thermal insulators and electrical conductors with large Seebeck coefficients. One way to deal with this antagonist combination of properties is to generate and tailor the material's nano/microstructure. Following a coupled experimental and modelling approach, we investigate the metallurgy of advanced thermoelectrics in order to gain a better understanding of the underlying physics of this class of materials and design guidance to obtain the desired properties through the quantitative nano/microstructure control. In this presentation, we will describe two examples. The first concerns an approach that involves coupling modelling, combinatorial synthesis and localized property measurement for the study of $Mg_x(Si,Sn)$ alloys. The second is related to the relationship between structure, microstructure and properties of incommensurate higher manganese silicides.

10:15

Structure and Dynamic Behavior of a Metastable Cu Phase Formed at a Solid Si-liquid Al Interface in Al-Si-Cu-Mg Alloy: *James Howe*¹; *Matthew Schneider*²; ¹University of Virginia; ²University of Central Florida

The structure and properties of solid-liquid interfaces affect solidification, wetting, and crystal growth mechanisms. This study employed in-situ high-resolution transmission electron microscopy (HRTEM) to quantify the structure and dynamic behavior of a metastable Cu phase that was found to form at the interface between solid Si and liquid Al in an Al-Si-Cu-Mg alloy at 650°C. HRTEM image simulations were used to determine the interfacial structure and the (113)Si||[076]Cu; [110]Si||[100]Cu orientation relationship (OR) between the solid phases. Atom-row matching showed that 44% of the Si atom-rows aligned with Cu atoms in this OR. The fluctuating Cu islands displayed a log-normal distribution in lengths ranging from 0.4 to 13.2 nm, and a Gaussian distribution in heights ranging from 0.2 to 1.3 nm. Dynamic fluctuations of the

(113)Si solid-liquid interface were damped where the solid-solid OR formed between the Si and Cu phases. This research was supported by NSF Grant DMR-1106230.

10:30

Functionally Graded Iron Based Alloys Showing Twinning and Martensitic Transformation: Processing, Microstructure and Properties: *Thomas Niendorf¹; Florian Brenne²; Christian Rüsing³; Matthias Droste¹; TU Bergakademie Freiberg; ²University of Paderborn; ³Benteler Automotive*

In order to provide materials suited for advanced light-weight design, steels showing twinning induced plasticity (TWIP) and transformation induced plasticity (TRIP) have been developed in the last decades. Through alloying, e.g. by manganese, aluminum and carbon, the stacking fault energy (SFE) is set to a value leading to activation of TWIP/TRIP upon deformation. The actual deformation mechanism is additionally influenced by parameters such as texture, grain size and deformation temperature. In order to further improve the properties of these high-performance materials, functional gradation, i.e. setting of local mechanical properties, can be used. The current work introduces concepts suitable for functional gradation of high-manganese iron-based alloys. Thermo-mechanical treatments as well as additive manufacturing were employed for direct microstructure manipulation and, thus, property optimization. Based on mechanical testing including local strain analyses employing digital image correlation and thorough microstructure analyses using electronoptical techniques solid process-microstructure-property relationships are deduced.

10:45 Invited

In Situ Evaluation of Metallurgical Phenomena Using Laser Generated Ultrasonic Waves: *Thomas Garcin¹; Matthias Miltzer¹; ¹University of British Columbia*

Over the past decade, laser ultrasonics has gained tremendous maturity to in-situ characterize microstructure evolution during thermo-mechanical processing of metals and alloys. In this technique, pulse lasers are used for the generation and detection of ultrasound in materials. The ultrasound wave properties are correlated with microstructure parameters such as grain size and phase fractions transformed or recrystallized. Meanwhile the new Laser Ultrasonics for Metallurgy (LUMet) system has been developed such that this technology can be used as a user-friendly tool in the laboratory. Attached to a Gleeble thermomechanical simulator, it allows for the systematic in-situ investigation of a large number of metallurgical phenomena observed in metals and alloys with complex microstructures including advanced steels, superalloys and titanium alloys. This contribution aims at demonstrating that this technology provides fast and reliable measurements of microstructure evolution during complex thermomechanical treatments including rapid heating and cooling as well as hot deformation conditions.

11:15 Break

Phase Transformations in Superalloys

FRIDAY AM ROOM: ALPINE A-B-C
SESSION CHAIR: WALTRAUD KRIVEN,
UNIVERSITY OF ILLINOIS AT URBANA-CHAMPAIGN

11:45 Invited

Evolution of γ - γ' Microstructure in Ternary Co-Al-W Alloys: *Eric Lass¹; Yaakov Idell¹; ¹NIST*

The discovery of a two-phase γ (FCC)- γ' (L12) field in the ternary Co-Al-W phase diagram has sparked significant research interest into possible Co-based analogs to traditional Ni-based superalloys used in turbine engine applications. This work experimentally investigates microstructural evolution ternary Co-Al-W alloys. Nucleation of ordered γ' precipitates 2 nm to 10 nm in diameter cannot be suppressed even under rapid solidification conditions. Upon subsequent annealing, growth of these nuclei into irregular, non-cube shaped precipitates is very rapid,

resulting in a volume fraction of γ' roughly equal to that in metastable equilibrium with the γ phase after only a few minutes. The microstructure then slowly coarsens to reveal the familiar cuboidal γ - γ' microstructure similar to that found in Ni-based superalloys. The two-phase microstructure is ultimately destroyed by the nucleation and growth of the additional phases Co_3W (D019) indicating γ' is metastable in ternary Co-Al-W.

12:15

Simulations of Early Stage Phase Separation in Al-Cr-Ni Superalloys: *Stefan Paulsen¹; Peter Voorhees²; ¹Northwestern University; ²Northwestern University*

Nickel-based superalloys owe many of their desirable properties to gamma prime (ordered FCC) precipitates in the gamma (disordered FCC) matrix, thus understanding the phase separation process, i.e. nucleation and growth of gamma prime precipitates and the resulting microstructure is of great technological interest. We have examined the early stages of phase separation in Al-Cr-Ni alloys with a phase-field model, that employs CALPHAD free energies and CALPHAD-style assessed interdiffusion mobilities to make quantitative predictions about the phase separation process. The approach takes into account that 1) The microstructure consists of an ordered and a disordered phase, 2) The diffusivities depend on the local composition, and vary between the phases, and 3) Departures from the equilibrium tie lines as a result of the diffusional growth process. The evolution of the phase compositions as a function of time and radius are determined and compared to results from experimental investigations using atom probe tomography.

12:30

Coupling of Precipitation and Recrystallization Phenomena in a γ - γ' Ni Base Superalloy: *Marie-Agathe Charpagne¹; Nathalie Bozzolo¹; Thomas Billot²; Jean-Michel Franchet³; ¹Mines Paristech; ²Snecma-Safran Group; ³Safran SA*

Recrystallization and second phase precipitate evolution during hot forging sequences were investigated in a Ni base superalloy. The alloy under study consists of a γ matrix and γ' particles ($\text{Ni}_3(\text{Al,Ti})$): large primary particles aiming at grain boundary pinning, and fine hardening ones which are dissolved at the forging temperatures but form again during cooling. The applied forging conditions allow (dynamic and post-dynamic) recrystallization to occur and precipitation to evolve simultaneously. While many studies are dedicated either to recrystallization in γ matrix or γ' precipitation phenomena, the focus is placed here on the coupling of both phenomena: recrystallization influencing γ' precipitation, and γ' particles influencing recrystallization mechanisms. Nucleation and growth of γ' into γ and possibly of γ into γ' occur as diffusional transformations. Scenarios are proposed to account for the observed evolutions, based on consideration of stored energy, chemical composition of grains and precipitates, boundary energies and migration.

12:45

Coexisting α '- β ' Nanoscale Precipitation in an Fe-Cr-Al-Ti Alloy: *Carlos Capdevila-Montes¹; J. Chao¹; Gemma Pimentel²; María Martín-Aranda¹; Esteban Urones-Garrote³; Mike K. Miller⁴; ¹CENIM-CSIC; ²University of Oxford; ³Centro Nacional de Microscopía Electrónica (CNME), Universidad Complutense de Madrid; ⁴Oak Ridge National Laboratory*

The strengthening mechanisms observed in the oxide dispersion strengthened Fe-Cr-Al-Ti system have been investigated during ageing between 435 and 475 °C. The alloy underwent simultaneous nanoscale phase separation into TiAl-rich β' , Fe-rich (α), and Cr-rich (α') phases that were responsible for the anomalous hardness increase observed. Atom probe tomography indicated that the composition of the intermetallic β' phase was $\text{Fe}_2\text{AlTi}_{0.6}\text{Cr}_{0.4}$. High-resolution transmission electron microscopy determined that the β' precipitates were a cubic phase with the Heusler-type Fe_2AlTi (L21) structure with lattice parameter $a=0.5879$ nm and a Fm-3m space group. The β' particles were oriented along the [110] α zone axis. The strengthening could be explained by two simultaneous hardening effects: a modulus effect due to α - α' phase separation, and the interaction of the coherent β' particles with dislocations. Atom probe tomography was conducted at the Center for Nanophase Materials Sciences, which is a DOE Office of Science User Facility.

13:00

Time-resolved X-ray Diffraction of Phase Transformations in High Strength Nickel-based Superalloys: *David Collins¹; David Crudden¹; Thomas Conolly¹; Mark Hardy; Roger Reed¹; ¹University of Oxford*

Phase transformations in a number of prototype high strength polycrystalline nickel-based superalloys are studied using time-resolved X-ray synchrotron diffraction. The dissolution kinetics of the ordered phase $\text{Ni}_3(\text{Al,Ti,Ta})$ upon heating to the solutioning temperature of $\sim 1200^\circ\text{C}$ and its reprecipitation on cooling are deduced; effects of varying Nb and Ti alloy composition on the reaction kinetics are identified. Heating to 800°C does not alter substantially the fraction of the strengthening phase $\text{Ni}_3(\text{Al,Ti,Ta})$ but further heating causes its rapid dissolution. At higher temperatures, evidence is provided for the formation of further ordered phases Ni_3Ti and possibly Ni_3Ta ; cooling causes their dissolution and reprecipitation of $\text{Ni}_3(\text{Al,Ti,Ta})$, indicating the reactions may be coupled. The unforeseen phases could contribute to the high temperature mechanical behaviour of these materials, rather than solely dependent on the $\text{Ni}_3(\text{Al,Ti,Ta})$ precipitates. The MC carbide is stable even at the solution temperature; no evidence of reactions involving carbides, e.g. M_{23}C_6 , is found.

Interfaces and Phase Transformations

FRIDAY AM ROOM: ALPINE D-E
SESSION CHAIR: PAVEL LEJCEK,
INSTITUTE OF PHYSICS, AS CR

11:45

Atomistic Prediction of Solute Segregation Kinetics and Associated Heterogeneous Precipitation at Dislocations: *Evgeniya Dontsova¹; Joerg Rottler¹; Chad Sinclair¹; ¹University of British Columbia*

Solute enrichment due to strong binding between solute atoms and the elastic field of a dislocation can lead to second phase formation if the local concentration is brought within a spinodal. Prediction of the time evolution of the solute field around a dislocation is, however, a complex problem, involving temporal and spatial dependent diffusivity, non-dilute solid solutions and the atomistic topology of the defect. In this work we have used a recent adaptation of the "diffusive molecular dynamics" (DMD) model to examine the kinetics of solute segregation to dislocations on diffusive timescales and atomistic length-scales. Under specific conditions for model Al-Mg alloys it is found that the segregation can promote a first order phase transition in the region of high segregation, leading to an ordered precipitate phase. These results are discussed in relation to previous theoretical and experimental work on the interaction between segregation and heterogeneous precipitation in other alloys.

12:00

Volumetric Origin of Hydrogen Trapping at Grain Boundaries in FCC Metals: *Xiao Zhou¹; Jun Song¹; ¹McGill University*

Since the first discovery of the deleterious effects of hydrogen on mechanical properties of structural metals over one century ago, hydrogen embrittlement has been a persistent challenge in the design of high-strength metals. One essential piece in mechanistic understanding of hydrogen embrittlement of structural metals is the interaction between hydrogen and grain boundaries. In this study, we utilized one novel algorithm based on space tessellation to effectively partition grain boundary structures to identify hydrogen adsorption sites. The space tessellation, coupled with first-principle calculations, allows us to systematically investigate the interplay between hydrogen and grain boundaries. Applying the approach to several fcc materials, we identified a generic volumetric origin underlying hydrogen adsorption at grain boundaries. This enables us to make accurate predictive assessments of hydrogen energetics and segregation at grain boundaries, providing valuable insights towards hydrogen-induced cracking at grain boundaries.

12:15

The Effect of Alloying Element Partitioning on the Interface Velocity during the Isothermal Bainite Formation: Hussein Farahan¹; Wei Xu¹; Sybrand van der Zwaag¹; ¹Delft University of Technology

Following the previous study on the effect of alloying elements on the isothermal bainitic ferrite formation in quaternary steels with the mean field approximation, the Gibbs Energy Balance (GEB) model is further developed to incorporate the effect of partitioning of alloying element in both austenite and ferrite domains. In the new model, distributions of alloying elements are updated according to their initial profiles, progresses of the interface and corresponding local equilibrium condition at each time step. The dissipation of carbon (interstitial) diffusion inside and across the interface is calculated and added to the contributions of substitutional alloying elements, e.g. Mn, Si, Ni and Mo. In addition to the final fraction of bainitic ferrite, the new model allows to explore the effect of alloying element partitioning on the interface velocity during the entire transformation. The results are compared to previous simulations and the metallurgical insights are discussed.

12:30

Ab Initio Based Displacive-diffusional Theory for Structural Transformations among Austenite, Ferrite and Cementite in Fe-C Alloys: Xie Zhang¹; Tilmann Hickel¹; Jutta Rogal²; Ralf Drautz²; Jörg Neugebauer²; ¹Max-Planck Institute for Iron Research; ²Interdisciplinary Centre for Advanced Materials Simulation, Ruhr University Bochum

Structural transformations in Fe-C alloys are decisive for the mechanical properties of steels, but their modeling remains a theoretical challenge due to the coupling between the displacive rearrangement of Fe matrix and the diffusion of C. Within an ab initio approach we have successfully decoupled the two aspects in the displacive-diffusional transition. For the displacive part, a proper combination of the orientation-relationships between austenite, ferrite and cementite is decisive. We identify an intermediate structure, which consists of $\Sigma 3$ twin boundaries in bcc Fe and can serve as a bridge between the three phases. Meanwhile, these microstructure features trigger the diffusion of C during the transformation. Within this framework, different mechanisms depending on the local conditions (magnetism, C concentration and strain) have been investigated using ab initio techniques and solid-state nudged elastic band simulations. They allow us to derive a unified displacive-diffusional understanding of the structural transformations among austenite, ferrite and cementite.

12:45

Computational Materials Design: From Atoms to Applications: Ilya Elfimov¹; Hao Jin¹; Joerg Rottler¹; Chad Sinclair¹; Benqiang Zhu¹; Matthias Militzer¹; ¹University of British Columbia

Phase transformations assume a crucial role to tailor material properties during materials processing, e.g. the austenite-ferrite transformations are a key metallurgical tool for advanced low-carbon steels with improved mechanical properties. Computational materials science offers now tremendous opportunities to formulate transformation models containing fundamental information on the basic atomistic mechanisms that can be implemented across different length and time scales. The kinetics of phase transformations depends critically on interface migration rates that are frequently significantly affected by the presence of alloying elements, e.g. Mn, Mo and Nb in iron and steel. Here, an approach is illustrated that links atomistic scale models for the solute-interface interaction with phase field modelling to describe the formation of microstructures with complex morphologies. The overall status and challenges of multi-scale phase transformation modelling will be analyzed for continuous cooling and intercritical annealing of low-carbon steels.

Spinodal Decomposition

FRIDAY AM

ROOM: CALLAGHAN

SESSION CHAIR: MICHEL PEREZ, UNIVERSITÉ DE LYON - INSA DE LYON -MATEIS - UMR CNRS 5510

11:45

Electric Field Induced Microstructure Formation in Polymers: Application in Polymer Blends and Diblock Copolymers: Arnab Mukherjee¹; Kumar Ankit²; Rajdip Mukherjee³; Britta Nestler²; ¹Karlsruhe University of Applied Sciences; ²Karlsruhe Institute of Technology; ³Indian Institute of Technology

There has been a long-standing interest on the application of external fields to control the morphology of polymer mixtures. Electric field is appealing because of the ease with which it can be applied, its ability to modulate morphologies and scales linearly with sample geometry, leading to a wide range of application in nano-devices. Experimental evidences show that external electric field leads to stretching and orientation of the phase separated domains along the direction of field leading to stripe or column formation. Motivated by experimental findings, we study the effect of electric field on the microstructure evolution of polymer mixture using phase-field method. In addition, coarsening and alignment kinetics is also studied for critical and off-critical mixtures. A close agreement with the existing experiments and theory is established.

12:00

Spinodal Decomposition of Fe-Ni-C Martensite by Room Temperature Redistribution of Carbon Investigated by Correlative ECCI/TEM/APT: Michael Herbig¹; Ross Marceau²; Lutz Morsdorf¹; Dierk Raabe¹; ¹Max-Planck-Institut für Eisenforschung GmbH; ²Deakin University

Carbon in martensite is mobile enough to form nm-scale substructures within hours/days via spinodal decomposition. We investigate this process in Fe-15Ni-1C (wt.%). After homogenization followed by water quench the alloy consists of 100% austenite. Quenching in liquid nitrogen triggers the transformation into martensite and when brought back to room temperature the carbon in the martensitic phase undergoes spinodal decomposition. This process has already been investigated by atom probe tomography (APT) and transmission electron microscopy (TEM), but not at the exact same location in the microstructure. Therefore, it is still unclear which part of the complex lenticular martensite microstructure has been measured by APT and how this corresponds to TEM measurements. We illuminate this topic by correlative microstructure characterization using electron channeling contrast imaging (ECCI) and targeted preparation of needle-like APT samples at selected regions of interest, followed by TEM investigation of these needle samples and then subsequent APT investigation.

12:15

Spinodal Decomposition and the Carbon Solubility in BCC Fe-C: Bij-Na Kim¹; Jilt Sietsma¹; Maria J. Santofimia²; ¹TU Delft

Recent findings have indicated that (i) carbon solubility in ferrite is larger than that predicted by the conventional Fe-C phase diagram, where a non-cubic structure of ferrite has been proposed, and (ii) local variations in carbon concentration consistently form within the matrix, thought to be the product of spinodal decomposition. These observations give rise to the scientific question of how carbon is distributed within ferrite, which remains under discussion in literature. The current study aims at establishing a thermodynamic explanation for the carbon solubility and partitioning within ferrite. Topics on carbon-competing processes such as spinodal decomposition in the Fe-C system and carbon segregation to defects have been revisited. Particular emphasis is put on the atom probe tomography (APT), a recurrent technique in the literature in the study of carbon redistribution in ferrite, and on its ambiguity in interpreting carbon profiles.

12:30

Phase Separation during Long Term Aging of a Complex Stainless Steel: Laurent Couturier¹; Frédéric de Geuser¹; Alexis Deschamps¹; ¹Univ. Grenoble Alpes, SIMAP, F-38000 Grenoble, France; CNRS, SIMAP, F-38000 Grenoble, France

The 15-5PH is a martensitic Fe-15%Cr based stainless steel used for aerospace applications, which can be strengthened up to 1200MPa by copper precipitation. This material may be subjected to in-service thermal aging at moderate temperatures (250°C-400°C), which results in microstructural changes leading to modifications of its mechanical properties. Those changes include spinodal decomposition and formation of the G phase. In this presentation, we focus on the quantification of the Chromium spinodal decomposition kinetics. We use a combination of small-angle X-ray and neutron scattering (SAS) and atom probe tomography (APT) to quantitatively describe the kinetics of this transformation both in terms of amplitude and length scale of the composition fluctuations. This evolution is further characterized by differential scanning calorimetry experiments (DSC) and finally we show that it controls the strength evolution of the alloy.

12:45

Phase Transformations, Spinodal Decomposition, Precipitation Reaction, and Eutectoid Reaction, of an Fe-1.28 C-12.5 Mn-6.53 Al Austenitic Steel: Wei-Chun Cheng¹; Chih-Yao Cheng¹; Chia-Wei Hsu¹; ¹National Taiwan University of Science and Technology

Phase transformations of an Fe-12.5 Mn-6.53 Al-1.28 C (wt%) austenitic steel, that include spinodal decomposition, precipitation transformation, and eutectoid reaction, have been studied after quenching from 1100°C and annealing at low temperatures. Spinodal decomposition takes place in the as-quenched steel. Fine coherent gamma' particles precipitate homogeneously in the austenite. After annealing at temperature below 875°C, precipitation transformation occurs and kappa-carbide appears in the austenite as either grain boundary precipitates or cellular precipitates. The cellular precipitates are composed of lamellar austenite and kappa-carbide. The lamellar kappa-carbide grains are always accompanied with austenite twins in the lamellar austenite grains. The presence of FCC twin layers adhered to the carbide plates may attribute to the lower activation energy for the precipitation of carbide plates. At temperatures below 700°C, the eutectoid reaction takes place and the supersaturated austenite decomposes into lamellar ferrite and kappa-carbide called kappa-pearlite.

13:00

The Co-Pt Nanochessboard: Pseudospinodal Decomposition and the Resultant Ferromagnetic Properties: Priya Ghatwai¹; Eric Vetter¹; William Soffa¹; Jerrold Floro¹; ¹University of Virginia

Eutectoid decomposition of Al Co-Pt alloys near 60% Pt can result in the nanochessboard structure – a 2+1D quasi-periodic tiling of L10 and L12 phases with a periodicity of 15-30 nm. Fundamentally, the transformation can be analyzed as pseudo-spinodal decomposition, where the alloy composition must be slightly hyperstoichiometric with respect to the composition where the free energy curves for the A1 and L10 phases cross. We find that the chessboard is obtained when a slow-cooling regimen through the eutectoid isotherm is used, followed by isothermal annealing. We are investigating the magnetic properties since the lengthscales and coherent interfaces should be conducive to exchange-coupling between the hard, uniaxial L10 and the softer, more isotropic L12. This talk will discuss how the chessboard microstructure depends on the thermal processing parameters, and how the aging process affects the coercivity, remanence and magnetic recoil properties. The mechanisms for magnetization reversal will also be discussed.

Novel Processing & Novel Materials II

FRIDAY AM

ROOM: NORDIC

SESSION CHAIR: BALA RADHAKRISHNAN,
OAK RIDGE NATIONAL LABORATORY

11:45 Invited

Surface Precipitation on Engineering Alloys:

*Christopher Hutchinson*¹; Yu Chen¹; Xiya Fang¹; Yves Bréchet²; ¹Monash University; ²Grenoble Institute of Technology

The nucleation and growth of solid state precipitates is used extensively to tailor the bulk mechanical properties of many engineering alloys. It is less well appreciated that precipitation can also be induced to occur on the surfaces of engineering alloys using simple heat treatments raising the possibility of using precipitation as a form of surface treatment. Surface precipitation occurs through a nucleation and growth process with kinetics that suggest mass transfer by surface (or interface) diffusion plays the dominant role. In this presentation, surface precipitation in a number of Al based alloys is presented, the physical principles underlying the phenomena are discussed and some interesting possibilities for 'surface physical metallurgy' are highlighted. Questions of the competition in phase formation on the surface, the compositions inherited by the growing surface precipitates and the coupling of bulk and surface diffusion are discussed.

12:15

Precipitation Processes in Nanostructured 7475

Aluminium Alloy: *Malgorzata Lewandowska*¹; Agnieszka Krawczynska¹; Ajit Panigrahi²; Erhard Schafner²; Michael Zehetbauer²; ¹Warsaw University of Technology; ²University of Vienna

In ultrafine and/or nanogained materials, precipitation phenomena are significantly affected by the high surface area of grain boundaries. Therefore, this work tried to evaluate the influence of grain boundaries on precipitation processes in detail. Samples of 7475 aluminium alloy were solution annealed, water quenched and processed at RT by hydrostatic extrusion (HE) and high pressure torsion (HPT). While both processing procedures yield significant reductions in grain size there are differences in the resulting grain shape (fibre-like for HE, pancake-like for HPT) and in the grain boundary type. Extensive grain boundary precipitation occurs in both samples, more pronounced and faster in HPT ones, which can be attributed to the different characters of grain boundaries involved. Inside the grains, precipitates are significantly smaller than in micrograined materials, which has been discussed in terms of HE / HPT induced vacancy concentrations in micro- and nanostructured samples.

12:30

Metallurgy in High Magnetic Field : From Phase Equilibria to Enhanced Soft Magnetic Properties of Fe-Co Alloys:

*Sophie Rivoirard*¹; Bianca Frincu¹; Rajasekhar Madugundo¹; Olivier Geoffroy²; Thierry Waeckerle³; ¹CNRS/CRETA; ²G2Elab; ³Aperam

Reducing the energy consumption is one of the driving forces for the development of improved materials. In this respect, both new metallurgical processes and improved magnetic materials can provide future solutions for a sustainable development. Thermo-magnetic processing is presented as a new technology which can lead to improved soft magnetic properties in FeCo alloys unattainable through conventional processing. In this work, the effect of a high magnetic field on the α - γ phase transformation in FeCo alloys was quantitatively measured by dilatation measurements up to 16 T. A linear shift of about 2°C/T to higher temperature of the α - γ phase transformation is observed leading to the stabilization of ferrite with a coarse grain microstructure and large Goss oriented grains. This leads to an improvement of coercivity and a reduction of the total magnetic losses. The effect of magnetic field on the α / γ phase transition is explained using a thermodynamic analysis.

12:45

Enhanced Recovery and Recrystallization of Pure Copper Due to an Applied Current:

*Damien Fabrègue*¹; Xavier Boulnat¹; Bassem Mouawad¹; Christopher Hutchinson²; ¹MATEIS, INSA Lyon; ²Monash University

Applying a high current to metals can have drastic effects on their microstructure. But usually the applied currents are very high. However, some recent studies has shown that reasonable currents during straining can permit, for example, to increase the ductility of aluminum alloys. Thus we have investigated the influence of an applied current on the recovery and recrystallization using a SPS machine on a cold drawn pure copper. By comparing samples heated by the Joule effect with those heated in a salt bath, it is shown that recovery and recrystallization are greatly accelerated by the current. At low temperatures, where only recovery occurs during conventional thermal treatments, fully recrystallized microstructures are obtained when the heating is applied through the Joule effect. The influence of the time and of the density of current for a given temperature is also studied.

13:00

Kinetics of Precipitation in New Generation of Cobalt-

based Superalloy: *Ahmad Azzam*¹; *Thomas Philippe*²; Frédéric Danoix²; Annie Hauet²; Didier Blavette²; ¹GPM Laboratory, Université de Rouen; ²GPM Laboratory, Université de Rouen

Nickel superalloys are widely used in aerospace industry and especially for advanced turbine engines. These materials derive their excellent mechanical properties at high temperature (creep) from the presence of a high volume fraction of ordered L12 γ' precipitates embedded in a disordered face centered cubic (FCC) γ matrix. New Co-based superalloys hardened by Co,(Al,W) γ' precipitates were recently investigated [1,2]. In this work, we study the kinetics of precipitation (nucleation, growth and coarsening) in model Co-Al-W ternary superalloys after heat treatment at 900°C. We use Atom Probe Tomography (APT) and Transmission Electron Microscopy (TEM) to determine atomic scale structural and composition information. APT 3D atomic maps will be confronted to kinetic Monte Carlo simulations (rigid lattice, residence time algorithm).[1] Peter J. Bocchini & al., Scripta Materialia 68 (2013) 563 [2] S. Meher & al., Ultramicroscopy 148 (2015) 67-74

Author Index

A			
Abart, Rainer	32	Berek, Harry	12
Abdank-Kozubski, Rafal	17	Bezencon, Cyrille	11
Adachi, Kazuhiko	45	Biborski, Andrzej	17
Aeby-Gautier, Elisabeth	31, 44	Bihan, Quentin Le	31
Ågren, John	6, 19, 24, 27, 35	Billot, Thomas	46
Agudo, Leonardo	19	Bjerkén, Christina	36
Ahmed, Mansur	33	Blavette, Didier	10, 14, 39, 48
Aindow, Mark	16	Blomqvist, Andreas	32
Akai, Hisazumi	24	Bobruk, Elena	41
Akama, Daichi	14	Bolfarini, Claudemiro	41
Akamatsu, Silvere	38	Bönisch, Matthias	44
Akamine, Hiroshi	21	Bonvalet, Manon	39
Akbary, Farideh Hajy	30	Borgenstam, Annika	8, 11, 19, 21, 24, 38
Akhlaghi, Maryam	23	Borgh, Ida	32
Akyildiz, Oncu	35	Borodin, Vladimir	29
Alam, Talukder	15, 33	Botta, Walter	41
Alexander, David	28	Böttger, Bernd	27
Alizamini, Hamid Azizi	44	Bottin-Rousseau, Sabine	38
Allain, Sébastien	11, 20, 38	Botton, Gianluigi	30
Allais, Lucien	9	Bouar, Yann Le	42
Almer, Jonathan	33	Bouaziz, Olivier	30, 32
Alonso, Thais	15	Boucard, Elodie	26
Ambard, Antoine	11	Boulnat, Xavier	48
Amino, Takafumi	6	Bourgeois, Laure	7, 10, 20, 43
Amram, Dor	31, 43	Boyd, Doug	33, 42, 45
Ando, Daisuke	20, 37	Bozzolo, Nathalie	46
Aneziris, Christos	12	Bréchet, Yves	27, 32, 31, 48
Angelkort, Joachim	25	Brenne, Florian	46
Ankit, Kumar	47	Brodacka, Sylwia	17
Aparicio-Fernandez, Rosaura	41	Brommer, Peter	12
Apel, Markus	27, 35	Brosek, Cedrik	12
Apostolov, Zlatomir	25, 32	Brown, Donald	28, 30, 33
Appolaire, Benoît	42, 44	Buken, Heinrich	40
Aranas, Clodualdo	22, 45	Bunkholt, Sindre	37
Arlazarov, Artem	30	Buy, François	9
Arroyave, Raymundo	40		
Arsene, Sylvie	11	C	
Asta, Mark	8, 12	Calin, Mariana	44
Auger, Maria	28	Campbell, Carelyn	7
Averback, Robert	38	Cao, Shanshan	23
Avila-Davila, Erika	29	Capdevila, Carlos	9
Azuma, Masafumi	6	Capdevila-Montes, Carlos	46
Azzam, Ahmad	48	Caram, Rubens	15
		Carron, Denis	11
		Caruso, Matteo	37
		Casero, Carola Celada	16, 42
B		Castro, Felipe	42
Babu, Sudarsanam	7, 8, 12, 34, 44	Catteau, Simon D.	6
Bagot, Paul	28	Cayetano-Castro, Nicolas	21
Bajaj, Saurabh	40	Cayron, Cyril	27, 40
Banerjee, Dipankar	33	Cazottes, S.	20
Banerjee, Rajarshi	15, 21, 31, 33	Cerreta, Ellen	33
Barbier, David	26, 28	Chakrabarti, Debalay	19
Bardel, Didier	37	Chantrenne, Patrice	10
Barges, Patrick	19, 35	Chao, J.	46
Barker, Thomas	27	Chao, Jesus	16, 42
Barker, Simon	11	Charpagne, Marie-Agathe	46
Baron, Christian	41	Chaudhary, Anil	8
Barrallier, Laurent	6	Cheng, Chih-Yao	47
Bauche, Aurelien	19	Cheng, Wei-Chun	47
Beladi, Hossein	27, 33, 38, 41	Chen, Hao	19, 31, 32
Béland, Laurent	12	Chen, Long Qing	36
Bellanger, Philippe	39, 45	Chen, Yan	34
Bellon, Pascal	38, 42	Chen, Ying	6
Belova, Irina	17	Chen, Yu	48
Ben-Haj-Slama, Meriem	26		
		Cheong, Sang-Wook	36
		Chevalier, Laurence	10
		Chiba, Akihiko	24
		Chiba, Tadachika	40
		Chobaut, Nicolas	11
		Choi, Jeom	45
		Choi, Pyuck-Pa	7
		Choi, Won Seok	34
		Choudhuri, Deep	15, 21, 33
		Choudhury, Abhick	42
		Chumlyakov, Yuri	22
		Clarke, Amy	9, 16, 28, 31, 33
		Clarke, Kester	9, 11, 16, 28, 31, 39
		Clausen, Bjorn	28, 33
		Clemens, Helmut	16
		Clouet, Emmanuel	25
		Cobo, Sebastian	26
		Collins, David	46
		Conforto, Egle	41
		Connolley, Thomas	46
		Contieri, Rodrigo	15
		Cooman, Bruno De	9, 34, 45
		Cortial, François	9
		Cottura, Maeva	25, 42
		Coughlin, Daniel	9, 16, 28
		Courteaux, Marc	6
		Coury, Francisco	41
		Couturier, Laurent	47
		Couvat, Yves Du Terrail	16
		Crudden, David	46
		Cuvilly, Fabien	10
		D	
		Dahmen, Ulrich	9
		Dai, Fu-Zhi	41
		Damm, E.	19
		Dancette, Sylvain	37
		Danielsen, Hilmar	41
		Danoix, Frédéric	10, 20, 21, 24, 38, 48
		de Geuser, Frédéric	15, 21, 37, 39, 47
		De Moor, Emmanuel	9, 16, 30
		Debreux, Claire	10, 24
		Dehmas, Moukrane	6, 31, 44
		Dehoff, Ryan	8
		Delacroix, Jessica	16
		Delfosse, Jérôme	44
		Demkowicz, Michael	8
		DeMoor, Emmanuel	28
		Denand, Benoît	31
		Denis, Sabine	6, 31
		Denoual, Christophe	45
		Dépinoy, Sylvain	28
		Deschamps, Alexis	15, 21, 27, 37, 39, 47
		Devaraj, Arun	15
		Ding, Wenjiang	21
		Dippenaar, Rian	28
		Doi, Minoru	39
		Domain, Christophe	8
		Dontsova, Evgeniya	46
		Dorantes-Rosales, Hector	21
		Dorin, Thomas	7, 8, 26
		Drautz, Ralf	47
		Drezet, Jean-Marie	11
		Driemeyer, Patrick	25
		Droste, Matthias	48

Duarte, Jazmin	41	Geoffroy, Olivier	48	Hong, Jaekeun	36
Dulcy, Jacky	6	Georges, Cédric	22	Horibe, Yuta	42
Dumont, Myriam	6	Germain, Lionel	11, 26, 44	Horie, Hiroyasu	26
Duong, Thien	40	Geslin, Pierre-Antoine	42	Hou, Ziyong	10
Du, Qiang	25, 44	Gey, Nathalie	10, 11, 26, 44	Howe, James	31, 45
Dutta, Biswanath	12	Gharghour, M.A.	45	Hoyt, Jeffrey	10, 12, 17
Dwyer, Christian	7	Ghatwai, Priya	47	Hsu, Chia-Wei	47
E					
Eberhart, Mark	19	Ghosh, Chiradeep	45	Huallpa, Edgar Apaza	22
Ebner, Reinhold	14, 32	Ghosh, Supryio	38	Huang, Bo-Ming	16
Eckert, Jürgen	44	Gibbons, Sean	40	Huang, Ching-Yuan	19
Ehteshami, Hossein	25	Gibbs, John	15	Huang, Mingxin	23, 40
Elder, Ken	27, 38	Gibbs, Paul	28	Huber, Liam	10
Elfimov, Ilya	47	Gibouin, David	10	Hughes, Robert	25, 32
El-Mellouhi, Fadwa	12	Gibson, Mark	21, 37	Hulme-Smith, Chris	42
Emigh, Megan	39	Glensk, Albert	6	Hutchinson, Christopher	28, 37, 39, 45, 48
Enikee, Nariman	41	Gloriant, Thierry	12	Huyan, Fei	24
Enomoto, Masato	18, 32	Godet, Stéphane	22, 36, 37	Hu, Yang	12
Epicier, Thierry	14	Goehring, Holger	27	Huyghe, Pierre	22
Escobar, Julian	18, 22	Goldenstein, Hélio	14, 16, 19, 22	Hu, Zhiping	18
Esin, Vladimir	31	Gonzalez-Velazquez, Jorge	21	I	
Esmaili, Shahrzad	11, 25	Gorsse, Stephane	39, 45	Ichiji, Shota	26
Etheridge, Joanne	43	Gorti, Sarma	44	Idell, Yaakov	7, 9, 23, 46
Evteev, Alexander	17	Goulas, Constantinos	11, 42	Idrissi, Hosni	33
F					
Fabrègue, Damien	10, 24, 48	Gouné, Mohamed	20, 24, 30, 32, 38	Il, Seichiro	21
Faivre, Gabriel	38	Gourdet, Sophie	44	Ikehata, Hideaki	37
Fallah, Vahid	11	Gourgues-Lorenzon, Anne-Françoise	28	Inamura, Tomonari	23
Fang, Xiya	48	Goyhenex, Christine	17	Inomoto, Makoto	20
Farahani, Hussein	47	Grabowski, Blazej	6, 10, 12	Inoue, Junya	28, 42
Faria, Guilherme	15, 18, 22	Grewal, Rupanjit	22	Ismail, Andi Idhil	44
Farjami, Sahar	21	Griesser, Stefan	28	Ito, Hirofumi	37
Farrow, Adam	7, 11	Gruber, Marina	14, 32	Ivanov, Rosen	37
Fazeli, Fateh	18, 30, 33, 34	Guenther, Johannes	22	Iwanaga, Kengo	14
Feaugas, Xavier	41	Guilbert, Thomas	9	J	
Field, Robert	28	Guiz, Robin	35	Jacques, Pascal	12, 22, 29, 33, 39, 44
Fillon, Amelie	14	Gulsoy, E.B.	43	Jaeger, David	21
Finel, Alphonse	42	Gumbmann, Eva	37	Jaegle, Eric	7, 33
Fischer, Franz	38	Gupta, Rajeev	26	Jahazi, Mohammad	22, 23
Floro, Jerrold	47	Gururajan, M P	27	Janczak-Rusch, Jolanta	17
Fonseca, João Quinta da	11	Gu, Xinfu	41	Jegou, Sébastien	6
Fraczkiewicz, Anna	24, 35, 41	H			
Franchet, Jean-Michel	46	Haataja, Mikko	15, 32	Jen, Chih-Hung	19
Fraser, Hamish	15, 31, 33	Habler, Gerlinde	32	Jensen, Wade	20
Freibert, Franz	33	Hackenberg, Robert E.	9, 31, 39, 40	Jeon, Jongbae	34
Fries, Suzana	15	Hadian, Sherri	10	Jerábek, Petr	32
Friis, Jesper	40, 44	Haggerty, Ryan	21, 25	Jiang, Fulin	23
Frincu, Bianca	48	Hanamura, Toshihiro	9, 40	Jin, Hao	47
Frolov, Timofey	8	Han, Heung Nam	45	Jin, Xuejun	13, 22
Fujii, Toshiyuki	26	Han, Jian	10	Jin, Yongmei	17, 29
Fujimoto, Kousuke	40	Hardy, Mark	46	Ji, Yanzhou	36
Fujiyama, Hideki	42	Hariharaputran, Ramanarayan	27	Johnson, Duane	12
Fukuda, Takashi	22, 24, 38	Hata, Satoshi	39	Jolly, William	9
Fultz, Brent	6, 12	Hauet, Annie	48	Joly, Jean-François	12
Furtado, Jader	24	Hayashi, Koutarou	32	Jonas, John	22, 45
Furuhara, Tadashi	6, 10, 13, 22, 35, 38, 40, 41	Hazotte, Alain	30	Jones, Zachary	21, 25
G					
Gamsjäger, Ernst	9, 14	He, Binbin	23	Jung, Minsu	40
Gao, Yipeng	29	Hecht, Matthew	35	Junior, José da Cruz	19
Garat, Xavier	19	Hedström, Peter	10, 19, 21, 32	K	
Garcia-Riesco, Pedro Manuel	8	Hell, Jean-Christophe	20	Kadletz, Peter	22
Garcin, Thomas	15, 24, 26, 46	Helmreich, Grant	8	Kainuma, Ryosuke	9
Gautam, Abhay	9	Heo, Yoon-Uk	38	Kajihara, Masanori	16, 20
Gazder, Azdiar	33	Herbig, Michael	47	Kakeshita, Tomoyuki	22, 24, 38
Geandier, Guillaume	20, 31	He, Yongjun	36	Kalbfleisch, Anne-Sophie	29
Geng, Liwei	29	Hickel, Tilmann	6, 12, 47	Kammuri, Kazuki	26
Gentils, Aurelie	29	Hillert, Mats	11	Kamyabi-Gol, Ata	15
H					
Geoffroy, Olivier	48	Hirako, Takaaki	20	Kaneshita, Takeshi	22
Georges, Cédric	22	Hodgson, Peter	8, 19, 26, 27, 33, 38	Kang, DaeHoon	21
Germain, Lionel	11, 26, 44	Hoerner, Michael	19	Kang, Joo-Hee	24
Geslin, Pierre-Antoine	42	Höglund, Lars	19, 27, 35	Kang, Singong	30
Gey, Nathalie	10, 11, 26, 44	Holm, Elizabeth	44	K	
Gharghour, M.A.	45	Holmestad, Randi	44	Kadletz, Peter	22
Ghatwai, Priya	47	I			
Ghosh, Chiradeep	45	Ichiji, Shota	26	Idell, Yaakov	7, 9, 23, 46
Ghosh, Supryio	38	Idrissi, Hosni	33	Il, Seichiro	21
Gibbons, Sean	40	Ikehata, Hideaki	37	Inamura, Tomonari	23
Gibbs, John	15	Inomoto, Makoto	20	Inoue, Junya	28, 42
Gibbs, Paul	28	Ismail, Andi Idhil	44	Ito, Hirofumi	37
Gibouin, David	10	Ivanov, Rosen	37	Iwanaga, Kengo	14
Gibson, Mark	21, 37	J			
Glensk, Albert	6	Jacques, Pascal	12, 22, 29, 33, 39, 44	Jaeger, David	21
Gloriant, Thierry	12	Jaegle, Eric	7, 33	Jahazi, Mohammad	22, 23
Godet, Stéphane	22, 36, 37	Jahazi, Mohammad	22, 23	Janczak-Rusch, Jolanta	17
Goehring, Holger	27	Janczak-Rusch, Jolanta	17	Jegou, Sébastien	6
Goldenstein, Hélio	14, 16, 19, 22	Jegou, Sébastien	6	Jen, Chih-Hung	19
Gonzalez-Velazquez, Jorge	21	Jensen, Wade	20	Jeon, Jongbae	34
Gorsse, Stephane	39, 45	Jeon, Jongbae	34	Jerábek, Petr	32
Gorti, Sarma	44	Jerábek, Petr	32	Jiang, Fulin	23
Goulas, Constantinos	11, 42	Jiang, Fulin	23	Jin, Hao	47
Gouné, Mohamed	20, 24, 30, 32, 38	Jin, Hao	47	Jin, Xuejun	13, 22
Gourdet, Sophie	44	Jin, Xuejun	13, 22	Jin, Yongmei	17, 29
Gourgues-Lorenzon, Anne-Françoise	28	Jin, Yongmei	17, 29	Ji, Yanzhou	36
Goyhenex, Christine	17	Ji, Yanzhou	36	Johnson, Duane	12
Grabowski, Blazej	6, 10, 12	Johnson, Duane	12	Jolly, William	9
Grewal, Rupanjit	22	Jolly, William	9	Joly, Jean-François	12
Griesser, Stefan	28	Joly, Jean-François	12	Jonas, John	22, 45
Gruber, Marina	14, 32	Jonas, John	22, 45	Jones, Zachary	21, 25
Guenther, Johannes	22	Jones, Zachary	21, 25	Jung, Minsu	40
Guilbert, Thomas	9	Jung, Minsu	40	Junior, José da Cruz	19
Guiz, Robin	35	Junior, José da Cruz	19	K	
Gulsoy, E.B.	43	K			
Gumbmann, Eva	37	Kadletz, Peter	22	Kainuma, Ryosuke	9
Gupta, Rajeev	26	Kainuma, Ryosuke	9	Kajihara, Masanori	16, 20
Gururajan, M P	27	Kajihara, Masanori	16, 20	Kakeshita, Tomoyuki	22, 24, 38
Gu, Xinfu	41	Kakeshita, Tomoyuki	22, 24, 38	Kalbfleisch, Anne-Sophie	29
H					
Haataja, Mikko	15, 32	Kalbfleisch, Anne-Sophie	29	Kammuri, Kazuki	26
Habler, Gerlinde	32	Kammuri, Kazuki	26	Kamyabi-Gol, Ata	15
Hackenberg, Robert E.	9, 31, 39, 40	Kamyabi-Gol, Ata	15	Kaneshita, Takeshi	22
Hadian, Sherri	10	Kaneshita, Takeshi	22	Kang, DaeHoon	21
Haggerty, Ryan	21, 25	Kang, DaeHoon	21	Kang, Joo-Hee	24
Hanamura, Toshihiro	9, 40	Kang, Joo-Hee	24	Kang, Singong	30
Han, Heung Nam	45	Kang, Singong	30	K	
Han, Jian	10	K			
Hardy, Mark	46	Kadletz, Peter	22	Kainuma, Ryosuke	9
Hariharaputran, Ramanarayan	27	Kainuma, Ryosuke	9	Kajihara, Masanori	16, 20
Hata, Satoshi	39	Kajihara, Masanori	16, 20	Kakeshita, Tomoyuki	22, 24, 38
Hauet, Annie	48	Kakeshita, Tomoyuki	22, 24, 38	Kalbfleisch, Anne-Sophie	29
Hayashi, Koutarou	32	Kalbfleisch, Anne-Sophie	29	Kammuri, Kazuki	26
Hazotte, Alain	30	Kammuri, Kazuki	26	Kamyabi-Gol, Ata	15
He, Binbin	23	Kamyabi-Gol, Ata	15	Kaneshita, Takeshi	22
Hecht, Matthew	35	Kaneshita, Takeshi	22	Kang, DaeHoon	21
Hedström, Peter	10, 19, 21, 32	Kang, DaeHoon	21	Kang, Joo-Hee	24
Hell, Jean-Christophe	20	Kang, Joo-Hee	24	Kang, Singong	30
Helmreich, Grant	8	Kang, Singong	30	K	
Heo, Yoon-Uk	38	K			
Herbig, Michael	47	Kadletz, Peter	22	Kainuma, Ryosuke	9
He, Yongjun	36	Kainuma, Ryosuke	9	Kajihara, Masanori	16, 20
Hickel, Tilmann	6, 12, 47	Kajihara, Masanori	16, 20	Kakeshita, Tomoyuki	22, 24, 38
Hillert, Mats	11	Kakeshita, Tomoyuki	22, 24, 38	Kalbfleisch, Anne-Sophie	29
Hirako, Takaaki	20	Kalbfleisch, Anne-Sophie	29	Kammuri, Kazuki	26
Hodgson, Peter	8, 19, 26, 27, 33, 38	Kammuri, Kazuki	26	Kamyabi-Gol, Ata	15
Hoerner, Michael	19	Kamyabi-Gol, Ata	15	Kaneshita, Takeshi	22
Höglund, Lars	19, 27, 35	Kaneshita, Takeshi	22	Kang, DaeHoon	21
Holm, Elizabeth	44	Kang, DaeHoon	21	Kang, Joo-Hee	24
Holmestad, Randi	44	Kang, Joo-Hee	24	Kang, Singong	30

Kang, SungJin	7	Lenci, Matthieu.....	41	Mei, Paulo Roberto	18
Kante, Stefan	27	Lépinoux, Joël	17	Meka, Sai Ramudu	23, 40
Kaoumi, Djamel	22	Letourneau, Steven	25	Melado, André	16
Kapikranyan, Oleksandr.....	8	Levasseur, Tom.....	22, 23	Mendez, Patricio.....	15
Karmakar, Anish	19	Levchenko, Elena.....	17	Mikheev, Alexander	25, 42
Kattner, Ursula	15, 17	Levine, Lyle.....	7	Mikolaychuk, Mikhail	15
Kaufman, Michael.....	41	Lewandowska, Malgorzata	48	Militzer, Matthias 6, 8, 10, 15, 19, 24, 26, 32, 33, 44, 46, 47	
Kawai, Ryutaro	21	Leyson, Gerard	6	Milkereit, Benjamin	12
Kawai, Yuichiro	29	Li, Huijun.....	19	Miller, Allison	8
Kawamoto, Yuzo	28	Liss, Klauss	38	Miller, Michael	28
Kegel, Frédéric	30	Liu, Chenglu	44	Miller, Mike K.....	46
Kellezi, Gert	16	Liu, Chenxi	19, 34	Mitchell, Jeremy	11, 29, 33
Keplinger, Andreas.....	14	Liu, Junliang	22	Mitchell, Terence	11, 33
Kerber, Michael	23	Liu, Lu	20	Mithieux, Jean-Denis	16
Keßler, Olaf.....	12	Liu, Naiming	20	Mittemeijer, Eric.....	17, 21, 23, 27, 36, 40
Kestens, Leo.....	30	Liu, Tianyu.....	20, 43	Miyamoto, Goro	6, 10, 15, 22, 35, 38, 40
Ke, Xiaojin	29	Liu, Yongchang	19, 34	Miyazawa, Tomotaka.....	26
Keyvani, Mahsa	24	Li, Xin	43	Miyoshi, Takayuki	23
Kim, Bij-Na.....	47	Li, Yanjun.....	25	Mohles, Volker	12
Kim, Dong Hwi	38	Li, Yuanyuan.....	23	Mohri, Tetsuo.....	6, 25, 30
Kiminami, Claudio.....	41	Li, Yunguo	25	Monzen, Ryoichi	21
Kim, Miyoung	7	Li, Zhaodong.....	26	Moody, Michael	28
Kim, Sung-Joon.....	38	Llobet, Anna	39	Moritani, Tomokazu	42
Kirka, Michael.....	8, 11	Lo, Jason	30	Morsdorf, Lutz	47
Kléber, X.....	20	Longo, Paolo.....	23	Mosquero, Maria	19
Klinger, Leonid.....	31	Lopes, Eder	15	Motoyama, Kojiro	42
Knapp, Cameron.....	11	López, Beatriz.....	8, 18	Mouawad, Bassem	48
Knijf, Dorien De	30	Lopez-Hirata, Victor	21, 29	Moumni, Ziad	36
Koga, Norimitsu.....	10	Lousada, Cláudio	25	Mousseau, Normand	12
Koike, Junichi	20, 37	Lucas, Matthew	12	Mroz, Michal.....	41
Komiyama, Shoko.....	20	Luo, Haiwen	18	Mukherjee, Arnab.....	47
Korbmacher, Dominique	6	Luo, Na	16	Mukherjee, Rajdip	47
Körmann, Fritz.....	6, 12	Lu, Qi	14, 28	Mukherjee, Subrata	19
Korzekwa, Deniece.....	11	LV, Duchao	29	Munoz, Jorge.....	12
Korzhavyi, Pavel	25			Murakami, Masahiro	14
Kosaka, Makoto	10	M		Murakami, Yasukazu.....	9
Koseki, Toshihiko	28, 42	Madugundo, Rajasekhar	48	Murashkin, Maxim.....	41
Kostka, Aleksander.....	41	Maetz, Jean-Yves.....	20	Murata, Yoshinori.....	29
Kovalenko, Oleg	31, 43	Maier, Hans	22	Murch, Graeme	17
Koyama, Toshiyuki	29	Majumdar, Bhaskar	30		
Koyano, Tamotsu	45	Malet, Loïc.....	36	N	
Kozakai, Takao	42	Ma, Li	7	Nag, Soumya	15, 31
Kozeschnik, Ernst.....	28, 29, 38, 39, 40	Malik, Amer	35	Nakada, Nobuo	10, 14, 45
Kozłowski, Miroslaw	17	Maminska, Karolina	24	Nakashima, Philip.....	7, 20, 41, 43
Krauss, George.....	28	Mandal, Abhisek	19	Nakayama, Misako	20
Krawczynska, Agnieszka	48	Mandal, Madhumanti.....	19	Nambu, Shoichi	28, 42
Kristoffersen, Hans	38	Marceau, Ross.....	7, 26, 28, 47	Nanese, Hadi Ghasemi	22, 23
Kriven, Waltraud	21, 25, 32, 46	Marini, Bernard	9, 28	Nasedkina, Yana	41
Kroke, Edwin	16	Marioara, Calin	44	Navarro-Lopez, Alfonso	40
Krooß, Philipp.....	22	Mark, Alison	45	Navarro, Maria Santofimia.....	17
Kubo, Hironori	6	Marsoner, Stefan	14, 32	Nazarov, Andrei	25, 42
Kwakernaak, Kees	30	Marteleur, Matthieu	12, 22, 33	Nelias, Daniel	37
		Marthinsen, Knut.....	25, 37	Nes, Erik.....	37
L		Martin-Aranda, María	9, 46	Nestler, Britta	42, 47
Laas, Tõnu.....	20	Martin, David San	16, 42	Neugebauer, Jörg	6, 10, 12, 47
LaGrange, Thomas	9	Mas, Fanny.....	27	Nguyen, Toan	11
Lai, Qingquan	32	Massih, Ali	36	Nie, Jian-Feng	7, 39, 41
Lancon, Frederic.....	9	Masumura, Takuro.....	45	Niendorf, Thomas.....	22, 46
Landa, Alexander.....	40	Ma, Taoran	32	Niitsu, Koudai.....	9
Landeghem, Hugo P. Van.....	6, 31	Mateo, Antonio Manuel	45	Nishibata, Toshinobu	32
Langelier, Brian.....	31	Matsuda, Mitsuhiro	23	Nishida, Minoru	21, 23
Lass, Eric.....	7, 15, 32, 46	Matsumura, Syo.....	24, 39	Nishikawa, Arthur	16, 19
Lathe, Christian	16	Mauger, Lisa.....	12	Nolze, Gert	19
Lawrence, Ben	14	Ma, Weijie.....	28	Nomoto, Sukeharu.....	24
Leach, Lindsay	19	Ma, Xiao	23, 25	Northover, Peter	39
Lee, Hak Sung	36	Mayer, Walter.....	39	Northover, Shirley	39
Lee, Woei-Shyan	22	McLeod, Michael	30	Nozaki, Takayuki.....	6
Lefebvre, Williams.....	37	McReynolds, Kevin	10	N'Tsouaglo, Gawonou	12
Leineweber, Andreas	23, 27	Mecozzi, Pina	11		
Leitner, Harald	16	Medhekar, Nikhil	7, 20	O	
Lejcek, Pavel	45, 46	Medrano, Sebastian.....	21		

Odqvist, Joakim	10, 19, 21, 27, 32, 35
Ogata, Keisuke	39
Ogawa, Yukiko	20, 37
Oguma, Ryuichiro	39
Ogura, Masako	24
Oh, Chang-Seok	24, 36
Oikawa, Katsunari	20
Ojima, Mayumi	28
Olson, Greg	33, 36, 44
Ono, Toshiyuki	26
Ophus, Colin	9
Ortiz-Mariscal, Arturo	29
Orvananos, Bernardo	35
Ou, Xiaoqin	17
P	
Paju, Jana	20
Palumbo, Mauro	15
Panahi, Damon	25, 31
Panigrahi, Ajit	23, 44, 48
Papaefthymiou, Spyros	42
Papin, Pallas	39
Pardoen, Thomas	32
Pareige, Cristelle	8
Pareige, Philippe	8
Park, C.-L.	43
Park, Hyun Soon	9
Park, Kyung-Tae	45
Park, Yun Chang	25
Pascan, Oana Zenaïda	36
Patte, Renaud	8
Paul, Francois-Liguori	22
Peet, Mathew	42
Peng, Liming	21
Pereloma, Elena	33, 41
Perez, Michel	10, 14, 37, 47
Perlade, Astrid	32
Petit, Philippe	9
Petrov, Roumen	30, 42
Phillippe, Thomas	14, 39, 48
Picard, Yoosuf	35
Pierce, Dean	9, 16, 28
Pierron-Bohnes, Veronique	17
Pilkey, Keith	33
Pimentel, Gemma	46
Plapp, Mathis	38
Ploberger, Sarah	32
Pogatscher, Stefan	12
Pohu, Benjamin	37
Polak, Micha	43
Polatidis, Efthymios	21, 36
Poole, Warren	26, 33, 44
Poplawsky, Jonathan	9
Poulsen, Stefan	46
Povoden-Karadenitz, Erwin	32
Preuss, Michael	11
Priimets, Jaanis	20
Prima, Frédéric	12, 22, 33
Primig, Sophie	16, 29
Purdy, Gary	14, 23, 25, 31
Puype, Athina	30
R	
Raabe, Dierk	7, 38, 41, 47
Rabkin, Eugen	31, 43
Race, Christopher	10
Radhakrishnan, Bala	48
Radiguet, Bertrand	8
Raeisia, Babak	11, 21
Rafaja, David	16
Rakha, Khushboo	38
Ramajayam, Mahendra	7
Ramirez, Antonio	15, 16, 18, 22
Ravi, Ashwath M.	22
Razumovskiy, Vsevolod	7
Redjaïmia, Abdelkrim	6, 45
Reed, Roger	46
Reiche, H. Matthias	30
Reichert, Jennifer	33
Rementeria, R.	9
Ren, Xiaobing	17, 29
Ressel, Gerald	14, 32
Restrepo, Oscar	12
Reyes-Huamantincó, Andrei	7
Rheingans, Bastian	17, 40
Ribero, Daniel	32
Ribis, Joël	29
Rigal, E.	16
Ringer, Simon	7, 9
Ringeval, Sylvain	9
Rivera-Díaz-del-Castillo, Pedro	14
Rivoirard, Sophie	48
Rizzo, Fernando	19
Roa, Joan Josep	45
Robinson, Isaac	26
Robson, Joseph	37, 39
Roch, François	27, 28
Rodriguez-Ibabe, Jose	8, 18, 36
Rogal, Jutta	47
Rohrer, Gregory	27, 36, 41
Rollett, Anthony	27
Romankov, Sergey	25
Romero, Javier	11
Ropars, Ludovic	44
Rosalie, Julian	7
Rosker, Eva	20
Rottler, Joerg	46, 47
Rottler, Jörg	10
Roy, Arijit	27
Roy, Geoffrey	39
Ruban, Andrei	7, 40
Rubinovich, Leonid	43
Rüsing, Christian	46
Rutkevych, Pavlo	27
S	
Sackl, Stephanie	16
Saengdeejing, Arkapol	6
Saidi, Peyman	12
Saied, Mahmoud	16
Sakaguchi, Hidetsugu	21
Saleh, Ahmed	33
Saleh, Tarik	11
Salib, Matthieu	44
Sánchez, Julio Antonio Capó	22
Santofimia, Maria J.	22, 30, 40, 47
Santos, Dagoberto	19
Sapezanskaïa, Ina	45
Saragosa, James	30
Sarin, Pankaj	21, 25, 32
Sato, Hisashi	20, 40, 42
Sato, Kazunori	24
Saucedo-Muñoz, Maribel	21, 29
Sauvage, Xavier	14, 24, 39, 41, 43
Sawatzky, George	35
Schäfer, Norbert	27
Schafler, Erhard	48
Schick, Christoph	12
Schimpf, Christian	16
Schloth, Patrick	11
Schneider, Daniel	42
Schneider, Matthew	45
Schryvers, Dominique	23, 36
Schumacher, Philipp	12
Schwartz, Daniel	17, 33
Schwarz, Marcus	16
Scott, Colin	14, 18, 34
Scott, Hayley	33
Segawa, Masahito	24
Seidman, David	27
Selzer, Michael	42
Seo, Seong Moon	24
Sepehrband, Panthea	25
Seymour, Kevin	25, 32
Shalchi-Amirkhiz, B.	34
Shang, Chengjia	37
Shan, Yao	38, 39
Shassere, Benjamin	34
Shchyglo, Oleg	15
Sheng, Zhendong	7
Sherstnev, Pavel	40
Shi, Lei	34
Shi, Rongpei	15, 31
Shigesato, Genichi	6
Shinbine, Alyssa	24
Shinbo, Kunio	35
Shindo, Daisuke	9
Shin, Dong Jun	25
Shin, Sunmi	34
Shirokova, Veronika	20
Sidhu, Gagan	33
Sietsma, Jilt	11, 17, 22, 28, 30, 32, 40, 42, 47
Sigli, Christophe	14, 17, 37
Simar, Aude	39
Sinclair, Chad	8, 14, 19, 21, 24, 34, 35, 46, 47
Siqueira, Luana	33
Skibinski, Wojciech	20
Skrotzki, Werner	44
Slama, Meriem Ben Haj	11
Smith, Andrew	7, 20
Smith, George	28
Sob, Mojmir	45
Soejima, Yohei	23
Soffa, William	20, 47
Soler, Michel	20
Somsen, Christoph	22
Song, Huajing	17
Song, Jun	46
Song, Pengcheng	20
Soroka, Inna	25
Sourmail, Thomas	10, 24, 31
Sowa, Piotr	17
Speer, John	9, 16, 19, 28, 30
Springer, Hauke	41
Sridharan, Niyanth	8
Srivilliputhur, Srinivasan	21
Srolovitz, David	10
Stanford, Nicole	7, 8, 12, 19, 26, 33
Starink, Marco	12
Stechauner, Georg	29
Steinbach, Ingo	6, 9, 15
Steiner, Tobias	23
Stone, Howard	42
Stormvinter, Albin	38
Styles, Mark	37, 39
Subramanian, S.V.	37
Sundman, Bo	15
Sun, Fan	12
Sun, Weiwei	25
Sun, Wenwen	28
Sun, Xinjun	26
Sutou, Yuji	20, 37

Suzon, Eric9
 Suzuki, Tetsu37
 Svoboda, Jirí32, 38

T

Takaki, Setsuo 10, 14, 31, 45
 Tanaka, Kouji37
 Tanaka, Tomoyuki40
 Tanguy, Perrine22
 Tang, Yijin21
 Tanigaki, Toshiaki9
 Tan, Xiaodong18
 Tari, Vahid27
 Tassin, Catherine16, 27
 Taylor, Adam7, 8, 19
 Teixeira, Julien6, 31, 44
 Terai, Tomoyuki24
 Teshima, Toshihiko10
 Thompson, J.43
 Thornton, Katsuyo35, 43
 Tian, Ye21
 Timokhina, Ilana33, 38
 Toda-Caraballo, Isaac14
 Toda, Yoshiaki28
 Todeschini, Patrick27
 Toffolon-Masclat, Caroline9, 28
 Torizuka, Shiro9, 40
 Tracy, Sally12
 Trickers, David44
 Trochet, Mickaël12
 Tsai, Shao-Pu9, 19
 Tsai, Yu-Ting22
 Tschukin, Oleg42
 Tsuchiya, Koichi21
 Tsuchiyama, Toshihiro10, 14, 45
 Tsukada, Yuhki29
 Tucker, Tim39
 Turchi, Patrice40
 Tyne, Chester Van31

U

Udovsky, Aleksandr15
 Ueda, Keiji15
 Ugaste, Ülo20
 Umantsev, Alexander24, 43
 Uranga, Pello8
 Urones-Garrote, Esteban9, 46

V

Valdenaire, Pierre-Louis42
 Valiev, Ruslan41
 Van der Rest, Camille39
 Van der Zwaag, Sybrand14, 27, 28, 31, 47
 Van Petegem, Steven33
 Vanacken, Johan29
 Vasilyev, Dmitry15
 Vattré, Aurélien8, 45
 Verdu, C.20
 Vermaut, Philippe12
 Véron, Muriel16
 Vetter, Eric47
 Vieira, Estéfano16
 Vigil, Chastity31
 Vijayan, Sriram16
 Viljus, Mart20
 Villegas-Cardenas, Jose29
 Vitek, Vaclav10
 Vitos, Levente40
 Vivès, Solange45
 Vogel, Sven30

Vollmer, Malte22
 Volz, Heather39
 Voorhees, Peter10, 14, 43, 46

W

Waeckerle, Thierry48
 Waitz, Thomas23, 44
 Wang, Dong17, 29, 31
 Wang, Jian17
 Wang, Xiang33
 Wang, Xueyun36
 Wang, Yu17, 29, 33
 Wang, Yuan-Tsuong19
 Wang, Yunzhi15, 17, 29, 31, 33
 Wang, Zhiquan37
 Watanabe, Chihiro21
 Watanabe, Yoshimi20, 40
 Webler, Bryan35
 Wedrychowicz, Stanislaw20
 Weigelt, Christian12
 Wei, Ran32
 Wei, Zhaozhao25
 Wenner, Sigurd44
 Wexler, David33
 Weyland, Matthew7
 Wicaksono, Tegar8
 Wident, Pierre9
 Wierzba, Bartek20
 Wierzba, Patrycja20
 Wiessner, Manfred14, 32
 Wiezorek, Jorg23
 Williamson, Don16
 Williams, Robert31, 33
 Wilson, Alison39
 Wolverton, Chris38, 40
 Wu, David T27
 Wu, Di10, 18
 Wu, Kuo-An10
 Wu, Leonardo15, 18

X

Xiao, Fei22
 Xia, Yuan8, 20
 Xie, Zhenjia37
 Xiong, Xiang-Yuan38
 Xue, Fei36
 Xu, Wei14, 23, 27, 28, 47
 Xu, Xin19
 Xu, Yunbo18

Y

Yablinsky, Clarissa39
 Yamada, Yasunori25
 Yamaguchi, Takashi38
 Yamamoto, Sukeyoshi24
 Yamamoto, Tomokazu24
 Yamamoto, Yukinori34
 Yamanaka, Akinori24, 36
 Yamanaka, Kenta24
 Yang, Jer-Ren9, 16, 19, 22, 31, 35
 Yang, Ke28
 Yang, XiaoLong18
 Yang, Ze nan8, 27
 Yang, Zhi-Gang8, 20, 26, 27
 Yan, Jiayi24, 33
 Yan, Wei28
 Yao, Xiayang23
 Yasuda, Kazuhiro24
 Yeli, Guma28
 Yen, Hung-Wei22

Yeom, Jong-Taek24, 36
 Yingjun, Gao25
 Yin, Jiaqing11
 Yokomine, Tomohito24
 Yong, Qilong26
 Yoon, Jeong Mo25
 Yoshioka, Satoru24
 Yu, Hui-Chia35
 Yu, Liming19, 34
 Yu, Yongmei18

Z

Zapolsky, Helena8, 21, 38
 Zarkevich, Nikolai12
 Zehetbauer, Michael44, 48
 Zhang, Chi8, 20
 Zhang, Gufei29
 Zhang, Han41
 Zhang, Hui23
 Zhang, Liangxiang17
 Zhang, Wenzheng35, 41
 Zhang, Xie47
 Zhang, Xiping23, 25
 Zhang, Yongjie35
 Zhang, Zezhong7, 20
 Zhang, Zhenyan21
 Zheng, Ce29
 Zheng, Yufeng15, 31, 33
 Zhou, Wei23, 43
 Zhou, Weihao37
 Zhou, Xiao46
 Zhou, Xiaosheng19
 Zhu, Benqiang19, 32, 47
 Zhu, Guo-zhen23, 43
 Zhu, Kangying11
 Zotov, Nikolay21, 36
 Zou, Ying18
 Zuazo, Ian19, 35
 Zuo, Jian-Min7, 12
 Zurob, Hatem13, 19, 23, 25, 31

Who are Aperam?



> 2.5mt flat stainless steel capacity in Europe and South America



> 1.81mt shipped in 2014



Employees



R&D Europe

us\$5.485bn

> 2014 revenues in 40 countries

Principal operations including significant production plants

Stainless Europe	Belgium	France			
	Genk	Châtelet	Gueugnon	Isbergues	
South America	Brazil	Alloys & Specialties		France	
	Timoteo	Imphy	Amilly	Rescal	
Services & Solutions	Worldwide	16	Steel Service Centres	19	sales offices
		8 transformation facilities			

What makes us unique?

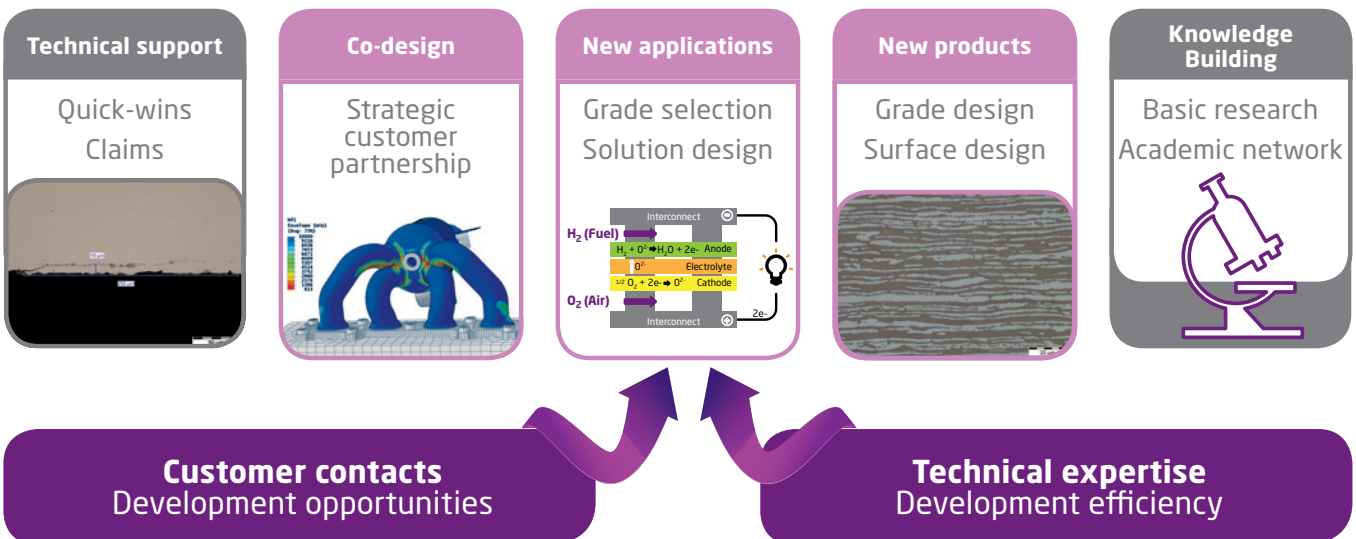
- > Leading global stainless and specialty steel producer
- > Long-term growth potential of the stainless and specialty steel industry
- > Global, integrated distribution network and proximity to customer
- > Effective working capital and risk management
- > Leading R&D capabilities

A complete range of R&D activity to feed Aperam innovation

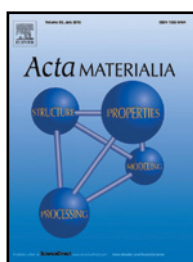
From short term...

THIS IS INNOVATION!

...to long term

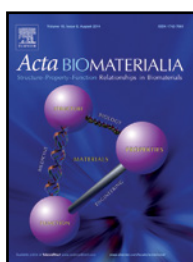


The Materials Engineering Collection from Elsevier



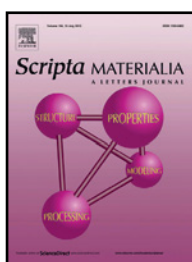
2013 Impact Factor
3.940

Coordinating Editor: Professor S. Mahajan, University of California, USA



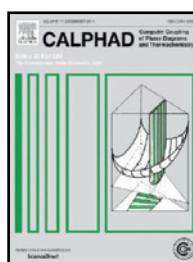
2013 Impact Factor
5.684

Editor-in-Chief: Professor W.R. Wagner, University of Pittsburgh, USA



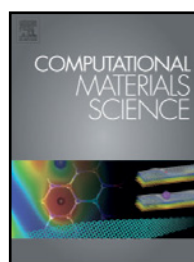
2013 Impact Factor
2.968

Principal Editor: K. Hono, National Institute of Minerals Science, Japan



2013 Impact Factor
1.394

Editor-in-Chief: Z.-K. Liu, Pennsylvania State University, USA



2013 Impact Factor
1.879

Editor-in-Chief: Susan Sinnott, University of Florida, USA



2013 Impact Factor
3.171

Editor-in-Chief: A.M. Korsunsky, University of Oxford, UK



2013 Impact Factor
1.925

Editor-in-Chief: I. Baker, Dartmouth College, USA



The 2014 Acta Materialia Gold Medal has been awarded to: Professor J. David Embury

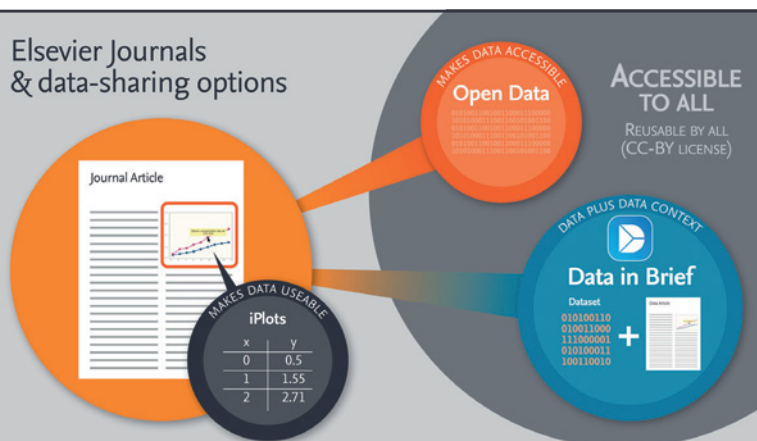
The Acta Materialia Gold Medal is awarded annually by the Board of Governors of Acta Materialia, Inc., with partial financial support from Elsevier, Ltd. Nominees are solicited each year from the Cooperating Societies and Sponsoring

Societies of Acta Materialia, Inc., based on demonstrated ability and leadership in materials research.

Elsevier Materials Science Journals Offers Entire Suite of Data Sharing Options

From early 2015, 13 journals published by Elsevier have three new capabilities to store, share, discover and facilitate re-use of data: iPlots, Open Data on ScienceDirect and linking to Data in Brief.

Elsevier Journals & data-sharing options



For further information, please visit www.materialstoday.com/materials-genome-initiative